

***A STUDY OF CHANGE IN HUMAN TRABECULAR BONE STRUCTURE
WITH AGE AND DURING OSTEOPOROSIS***

A thesis submitted for the degree of
Doctor of Philosophy
in the University of London by
JAYASINGHE ARACHCHILAGE PREMASIRI JAYASINGHE

Hard Tissue Research Unit
Department of Anatomy and Developmental Biology
University College London
Gower Street
London WC1E 6BT

June 1991

ProQuest Number: 10610823

All rights reserved

INFORMATION TO ALL USERS

The quality of this reproduction is dependent upon the quality of the copy submitted.

In the unlikely event that the author did not send a complete manuscript and there are missing pages, these will be noted. Also, if material had to be removed, a note will indicate the deletion.



ProQuest 10610823

Published by ProQuest LLC (2017). Copyright of the Dissertation is held by the Author.

All rights reserved.

This work is protected against unauthorized copying under Title 17, United States Code
Microform Edition © ProQuest LLC.

ProQuest LLC.
789 East Eisenhower Parkway
P.O. Box 1346
Ann Arbor, MI 48106 – 1346

ABSTRACT

The objective of this work was to develop new techniques to view trabecular bone three-dimensionally, and to study its structure and the changes that occur with age and in osteoporosis: the methods used included 3D methods in the SEM, laser confocal microscopy, pseudo-holograms and a "continuous motion parallax method".

A detailed analysis of trabecular bone from fourth lumbar vertebral bodies used macro-stereophotographs produced by tilting a sample 10° . Models are proposed for both normal and osteoporotic architecture. A quantitative analysis of the lengths of horizontally oriented trabeculae was carried out. A significant decrease in the number of both vertically and horizontally oriented trabeculae was found. The importance of the influence of different developmental patterns on the formation of the normal structure and of the changing vascularisation on osteoporotic structure are emphasised.

Two-dimensional fast Fourier transform methods were employed to study changes in the spatial frequency of trabeculae as a function of orientation. A decrease in spatial frequency was observed in both sexes, but in males this was evident only after the mid-sixth decade in the limited sample studied. Contoured power spectra discriminated different trabecular patterns and the intensity mapping of optical density provided volume density information. Templated reverse transformation was used to study individual orientations of trabeculae.

Changes in the quality of trabecular bone with age were also investigated using techniques that analyse bone before and after removal of unmineralised matrix. All specimens were less stiff after removal of osteoid; this was more marked in older specimens. Locally defective mineralisation would explain the changed behaviour observed in some old and osteoporotic specimens. Trabecular fracture patterns had a strong relationship to architecture and microstructure.

Scanning electron microscopy was used to study trabecular surfaces. An uncoupling between resorption and formation was evident in older specimens. Two resorption patterns responsible for thinning and perforation and removal trabecular elements were identified. Trabecular microfractures were also investigated.

"That regular decay of nature which is called old age, is attended with changes which are easily detected in the dead body; and one of the principal of these is found in the bones, for they become thin in their shell, spongy in their texture"

| Sir Astley Cooper 1824.

ACKNOWLEDGEMENTS

I have received much support both material and moral, from a great number of people during the course of this study. Professor Alan Boyde deserves special thanks for supervising this work and for spending his valuable time reading my thesis and giving expert advice. I am also grateful to him for securing funds to complete the last year of the study. Professor Sheila Jones helped me in many respects and my special thanks go to her for the continuous encouragement given to me throughout the period I have spent at the Hard Tissue Research Unit.

Thanks are also due to Marios Karseras of University College Hospital and to Dr. Paul Thompson of London Hospital Medical College for providing many of the bone specimens. I also wish to thank Dr. Tim Arnett for providing some materials and support and Dr. Gavin Pearson of University College Dental Hospital for helping with the stiffness testing machine.

Several friends gave me a great deal of help. Ranjith Perera spent hours helping with statistics. Jayantha Pattapola assisted me with parallax measurements and Gamini Rajapaksa with the theory of Fourier transform. I acknowledge and appreciate their support.

I would also like to offer my sincere thanks to my colleagues: Helen Liversidge for her help in preparing radiographs and for various other assistance given throughout this work; and to Pinkoo Bose for translating much valued German references. Special thanks are also due to Ann Ginger for her kindness and for typing some parts of the thesis.

I am grateful to the late Elaine Maconnachie for technical assistance given to me and especially for her skilled help with the scanning electron microscope. Roy Radcliffe also provided technical assistance throughout this work and Maureen Arora helped with the photography. Michaela Kneissel provided some help with illustrations. I wish to acknowledge their assistance.

I also wish to thank the Commonwealth Association in the UK for sponsoring the first two years of this study through an Academic Staff Scholarship.

Finally, I am indebted to my parents for their continuous support and especially for excusing my years of long absence from home. It is to them that this thesis is dedicated.

TABLE OF CONTENTS

	Page
Abstract.....	p2
Acknowledgements.....	p4
Table of contents.....	p5
List of figures.....	p10
List of tables.....	p16
CHAPTER 1 – INTRODUCTION.....	p17
1.1 BONE.....	p17
1.2 TRABECULAR BONE – DEFINITIONS.....	p17
1.3 DISTRIBUTION.....	p17
1.4 HISTORICAL PERSPECTIVE.....	p18
1.5 AGE RELATED BONE LOSS AND OSTEOPOROSIS.....	p21
1.5.1 Osteoporosis – Definition.....	p21
1.5.2 Epidemiology of Osteoporosis.....	p21
1.5.3 Classification of Osteoporosis.....	p22
1.5.4 Loss of bone with age.....	p23
1.6 CURRENT METHODS OF BONE MEASUREMENTS AND THEIR SUITABILITY IN ANALYSING TRABECULAR BONE ARCHITECTURE.....	p24
1.6.1 Non invasive methods.....	p24
1.6.2 Bone Histomorphometry.....	p25
1.7 OBJECTIVES OF PRESENT WORK.....	p28
1.8 ORGANISATION OF THESIS.....	p29
1.9 REFERENCES.....	p30
CHAPTER 2 – THE DEVELOPMENT OF NOVEL, ALTERNATIVE METHODS FOR THREE DIMENSIONAL ANALYSIS OF TRABECULAR BONE ARCHITECTURE.....	p34
2.1 MATERIALS AND SPECIMEN PREPARATION.....	p34
2.2 MICROSCOPY.....	p34
2.3 METHODS AND RESULTS.....	p35
2.3.1 Observations with a binocular microscope.....	p35
2.3.2 Stereopairs in the SEM.....	p35
2.3.3 Stereopairs in the MRC–500 Bio–Rad Lasersharp microscope.....	p35
2.3.4 Studies with a high definition light microscope (Olbrich 4000).....	p36
2.3.5 Studies with a tandem scanning reflected light microscope (TSM).....	p37
2.3.6 Construction of models of trabecular bone.....	p39

2.3.7 Construction of three dimensional integram images using SEM and Laser confocal microscopic images.....	p39
2.3.7.1 Integram from SEM images.....	p40
2.3.7.2 Integrams from laser confocal images.....	p40
2.3.7.3 Results.....	p40
2.3.8 Three dimensional display and analysis of trabecular bone architecture by continuous motion parallax.....	p41
2.3.8.1 Specimen preparation.....	p41
2.3.8.2 Methods.....	p42
2.3.8.3 Results.....	p42
2.3.9 35mm Macro stereophotographs of trabecular bone.....	p44
2.4 DISCUSSION.....	p44
2.5 REFERENCES.....	p45

CHAPTER 3 – TRABECULAR BONE ARCHITECTURE OF THE LUMBAR VERTEBRAL BODY; ITS RELATIONSHIP TO DEVELOPMENT AND VASCULARISATION; AND CHANGES WITH AGING – A STUDY USING MACRO STEREOPHOTOGRAPHS.....	p51
3.1 INTRODUCTION.....	p51
3.1.1 Current concepts of trabecular bone structure and age changes.....	p52
3.1.2 The development of the vertebrae.....	p53
3.1.3 The arterial supply of the adult lumbar vertebral bodies.....	p54
3.1.4 The venous drainage from the lumbar vertebrae.....	p55
3.2 MATERIALS AND METHODS.....	p56
3.3 RESULTS AND DISCUSSION.....	p57
3.3.1 Normal structure.....	p57
3.3.1.1 Mid–sagittal sections.....	p57
3.3.1.2 Coronal sections.....	p58
3.3.1.3 Horizontal sections.....	p58
3.3.2 Vertically oriented trabeculae.....	p59
3.3.3 Horizontally oriented trabeculae.....	p60
3.3.4 Changes in trabecular structure with age and during osteoporosis.....	p62
3.3.5 Microfractures and microcallus.....	p64
3.3.6 Changes in the length of horizontal trabeculae.....	p66
3.3.7 Changes in the number of vertical and horizontal trabeculae with age.....	p67
3.3.8 Biconcavity index.....	p68
3.3.9 Osteoporotic state.....	p68

3.3.10 Implications of changing vascularity of lumbar vertebral bodies with age.....	p71
3.4 CONCLUSION.....	p74
3.5 REFERENCES.....	p75
CHAPTER 4 – THE ANALYSIS OF TRABECULAR BONE IN THE FREQUENCY DOMAIN.....	p102
4.1 INTRODUCTION.....	p102
4.1.1 Image processing in the frequency domain.....	p102
4.1.1.1 Frequency methods.....	p102
4.1.1.2 Fourier transformation of an image.....	p102
4.1.1.3 The discrete Fourier transform.....	p103
4.1.1.4 The fast Fourier transform.....	p103
4.1.2 Applications of the Fourier transform.....	p103
4.1.3 Use of Fourier techniques in biological sciences.....	p104
4.1.4 Applications of Fourier techniques to trabecular patterns in bone.....	p105
4.2 PRELIMINARY, EXPERIMENTAL WORK.....	p106
4.2.1 Analysis of simulated trabecular patterns.....	p106
4.2.1.1 Methods.....	p106
4.2.1.2 Results.....	p106
4.2.2 Preliminary studies with trabecular bone patterns.....	p107
4.2.2.1 Materials and methods.....	p107
4.2.2.2 Image input.....	p108
4.2.2.3 Image analysis.....	p108
4.2.2.4 Results.....	p109
4.3 A STUDY OF CHANGES IN VERTEBRAL TRABECULAR BONE WITH AGE USING FREQUENCY DOMAIN ANALYSIS.....	p110
4.3.1 Method.....	p110
4.3.2 Results.....	p111
4.3.2.1 The comparison of contoured power spectra.....	p111
4.3.2.2 The analysis of changing spatial frequency with age.....	p112
4.3.2.3 The volume density of radiographs and the study of individual groups of trabeculae using templated images.....	p116
4.4.3 Discussion.....	p119
4.4.3.1 Contoured power spectra.....	p119
4.4.3.2 The analysis of changing spatial frequency with age.....	p120
4.4.3.3 The study of trabecular groups using templated images.....	p122

4.5 CONCLUSION – FREQUENCY DOMAIN ANALYSIS.....	p123
4.6 REFERENCES.....	p124

CHAPTER 5 – CHANGES IN QUALITY OF TRABECULAR BONE ON AGING AND IN OSTEOPOROSIS AND THE CONSEQUENCES OF THESE CHANGES ON BONE STRENGTH.....	p143
5.1 INTRODUCTION.....	p143
5.2 METHODS.....	p144
5.2.1 <i>Sample preparation</i>	p144
5.2.2 <i>Measurements of the apparent density</i>	p144
5.2.3 <i>Mechanical testing</i>	p145
5.2.4 <i>Study of trabecular fractures</i>	p145
5.3 RESULTS.....	p145
5.3.1 <i>Mechanical behaviour of trabecular bone</i>	p145
5.3.2 <i>Fracture behaviour of the samples</i>	p147
5.4 DISCUSSION.....	p148
5.5 CONCLUSION.....	p152
5.6 REFERENCES.....	p152

CHAPTER 6 – AN INVESTIGATION OF THE MICROMORPHOLOGY OF HUMAN LUMBAR VERTEBRAL TRABECULAR BONE SURFACES USING SCANNING ELECTRON MICROSCOPE.....	p166
6.1 INTRODUCTION.....	p166
6.2 MATERIALS AND METHODS.....	p167
6.3 RESULTS.....	p167
6.3.1 <i>Identification and distribution of activities</i>	p167
6.3.2 <i>Collagen organisation</i>	p167
6.3.3 <i>Resorption</i>	p168
6.3.4 <i>Mineralising surfaces</i>	p170
6.3.5 <i>Osteocyte lacunae</i>	p171
6.3.6 <i>Microfractures</i>	p171
6.4 DISCUSSION.....	p172
6.5 CONCLUSION.....	p173
6.6 REFERENCES.....	p174

CHAPTER 7 – SUMMARY AND CONCLUSIONS.....	p188
7.1 TRABECULAR BONE.....	p188
7.2 NOVEL METHODS.....	p188
7.3 TRABECULAR BONE ARCHITECTURE OF THE LUMBAR VERTEBRAL BODY.....	p189
7.4 FREQUENCY DOMAIN ANALYSIS.....	p190
7.5 QUALITY OF TRABECULAR BONE.....	p191
7.6 TRABECULAR BONE SURFACE.....	p191
7.7 FINAL REMARKS.....	p192

APPENDIX I – <i>Details of subjects from whom bone used in the study was obtained.....</i>	p193
APPENDIX II – <i>Calculated values for L and R₂ for multiple regression analysis in Chapter 4.....</i>	p195
APPENDIX III – <i>Publications.....</i>	p196

LIST OF FIGURES

CHAPTER 2

Figure	Page
1. A stereopair SEM micrograph of sagittal section of the 2nd lumbar vertebral body from a 42 year old male.....	p46
2. A stereopair synthesised in the MRC-500 Lasersharp confocal microscope (69 year female, mid-sagittal section of the 4th lumbar vertebral body).....	p47
3. A stereopair micrograph from a high definition light microscope (Olbrich 4000) showing callus formation on trabeculae.....	p48
4A. A model for osteoporotic trabecular bone.....	p49
4B. A model for normal trabecular bone.....	p49
5A. A lumbar vertebra showing the positions of three square beams used for the "continuous parallax method".....	p50
5B-5D. Figures showing the methods employed for imaging and displaying continuous motion parallax information.....	p50

CHAPTER 3

Figure

1-10 and 12-20. – All trabecular bone sections in these figures were derived from 4th lumbar vertebrae. The figures are stereopairs with a tilt angle of 10° .

1. A drawing of mid-sagittal section of a 4th lumbar vertebra showing planes where trabecular counts were made.....	p78
2. Three zonal distribution of trabeculae in a mid-sagittal section from a 31 year old male.....	p79
3. Trabecular arrangement in a coronal section of a 30 year old female.....	p80
4. Trabecular arrangement in a horizontal section through middle zone of a 30 year old female.....	p81
5. Trabecular arrangement in a horizontal section through superior zone of a 30 year old female.....	p82
6. A mid-sagittal section showing large canals for blood vessels in the middle zone. 60 year old male.....	p83
7. A mid-sagittal section from a 64 year old male showing a certain degree of thinning and removal of trabeculae.....	p84
8. A coronal section through the anterior-most part of the vertebral body. 30 year old female.....	p85

9. A coronal section through the posterior-most part of the vertebral body. 30 year old female.....	p86
10. Trabecular arrangement in a para-sagittal section. 69 year old male.....	p87
11. The proposed two dimensional models for normal and osteoporotic trabecular bone architecture at mid-sagittal plane.....	p88
12. A mid-sagittal section showing long horizontal trabeculae at the middle zone. 71 year male.....	p89
13. An osteoporotic mid-sagittal section showing complete loss of normal trabecular architectural pattern. 89 year old female.....	p90
14. A mid-sagittal section from an 89 year old male showing maintenance of normal architecture irrespective of thinning of trabeculae.....	p91
15. A mid-sagittal section from an 88 year old female showing typical osteoporotic trabecular bone architecture.....	p92
16. A coronal section through middle of a vertebral body showing trabecular thinning. 88 year old female.....	p93
17. A mid-horizontal section showing thinning of trabeculae at this plane. 88 year old female.....	p94
18. A horizontal section through superior zone showing trabecular thinning, collapse and microcallus. 88 year old female.....	p95
19. A mid-sagittal section from an 89 year old osteoporotic male showing thickened vertical trabeculae at the superior zone.....	p96
20. A segment of a mid-sagittal section showing microcallus on horizontal trabeculae.....	p97
21-23. A graphical comparison of changes in the real lengths of horizontal trabeculae with age at three zones of mid-sagittal sections.....	p98
24. Changes in the number of horizontal trabeculae with age at mid-sagittal plane of the 4th lumbar vertebral body.....	p99
25-27. Changes in the number of vertical trabeculae with age at three zones of mid-sagittal sections of the 4th lumbar vertebral body.....	p100
28. Changes in the biconcavity index of the 4th lumbar vertebral body with age.....	p101

Figure

2-8 and 11-16 – Trabecular bone images in these figures were derived from X-ray images of 3mm mid-sagittal sections of 4th lumbar vertebral bodies.

1. Templated images used for individual analysis of vertically, horizontally and diagonally oriented elements in trabecular bone images.....	p126
2. A trabecular bone image and its contoured power spectrum from a 30 year old female.....	p127
3. A trabecular bone image from a 55 year old female and its contoured power spectrum showing vertical and horizontal arrangements of frequencies.....	p128
4. A trabecular bone image from a 71 year old female and its contoured power spectrum showing an increase in spacing among horizontal elements.....	p129
5. A trabecular bone image from a 74 year old female and its contoured power spectrum showing loss of both vertical and horizontal elements.....	p130
6. A trabecular bone image from an 89 year old osteoporotic female and its contoured power spectrum.....	p131
7. A trabecular bone image from a 50 year old male and its contoured power spectrum showing an increased spacing in 45 ^o direction.....	p132
8. A trabecular bone image from an 89 year osteoporotic female and its smaller (contoured) power spectrum showing the presence of fewer, larger elements in the image.....	p133
9. A graph showing change in spatial frequency with age in the male group studied.....	p134
10. A graph showing change in spatial frequency with age in the female group studied.....	p134
11A-D. Intensity mapped, colour coded, X-ray images of trabecular bone sections from 30 year old female (11A), 31 year old male (11B), 89 year old female (11C) and 89 year old osteoporotic female(11D).....	p137
12. An intensity mapped image from a 30 year old female and its templated images.....	p138
13. An intensity mapped image from a 50 year old male and its templated images.....	p139
14. An intensity mapped image from a 71 year old male and its templated images.....	p140
15. An intensity mapped image from an 89 year old osteoporotic female and its templated images.....	p141

16. An intensity mapped image from a 75 year old female showing a schmorl's node and its templated images.....	p142
--	------

CHAPTER 5

Figure

1. The three line rig used for mechanical testing of trabecular bone.....	p154
2. The load deformation curves for trabecular bone samples from a 35 year old male, 55 year old female and 89 year old female.....	p156
3. Apparent density distribution of the trabecular bone samples used.....	p157
4. A bar chart showing the load required to deform female samples by 1mm after removal of osteoid.....	p158
5. A bar chart showing the load required to deform male samples by 1mm after removal of osteoid.....	p158
6. Graphs showing the relationship between apparent density and the load required for a constant deformation of female samples.....	p159
7. Graphs showing the relationship between apparent density and the load required for a constant deformation of male samples.....	p159
8. Graphs showing the relationship between drop of force and loss of bone in the female group after treatment with hydrogen peroxide.....	p160
9. Graphs showing the relationship between drop of force and loss of bone in the male group after treatment with hydrogen peroxide.....	p160
10. A stereopair of fractured trabecular bone specimen from a 60 year old female.....	p161
11. A stereopair of fractured trabecular bone specimen from a 62 year old male.....	p162
12. A stereopair of fractured trabecular bone specimen from a 74 year old female.....	p163
13. A stereopair of fractured trabecular bone specimen from an 89 year old osteoporotic female.....	p164
14. An SEM micrograph of a fractured plate from a middle third of a vertebral section.....	p165
15. A fracture face of a plate from the specimen in figure 14.....	p165
16. An SEM micrograph showing fracture line of a vertebral section from a 30 year old female.....	p165
17. A fractured rod from a specimen from an 89 year old female.....	p165

18. A long horizontal trabeculae from a specimen from an 89 year old osteoporotic female.....	p165
19. High power view of fracture of the trabeculum in figure 18.....	p165

CHAPTER 6

All figures are SEM micrographs of anorganic mid-sagittal sections of 4th lumbar vertebral bodies.

Figure

1. The surface of a rod-shaped trabeculum.....	p176
2. The arrangement of collagen bundles into domains on a rod surface.....	p176
3. A mineralising and a resorbing surface on a rod shaped trabeculum.....	p176
4. A rod showing resting surface and superficial resorption.....	p176
5. A rod showing forming surface.....	p176
6. A plate shaped trabeculum from middle zone of a mid-sagittal section.....	p176
7. The arrangement of collagen domains around an opening of a plate.....	p177
8. The fracture face of junction between a rod and a plate. Stereopair.....	p177
9. The "snail track" type of resorption bays around an opening of a plate.....	p177
10. Trabecular surface showing formation on a superficially resorbed region.....	p177
11. Several generations of "snail track" type of resorption on a trabeculum.....	p177
12. A "node" showing advancing resorption towards surrounding rods and plates.....	p178
13. Initiation of resorption on a trabeculum.....	p178
14. A trabeculum showing different morphological types of resorption bays.....	p178
15. Deep resorption bays at the junction between a rod and a plate.....	p178
16. A plate showing two disproportionately large mineralising fronts approaching each other from the sides to cover up several generations of resorption bays.....	p178
17. High power view of a mineralising front from figure 16.....	p178

18. A half-formed osteocyte lacuna from the mineralising front shown in figure 17.....	p179
19. A stereopair showing a deep resorption at the centre of a node.....	p179
20. A superficially resorbed plate with beginning of a perforation at the centre.....	p179
21. A high power stereopair of central, deeply resorbed area from the plate in figure 20.....	p180
22. Superficially resorbed surface showing exposed canalicular openings.....	p180
23. Trabecular surface showing a massive mineralising front, superficial resorption and resting surface.....	p180
24. A stereopair showing a deeply grooved trabeculum.....	p180
25. A stereopair of floor of the groove in figure 24.....	p181
26. The appearance of perforations from the floor of a groove.....	p181
27. A stereopair showing a deep pit made presumably by a single osteoclast.....	p181
28. A disconnected rod showing deep resorption bays on the fracture face.....	p181
29. High power view of resorption lacunae from figure 28. Stereopair.....	p182
30. A stereopair showing a grooved and "tunnelled" trabeculum.....	p182
31. A rod showing several "tunnelled" grooves.....	p182
32. A deep groove on a superficially resorbed surface.....	p182
33. A section of a trabeculum through a deep groove.....	p182
34A. A trabeculum completely disconnected by osteoclastic resorption.....	p183
34B. A montage of resorbed trabecular surface showing many morphological types of resorption bays.....	p183
35. The surface of a long, thin, rod-shaped trabeculum from an osteoporotic section.....	p184
36. Junction between a rod and a plate showing irregular arrangement of collagen bundles and initiation of inward resorption.....	p184
37. Irregularly arranged collagen bundles from figure 36.....	p184
38. Rounded resorption from figure 36.....	p184
39. Irregular collagen bundles around microcracks on a rod.....	p184

40. A fractured rod showing shallow resorption on one side.....p184

41. A disconnected rod in which resorption was responsible for most of the disconnection.....p185

42. A tip of a rod which has been severed by complete osteoclastic resorption.....p185

43. A disconnected end of a trabeculum.....p185

44. A disconnected tip of a rod covered by extensive formation of collagen bundles.....p185

45. A stereopair showing tip of a disconnected trabeculum "wrapped" by collagen bundles.....p185

LIST OF TABLES

CHAPTER 3

TABLE I – The increase in vertical trabecular spacing in old and osteoporotic specimens.....p67

CHAPTER 4

TABLE I – The increase in trabecular spacing at different angles and intensities in the male group.....p135

TABLE II – The increase in trabecular spacing at different angles and intensities in the female group.....p136

CHAPTER 5

TABLE I – Density, loss of tissue and stiffness in female L4 sections.....p155

TABLE II – Density, loss of tissue and stiffness in male L4 sections.....p155

CHAPTER 1

INTRODUCTION

1.1 BONE

Bone is a highly vascular, living, constantly changing mineralised connective tissue. It is remarkable for its hardness, resilience and regenerative capacity, as well as its characteristic growth mechanisms. Similar to all other connective tissues, bone consists of cells and an intercellular matrix. The majority of its cells, the osteocytes, lie embedded within the matrix which is composed of organic materials, mainly collagen fibres, and inorganic salts rich in calcium and phosphate which structurally resemble hydroxyapatite crystals.

Vascular canals ramify within bone, providing its cells with nourishment and creating avenues of entry for other cells, including osteoblasts, capable of depositing bone, and osteoclasts which can remove it.

1.2 TRABECULAR BONE – DEFINITIONS

From the macroscopic appearance of cut surfaces, two types of bone can be recognised; one with a dense texture like ivory (*compact bone*) and the other honeycombed by large cavities, the bone being reduced to a lattice work of bars and plates (*trabecular*, *cancellous* or *spongy bone*). All the three terms used for the latter group also reflect merely some aspect of its macroscopic appearance.

The adjective **trabecular** and the (plural) noun **trabeculae** are derived from Latin words *trabecula* or *trabacula* which means a little beam. The word *trabs* in Latin denotes a tree or anything made up of beams or timbers. As these meanings suggest, these words were originally used in architectural rather than in medical literature.

The term **cancellous** has its origin in the Latin word *cancelli* which means a lattice, enclosure, bars or railings. The Latin word *cancellus* denotes the meaning "covered with bars or railings".

The term **spongy** is derived from the Latin words *spongia* or *spongiea* which means a sponge (Adjectives *spongiosus* or *spongeosus* express the meanings spongy or porous). Most of the nineteenth century German scientists had a preference for the German equivalent of this word (*spongiös*) when referring to the second group of bone described above.

With no special reason whatsoever, the term **trabecular bone** will be used in this thesis to refer to this second group of bone while for the first group the more popular term **compact bone** (or **cortical bone** depending on disposition) will be maintained.

1.3 DISTRIBUTION

The distribution and disposition of trabecular bone varies in different bones and in different parts of the same bone. The shafts of the long bones of adults are composed of thick compact bone and present only a few trabeculae on their inner surface while their expanded ends

(metaphyses and epiphyses) consist chiefly of trabecular bone. In short bones such as vertebrae the bone is mainly trabecular with a thin layer of compact bone covering the outer surface shell. In flat bones such as the ribs and the ilium, the interior is uniformly cancellous, compact bone forming the surface. In the skull, the cranial bones mainly consist of two tables of compact bone with an intervening layer of trabecular bone or diploë.

1.4 HISTORICAL PERSPECTIVE

Interest in the study of bone has been intimately related to its mechanical properties. The earliest recorded comments on the mechanical significance of bone were accredited to Galileo (1638) (quoted by Koch, 1917 and Evans, 1957) who pointed to the mechanical implications of bone shape and stated that smaller bones are proportionally stronger than larger ones. However, until the early nineteenth century no significant observations were made regarding the structure of bone and no studies were undertaken to relate the inner architecture of the bone (tissue) to its mechanical properties.

Bourguery (1831) published an anatomy book illustrating the inner structure of the femur, tibia, humerus and many other bones with great accuracy. However, the first real attempt at a mechanical interpretation of the arrangement of trabeculae was made by Ward (1838), an English anatomist, who, in his classic book "**Outlines of Human Osteology**", described the significance of the trabecular arrangement in the upper part of the human femur. Mechanical adaptations of bones were known to many people before this date. For example, Ward (1838) in an analysis of pelvic bones from King's college museum in London for the curvature of the sacrum, states "*The curvature of the sacrum is liable to be changed after birth by pressure. A dealer in bones, who obtains his supplies from a French military hospital, informs me that the skeleton of a horse-soldier may generally be distinguished from that of a foot-soldier, by the more sudden curvature of the sacrum*".

Ward (1838) compared the arrangement of the trabeculae of the proximal end of the femur to a triangular bracket, attaching a street lamp to an upright pole. The oblique (compression) bar of the bracket was compared with the trabeculae extending from the head of the femur to the inferior wall of the neck, while the horizontal (tension) bar of the bracket was considered to be to be analogous to the more horizontally oriented trabeculae in the upper part of the neck.

An American anatomist, Jefferies Wyman, (1849) described the arrangement of the trabeculae in sections of the femur, vertebrae, talus and calcaneum. His interpretation divided the trabeculae into two main groups; "studs" or those bars that resist compression and "braces" those that resist tension. He advanced the study of inner architecture of the proximal femur by analysing and grouping the trabeculae into three groups. A tensile group, a compressive group and a third group of short trabeculae that bind the two preceding groups together. Nevertheless, as pointed out by Koch (1917) his explanation of the position and action of the third group was erroneous. However, in his analysis of lumbar vertebrae, Wyman (1849) accurately described the vertical and horizontal arrangement of the trabeculae in vertical sections. He postulated that the vertical trabeculae resist the compressive forces while the horizontal ones which are placed at right angle to

the vertical ones, serve the purpose of "braces".

Humphry (1858) published observations on the inner architecture of the bone, in which he pointed out that in frontal sections of the femur the trabecular lines are perpendicular to the articular surface of the head and cross each other at right angles. The importance of these observations was not appreciated at the time but later they played an important part in the mathematical analysis of the functional significance of trabecular orientations.

The next major contribution was made by von Meyer (1867) who demonstrated before a meeting of naturalists held at Zurich a collection of preparations of human bones and discussed the significance of the arrangements of the trabeculae in many of the bones. Culmann, a Zurich mathematician and engineer, attended this meeting and became much interested in the structure of the bones. He observed a resemblance between the arrangement of the trabeculae and the calculated lines of maximum internal stress in a mechanical structure of similar form and similarly loaded. Later he calculated the lines of maximum stress (trajectories) in a Fairbairn crane, which he assumed was a homogeneous solid structure approximating the femur in shape. From this analysis Culmann concluded that the bony trabeculae were laid down along the lines of maximum internal stress, thus enabling the femur to transmit a maximum load with a minimum of material.

Von Meyer's article described Culmann's discovery and is the basis for the Trajectorial Theory of bone form. According to this theory the trabeculae follow lines of maximum internal stress (trajectories) in the bone, cross each other at right angles, and arise perpendicularly from the surface of the bone or articular cartilage. Some of these trajectories are considered to be compressive and others tensile resistant.

Wolff (1869) advanced these studies by examining photographs of thin sections of bone. He emphasized the importance of right angle crossing of the trabeculae in the proximal end of the femur and described the tensile and compressive lines according to Culmann's calculations for the Fairbairn crane. Wolff (1892) also criticised Ward's comparison of the proximal end of the femur to a triangular bracket. However, this was inevitable: the correct analogy, the Fairbairn crane, had not yet been invented during Ward's time.

After the publication of von Meyer's paper, large numbers of investigations were carried out on the subject by numerous workers: Wolfermann (1872), Aeby (1873), Bardeleben (1874), Humphry (1888) and Wolff (1891, 1892, 1896, 1899) are some of the writers who contributed immensely to this field. Roux's (1885) interpretation of the functional significance of the arrangement of the trabeculae in an ankylosed knee joint was totally based on the trajectorial theory.

The classic monograph entitled *The Law of Bone Transformation* (Wolff, 1892) developed the theory of the functional form of bone and the transformation of bone in normal and pathological cases, and discussed in detail the structural changes in bone due to changed static conditions. According to this law, every change in the form and function, or in the function alone of a bone, produces changes, in accordance with mathematical laws, in its architecture and external form. Wolff's law, as it has since been known, was based upon the orientation of the trabecular bone in the proximal end of the femur.

From its inception, Wolff's law was criticised on various grounds by many investigators. Ritter (1888) put forward a new theory in which trabeculae were related to parabolic lines that cross each other randomly. Zschokke (1892) argued that the inner architecture of bone is designed to resist only compressive stresses.

Von Meyer, Roux and Wolff all believed that tensile stresses are primarily responsible for bone formation and growth. This view has also been denied by many investigators, among them Janssen (1920) and Carey (1929) who also emphasized the role of muscle action in determining the form and structure of bone. Culmann and von Meyer interpreted femoral architecture entirely from the view of static body weight without any consideration of muscle action. Janssen argued that the jerking force exerted by muscles combined with the gravity was the chief mechanical stimulus for bone formation.

One of the harsh critics of the trajectorial theory of bone structure was Triepel who according to Murray (1936) cited twenty objections to the theory. Janssen (1920) and Carey (1929) were also in agreement with Triepel in rejecting the trajectorial nature of bone structure.

Some of the important objections to the trajectorial theory are as follows:-

- i. The original trajectorial diagram of a Fairbairn crane, which was the basis for the theory, was drawn for a solid composed of homogeneous material which is quite different from a hollow bone consisting of heterogeneous materials.
- ii. A femur is not loaded or subjected to stresses similar to those in a Fairbairn crane.
- iii. The tension trabeculae of the femur only resemble tension trajectories of a crane in frontal section and present an entirely different picture in a section slightly away from the midline.
- iv. The basic nature of stress trajectories does not agree with the orientation of the trabeculae.

It should be mentioned that while considerable evidence has been gathered regarding mechanical adaptation of bones, even at the end of this twentieth century controversy still exists as to the total validity of Wolff's law.

Koch (1917) in a comprehensive study of human femur, first demonstrated quantitatively that bone responds to its mechanical environment.

D'Arcy Thompson (1917) investigated the stress and strains in different bones. He was the first to suggest that strain might be the causative stimulus for functional adaptation. Evans (1957) described extensively the results of experimental studies on stress and strains in many human bones.

Early tissue culture work of Glucksmann (1938) and Lanyon and Smith's (1969) pioneering experiments measuring bone strains in living animals strengthened the idea of strain as the causative factor. An hypothesis that strain-related electrical potentials mediate the adaptive response originated from the work of Fukada and Yasuda (1957) and Becker and Murray (1967).

Frost (1964) introduced the Flexural Neutralization Theory of bone remodelling which was the first mathematical formulation of bone remodelling as a function of mechanical variables.

1.5 AGE RELATED BONE LOSS AND OSTEOPOROSIS

Astley Cooper (1824) stated that in old age bones "*become thin in their shell, and spongy in their texture*", he also noted that fractures of the neck of the femur often followed moderate trauma. Hip fractures were recognised as a complication in old age even during nineteenth century. Hyde (1875) provided an analysis of 322 cases of fractures of the femur from an American hospital. However, bone loss as a syndrome was first recognised by Pommer in 1885. It was Albright and his colleagues (1941) who linked osteoporosis with the postmenopausal state and the credit for its introduction as a disorder of clinical interest goes to Albright and Reifenstein (1948).

1.5.1 Osteoporosis – Definition

The terminology associated with osteoporosis was originally developed to distinguish diseases of bone, notably osteomalacia, osteoporosis and osteitis fibrosa cystica. However, when bone began to be studied radiologically, confusion arose as osteoporosis was not readily distinguished from osteomalacia. The classical definition of osteoporosis in 1948 by Albright and Reifenstein "*Too little bone, but what bone there is, is normal*" rectified this situation to some extent because it differentiated osteoporosis from osteomalacia. This definition of osteoporosis is, however, impractical as it is based on histo-pathology for a condition that has to be identified clinically or radiologically. For any specific age and sex, there is a wide and continuously distributed range of bone mass and, therefore, it is not possible to define the norm for the amount of bone tissue by which we can identify loss of bone. Generally, the bone mass expected at skeletal maturity is taken as for this value.

At present, the term "**osteopenia**" is used to refer to a reduction in the amount of bone per unit volume relative to that expected for the age and sex of the subject and the term "**osteoporosis**" has been reserved for the clinical syndrome which occurs as a complication of osteopenia and includes the most common fractures which involve the hip, vertebrae, radius and humerus (Gallagher, 1990). Consequently, many elderly people have osteopenia, but never develop a clinical fracture.

1.5.2 Epidemiology of Osteoporosis

Osteoporosis is an enormous public health problem in the western world. Its associated fractures are especially common among elderly white women. This high incidence among women is not only related to an increased life expectancy which has led to a growing elderly population and to the link between osteoporosis and postmenopausal state, but to the fact that more women survive to the age at which osteoporotic fractures occur than men. In the United States alone osteoporosis is responsible for at least 1.2 million fractures each year (Riggs and Melton, 1986).

The main age related fractures associated with osteoporosis are fractures of the distal forearm (Colles' fracture), vertebrae and femur. These fractures could occur in anyone subjected to sufficient force, but they are considered as being osteoporotic when they occur in the elderly or as a result of trauma that is no more severe than falling from a standing height (Cummings et al. 1985).

Colles' fractures are the most common fractures among women until the age of 70, when

their frequency is surpassed by fractures of the hip. At the time of menopause (approximately age 45–50) there is a rapid increase in the number of fractures of the wrist but there is no significant increase among men of the same age (Office of Health Economics, 1990). Vertebral fractures become more frequent after the age of 50 – particularly among women – and by age 70, over 35% of white women will have sustained at least one such fracture (Kleerekoper and Avioli, 1990). The incidence of vertebral fractures has been estimated as seven times more in women than men. However, current statistics of these fractures cannot be considered as accurate because 35% of vertebral fractures are "silent" or left undetected.

The prevalence and incidence of hip fractures increase rapidly after the age of 70, and women are affected two times more often than men. Kleerekoper and Avioli (1990) estimated that up to 33% of women and more than 17% of men experience a femoral fracture by age 90 years. Using current age and sex specific incidence rates for England and Wales the probability of women suffering a fractured femur before the age of 85 is 12% compared with only 5% for men (Royal College of Physicians, 1989). Fractures of the hip are associated with more deaths, disability, and medical costs than all other osteoporotic fractures combined. Thus, the scale of the problem is huge and in 1985, over 35,000 people in England and Wales (Purdie, 1988) and about 250,000 in the USA (Consensus Development Conference, 1987) fractured a femur.

In UK the estimated cost of osteoporosis and osteoporotic fractures to the Department of Health is in the region of 500 million pounds annually (Stevenson et al. 1989) and in USA in 1983 around 6.1 billion dollars (Holbrook et al. 1984).

1.5.3 Classification of Osteoporosis.

Usually, osteoporosis is classified into two types; primary and secondary osteoporosis. Secondary osteoporosis can often be attributed to a known single cause, either a disease or a drug, and can occur in both sexes and in children as well as adults.

Albright (1947) originally described two forms of primary osteoporosis; postmenopausal and senile. He evidently implicated the role of oestrogen deficiency in postmenopausal osteoporosis. Riggs and Melton (1983) reclassified the primary osteoporosis into two types. **Type I** (postmenopausal) osteoporosis is presumably caused by the reduction in oestrogen which occurs in women around the time of menopause, affects primarily trabecular bone, and results in vertebral and colles' fractures. **Type II** (senile osteoporosis) is said to occur in the very elderly as a result of impaired bone formation and increased bone resorption associated with reduced calcium absorption. It affects both cortical and trabecular bone and leads to fractures of the hip and humerus.

Another small group, Type IA, has also been described (Riggs et al. 1978). This group presents clinically as Type I, but behaves biochemically as Type II. Secondary osteoporosis has also been classified as Type III osteoporosis by some authors (Gallagher, 1990).

1.5.4 Loss of bone with age

Loss of bone is usually expressed as the loss in amount of bone or bone mass. The often used term "bone density" has its origin mainly in different X-ray densitometric techniques that are frequently employed for bone mass measurements.

Bone mass increases rapidly in childhood and adolescent years, reaching a peak in the third decade of life (Exton-Smith et al. 1969, Garn 1970). Loss of bone may begin as early as the third decade of life and occurs in both sexes and in all races studied so far (Mazess 1982, Newton-John and Morgan 1970, Cohn et al. 1977, Yano et al. 1984). It has also been shown that bone loss starts at different periods of life throughout the skeleton and occurs at different rates. In the femoral neck and Ward's triangle of the proximal femur, there is a 30% decrease in bone mineral density during the premenopausal period (Riggs et al. 1981, Gallagher et al. 1989). However, no significant loss of bone prior to the menopause has been observed in the spine (Mazess et al. 1987, Ribot et al. 1988) and in the trochanteric region of the proximal femur (Mazess et al. 1987, Gallagher et al. 1989). The radius show an increase in density up to the fourth decade and no significant loss before the menopause (Johnston et al. 1985).

The proportions of cortical and trabecular bone varies in these regions, except in the radial mid shaft region which consist almost entirely of cortical bone. The influence of the menopause should be uniform throughout the skeleton, but, it has been shown that the largest decrease in bone occurs in the central part of the vertebrae which is predominantly trabecular bone (Cann et al. 1980). The rate of loss in the central region of the vertebrae has been estimated at 10% per year for the first two years after the menopause. By contrast, the rate of cortical bone loss in the radius averages 2–3% per year (Johnston et al. 1985). It has been suggested that these differences between cortical and trabecular bone loss reflect the fact that trabecular bone has a larger surface area for resorption (Gallagher 1990).

The rate of bone turnover is determined mainly by the frequency of activation of new bone remodelling units. In normal young adults, the resorption and formation phases are tightly coupled and bone mass is maintained. An uncoupling of the phases of bone remodelling, with a relative or absolute increase in resorption over formation results in a net bone loss.

For both cortical and trabecular bone, a biphasic pattern of bone loss has been identified. There is a prolonged slow phase that occurs in both sexes and a transient accelerated phase that occurs in women after the menopause (Riggs and Melton 1986). These two phases are associated with two different abnormalities of bone remodelling (Parfitt 1979, Parfitt et al. 1983). The slow, age-dependent phase results mainly from impaired bone formation; osteoclasts cause resorption cavities of normal depth, or even decreased depth (Eriksen et al. 1985) but osteoblasts fail to refill them completely. The accelerated phase of bone loss occurs in women soon after the menopause and is associated with a high rate of bone turnover; there are more osteoclasts and each creates a deeper resorption cavity (Parfitt 1979, Eriksen et al. 1985). An increase in bone accretion, but an even greater increase in bone resorption has been reported during this phase (Parfitt 1979, Heaney et al. 1978).

1.6 CURRENT METHODS OF BONE MEASUREMENTS AND THEIR SUITABILITY IN ANALYSING TRABECULAR BONE STRUCTURE.

1.6.1 Non invasive methods

Conventional radiography is the most readily available and most frequently used method of studying bone in clinical practice. It provides some information about the quality, quantity and structure of bone. The occurrence of fractures and collapsed vertebrae can easily be detected by radiography and some assessment can be made regarding trabecular patterns and cortical thickness. However, it is currently agreed that bone loss does not become radiologically perceptible until it exceeds 30% (Cohen and Martin 1990). Further, the appearance of different features on radiographs depends too much on technical conditions for them to be used reliably as indicators of the degree of bone loss. Moreover, simple radiographs can not be quantified; nevertheless, several indices have been introduced for this purpose, including the following :-

Singh's index – The neck of the femur is made up of different trabeculae arranged in several systems. These trabeculae tend to disappear with advancing age, and this loss of trabecular bone can be graded according to a six-point index (Singh et al. 1970). This method requires subjective judgments which are susceptible to inter observer variability and is therefore poorly reproducible.

Metacarpal cortico-medullary index – This is a measure of cortical thickness in long bones. From radiographs of the hand, the width and areas of the cortex of metacarpals can be measured. The index can be expressed either as a function of the cortical thickness or by using the ratio of the cortical surface area to the total metacarpal surface area. The main limitation of the approach is that bone mass is measured at a predominantly cortical site and this may not be representative of sites of greater clinical interest, such as vertebral body trabecular bone. The reproducibility of the technique is also poor.

With the advancement of technology new techniques have been developed for clinical use, which enable "bone density" to be more accurately measured. Some of more popular such techniques are as follows :-

Single photon absorptiometry (SPA) – SPA is used to study cortical bone in the appendicular skeleton by measuring the bone density of the forearm. Measurements are usually made at the middle of the radius, which contains over 90% cortical bone, and near the distal end of the radius, which contains about 25–75% trabecular bone. The reproducibility of the measurement varies from 1 to 3%, depending on the method employed. However, the measurements are made on the wrist and not on clinically relevant sites. The correlation between density in the lumbar spine and the radius is too low for vertebral density to be predicted accurately for individual patients (Riggs and Melton 1986). Moreover, because of the monochromatic character of the radiation, the absorption attributable to the soft tissues in the total attenuation of the radiation cannot be known.

Dual photon absorptiometry (DPA) – DPA can be used to measure bone density directly at clinically relevant sites such as spine and hip, where it provides reasonably accurate measurements of both cortical and trabecular bone mineral content. A reproducibility of about 2.3% can be obtained by this method. The use of dual energy character radiation enables the coefficient of attenuation to be corrected for the part accounted for by soft tissue absorption. However, it is sensitive to the effects of dystrophic calcification and of vertebral compression in the scanning area. Recently, a newly developed instrument utilises an X-ray generator instead of the DPA radionuclide source. This method is called dual-energy X-ray absorptiometry (DEXA). The DEXA method permits more precise measurement of body composition than DPA with much faster determinations.

Computerised tomography (CT scanning) – CT scanning allows the measurement of the density of either the entire bone or just the trabecular portion of bone. Thus, it can be employed to measure the trabecular bone in the centre of the vertebral body exclusively. However, reproducibility of the technique is less good (3–5%) and accuracy is poor (12–30%), depending on the quantity of fat in the bone marrow. Further, exposure to radiation is relatively high compared with any of the other techniques.

Neutron activation analysis – This method allows an estimation of total body calcium content and is thus a measure of total bone mass. It can also be used to determine local bone mass. However, its reproducibility is not so good as the measurement of total bone mass. This technique is more useful for assessing the skeletal response to experimental therapies.

There are also other less well used techniques for bone mass measurements. **Compton scattering** is another technique that measures bone mineral content. It also allows separate measurements of cortical and trabecular bone mineral content. **Radioisotope scanning** provides a functional assessment of bone and is more useful in differential diagnosis of osteoporosis rather than in its assessment. Skeletal **uptake of diphosphonate** can be quantitated and can be used to measure increased bone turnover. This method is mostly used in differential diagnosis and as a research technique.

All these clinical techniques measure amount of bone and do not consider its structure or spatial arrangement. Therefore, it would not be possible to employ any of these techniques to analyse the structure of trabecular bone.

1.6.2 Bone Histomorphometry

Histological analysis of a bone biopsy is the most widely employed technique in studying the bone tissue changes. Much of our present knowledge of physiology of bone and bone disease has been gained from such biopsy techniques, especially after the introduction of in vivo labelling of bone with the antibiotic tetracycline. Earlier bone histological studies used rib biopsies, because of the easy availability of comparable rib autopsy samples. However, the ilium is presently the most popular site because it offers several advantages over the rib. There is less patient discomfort,

no body cavity is threatened, it is less dangerous, and a trained surgeon is not required. It is also believed that the ilium behaves more like the vertebrae where metabolic bone disease is prominently expressed (Recker 1983).

Histomorphometrical techniques used for bone biopsies are generally direct extensions of the techniques used for other tissues of the body. Thin sections from the biopsy, when looked at through a microscope, give a two-dimensional image. This image consists of profiles which are the projections of structures in three dimensions on to a plane. Measurements of these profiles are usually accomplished by randomly superimposing on the image a set of lines and a set of points to form a stereological grid or graticule. This may be accommodated in the eyepiece of a conventional microscope. Alternatively, the microscopic image can be projected on to a large scale grid on a flat surface. For the analysis of sections in the SEM, an electronically generated grid can be superimposed on the visual display (Boyde et al. 1974). The data derived from such techniques are known as primary data. Two-dimensional quantities such as area and perimeter can be calculated from the primary data. This is the province of quantitative microscopy, whereas the extrapolation of these two-dimensional quantities to three-dimensional quantities such as volume and surface area is the province of stereology (Parfitt 1983). According to Weibel (1979) *stereology is a body of mathematical methods relating three-dimensional parameters defining the structure to two-dimensional measurements obtainable on sections of the structure*. Many mathematical formulae have been derived for different stereological parameters and have been applied in the field of bone histomorphometry for both cortical and trabecular bone (Recker 1983).

Frost (1983) described applications of histomorphometrical techniques to trabecular bone dynamics. His analysis consisted of three levels:– primary data, first order derived quantities, and second order derived quantities. The primary data consist of the actual grid and cell counts and simple measurements of lengths performed at the microscope. The first order derived quantities are computed directly from the primary data and the second order derived quantities are computed from the first order quantities and generally relate more clearly to the kinetic features of bone physiology.

The nomenclature, symbols and units used in bone histomorphometry may be confusing, since several names and symbols are in use for the same measured quantity. It has been reported that for some measurements as many as nine different terms were in use (Parfitt et al. 1987). Recognition of this difficulty led the American Society of Bone and Mineral Research (ASBMR) to convene a committee to develop a unified system of terminology. Their report (Parfitt et al. 1987) recommended a more acceptable system for bone histomorphometry, but arbitrary terminology can still be encountered in the literature.

In analysing a complex three-dimensional tissue such as trabecular bone, the techniques described so far are barely sufficient. Trabecular bone is usually considered as made up of bars or plates of bone connected to each other in space in different ways and in different directions. The structure could vary from thin needles like trabeculae to thick tubes having holes at various intervals. Qualities such as *spatial distribution*, *connectivity*, and *shape*, cannot be described accurately using these techniques. During the past decade, an awareness of these special problems

related to trabecular bone has impelled many investigators to develop new techniques for analysis of trabecular bone especially using computer image analysis techniques.

Garrahan et al. (1986) introduced a technique in which an image of trabecular bone from an iliac crest biopsy was processed by a computer to produce a skeletonised image. By describing different "strut types" and "nodes", these authors derived several indices to analyse microanatomic structure of trabecular bone. Age-related structural changes in iliac crest trabecular bone have been studied using this method (Compston et al. 1987). However, the two-dimensional images were derived from thin histological sections and the struts and nodes described, do not therefore necessarily represent the real struts and nodes found in three-dimensional trabecular bone. An image analysis technique has also been described by Merolli et al. (1990) for trabecular bone morphometry and to determine mean trabecular orientation in small areas of histological sections.

Another development in bone structural analysis is the introduction of a new stereological parameter called the "star volume" (Vesterby et al. 1989). The star volume can provide an unbiased estimate of the mean size of the marrow space in three-dimensions and can therefore be used to describe structural changes in trabecular bone. A significant age-related increase in marrow space star volume in both lumbar vertebra and iliac crest has been shown (Vesterby et al. 1989, Vesterby 1990).

Feldkamp et al. (1989) described a technique based on high-resolution computed tomography to study three-dimensional bone structure directly in vitro. They were able to determine all structural indices commonly determined from two-dimensional histologic sections non-destructively and also to determine a measure of three-dimensional connectivity in human cancellous bone.

A mathematical model for vertebral trabecular bone architecture has also been presented by Jensen et al. (1990) based on studies of samples taken from the central parts of the vertebral bodies. The model was a three-dimensional lattice with a unit cell geometry that is typical for the trabecular lattice of the vertebral body underneath the end plates. By introducing a measure for the randomness of lattice joint positions, they demonstrated that the apparent stiffness varies by a factor of between 5 and 10 from a perfect cubic lattice to a network of maximal irregularity, even though trabecular bone volume remains almost constant.

It is a common observation that the structure of trabecular bone differs from site to site and even within the same site of the skeleton. In the centre of the vertebral body for example, plate-like trabeculae dominate while towards the periphery the structure is more rod- or needle-like. Most of the existing techniques sample small amount of tissues from one region and generalise the results to the rest of the bone. Such procedures therefore do not provide accurate results regarding the structure of trabecular bone. On aging, the shape of the trabeculae also changes (mainly to a structure dominated by rods) and the connectivity is also altered by perforation and removal of entire trabecular elements. None of the present techniques can describe such changes completely or measure them quantitatively.

Techniques for the description of gross biological shapes and patterns have been developed in other areas of biological sciences such as physical anthropology. They have mainly been applied

in characterising and comparing the external shapes of bones such as the cranium and pelvis. Many of these methods have been borrowed from areas other than biology and many involve attempts to isolate individual features in shapes and patterns, such as edges, corners, nodes, tangents, vectors, inflection points and central axes, as well as curve-fitted images and skeletal transforms. Some techniques have also been devised to assess directly the form or pattern of a picture or an object. Some of these depend on studying contours of objects and many involve application of Moiré fringe analysis (Takasaki 1970). Such methods produce field views of overall shape that do not depend upon defining precise points upon an object. They have been very useful in analysing complicated three dimensional surfaces such as the surfaces of teeth (Chmielewski and Varner 1969).

Other techniques assess shapes by comparing the difference between two field views of shapes. The best known of these is the D'Arcy Thompson's (1917) method of transformations. Trend surface analysis is another technique borrowed from geology and applied to characterise hominid skulls (Sneath 1967). Bio-orthogonal grids developed in other fields have been applied to primate crania (Bookstein 1978).

Fourier and other related frequency domain transformations have also been employed to study biological shapes and patterns. Most of such studies have been aimed at characterising external shape by treating the curve of the shape as a one-dimensional wave to be transformed into its simple harmonic functions. Examples for such uses include studies of the outline of the face (Lu 1965) and of the growth of the cranial vault (Lestrel and Brown 1976).

It is apparent that these methods cannot be used directly to study microscopic patterns and shapes such as that of trabecular bone and there have not been many attempts to do so. However, Oxnard (1972, 1973) used Fourier transform methods to analyse trabecular bone patterns of human lumbar vertebral bodies. Not only he was able to describe different trabecular patterns using power spectra of bone images, but he was able to reveal hidden structures from radiographs by the use of spatial filtering techniques. This is therefore, a useful approach to explore in developing methods for structural analysis of trabecular bone.

1.7 OBJECTIVES OF PRESENT WORK.

Several important conclusions can be deduced from the above review. Firstly, the structure of the trabecular bone cannot be described accurately using the existing techniques. Secondly, the story of trabecular bone loss on aging and during osteoporosis will never be complete unless the changes in its connectivity, shape and spatial distribution are also told. Two-dimensional techniques or reconstruction of the third dimension from such techniques offer no or little support in understanding such properties completely.

In studying the structure of three-dimensional trabecular bone therefore, none other than a non-destructive technique that would view and analyse the whole structure three-dimensionally could be of any help. Hence, the first objective of this work was to experiment on developing three-dimensional techniques using trabecular bone derived from clinically important sites such as lumbar vertebral bodies, iliac crest and proximal end of the femur.

In reviewing research on trabecular bone structure, it was observed that many investigators have over-emphasised the role played by mechanical factors in its architectural design, but have paid no or little attention to other factors that may influence bone in vivo. Two such factors, the development and vascularisation, play important roles in the original design of the architecture in an individual bone, and vascular changes on aging could also influence the changes in architecture, quite apart from mechanical factors. The part played by such factors have been discussed during this work and age changes in trabecular bone have been analysed taking into consideration both the development and vascularisation.

The analysis of bone using Fourier techniques can provide information regarding trabecular spacing. Spatial filtering involving Fourier analysis allows the study of individual trabecular groups as a function of orientation. Therefore, even though this is a two-dimensional technique, structural information can be obtained using images such as radiographs, without having to involve cumbersome histological techniques. Fourier techniques for the analysis of trabecular bone using state of the art image analysis techniques have been used during this study to analyse structural changes of trabecular bone with age.

The occurrence of osteomalacia in the elderly and in patients with osteoporosis has been reported by many investigators. However, prior studies have considered only the quantitative rather than qualitative aspects of age related bone loss. Another objective of this work was to investigate the mineralisation of trabecular bone and to observe changes of its quality on aging and during osteoporosis.

The examination of surfaces of bone by scanning electron microscopy (SEM) reveals substantial information regarding both microstructure and the activity status of surfaces. An enormous amount of knowledge has been gathered by examining endosteal surfaces of bone by SEM. Nevertheless, little work has been carried out on trabecular surfaces. Further, the occurrence of microfractures are a common phenomenon seen in aged trabecular bone, but these have not been investigated adequately. Therefore, an SEM study of trabecular surfaces was also be carried out on normal, old and osteoporotic bone.

1.8 ORGANISATION OF THE THESIS.

After this first introductory Chapter, Chapter 2 describes different experimental work carried out to develop three-dimensional methods to analyse trabecular bone. Two new techniques, the construction of "pseudo-holograms" or "integrations" and "continuous motion parallax method" are presented in this Chapter.

Chapters 3, 4, 5 and 6, even though they share common objectives, should be considered as separate pieces of work having their own introductions, materials and methods, results, discussions and conclusions.

Chapter 3 presents a detailed analysis of the trabecular bone structure of 4th lumbar vertebral bodies and related age changes using macro stereophotographs generated by tilting a specimen stage under a 35mm camera. Models for the trabecular bone architecture of both normal and old vertebral bodies are proposed and quantitative results have been presented where possible.

Cohen J, Martin J-L (1990) Menopause and Osteoporosis. Bone Diseases. Coissac P, Ed. Sandoz
Ltd. CH-4002 Basle, Switzerland.

The development and vascularisation of lumbar vertebral bodies are discussed in relation to their adult structure. The literature on changes in vascularisation with age is reviewed and the possible consequences of age changes on trabecular bone structure are discussed.

Chapter 4 describes the Fourier transform, its previous applications in both non-biological and biological fields and different experimental work carried out to find possible applications of these techniques to analyse trabecular bone. At the end of the chapter three examples are presented where Fourier analysis has been applied to study age changes in trabecular bone in lumbar vertebral bodies.

Chapter 5 presents a study of change in quality of trabecular bone on aging and in osteoporosis. The stiffness of trabecular bone was tested before and after removal of osteoid tissue, in order to observe the changes in bone strength after removal of un-mineralised bone in different age groups. The fracture patterns of trabeculae have also been studied using stereophotographs and scanning electron micrographs.

Chapter 6 presents an SEM study of trabecular bone surfaces from lumbar vertebral bodies of normal, old and osteoporotic subjects. The changes in different surface activities with age and their relationships to structural changes of trabecular bone and possible mechanisms for the occurrence of microfractures have also been discussed.

Chapter 7 summarises and discusses the findings and makes suggestions for future work.

Appendix I presents details of subjects from whom bone used in this study was obtained.

1.9 REFERENCES

- Aeby (1873) Zur Architectur der Spongiosa. *Centralblatt für die medizin. Wissenschaft.* **50**:786.
- Albright F, Reifenstein EC (1948) The parathyroid glands and metabolic bone disease. Williams and Wilkins, Baltimore.
- Albright F, Smith PH, Richardson AM (1941) Postmenopausal osteoporosis: Its clinical features. *JAMA* **116**:2465-2474.
- Bardeleben (1874) Beiträge zur Anatomie der Wirbelsäule. Jena.
- Becker RO, Murray DG (1967) A method for producing cellular dedifferentiation by means of very small electrical currents. *Trans New York Acad Sc* **29**:606-615.
- Bookstein FL (1978) The measurement of biological shape and shape change. Springer-Verlag, New York.
- Bourguery (1831) *Traité complet de l'anatomie de l'homme.* Paris.
- Boyde A, Howell PGT, Jones SJ (1974) Measurement of lacunar volume in bone using a stereological grid counting method evolved for the scanning electron microscope. *J Micros* **101**:261.
- Cann CE, Genant HK, Ettinger B, Gordon GS (1980) Spinal mineral loss in oophorectomized women. *J Am Med Assoc* **244**:2056-2059.
- Carey EJ (1929) Studies in the dynamics of histogenesis. Experimental, surgical and roentgenographic studies in the architecture of human cancellous bone, the resultant of back pressure vectors of muscle action. *Radiology* **13**:127-168.
- Chmielewski N, Varner JR (1969) An application of holographic contouring in dentistry. *Biomed Sci Instrum* **6**:72-79.
- Cohn SH, Abesamis C, Yasumura S (1977) Comparative skeletal mass and radial bone mineral content in black and white women. *Metabolism* **26**:171-178.
- Compston JE, Mellish RWE, Garrahan NJ (1987) Age-related changes in iliac crest trabecular microanatomic bone structure in man. *Bone* **8**:289-292.
- Consensus Development Conference (1987) Prophylaxis and treatment of osteoporosis. *Br Med J* **295**:914-915.

- Cooper A (1824) A treatise on dislocations, and on fractures of the joints. 4th Ed. Longman, Hurst, Rees, Orme, Brown and Green. London.
- Cummings SR, Kelsey JL, Nevitt C, O'Dowd KJ (1985) Epidemiology of osteoporosis and osteoporotic fractures. *Epidemiologic Rev.* 7:178–208.
- Eriksen EF, Mosekilde L, Melsen F (1985) Trabecular bone resorption depth decreases with age: differences between normal males and females. *Bone* 6:141–146.
- Exton-Smith AN, Millard PH, Payne PR (1969) Pattern of development and loss of bone with age. *Lancet* 2:1154–1157.
- Evans FG (1957) *Stress and Strains in Bones: Their relation to fractures and osteogenesis.* Charles C Thomas, USA.
- Feldkamp LA, Goldstein SA, Parfitt AM, Jesion G, Kleerekoper M (1989) The direct examination of three dimensional bone architecture in vitro by computed tomography. *Bone* 4(1):3–11.
- Frost HM (1964) *The laws of bone structure.* Charles C Thomas, Springfield.
- Frost HM (1983) Bone histomorphometry: Analysis of trabecular bone dynamics. In: *Bone histomorphometry: Techniques and interpretation.* Recker RR eds. CRC press, Boca Raton, Florida. 109–131.
- Fukada E, Yasuda I (1957) On the piezoelectric effect of bone. *J Phys Soc Japan* 10:1158–1169.
- Gallagher JC (1990) The pathogenesis of osteoporosis. *Bone Mineral* 9:215–227.
- Gallagher JC, Hedlund LR (1989) The effect of age and menopause on bone mineral density of the proximal femur. *J Bone Mineral Res* 4:639–642.
- Garn SM (1970) *The earlier gain and later loss of cortical bone.* Springfield, Charles C Thomas.
- Garrahan NJ, Mellish RWE, Compston JE (1986) A new method for the two-dimensional analysis of bone structure in human iliac crest biopsy. *J Microsc* 142(III):341–349.
- Glucksmann A (1938) *Studies on bone mechanics in vitro. I. Influence of pressure on orientation of structure.* *Anat Rec* 72:97–113.
- Heaney RP, Recker RR, Saville PD (1978) Menopausal changes in bone remodelling. *J Lab Clin Med* 92:964–970.
- Holbrook TL, Grazier K, Kelsey JL, Stauffer RN (1984) The frequency of occurrence, impact and cost of selected musculoskeletal conditions in the united states. *American Academy of Orthopaedic Surgeons, Chicago.*
- Humphry GM (1858) *A Treatise of the Human Skeleton.* Cambridge.
- Humphry GM (1888) On the angle of the thigh bone with the shaft at various angles, etc. *Lancet.*
- Hyde FE (1875) Analysis of 322 cases of fracture of the femur, Bellevue Hospital. *New York Med. Record* 10:513–519.
- Janssen M (1920) *On Bone Formation: Its relation to Tension and Pressure.* 1–114, Longmans, London.
- Jensen KS, Mosekilde L, Mosekilde LE (1990) A model of vertebral trabecular bone architecture and its mechanical properties. *Bone* 11:417–423.
- Johnston CC Jr, Hui S, Witt RM, Appledorn R, Baker RS, Longcope C (1985) Early menopausal changes in bone mass and sex steroids. *J Clin Endocrinol Metab* 61(v):905–911.
- Kleerekoper M, Avioli LV (1990) Evaluation and treatment of postmenopausal osteoporosis. In: *Primer on the metabolic bone diseases and disorders of mineral metabolism,* Favus MJ eds. American Society for Bone and Mineral Research, California. pp 151–154.
- Koch JC (1917) The laws of bone architecture. *Am J Anat.* 21(II):177–298.
- Lanyon LE, Smith RN (1969) Measurement of bone strain in the walking animal. *Res Vet Sci,* 10:93–94.
- Lestrel PE, Brown HD (1976) Fourier analysis of adolescent growth of the cranial vault: a longitudinal study. *Hum Biol* 48:517–528.
- Lu KH (1965) Harmonic analysis of the human face. *Biometrics* 21:491–505.
- Mazess RB (1982) On aging bone loss. *Clin Orthop* 165:239–252.
- Mazess RB, Barden SH, Ettinger M, Johnston C, Dawson-Hughes B, Baran C, Powell M, Notelowitz M (1987) Spine and femur density using dual-photon absorptiometry in US white women. *Bone Mineral* 2:211–219.
- Merolli A, Tranquilli Leali P, Gabbi C (1990) Una metodica per lo studio della struttura tridimensionale dell'osso trabecolare. *Biomateriali* 1/2:29–35.
- Murray PDF (1936) *Bones. A Study of the Development and Structure of the Vertebrate Skeleton.* 96–135 Cambridge Univ. Press.

- Newton-John HF, Morgan DB (1970) The loss of bone with age, osteoporosis, and fractures. *Clin Orthop* **71**:229-252.
- Office of Health Economics (1990) Osteoporosis and the risk of fracture. Office of Health Economics, Whitehall London.
- Oxnard CE (1972) The use of optical data analysis in functional morphology: investigation of vertebral trabecular patterns. In: *Functional and evolutionary biology of primates: methods of study and recent advances*. Tuttle RH eds. Chicago, Aldine. 337-347.
- Oxnard CE (1973) Form and pattern in human evolution: some mathematical, physical, and engineering approaches. The University of Chicago press, Chicago and London.
- Parfitt AM (1979) Quantum concept of bone remodelling and turnover: implications for the pathogenesis of osteoporosis. *Calcif Tissue Int* **28**:1-5.
- Parfitt AM (1983) Stereological basis of bone histomorphometry; Theory of quantitative microscopy and reconstruction of the third dimension. In: *Bone histomorphometry: Techniques and interpretation*. Recker RR eds. CRC press, Boca Raton, Florida. 53-87.
- Parfitt AM, Mathews CHE, Villaneuva AR, Kleerekoper M, Frame B, Rao DS (1983) Relationship between surface, volume and thickness of iliac trabecular bone in aging and osteoporosis. *J Clin Invest* **72**:1396-1409.
- Parfitt AM (1987) Bone histomorphometry: Standardization of nomenclature, symbols, and units. *J Bone Min Res* **2**(VD):595-610.
- Pommer G (1885) Untersuchungen über Osteomalacie und Rachitis, nebst Beiträgen zur Kenntniss der Knochenresorption und -apposition in verschiedenen Altersperioden und der durchbohrenden Gefässe. Vogel Leipzig.
- Purdie DW (1988) Broken bones, a gynaecological problem. *Br J Obstet Gynaecol.* **95**:737-739.
- Recker RR (1983) *Bone histomorphometry: Techniques and interpretation*. CRC press, Boca Raton, Florida.
- Ribot C, Tremollieres F, Pouilles JM, Louvet JP, Guiraud R (1988) Influence of the menopause and aging on spinal density in French women. *Bone Mineral* **5**:89-97.
- Riggs BL, Melton LJ (1983) Evidence for two distinct syndromes of involuntional osteoporosis. *Am J Med* **75**:899-901.
- Riggs L, Melton LJ (1986) Involuntional osteoporosis. *New Eng J Med*, **314**:1676-1686.
- Riggs L, Wahner HW, Dunn WL, Mazess RB, Offord KP, Melton LJ III (1981) Differential changes in bone mineral density of the appendicular and axial skeleton with aging: relationship to spinal osteoporosis. *J Clin Invest* **67**:328-335.
- Ritter (1888) *Anwendungen der graphischen Statik nach Culmann*. 128.
- Roux W (1885) Beiträge zur Morphologie der funktionellen Anpassung. 3. Beschreibung und Erläuterung einer knöchernen Kniegelenksankylose. *Arch Anat Physiol, Anat Abt.* **9**:120-158.
- Royal College of Physicians (1989) Fractured neck of femur, prevention and management. Royal College of Physicians of London.
- Sneath PHA (1967) Trend-surface analysis of transformation grids. *J Zool Lond* **151**:65-122.
- Stevenson JC, Lees B, Cust MP, Ganger KF, Hillard T (1989) The pathogenesis of postmenopausal osteoporosis. *Excerpta Medica*.
- Takasaki H (1970) Moiré topography. *Appl Optics* **9**:1457-1472.
- Thompson D'arcy W (1917) *On growth and form*. Cambridge.
- Vesterby A (1990) Star volume of marrow space and trabeculae in iliac crest: Sampling procedure and correlation to star volume of first lumbar vertebra. *Bone* **11**:149-155.
- Vesterby A, Gundersen HJG, Melsen F (1989) Star volume of marrow space and trabeculae of the first lumbar vertebra: Sampling efficiency and biological variation. *Bone* **10**:7-13.
- von Meyer H. (1867) Die Architectur der Spongiosa. *Reichert und Dubois- Reymond's Archiv.* 615.
- Ward FO (1838) *Outlines of Human Osteology*. London.
- Weibel ER (1979) *Stereological methods. Volume I Practical methods for biological morphometry*. Academic Press, London.
- Wolfermann (1872) Beitrag zur Kenntniss der Architectur der Knochen. *Reichert und Dubois-Reymond's Archiv.* 312.
- Wolff J. (1869) Ueber die Bedeutung der Architectur der spongiösen Substanz. *Centralbl f die med Wissensch.* **54**:849-851.
- Wolff J. (1891) Ueber die Theorie des Knochenschwundes durch vermehrten Druck und der Knochenanbildung durch Druckentlastung. *Archiv f klin Chirurgie.* **42**:302.
- Wolff J. (1892) *Das Gesetz der Transformation der Knochen*. Quarto. Berlin.

- Wolff J. (1896) Die Lehre von der funktionellen Pathogenese der Deformitäten. Archiv f kin Chirurgie. **53**:831.
- Wolff J. (1899) Die Lehre von der funktionellen Knochengestalt. Virchow's Archive **155**:256–315.
- Wyman J (1849) On the cancellated structure of the bones of the human .pabody. Boston J Nat His **6**125–140.
- Yano K, Wasnich RD, Vogel JM et al. (1984) Bone mineral measurements among middle-aged and elderly japanese residents in Hawaii. Am J Epidemiol **119**:751–764.
- Zschokke E. (1892) Weitere Untersuchungen ueber das Verhältniss der Knochenbildung zur Statik und Mechanik des Vertebratenskelettes. Quarto, Zurich.

CHAPTER 2

THE DEVELOPMENT OF NOVEL, ALTERNATIVE METHODS FOR THREE DIMENSIONAL ANALYSIS OF TRABECULAR BONE ARCHITECTURE.

2.1 MATERIALS AND SPECIMEN PREPARATION

Trabecular bone specimens for the study were derived from three sites; the iliac crest, femoral head and neck and the lumbar spine. The iliac crest was selected as it is the most popular site from the relevant literature and because it may be biopsied, while the upper part of the femur and the lumbar spine are important fracture sites.

Femoral heads, lumbar spine and part of the ilium (including anterior superior iliac spine) were removed at autopsy from eight subjects (3 males and 5 females) aged 30–95 years and were stored in of 70% ethanol. Two of the females were osteoporotics; one had Paget's disease of bone. Various sample preparation and staining methods were employed and these will be discussed under appropriate headings. However, for the preparation of cleaned and dry trabecular bone, the following procedure was used.

A slow speed diamond saw (Buehler Isomet 11–1180) was used for sectioning. From iliac bone samples, plane parallel sections of various thickness were cut below and behind the anterior superior iliac spine and similar sagittal and horizontal sections were also cut from 2nd, 3rd, 4th and 5th lumbar vertebral bodies. Vertical and horizontal sections were also cut from both femoral heads and necks. These samples were treated at 37^o with a (maximally) 3% solution of hydrogen peroxide (1:10 dilution of 30% stock concentrate) for 24 hours to remove marrow, soft tissues and unmineralised bone matrix. At the end of the treatment, samples were washed carefully with a jet of water, extracted with a 50:50 solution of chloroform and methanol and were air dried.

2.2 MICROSCOPY

The following microscopes were employed during this study.

- i) Vickers binocular microscope with magnifications of 10x and 30x.
- ii) Hitachi S–530 scanning electron microscope (Hitachi Limited, Tokyo, Japan).
- iii) Cambridge Stereoscan S4–10 scanning electron microscope (Cambridge Scientific Instruments Limited, England).
- iv) MRC–500 Bio–Rad Lasersharp confocal laser scanning microscope (BIO–RAD Microscience division, Watford, England).
- v) Olbrich 4000 high definition light microscope (Bayross International, Tokyo, Japan).
- vi) Tandem scanning reflected light (confocal, direct view) microscope (Tracor Northern, Inc. Middleton, Wisconsin).

2.3 METHODS AND RESULTS

2.3.1 *Observations with a binocular microscope*

The simplest method to view the 3-D architecture of trabecular bone is to examine the specimens under a binocular microscope: all the samples were first studied at magnifications of 10x and 30x. The lower magnification (10x) generated excellent views of three dimensional arrangement of different groups of trabeculae in all the sections. Since it was possible to handle specimens while looking through the microscope, trabecular architecture could be viewed at many different angles and the spatial distribution of trabeculae could readily be studied. However, it was not possible to examine the whole specimen in one view with many samples (especially vertebral and femoral head sections) and at higher magnification, (30x) the shallower depth of field limited a proper three dimensional view. Attempt were also made to produce stereopairs of bone images by tilting the samples under the microscope and recording photomicrographs at various angles. These proved to be unsatisfactory because of the limited depth of field.

2.3.2 *Stereopairs in the SEM*

In three dimensional analysis, the most popular method is the use of stereopair micrographs produced in the SEM (Boyde 1968, Howell and Boyde, 1984). This method was employed using a Hitachi S-530 SEM.

Dried specimens were mounted on a specimen stage using carbon conductive cement (Agar Aids, Essex, England) and coated with gold by sputtering in a sputter coater (Polaron Equipment Ltd., Watford, England). They were then examined using the secondary electron mode in the SEM operated at 2kV. With the lowest magnification possible in the SEM, stereopair micrographs were recorded with a tilt angle difference of 8°.

Figure 1 is a stereopair micrograph of trabecular bone from a mid-sagittal section of 2nd lumbar vertebral body. The trabecular architecture seen in this micrograph is typical of that usually found underneath the end plates. Approximately 2 to 3 layers of vertical trabeculae are clearly visible in this micrograph. Three dimensional structure of such limited areas of bone can reasonably be studied using similar stereopairs.

However, for a proper understanding of connectivity and spatial distribution, many more stereopairs at different angles should be studied and many more layers of trabeculae than can be seen by SEM should be examined. Furthermore, even with the lowest magnification possible in the SEM, enormous numbers of stereopairs should be produced to study one whole vertebral section. All these disadvantages makes SEM stereopairs impracticable for an efficient, cost-effective analysis.

2.3.3 *Stereopairs in the MRC-500 Bio-Rad Lasersharpe microscope*

The MRC-500 is a laser beam scanning confocal microscope. Confocal microscopy makes it possible to obtain a series of images of the sample at different focal levels without the need for mechanical sectioning. The MRC-500 has a motorised stage control for fine focus and this allows

all focussing functions to be controlled from the computer. The software has an extensive command capability for programming the system to acquire a series of images automatically and to store them in computer memory for subsequent display and analysis. The image on the monitor can be zoomed up several times.

Cleaned, defatted, dry trabecular bone specimens were mounted with the microscope focused on the topmost layer of the sample. Using the motorised stage, 25 confocal images were collected at 150 micron intervals and stored in the computer memory. Kalman averaging of 20 frames was used during the collection of each image. Anaglyph (red-green) stereo images were synthesised on the display monitor. Figure 2 shows a stereopair synthesised in this way mounted to view through a hand held stereo viewer. To obtain the lowest magnification with a reasonable resolution, a Planapo 2X objective lens was used when acquiring images for this stereopair.

When this stereopair was compared with that of SEM, the only advantage discovered was that a greater depth of tissue can be sampled in the laser confocal microscope. Since the optical sections are always in focus, the limiting useful depth is determined by the porosity of the sample. However, the total area that could be scanned was limited (by the magnification of the objective, by the limited use of the available field of view by the Laserssharp system and by the fundamental requirement that confocality is proportional to magnification), and all the disadvantages described for SEM stereopairs also apply to laser confocal stereopairs. Added to all these disadvantages there was also an intense reflection present at the centre of the image. Another problem concerns the fact that light reflected from deep optical sections is blocked by superficial trabecular layers. When the microscope is focussed deep into the bone, the amount of light reflected is continuously reduced until at a certain depth no further light was reflected. This depth differed from sample to sample, depending on porosity. In other words, it is a measure of porosity of these samples. This technique could therefore be developed as an index of porosity of trabecular bone in different conditions and at different age groups.

To demonstrate this possibility, two vertebral body trabecular bone samples derived from 30 year and 89 year old normal females were analysed. The maximum depth at which an image could be obtained was measured all over each section and the average value was calculated. In the 30 year old female, the average depth was 2.1mm while in the 89 year old female it was 6.0mm. This means that the vertebral body of this particular 89 year old female was approximately three times more porous than that of the 30 year old. An objective lens with a long working distance would be necessary for this kind of study especially when analysing extremely porous osteoporotic bone.

2.3.4. Studies with a high definition light microscope (Olbrich 4000)

The Olbrich 4000 has many advantages over conventional light microscopes. Its unique control of illumination and wide range of optical systems gives a great flexibility. The specimens can be viewed either with transmitted or incident light or both simultaneously. A fibre optic system provides a great flexibility in illuminating areas of interest in incident light. Most importantly, the

microscope provides the observer with a control over depth of field by means of an additional iris behind the objective.

To produce stereopairs using this microscope, a sample was mounted on a tilting stage. Photomicrographs were recorded using a Planapo-2x objective lens and the stereopairs were examined under a folding-mirror stereoscope (SB 180, Hilger and Watts, England).

One of the main problems in studying trabecular bone was that a large volume of tissue should be sampled in order to understand its three dimensional architecture. This microscope also allowed the study of an increased depth of tissue. However, only a limited area could be sampled and it therefore was not very practicable in analysing whole bone sections.

Some modifications were made to this microscope to permit its efficient use in low magnification - large depth of field - epifluorescence to study fluorescently-labelled samples. It was then possible to use it to study unmineralised bone collagen matrix (osteoid) on large, thick bone sections (hitherto, such studies were only carried out on thin histological sections). The following procedure was used in preparing samples for a pilot study.

4mm thick sagittal sections were cut from several normal and osteoporotic 4th lumbar vertebral bodies using the diamond saw. These samples were stored at 50°C with a 5% solution of an enzyme detergent (TERG-A-ZYME) for 24 hours to remove marrow and soft tissues. They were then washed with a jet of water and immersed in a solution of brilliant sulphaflavine to stain unmineralised bone matrix. Samples were then defatted and dehydrated with a 50:50 solution of chloroform and methanol and embedded in polymethyl-methacrylate (PMMA). Polished samples were mounted on the tilting stage as before and illuminated with ultra violet (UV) light using fibre optic leads. Stereopair micrographs were recorded at several tilt angle differences and at different magnifications with and without a yellow pass filter.

Osteoid patches could be identified clearly on trabecular surfaces and their three dimensional distribution could readily be studied. It is therefore possible to use this new technique to study the spatial distribution of osteoid in trabecular bone. Furthermore, new bone formation usually occurs in spinal crush fracture patients and the three dimensional structure of this callus can also be studied using this technique. A stereopair of callus formation on trabeculae after a crush fracture in a osteoporotic patient is shown in the Figure 3.

2.3.5 Studies with a tandem scanning reflected light microscope

(TSM)

The TSM is a real time, direct view confocal microscope. In the TSM, the image can be observed directly while moving the focal plane up and down through the sample. It is also possible to generate stereopairs in the TSM using extended focus images. Further, if it is possible to make light reflected from deep trabecular layers pass through superficial layers, much more information regarding the three dimensional arrangement of trabeculae could be obtained.

As a first step, hydrogen peroxide-digested, dry trabecular bone samples were viewed with different objective lenses. Light reflected from trabecular surfaces was insufficient to form a high contrast image with many lenses, while light reflected from deeper layers did not pass through

superficial layers with all the lenses tested. A Swift 3x (NA 0.12) lens brought about the best results, but the magnification of the image was too high for a proper analysis. A reasonably good and a low magnification image was produced by a Plan 2.5x lens (Reichert, Austria) and this lens was therefore, used during rest of the experiments.

Several preparative experiments were carried out to increase the amount of light reflected from trabecular surfaces.

Firstly, trabecular bone samples were digested with an enzyme detergent (TERG-A-ZYME) instead of hydrogen peroxide, thus leaving unmineralised bone collagen intact. When examined, these samples reflected more light than the hydrogen peroxide-treated samples, but the image was still far from satisfactory.

Secondly, to increase reflection, approximately 1cm^3 cubes of trabecular bone samples were painted with a dental varnish and air dried. These samples produced good reflective surfaces, but the light scattering effect of the varnish disturbed the image.

The TSM also permits examination of fluorescently-labelled samples. To experiment with this facility, several techniques were employed to prepare samples stained with fluorescent dyes.

i. Rhodamine was mixed with dental light-curing resin and dry trabecular bone cubes were coated with this mixture. These cubes were then embedded in hexa-ethyl methacrylate (HEMA) by painting and drying with a jet of air. They were then mounted on slides and examined under the TSM.

ii.a. Trabecular bone cubes cleaned with the enzyme detergent were immersed in a solution of brilliant sulphaflavine (100mg/100ml water) for 15 seconds and washed thoroughly with distilled water. Several similar cubes were decalcified in a solution of diluted hydrochloric acid and stained as above.

ii.b. Several of these samples were examined in water under the TSM, and some were air dried before the examination. Some of the samples were extracted from a solution of 50:50 chloroform and methanol and embedded in poly-methyl methacrylate (PMMA). A few of the embedded cubes with undecalcified trabecular bone were immersed in a solution of concentrated hydrochloric acid for a few hours to dissolve away bone, so that only the spaces previously occupied by trabecular bone were left behind in the cube. These cubes were immersed in glycerine and examined in the TSM.

iii. The procedure described in (ii)a and (ii)b was also repeated with the fluorescent dye fluorescein.

Appropriate filters were used to excite and to view the fluorescence of the dyes. Of the techniques tested, brilliant sulphaflavine-stained, PMMA-embedded samples provided the best results. However, none of these techniques allowed enough light reflected from deeper layers to pass through the superficial layers. This major problem remained unsolved. Further, at the very low magnification employed, the TSM was also not sufficiently confocal to produce good quality images.

2.3.6 Construction of models of trabecular bone

To study microscopic three dimensional structures such as trabecular bone, one of the best methods would be to make a macroscopic model representing a reasonable volume of tissue. Two trabecular bone samples from the upper part of the femur (one severely osteoporotic with almost rod like trabeculae and the other normal with thick plates and tubes) were used. Low power stereopair micrographs of these samples were generated in the SEM (Cambridge Stereoscan S4-10) with tilt angle difference of 10° . These micrographs were then enlarged to $20 \times 25 \text{cm}^2$ and examined using the Stereosketch (SB.115, Hilger and Watts Ltd. England: Boyde, 1966). Boyde (1966) described how to use this instrument to make a model by making a modelling material conform to the 3D image.

In a preliminary effort, pipe cleaners were used to make trabecular bone models. In the case of osteoporotic bone (Figure 4A), this task was not difficult as one rod could easily be represented by one or a part of one brush. However, with normal bone having thick plates and tubes it was not possible to use this as a modelling material and a "mental skeletonisation" had to be carried out. (Figure 4B).

The normal and osteoporotic models were different from each other, emphasising that osteoporosis is not a simple process of thinning of thick trabecular plates and tubes. In the normal model, trabecular elements were curved and actually represent walls of the tubes oriented in the long axis of the model. By contrast, the osteoporotic model had more or less straight and long elements. The model also presented a more open structure indicating increased porosity of the bone. The number of trabecular elements joining to form nodes (their meeting points) were also counted in both models. It was found that in the osteoporotic model most of the nodes were formed by the union of three elements, while in the normal model both three and four elements more or less equally contributed to form nodes.

The above findings suggest that the osteoporotic changes of trabecular bone are more complicated than could be explained by a simple thinning and a removal process. Further, more realistic models than those attempted here would be necessary for a proper understanding of the trabecular bone structure.

2.3.7 Construction of three dimensional integram images using

SEM and Laser confocal microscopic images

It was noted earlier that low power stereopair SEM images were of limited value in understanding trabecular bone architecture, and one reason for this was that foreground trabecular layers obscure back ground connections. A method that would produce large series of views with small tilt angle differences over a large range would greatly enhance the visualisation of the complex architecture of trabecular bone. The production of "pseudo-holograms" or "integram images" is one such means of generating three dimensional images of trabecular bone.

2.3.7.1 Integrations from SEM images

5mm thick, sagittal sections of 2nd to 5th lumbar vertebral bodies from several normal, osteoporotic and pagetic autopsy samples were used for this study. The technique of specimen preparation for the SEM has been described earlier.

The specimens were photographed in a Cambridge S4-10 SEM operated at 10kV for secondary electron (SE) imaging and at 10kV or 20 kV for backscattered electron (BSE) imaging. For the latter, a solid state four sector annular detector was used with the beam at mean normal incidence to the cut surface. Both the summed signal from all four sectors or the sum of the three sectors minus the fourth sector which gives directional topographic shading, was used during imaging. The basis of the procedure was to produce a large series (minimum 18 and maximum 36) of very well-registered images of the same point on the sample as seen from the chosen number of projections which were separated by small tilt angle differences. A precision eucentric goniometer stage was used in which the tilt angle difference could be read reliably to 0.1° and the series was recorded with symmetrical tilts about normal beam incidence, always progressing in the same direction.

To determine the optimum number of images for a series, several series were recorded, varying the number of images. Increments of tilt angle difference from 0.1° (maximum 3.6°) to 1.0° (maximum 22°) were tried to ascertain the best value increment. The images were presented as single uncut strips to the processing laboratory.

2.3.7.2 Integrations from laser confocal images

Hydrogen peroxide-digested, 5mm thick, dry sagittal sections from normal and osteoporotic lumbar vertebral bodies were used for the study. A sample was mounted on the axis of a shaft of a stepper motor which rotates in 1.8° increments. This setup was placed on the motor driven focussing stage of the MRC-500 Lasersharp confocal microscope and the laser beam was focussed on to the topmost layer of the sample. A 4mm deep, extended focus image was recorded using a Planapo 2x objective lens and a Kalman filter. After storing this image in the computer memory, the sample was rotated by one increment (1.8°) and another image was recorded. This process was continued until 22 images were stored in the computer. These images were then normalised and photographed in the same order and the uncut film was delivered to the processing laboratory.

During the production of integrations, the individual images of the series are printed through the lenticular screen so that they lie in vertical strips in register behind vertical prisms. When the screen is viewed from different directions, different members of the sequence were seen and this brings about a hologram type of visual effect.

2.3.7.3 Results

These integrations permitted a greater comprehension of trabecular bone architecture than can be obtained from a single stereopair.

In the SEM case, it was determined that the most satisfactory conditions were to use either

the secondary electron emission mode images from the centre of a large mass of bone (so that the remainder of the specimen blocks forward scattering to the Everhart Thornley detector) or backscattered electron images from a four sector detector with one sector switched to negative. A total tilt angle difference of 24° in increments up to one degree (to a total of 36 steps) produced the best results. This compares with the angle of view reproduced in the lenticular screen. When viewing integrams, the sequence jumps back again every 24° , causing the image to "flash". The integrams produced from laser confocal images were spoilt by the central reflection which further disturbed a proper comprehension of trabecular bone architecture.

The production of integrams is costly which will limit their use in research. The cost also prevented reproduction of integrams in this thesis.

2.3.8 Three dimensional display and analysis of trabecular bone architecture by continuous motion parallax

In techniques described so far, attempts were made to describe trabecular bone architecture by methods that involve the use of stereoscopic parallax. It was observed that for a proper comprehension of the three dimensional arrangement of trabecular bone, a large volume of bone should be viewed through a wide range of projections. The use of stereoscopic parallax methods for such a task is time consuming and cumbersome.

A method that allows the full 360° range of projections would secure the best results regarding the three dimensional structure and connectedness of trabecular bone. In developing a non-stereoscopic parallax method for this purpose, it was found that by rotating a large volume of bone under a microscope and displaying the resultant motion parallax information on a television monitor, a powerful three dimensional impression could be generated (Boyde et al. 1989). The success of such a method depends on the depth of focus of the microscope under which the sample was rotated. Conventional light microscopes do not satisfy this requirement due to their shallow depth of focus. The high definition light microscope described earlier (Olbrich 4000) has a greater depth of field and is therefore a suitable instrument for this purpose. By experimenting with trabecular bone samples, it was discovered that without much difficulty a thickness of 4mm of bone can be viewed in focus under this microscope.

2.3.8.1 Specimen preparation

Lumbar vertebral bodies removed at autopsy from two young patients (30 year, female and 35 year, male), two elderly patients (91 year, female and 74 year male) and two clinically confirmed osteoporotic patients (89 year, female and 89 year male) were used. An ideal sample for the study would be a 4mm diameter cylindrical rod extending from one end of a vertebral body to the other. It was attempted to prepare such a sample using a bone biopsy trephine. However, this was not successful as it was difficult to achieve an undisrupted trabecular architecture especially in osteoporotic samples. A compromise sample in the form of a 4mm square beam was chosen: it was not difficult to cut such beams using a diamond saw.

As a first step, 4mm thick, plane parallel, mid sagittal and mid transverse sections were cut

from different lumbar vertebral bodies from each patient. Subsequently, from some of the sagittal sections 4mm square beams were cut extending from one end plate to the other (these will be called **vertical beams**), and from the rest of the sagittal sections similar square beams were cut extending from the anterior to the posterior surface of the vertebral body (these will be called **antero-posterior beams or AP beams**). From the transverse sections beams were cut as above, but extending from one lateral wall of the vertebral body to the other (these will be called **horizontal beams**; Figure 5A).

These trabecular bone beams were treated with 2% hydrogen peroxide for 24 hours. Afterwards, the marrow was carefully washed away with a jet of water and the samples were extracted with 50:50 chloroform:methanol and air dried.

Some samples (cleaned using an enzyme detergent) were also prepared for fluorescence imaging. For this purpose, 4mm diameter cylindrical rods were prepared from brilliant sulphaflavine stained, PMMA embedded, sagittal vertebral sections.

2.3.8.2 Methods

To secure the 360⁰ range of projections necessary to capture all possible views from one rotation, one end of the beam was mounted on the axis of a slowly rotating shaft, which also moved continuously along its long axis (Figure 5B). This setup was fixed on the stage of the light microscope (Olbrich 4000) and the sample was illuminated using fibre optic leads (Figure 5C). Using an objective lens with 1.5x magnification the microscope was focussed on to the free end of the sample and the depth of focus was adjusted so that whole thickness of the sample was in focus. The sample was trans-illuminated with coloured light so that amount of light passing through the sample could be readily seen in contrast against the white light reflected from the sample. The image from the microscope was displayed via a high resolution television camera and a monitor and the optimum velocity for both rotation and long axis movement was established. The images were recorded at this constant velocity for playback analysis (Figure 5D).

For fluorescence imaging, the setup was similar to the above; however, the 2.3mm diameter cylindrical rod, PMMA-embedded (brilliant sulphaflavine stained) were machined and run inside a PMMA block, lubricated with glycerine. These samples were illuminated with ultra violet (UV) light using fibre optic leads to facets machined on the housing block.

2.3.8.3 Results

Displaying motion parallax information on a television monitor created a powerful three-dimensional impression of trabecular bone structure which proved to be best of all the techniques tested so far. Since the bone architecture could be observed from 360⁰ projections of instant sample volumes, the three-dimensional information obtained from this method was also more all-embracing than any other technique.

When displayed on the TV monitor an image width represented the thickness of the square beam. The vertical square beams were examined from one end plate to the other. Generally, trabecular bone structure has been described as consisting of plates and rods oriented in vertical

and horizontal directions. Some normal samples were dominated by plate like structures to the point that it was difficult to identify direction. However, the normal structure observed in the majority of the samples could be described as follows.

The end plate was composed of thick cortical bone. It was connected below into a second set of horizontally oriented plates by short, vertical rod-shaped trabeculae. Below this second set of plates, a broad, dominant rod-shaped trabecular zone could be seen. Here, vertical and horizontal orientations of rods could readily be identified. At the centre of the vertebral body the structure was almost plate like with several vertical trabeculae from the previous zone connecting to one plate. In fact, the structure in this region resembled vertical tubes having oval holes in them. These tubes were connected to each other by vertically oriented plates. Occasional rod-shaped horizontal trabeculae were also seen in this region. From here onward, the structure described above reversed up to the next end plate. Further, all four sides of these vertical square beams appear identical, indicating a similarity in trabecular arrangement in sagittal and coronal planes.

When old and osteoporotic vertical beams were examined, the first striking feature was the reduced amount of bone so that they were much more transparent to the transilluminating light. The end plates were very thin and were deformed to different degrees in osteoporotic samples. Overall, rod-shaped elements dominated in these samples and their orientations were very clear compared with the normal samples. The second set of horizontal plates seen in most young normal samples were absent in the majority of old and in almost all of osteoporotic samples. The number of both vertical and horizontal trabeculae was also less than that of normal samples, indicating that not only thinning but the removal of whole elements had taken place during aging.

The structure of AP square beams was different from that of vertical beams. Firstly, the four sides of the AP beams were not identical as in the vertical beams. The two sagittal faces of the beams consisted of horizontally cut vertical trabecular elements connected by horizontal plates or rods, whilst the two transverse faces appeared as transversely cut tubes. In normal beams, the anterior region was dominated by plate-like structures whereas the posterior region was almost rod-shaped. Other than thinning and loss of trabecular elements, the structural arrangement of old and osteoporotic AP beams did not appear to differ much from normal samples.

When horizontal beams were examined, it was discovered that they were not very different from AP beams. The four faces of the beams were more or less similar to AP beams, but, a complex trabecular structure was seen towards the lateral walls of the vertebral body. This was especially prominent in normal samples.

In many osteoporotic samples, microfractures, microcallus and new bone formation after trabecular collapse were observed. The size, shape and distribution of these lesions were readily perceptible as they could be studied in all possible projections.

The above description was based mainly on the structure of central beams from each section. However laterally, different degrees of variations were observed in different beams. Further, even though the terms vertical and horizontal were used in accordance with general acceptance, the real three-dimensional arrangement and connections of different trabecular elements is much more complicated than can be described by such terms.

In the fluorescently labelled samples, the embedding medium (polymethyl methacrylate) cleared and made the trabeculae transparent so that elements in the background could be viewed through elements in the foreground. Furthermore, it was possible to identify unmineralised areas of bone from the strong yellow green fluorescence, and the spatial distribution of these areas on trabeculae could readily be studied.

2.3.9 35mm Macro Stereophotographs of trabecular bone

For the best realisation of three dimensional structure, the whole trabecular bone specimen should be studied in one (focussed) view. However, the magnification given by lens systems described as "microscopes" make this task impossible. One possible way out of this problem would be to do away with "microscopy" and to produce stereopairs using "macro-photography".

An Olympus OM2 35mm camera with a 80mm macro lens was used for photography. Trabecular bone samples were mounted on a stage that can be tilted at a measurable angle. The camera was fixed and adjusted so that the whole specimen could be seen through the view finder. Using a very small aperture (F22) to ensure a large depth of field, stereophotographs were recorded by tilting the samples. For stereo viewing, the photographs were enlarged and examined under a Hilger and Watts SB 180 mirror stereoscope.

This experiment showed not only that the whole specimen could be examined three dimensionally in one view, but that the total thickness of the sample was also in focus. A tilt angle difference of 10° provided the best parallax for stereo viewing (example figures for this work can be found in Chapter 3).

2.4 DISCUSSION

For an accurate and efficient study of the 3-D architecture of trabecular bone, several conditions have to be satisfied. A large volume of bone should be sampled through as many projections as possible. To understand the three-dimensional arrangement within the site from which the samples were derived, it is important to study whole specimens in one view. None of the techniques described above were able to satisfy all these conditions.

SEM stereopairs provide only a limited understanding of the trabecular bone architecture. Larger depths could be sampled with the confocal microscopes, but the stereopairs did not satisfy other requirements. The integrations produced from SEM images would be useful in educating both the profession and the public about the structural changes in trabecular bone during aging and osteoporosis. Nevertheless, they are unsatisfactory as a research tool.

The "motion parallax method" provided the best technique for analysing a reasonable volume of tissue through a large number of projections and is useful in both education and research. However, it was not possible to view for example, a whole vertebral section by this method to understand the global three dimensional arrangement of trabeculae within the vertebral body. Furthermore, sample preparation, microscopy, filming and playback analysis were very time consuming.

The technique of producing 35mm macro stereophotographs provided the best method for

studying reasonably thick whole specimens in one view. However, the limitations of stereoscopic parallax prevented a proper three dimensional assessment of individual elements. Nevertheless, this is the simplest and easiest technique and would therefore be useful in analysing a large number of whole bone specimens such as vertebral sections. To clarify observations made while examining stereophotographs produced this way, it is always possible to examine original samples under a binocular microscope. Perhaps, this method could be considered as an improvement to binocular microscopy.

Two other interesting observations were also made during this experimental work. Confocal microscopes provide an easy means for measuring the porosity of trabecular bone and the high definition light microscope (Olbrich 4000) could be used to study the three-dimensional distribution of unmineralised bone matrix in trabecular bone.

2.5 REFERENCES

- Boyde A (1966) Photogrammetric studies of electron micrographs of replicas of the surface of developing dental enamel. *Advances in Fluorine Research and Dental Caries Prevention*. **4**:137-145.
- Boyde A (1968) Height measurements from stereopair scanning electron micrographs. *Beitrage zur Elektronenmikroskopische Direktabbildung von Oberflächen*. **1**:97-105.
- Boyde A, Radcliffe R, Watson TF, Jayasinghe JAP (1989) Continuous motion parallax in the display and analysis of trabecular bone structure. *Bone*, **11**:228 (1990).
- Howell PGT, Boyde A (1984) Three-dimensional analysis of surfaces. In: *Analysis of organic and biological surfaces*. Echlin P, eds. John Wiley and Sons, New York. 325-349.

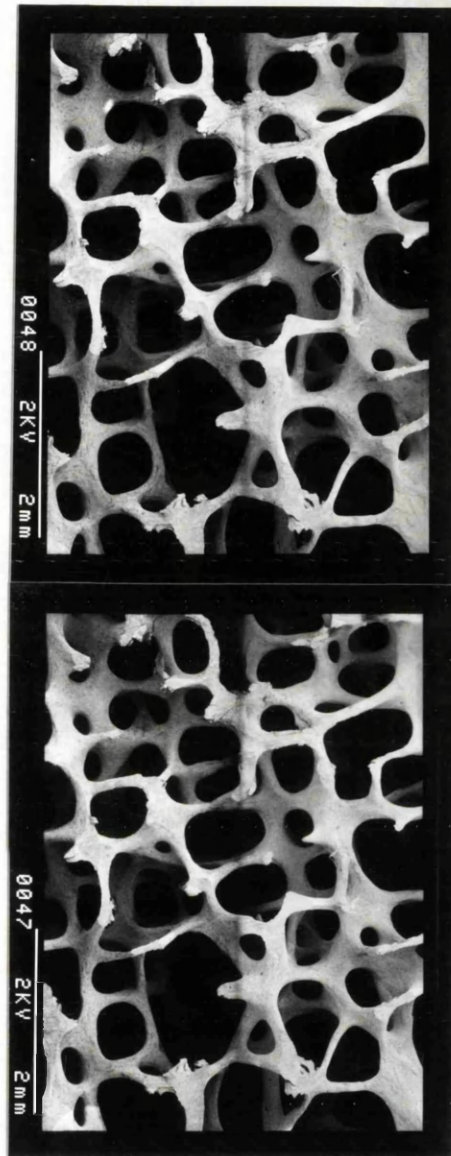


Fig. 1 A stereopair SEM micrograph (Hitachi S-530 SEM: tilt angle 8°) of a sagittal section of the 2nd lumbar vertebral body from a 42 year old man. Several layers of vertical trabeculae are visible in 3D. However, with this lowest magnification possible, only a maximum area of 22.4mm^2 was scanned and this makes analysis of a larger volume of bone impracticable.

Fig. 2 A stereopair synthesised in the MRC-500 Laserssharp confocal microscope (69 year female, mid-sagittal section of the 4th lumbar vertebral body). A greater depth of tissue can be sampled with this microscope depending on the porosity of the bone, but, as in the case with SEM, the total area scanned was limited and the available field for analysis was further reduced by the Laserssharp system.

TR0B2L Maximum projection projection of I to
25 (1), Shift -1.0 Thu May 10 15:50:28 1990 Zoom 1
TR0B2 12/12

TR0B2R Maximum projection projection of I to
25 (1), Shift 1.0 Thu May 10 15:50:28 1990 Zoom 1
TR0B2 12/12



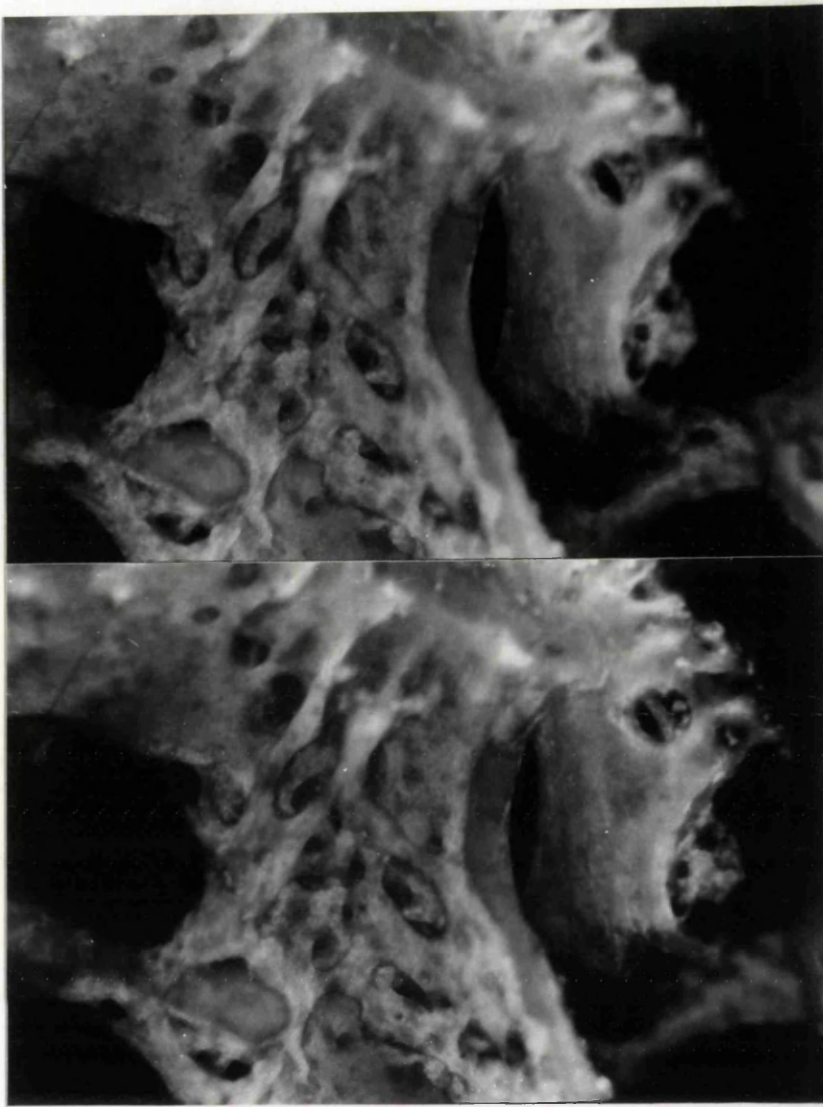


Fig. 3 A stereopair showing callus formation on trabeculae of the 4th lumbar vertebral body from a 80 year old osteoporotic man who had suffered from crush fractures of the spine. PMMA-embedded, brilliant sulphaflavine-stained samples were illuminated with UV light and viewed through a yellow pass filter in a high-definition light microscope (Olbrich 4000). The high depth of field that can be achieved in this microscope facilitates the analysis of unmineralised bone matrix in thick sections. Fieldwidth 550 μm .

Fig. 4A A model of a small volume of osteoporotic trabecular bone from a 4th lumbar vertebral body made in a Stereosketch with pipe cleaners using enlarged SEM micrographs. The structure resembles an open lattice with long interconnected elements. Fieldwidth 23 cm.

Fig. 4B A model similar to that in the figure 4A of a small volume of trabecular bone from a normal 4th lumbar vertebral body. Each element in this model represents the skeleton of a plate or part of a tube in normal bone. The dissimilarity between these two models is apparent, suggesting that neither simple thinning nor removal of elements would bring about osteoporotic structure. Fieldwidth 24cm.

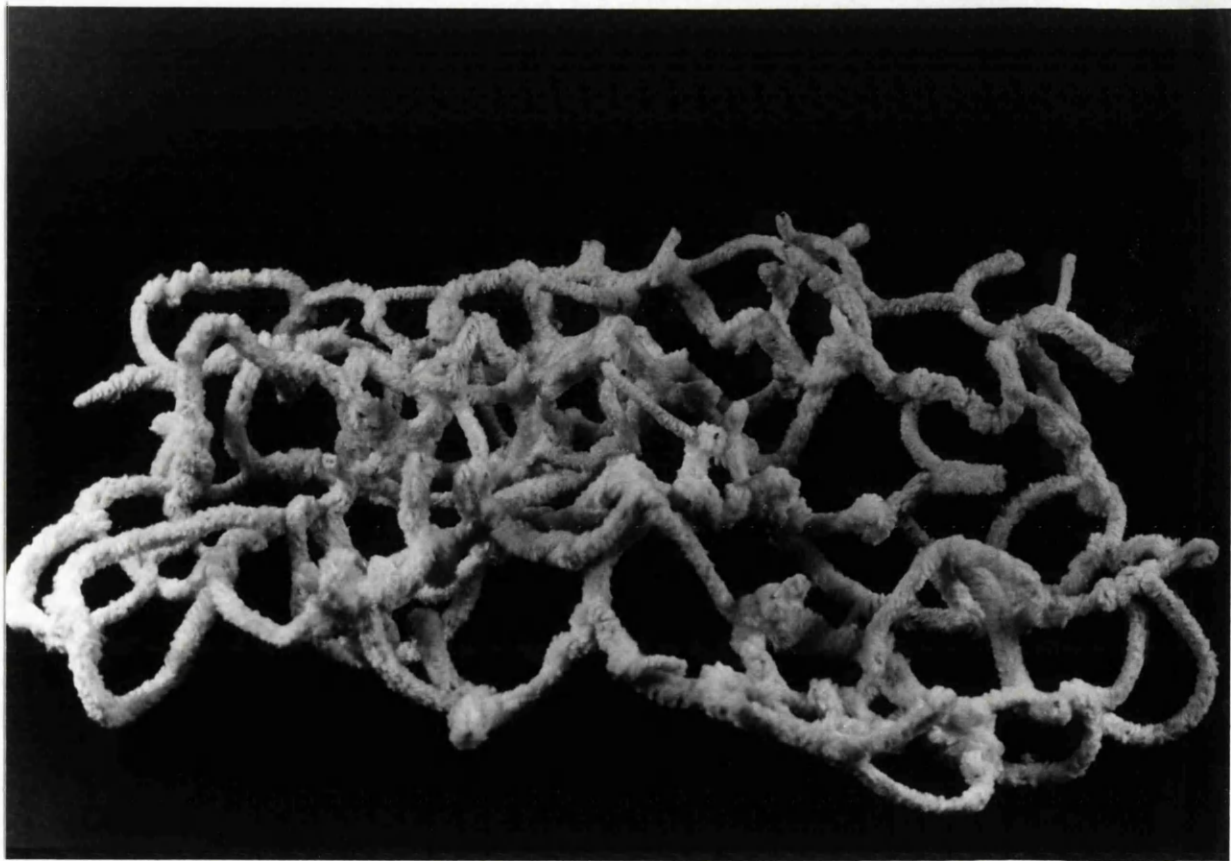
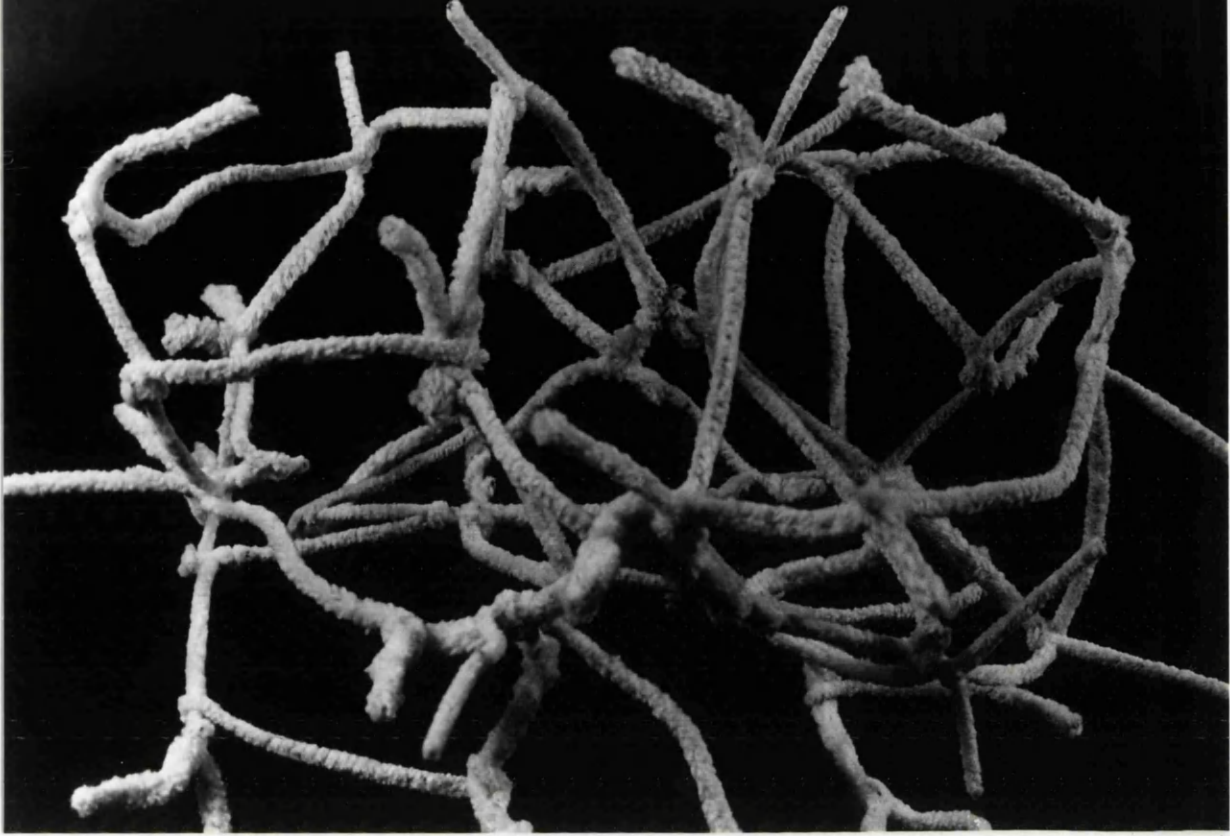
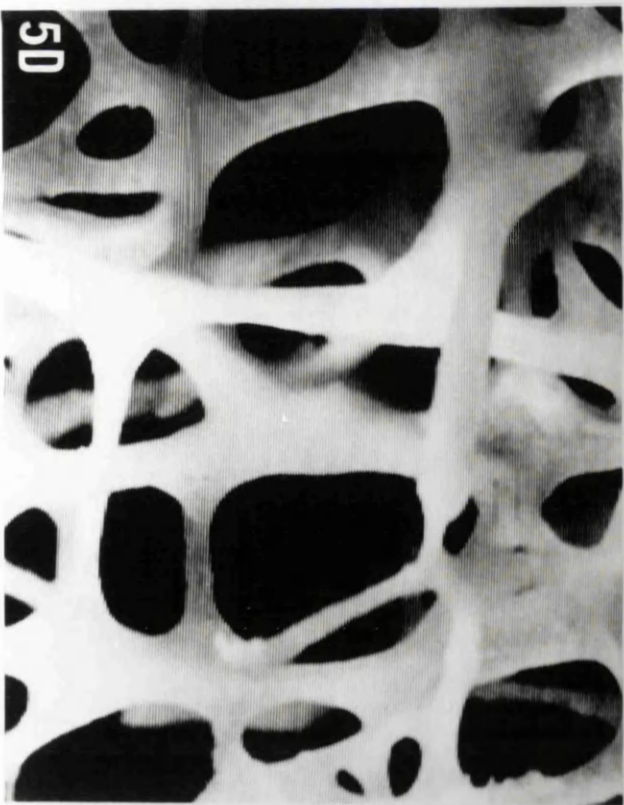
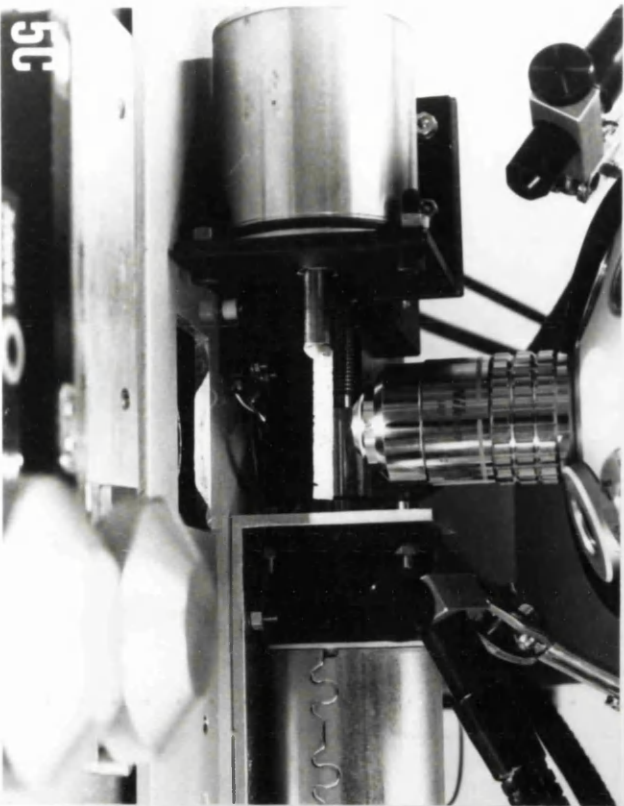
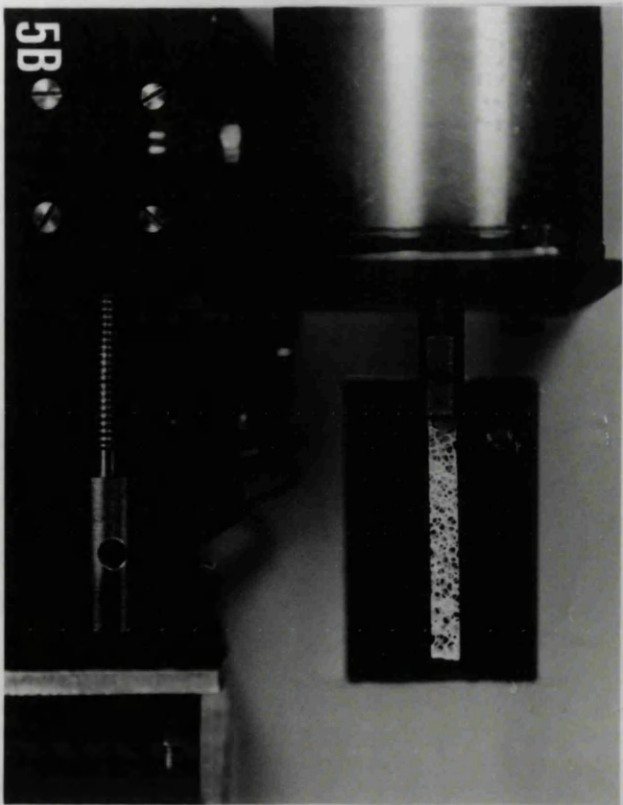
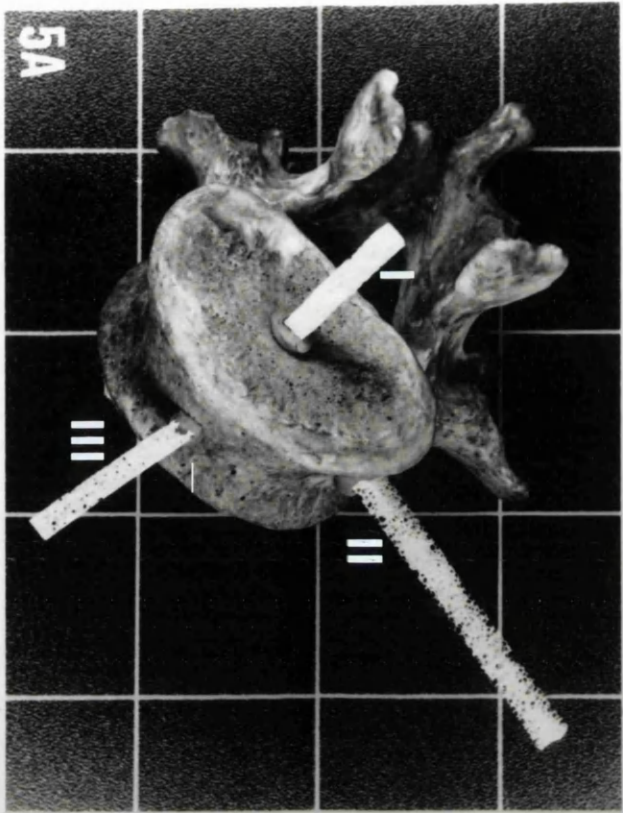


Fig. 5A A lumbar vertebra showing the positions of three square beams (I = Vertical, II = Horizontal and III = Antero-posterior) used for the "continuous motion parallax" method.

Figs. 5B-5D Beams were mounted axially on the shaft of a motor (5B) and rotated under the lens of a high definition light microscope with an increased depth of field (Olbrich 4000; 5C). The motion parallax information was displayed via a high resolution television camera on a television monitor (5D).



CHAPTER 3

TRABECULAR BONE ARCHITECTURE OF THE LUMBAR VERTEBRAL BODY; ITS RELATIONSHIP TO DEVELOPMENT AND VASCULARISATION; AND CHANGES WITH AGING – A STUDY USING MACRO STEREOPHOTOGRAPHS.

3.1 INTRODUCTION

That age related loss of vertebral trabecular bone leads to spinal osteoporosis and crush fractures has been well demonstrated (Arnold et al. 1966, Arnold 1973, Dunnill et al. 1967, Lindahl and Lindgren 1962, Atkinson 1967, Mosekilde et al. 1987, Cann et al. 1985). Bell et al. (1967) found that loss of strength of vertebrae is proportionately greater than loss of osseous tissue. This phenomenon has been explained by later work which revealed that the biomechanical competence of trabecular bone is dependent not only on the absolute amount of bone present but also on the trabecular microstructure (Galante et al. 1970, Pugh et al. 1973, Kleerekoper et al. 1985, Mosekilde et al. 1987). Trabecular bone architecture in both vertebral bodies and iliac crest biopsies has been described using measurements such as mean trabecular width, area, trabecular separation and interconnectedness (Bergot et al. 1987,1988, Wakamatsu and Sissons 1969, Aaron et al. 1987, Compston et al. 1987, Birkenhager–Frenkel et al. 1988). Such parameters were mainly derived from histological sections of bone using two dimensional standard statistical techniques or image analysis systems that analyse two dimensional digital images (Bergot et al. 1988, Garrahan et al. 1986, Merolli et al. 1990). Vesterby et al. (1989) described a stereological parameter for bone structure (the star volume) which provides an estimate of a characteristic size of the marrow space. An increase in star volume with age has been reported both for lumbar vertebra and iliac crest (Vesterby 1990). A high resolution computed tomographic technique for the direct examination of three dimensional bone structure in vitro has also been described (Feldkamp et al. 1989). Jensen et al. (1990) presented a mathematical model for vertebral trabecular bone architecture and described variations in apparent stiffness among different model types.

The above studies have described the age related bone loss to varying degrees, but the methods are not used to demonstrate changes in the three dimensional arrangement and architecture of bone which also contribute to the inability of the bone to withstand normal load. This work therefore concerns firstly the establishment of normal architectural pattern for lumbar vertebrae, taking the 4th lumbar vertebral body as a model. For this purpose a simple technique was employed to produce macro stereophotographs from vertebral sections. A literature survey on development and vascularisation of vertebral bodies was also carried out to understand the contribution of these processes in establishing normal trabecular architecture. Secondly, the changes in architecture were studied from young adult to old individuals and in osteoporotic subjects. Vascular changes on aging are also considered with the aim of finding possible correlations with trabecular structural changes.

3.1.1 Current concepts of trabecular bone structure and age

changes

According to Schmorl and Junghans (1975), cancellous bone of the vertebral bodies does not actually consist of trabeculae but of thin bone plates intersecting each other, containing numerous openings of different sizes varying from roughly circular to quadrangular. The main direction of these plates is craniocaudal, but this course varies somewhat in different sections of the spine, depending upon the direction of the principal functional stresses. Amstutz and Sissons (1969) studied a normal third lumbar vertebral body using macerated sections and enlarged models reconstructed from serial sections. They observed that even though vertical and horizontal structures predominate, the orientation of the plates depends on their exact position within the vertebral body. In the regions near the superior and inferior surfaces of the vertebral body, the bone structure is denser than in the intervening central region: predominantly horizontal plates were encountered in these regions compared with more vertically oriented plates at the centre. Plate thickness was greatest in the central part of the vertebral body. They suggested that plates inclining in many directions and joining together at various angles would serve to protect the vertebra against compressive and shearing stresses in various planes. Singh (1978) used macerated adult human bones to describe the arrangement of plates and rods in different parts of the vertebral body, grouping these arrangements into different types.

In a scanning electron microscopic study of a lumbar vertebral body, Whitehouse et al. (1971) observed that the bone structure contains many rod-like elements and resembles, in many respects, a cross-braced structure of short columns in the regions near the superior and inferior surfaces of the vertebral body. Near the central anterior part of the sagittal section, the structure consists predominantly of folded laminae of bone, enclosing large irregular marrow spaces. At the corners of the sagittal section, the trabecular structure appears to be heavier and to contain an above average proportion of bone. In horizontal sections, the structure appears to show irregular channels approximating to cylinders at right angle to the section. In some parts they have laminar walls and in others the structure is more like a lattice or cage of rods.

Arnold (1968, 1970) studied the macroscopic structure of vertebral trabecular bone using 2–3 mm thick sagittal and horizontal sections of vertebral bodies. He described regional variations of trabecular bone in normal sections and changes that occur during the process of aging. The first change observed was a decrease in the number of trabeculae forming transverse plates in the end zones. This change was detected during the third and fourth decades and no changes in longitudinal trabeculae were observed during this period. In the fifth decade, in addition to the progression of the above changes, the plate-like structure of the middle zone extends into the end zones to replace the lost transverse plates. In the sixth and seventh decades, perforations appeared on the plates of the middle zone, partially converting them into trabecular structures. The marked osteoporotic changes he observed in the eighth and ninth decades were a marked reduction to virtual absence of end zone transverse trabeculae or plates, an absence of middle zone vertical cylinders and plates, and the prominence of hypertrophied longitudinal trabeculae and the scarcity of persistent normal longitudinal trabeculae.

Parfitt et al. (1983) demonstrated that age-related bone loss occurs principally by a process that removes entire structural elements of bone. It was proposed that the process of removal is initiated by perforation of trabecular plates, progressive enlargement of the perforation leading to the conversion of plates to rods.

Delling and co-workers investigated sagittal sections of whole spines using a new preparative technique which permits combined two and three dimensional histomorphometrical analysis, revealing new information about this process (Delling 1989, Vogel et al. 1989, Hahn et al. 1989, Pompesius-Kempa et al. 1989). While confirming previous reports of the role of perforations and loss of horizontal trabeculae during age related bone loss, they found that the bone volume depends strongly on the number of plates, whereas there is no correlation, or even an inverse relation, between bone volume and the number of rods. Using an index of intertrabecular connectedness (trabecular bone pattern factor: TBPf) they reported a correlation between bone volume and trabecular connectedness. Further, they observed formation of microcallus only in subjects older than fifty years.

Vertebrae are developed by endochondral ossification of cartilagenous models. It is generally believed that bony elements are laid down around invading blood vessels: these elements are later remodelled, depending on the functional need and the mechanical forces that they are subjected to, into those seen in the adult vertebrae. What is less known is how far these first developed bone elements are maintained into adult life and to what extent they influence the adult structure and the different orientations seen in the adult structure. Further, the vascularisation of the vertebrae changes with age (Ratcliffe 1982, 1986). It is important to have a knowledge of the effects of these changes on the trabecular bone structure when interpreting bone loss with age.

The development and vascularisation of the vertebrae will be considered shortly at this point.

3.1.2 The development of the vertebrae

Each vertebra is usually described as formed from parts of two adjacent sclerotomes.

The notochord forms between the 2nd and 3rd weeks of gestation and plays a decisive role in the development and segmentation of the vertebral column. Mesenchymal cells from the most medial portion of somites migrate ventrally to surround the notochord and dorsally to surround the neural tube, thus providing for the future vertebral column and posterior neural arches. The cells of the primordial vertebral segments around the notochord (the sclerotomes) proliferate, with the caudal half of one primordial vertebral segment growing to meet the cranial half of the subjacent one. The vertebral bodies are formed from adjacent primordial vertebral segments that fuse and undergo chondrification at about the 5th and 6th week of gestation. Thus the intervertebral disc is a segmental structure that develops from the middle portion of the condensed vertebral segment.

The body's major part, the centrum, is ossified from a primary centre dorsal to the notochord. At approximately the same time as ossification appears in the cartilagenous vertebral bodies, the notochord disappears.

The upper and lower surfaces of the bodies and the apices of transverse and spinous

processes are cartilaginous until puberty when five secondary centres appear, one in the apex of each transverse and spinous process and two annular epiphyseal 'rings' for the circumferential parts of the upper and lower surfaces of the body. All these growth cartilages have disappeared by the age of 25 years.

3.1.3 The arterial supply of the adult lumbar vertebral bodies

The lumbar vertebrae are supplied by four pairs of lumbar arteries that arise from the aorta opposite the lumbar vertebrae. A fifth small pair occasionally arises from the median sacral artery, but lumbar branches of the iliolumbar arteries usually take their place (Williams et al. 1989). These arteries run posterolaterally on the four upper lumbar vertebral bodies. At the intervertebral foramen the lumbar artery sends a branch, the spinal artery, which enters the spinal canal. Deep to the posterior longitudinal ligament, the spinal artery divides into an ascending and a descending branch. Each branch anastomoses with its counterpart from above and below to form a longitudinal series of arches. The apex of each arch anastomoses with the apex of the opposite arch. Nutrient arteries to the vertebral body arise from these anastomoses and pass forward into the body through the centre of its dorsal surface. An anastomosis also exists on the anterolateral surface of the vertebral body (Wiley and Trueta 1959). From the upper and lower surfaces of the lumbar artery, periosteal arteries arise which pass upwards and downwards on the vertebral body. Some of these cross the disc spaces to anastomose with their counterparts on the vertebra above or below. Near the upper and lower surface of the vertebral body there is a generally horizontal vessel which anastomoses with the vertically directed periosteal arteries.

According to Ratcliffe (1980) the principal intra-osseous arteries are distributed into three horizontal layers, one equatorial and a metaphyseal layer near each end. The arteries of the equatorial plane are the main nutrient arteries from the posterior longitudinal anastomoses, with one or two arteries either side which arise directly from the lumbar artery as it traverses the anterolateral surface of the vertebral body. The long stemmed horizontally and radially disposed arteries in the metaphyseal layers have been called the metaphyseal arteries. They arise either from the periosteal arteries or from the metaphyseal anastomoses deep to the most superficial layer of the annulus fibrosus. A third type - called peripheral arteries - are short-stemmed, branch peripherally and have centripetally directed nutrient branches. They arise from the periosteal arteries and occur more frequently in older spines.

Ratcliffe (1980) also proposed a concept of zoned distribution of blood supply within the vertebral body. According to this, the central core, which lies behind the mid-axial point of the vertebral body and extends from disc surface to disc surface, is supplied by the equatorial arteries. An annulus at each end adjacent to the disc is supplied by the metaphyseal arteries. The surrounding collar from disc to disc is supplied by the peripheral arteries. The region of the vertebral body adjacent to the nucleus pulposus is therefore supplied by the equatorial arteries and the rest of the surface subjacent to the annulus fibrosus is supplied by the metaphyseal and peripheral arteries.

3.1.4 The venous drainage from the lumbar vertebrae

The veins of the vertebral column form intricate plexuses extending along its entire length. These plexuses can be divided into external and internal groups (outside or inside the vertebral canal), are devoid of valves, anastomose freely with each other, and end in the intervertebral veins (Williams et al. 1989).

The external vertebral venous plexuses consist of anterior and posterior plexuses which anastomose freely. The anterior external plexus lie in front of the bodies of the vertebrae, communicate with the basivertebral and intervertebral veins and receive tributaries from the vertebral bodies. The posterior external plexuses are on the posterior surfaces of the laminae and around the spines and the transverse and articular processes. These plexuses anastomose with the internal vertebral venous plexuses: in the lumbar region they end in the lumbar veins. The upper lumbar veins drains into the lumbar azygos veins and the lower lumbar veins drain directly into the inferior vena cava.

This "vertebral venous system" acts as a collateral system in the event of an obstruction of the superior or inferior vena cava. Batson (1957) has published a detailed description of this system. The internal vertebral venous plexus lies within the vertebral canal between the dura mater and vertebrae. It is essentially a series of irregular, valveless epidural sinuses that extends from the coccyx to the foramen magnum. Its channels are embedded in the epidural fat and are supported by a network of collagenous fibres (Parke 1986). They may be divided into anterior and posterior groups. The anterior internal plexuses consist of large veins which lie on the posterior surfaces of the vertebral bodies and intervertebral discs, on each side of the posterior longitudinal ligament. They are connected by transverse branches into which the basivertebral vein opens.

The posterior internal plexuses are on each side of the median plane in front of the vertebral arches and ligamenta flava, and anastomose, by veins passing through and between those ligaments, with the posterior external plexuses.

The basivertebral veins are the major vessels that drain the blood from the vertebral body. This system of veins is orientated horizontally in the centrum and is arranged in the middle of the vertebral body along with the radiate arteries, forming a large scale venous grid into which the vertical veins of the vertebral body flow from above and below (Crock et al. 1976,1977). They are large, and run tortuous courses to converge posteriorly to drain into the transverse branches uniting the anterior internal vertebral plexuses either as single or double veins. They also drain into the anterior external vertebral plexuses through small openings on the front and sides of the bodies of the vertebrae.

Crock et al. (1973, 1976) have described the arrangement of veins in the vertebral body in detail. The main venous channels that drain into the basivertebral venous system are formed by the confluence of numbers of equally large tributaries which enter the main stem obliquely and at regular intervals along their courses and around the circumferences. Individual tributaries themselves are formed by the union of innumerable short, fine radicles.

In the region of the vertebral body adjacent to the vertebral end-plate, Crock et al. (1973,1976) have described large venous channels that are orientated horizontally, running parallel

to the end-plate area when viewed in sagittal or coronal sections (the horizontal subarticular collecting vein system). These channels are built up in the central area of the vertebral body by large calibre tributaries of the vertical veins of the centrum. Posteriorly, some of the veins from the horizontally orientated network drain directly into the anterior internal vertebral venous plexus. They also communicate with the external vertebral venous plexuses anteriorly and around the vertebral body.

At the vertebral end plate level, Crock et al. described another vascular network that is orientated horizontally and parallel to the system described above. This system (the subchondral postcapillary venous network of the vertebral body) lies on the perforated cortical vertebral end-plate. Short, ventral tributaries from this network drain into the horizontal subarticular collecting vein system. It has been suggested that this network receives tributaries from capillaries in the vertebral end-plate cartilage.

3.2 MATERIALS AND METHODS

The fourth lumbar vertebral body was removed at post mortem from 36 adult subjects (18 male, 18 female, age range 30–91 years). Three females and one male had suffered fractures and were confirmed osteoporotics. Samples were clean and stored immediately in 70% ethanol.

Plane parallel mid sagittal sections of 4 mm in thickness were cut from each vertebrae using a diamond saw (Isomet). Some horizontal and coronal sections were also cut from some young and adult samples to compare with the sagittal sections. The samples were stored at 37 C with 2% hydrogen peroxide for 24 hrs to remove marrow and soft tissues. They were cleaned with a jet of water and were defatted for a few hours in a solution of chloroform and ethanol. Samples were then air dried.

When examined under a binocular microscope the three dimensional trabecular bone structure of these samples could clearly be discerned. However, at higher magnification, only a small area of bone was in the field of view and the depth of focus was insufficient for a favourable assessment. Therefore, the following procedure was used to produce stereophotographs of these sections.

A tilting stage in which the tilt angle is adjustable was constructed. Samples were mounted on it so that the tilting axis lay along the mid line of the sample. Using a 80 mm macro lens for an Olympus OM2 35mm camera, stereophotographs were produced with an angular difference of 10° between pairs. A very small aperture (F22) was used to increase the depth of field. Photographs were enlarged to the size of 165 mm x 115 mm and were examined under a Hilger and Watts SB180 mirror stereoscope with parallax measuring facility (Martin, 1966). The three dimensional structure of the whole section could be viewed this way and the whole thickness of the section was in focus. Therefore, in addition to the observation of three dimensional structure of trabeculae bone in different regions, different groups of trabeculae (e.g. vertical and horizontal) could be identified and counted across the section. Vertical trabeculae were counted from the anterior border and to the posterior border at superior, middle and inferior levels (AB, CD, EF Fig. 1). Horizontal trabeculae were counted at the midline (GH Fig. 1). The biconcavity indices of the

vertebral bodies used during the study were also calculated by dividing the mid-vertical height of each section from its anterior vertical height.

Using the parallax measuring facility, the height differences between pairs of points in the two photographs could be measured, and the real size of any elements could be calculated. This method was used to calculate the lengths of horizontal trabeculae at superior, middle, and inferior regions of selected young, old and osteoporotic samples, irrespective of their orientation in the horizontal plane.

3.3 RESULTS AND DISCUSSION

The method of producing stereopairs to view three dimensional structure of trabecular bone using macrophotographs proved to be very satisfactory. It allowed the observation of the three dimensional structure of any part of a whole section in a single view and thereby facilitated the comparison of different regions of the same section. Since the whole section was in focus, different layers of trabeculae could be identified, compared with each other and counted. The real length of the elements could also be calculated via the parallax measurements.

3.3.1 Normal structure

3.3.1.1 Mid-sagittal sections

Figure 2 is a stereopair of a mid sagittal section of a 4th lumbar vertebra from a 31 year-old male. The trabecular structure can be divided into three zones depending on the nature of the trabecular elements. The middle or equatorial zone consists of (relatively) huge plates or laminae orientated in the vertical plane, whereas the superior and inferior zones have short rod-like trabeculae arranged in orthogonal fashion. Three dimensional views show that the plates of the middle zone are in fact the common walls of tubes orientated in the cranio-caudal direction. However, examination of more specimens showed that the plates of the most anterior portion of the middle zone are arranged approximately in a triangular manner (Figures 2,6). (Whitehouse et al. (1971) described this region as consisting of folded laminae of bone enclosing large irregular, intercommunicating marrow spaces). Figure 8 is a stereopair of a coronal section through this region. The structure could be better studied in this plane. A different structure of the superior and inferior zones compared with the middle zone is apparent in this section. In the middle zone the structure appears to be tubes of different sizes orientated in the anterior posterior direction of the vertebral body. Some of these tubes are open to the outside and these are essentially tunnels for the entry of blood vessels.

The extent and the nature of this middle zone varied extensively in different specimens. A deficiency was usually encountered at the centre of the posterior border of these mid-sagittal sections (Figures 7,12). This is the point of entry of the basivertebral vein. The trabecular plates virtually formed the walls of this vein and its tributaries at this region (Figure 6,9). Thick plates forming their walls could clearly be identified in other regions of the middle zone when veins were present (Figures 6,7).

In describing the blood supply to the vertebral body, Crock and Yoshizawa (1977) state

that an arterial grid is formed in the centre of the vertebral body, from which vertical branches ascend and descend towards the respective vertebral end plates. The basivertebral vein is arranged in the middle of the vertebral body along with the radiate arteries, forming a large-scale venous grid into which the vertical veins of the vertebral body flow from above and below. This implies that the middle zone is highly vascularised. It is reasonable therefore to assume that the structure of this zone is highly dependent upon the arrangement of the vessels. Accordingly, it is erroneous to believe that the direction of trabecular plates of this region is solely determined by the mechanical forces that they are subjected to, without taking into consideration the vascular structure of the region.

3.3.1.2 Coronal sections

The above description was based on mid-sagittal sections of the vertebrae. However, a similar structural organisation could be observed when coronal sections were examined. Figure 3 is a stereopair of a coronal section through middle of a vertebral body. A clear middle zone with numerous openings for blood vessels and surrounding thick bony plates can clearly be seen in this section.

3.3.1.3 Horizontal sections

When horizontal sections through the middle zone were examined (Figure 4) the trabecular structure seemed to be a system of bony cylinders of different sizes orientated at right angles to the plane of the section. This implies that the orientation of these plates at the middle zone is mainly cranio-caudal. However, Figure 4 also shows two venous channels with their walls consisting of thick bony plates. They are directed sideways from the centre of the vertebral body.

When one compares the structure described above to the process of the development of lumbar vertebrae, what kind of relationship would be expected?

During embryonic life the ossification of vertebral bodies begins around the tenth and eleventh weeks. The invading arteries of the middle zone branch off and extend towards the upper and lower thirds of the vertebral body. Ossification proceeds parallel to the course of the radiating arteries and takes place more rapidly in the upper and lower thirds of the body, the central portion lagging behind (Willis 1949).

Bick and Cope (1950) studied the longitudinal growth of the human vertebra from a 14 weeks foetus to a 20 year-old female. While describing this process of ossification along the developing vessels, they also demonstrated an appearance of columnar cartilage with the form of an epiphyseal plate across the cephalic and caudal surfaces of the developing vertebral margin. However, much controversy exists about the occurrence of a true epiphysis during vertebral development. Francois and Dhem (1974), questioned if words like epiphysis, diaphysis and metaphysis, which were invented for long bones, can be transferred to short bones.

It is usually observed that the ossification centres of a newly formed vertebral body appear ovoid in lateral radiographs. Small indentations are visible anteriorly and posteriorly and sometimes they appear as more pronounced clefts. At the centre a linear radiolucency passes

across horizontally. Both these indentations and the linear radiolucencies are produced by the vascular channels passing horizontally through the ossification centres (Schmorl and Junghanns 1975). These vascular channels are also recognisable in the anteroposterior projection as small radiolucencies at the centre of the vertebral body. With growth these radiolucencies disappear in the anteroposterior projection but persist until growth ceases in the lateral projection. Schmorl and Junghanns (1975) also described the development of the bony rim at the periphery of the vertebral body. This rim ossifies separately and fuses with the body at around 14 or 15 years of age.

Another important aspect should be considered at this point. The vascularisation of the vertebral body of the foetus is not always uniform. Congenital vertebral malformations have been related to the abnormal distribution of the intersegmental arteries (Tanaka and Uthoff 1981). Further, in a study of coronal clefts (a vertical radiolucent band in the vertebral body found in a lateral projection) Tanaka and Uthoff (1982) suggested that, in cases of these clefts, endochondral bone formation progresses around two ossification centres which are connected by a vessel, giving it a dumb-bell shape. In some cases, the two ossifying centres merge just at the periphery so that a cartilaginous island remains in the middle. They concluded that the shape of the ossified area seems to be determined by the vascular distribution in foetuses.

In a study of ossification centres of the vertebral body, Cohen et al. (1956) concluded that no one type of ossification pattern exists universally in the formation of the vertebral body, some being formed as a single centre of ossification, some as doubled centres dorsoventrally arranged, and still others as paired lateral centres of ossification.

In a study of anomalies of vasculature in vertebral bodies, Schinz and Tondury (1942) showed a different arrangement of vessels where there is a double centre of ossification.

Thus different patterns of vascular supply are associated with and may even be responsible for the different patterns of ossification.

The above description suggests that variations observed in middle zones may be due to different patterns of ossification brought about by different patterns of vascular supply during development. However, the structure of the superior and inferior zones seems to be similar in all the specimens. This is because whatever variations exist at the centre, the branches sent off superiorly and inferiorly are approximately similar and the ossification process should therefore be uniform in these regions.

3.3.2 Vertically oriented trabeculae

Examination of normal vertebral sections (Figures 2,6) reveals that the number of vertical trabeculae per unit length of the section was much higher in superior and inferior thirds compared with the middle zone. Further, it was rarely possible to trace a vertical trabeculum from one end of the body to the other. When the three dimensional structure of these elements was examined, the most striking feature was that the huge tubes and plates at the middle zone in fact branch off (just as blood vessels branch off from the centre) to give rise to vertical trabeculae at the peripheral zones. Consequently, when we examine the three dimensional structure of the trabecular bone of the normal vertebral body, we may really be reading its developmental history.

The above finding can also be discerned by studying horizontal sections. Figure 4 is a mid horizontal section showing large cylinders mainly distributed at the front and sides of the vertebral body. A horizontal section through a metaphyseal region of the same vertebral body (Figure 5) shows that the number of cylinders has increased in this region, while their diameter has been diminished. Arnold's (1968) work also supports this description. He found that holes become larger when traced towards the middle zone from the peripheral zones in horizontal sections .

In some specimens, huge vertical trabeculae were seen at the centre, branching off to give rise to vertical trabeculae at the periphery (posterior region of the Figure 6). Nevertheless, in most of the specimens, even though the cut surfaces of the tubes at the middle zone were orientated in the cranio-caudal direction, separate vertical trabeculae could not be identified. This is, of course, due to the fact that the structure here consists of fused tubes and plates rather than separate trabeculae.

Even though a cross-braced trabecular structure is usually seen at the peripheral zones, it should also be mentioned that plates of different sizes exist in normal vertebrae at these regions, and in some regions the structure can be almost tube-like, when a cross braced structure may consequently not be visible.

A structure similar to the above description was also observed in para-sagittal sections. However, at the middle zone of para-sagittal sections, vertical trabeculae could be more readily identified than in mid-sagittal sections. At the region of the junction of the vertebral arch with the body (Figure 10), a different structure exists. These posterolateral parts of the vertebral body were formed from the ossification centres of the vertebral arch. Thick plate-like structures that were different from other regions could be seen in these areas. This structure could also be noticed in coronal sections through the most posterior part of the vertebral body (Figure 9).

Another interesting feature was that vertical trabeculae arose from the respective lateral walls near the walls of the vertebral body (Figures 2,3,10). It seems that loads from the vertebral rim region are transmitted through the lateral walls rather than the central part of the body.

The trabecular structure seems to be more orthogonal towards the vertebral end plates, and double vertebral plates were encountered in many specimens (Figures 2,6). Arnold (1968) considered that these thickened transverse plates below the end plates represented growth arrest lines in the trabecular structure of the vertebra, as may sometimes be seen in the long bones.

The above described structure has been schematically represented in figure 11A.

3.3.3 Horizontally oriented trabeculae

Since plates and tubes at the middle zone are fused to each other, the need for horizontal trabeculae should be minimal at this region. However, when a prominent middle zone was present, a horizontal trabecular type different from that of peripheral zones could be identified (Figures 2,6,12). These "mid-horizontal trabeculae" were longer and thicker than their peripheral counterparts and were not always exactly horizontal. At the anterior region of the section in Figure 12, very long horizontal trabeculae of this type can be seen. They could also be recognised in mid-horizontal sections (Figure 4).

At the periphery, the horizontal trabeculae were short, more horizontal and towards the end plates were more or less aligned into horizontal planes. In normal bone they can be presented as plates but most were thinner than the vertical trabeculae to which they were joined. Examination of horizontal sections (Figure 5) revealed that these horizontal trabeculae were more plate-like towards the walls of the vertebral body compared with more rod-like trabeculae at the centre. A quantitative analysis of these two types of horizontal trabeculae will be presented later.

In light of the above, it is apparent that when describing structural changes of vertebral trabecular bone, the regional variations of the normal anatomical structure should be taken into account. It should further be noted that the normal structure of the vertebra could be described from its developmental history alone without taking stress trajectories into consideration. This brings about several questions. Do the blood vessels grow with respect to stress trajectories? Are trabeculae laid down to resist the expected load? or, after initial formation, does strain history mould the structure during the remodelling process. Has loading got anything to do with the trabecular structure at all? Further research on development will be necessary for a proper understanding of these processes.

3.3.4 Changes in trabecular structure with age and during

osteoporosis

Figure 14 shows a 4th lumbar vertebral mid-sagittal section from an 89 year old male. The generalised thinning of trabeculae without a disruption of the normal architectural pattern shown in this sample was observed in many older specimens. A similar structure could also be seen in coronal sections (Figure 16). However, sections from osteoporotics (both clinically confirmed and histologically identified from loss of bone) showed a dramatic change in architecture (Figures 13,15,19). The most striking feature was that vertical trabeculae could be traced without much difficulty from one end of the body to the other (e.g. Figures 13,15). Further, these vertical trabeculae seem to be run approximately parallel to one another, the distance between vertical trabeculae being nearly constant. This also implies that the length of the horizontal trabeculae should also be nearly the same across the sections. If the normal structure is the one described above, what changes have occurred to bring about this revised arrangement in osteoporotic bone? The most prominent feature in "osteoporosis" is that the horizontal trabeculae in the superior and inferior zones have markedly increased in length (Figures 13,15). The length of the peripheral horizontal trabeculae now approaches that of mid-horizontal trabeculae. The most probable way of achieving this should be by removal of vertical trabeculae at the periphery leaving the remaining vertical trabeculae connected by long horizontal ones. Careful examination of these osteoporotic sections show that this is the case. Different stages of this process could be identified in samples from different age groups (Figures 7,15,16,19).

Arnold's (1968) observations of the changes that occur in the peripheral zones are in agreement with the above. He states that dilation of the pore size of the peripheral horizontal plates first occurs due to narrowing of the septal trabeculae forming the walls. Finally, the loss of four transverse trabeculae and the vertical trabeculae on which they impinge produces a single hole over twice the diameter of the original pores. This larger hole is now in continuity with that of an underlying cylinder of the middle zone of which it now becomes a part.

There are very few horizontal trabeculae remaining in osteoporotic bone. This indicates that most of the horizontal trabeculae have been completely removed from the periphery, causing increased trabecular separation. Further, the structure of these peripheral horizontal trabeculae of the osteoporotic bone was markedly different from that of normal bone. The structure has changed from thick, sturdy plates or rods to long, thin, frail strands. In addition, at the peripheral regions of osteoporotic bone, long oblique trabeculae connecting vertical trabeculae can be usually seen. These can be considered as horizontally transformed vertical trabeculae or trabeculae that have been formed from parts of vertical and horizontal trabeculae during the process of removal.

In the middle zone, very long horizontal trabeculae could be seen in severely osteoporotic sections, indicating that the horizontal trabeculae also increase in length in this zone. However, as observed from osteoporotic sections, the rate of increase was much lower in this zone compared with that of peripheral zones. Unlike normal bone, tubular structures cannot be recognised in the middle zone in osteoporotic specimens, but vertical trabeculae can now be clearly identified (Figure 13). However, comparatively thick plates were still present at the middle zone of some

osteoporotic sections (Figures 13,19), presumably because this region had thick tubes and plates to start with. Thus, when interpreting osteoporotic trabecular bone architecture, one should always keep its normal structure in mind and the regional variations in the vertebral body should also be taken into account.

A controversy exists as to whether the thickness of the remaining vertical trabeculae increases with age in response to increased mechanical loading brought about by bone loss. (Atkinson 1967, Pesh et al 1977, Twomey 1983, Bergot et al 1988, Mosekilde 1988). Most conclusions on this point have been drawn from histological parameters derived from two dimensional techniques. Comparing the structure of the trabeculae in the region indicated by the arrow in Figure 19 with the others in the same section, and imagining what sort of normal structure would have been present, it will be obvious that the trabeculae in this region must have thickened. Similar thickened vertical trabeculae were observed in many specimens during the present study. According to Frost (1964), the trabecular bone is used to withstand pure compression. Frost (1963, 1964), also stated that the cross sectional growth in size is controlled by the sizes of the bending loads, unequal and increasing loads causing increase in cross sectional size. He also considered that gain and loss of substance at bone surfaces is controlled by bending of the bone: increasing surface concavity as load is applied causes local gain, while increasing convexity causes loss of bone. If this explanation is correct, it is reasonable to assume that the remaining vertical trabeculae at the periphery increase in thickness to bear the additional load.

Arnold (1968) proposed that the extension of the large diameter cylinders peripherally from the middle zones occurs to replace the lost transverse plates of the end zones. When the bone loss occurs to a point where thinning of trabeculae can no longer occur without disrupting the architectural integrity, the process of removal of trabeculae should be more selective in order to preserve the strength to withstand compression. The resultant process would be the removal of both vertical and horizontal trabeculae at the peripheral zones, retaining just enough horizontal trabeculae to stabilise the remaining vertical trabeculae and thickening these remaining vertical trabeculae. Rather than an extension of cylinders from the middle zone to the periphery, the real process could be the thinning of the cylinders at the centre and thickening of vertical trabeculae at the periphery to produce more or less uniformly thickened vertical trabeculae extending from one end plate to the other.

Collapse of the trabecular bone has usually been reported to occur first at the central region of the vertebral body underneath the area adjacent to the nucleus pulposus (Twomey 1983). When the area below the vertebral rim of the osteoporotic samples were examined, vertical trabeculae were connected to the lateral walls as in normal bone. Therefore, even in the severe osteoporotic cases (Figures 13,19) loads can still be transferred to the lateral walls. With the architectural changes observed, the central region becomes the weakest part of the body. This perhaps explains the fact that collapse occurs first in the central region.

The architectural changes described above could also be detected in coronal and horizontal sections, but it is difficult to prepare horizontal sections from severely osteoporotic vertebral bodies due to insufficient support for the trabecular elements in this plane. Figure 16 is a coronal

section of a 4th lumbar vertebral body from an 88 year old female and Figures 17 and 18 are horizontal sections from mid and metaphyseal regions of the same vertebral body from another 88 year old female. Osteoporotic changes described above can also clearly be seen in these planes. In the section from the metaphyseal region (Figure 18), collapsing trabecular elements can easily be identified. In the normal bone at this plane, the structure showed cylinders (i.e. with mutual walls as in a honeycomb) at right angles to the plane of the section. However, in this osteoporotic section, the structure consists mainly of rods connected to form multi-sided shapes. These changes can also be seen in the area around anterior and posterior walls. The outline of the section is irregular due to formation of osteophytes where trabeculisation has also been taken place.

In many specimens, isolated depressions of the superior and inferior vertebral plates were observed from the 6th decade onward (Figures 10,16,19). They occurred to different degrees at different sites and sometimes typical Schmorl's nodes could be identified. It should be noted that when Schmorl's nodes or any other cystic lesions were present, the trabeculae around the lesion were thickened and were structurally very different from the rest of the vertebral body.

The structure of the osteoporotic bone described above has been schematically presented in Figures 11b and 11c.

In many severe osteoporotic cases, large collapsed regions were encountered within the vertebral body (Figures 13,19). The sections used during this study were prepared very carefully to prevent accidental breaking of the fine trabeculae. Other than the fracture of one corner of the section which occurred during preparation of the sample shown in Figure 13, very thin trabeculae around the collapsed region indicate that this is a "genuine" collapse of the osteoporotic bone. It should be noted that the collapse of the trabeculae within the vertebral body took place without a collapse in vertebral end plates or walls.

Schmorl and Junghanns (1975) observed that the radiodensity of the vertebral rim in the adult is less than that of young individuals. In younger samples, a vertebral rim could clearly be recognised and mostly consisted of thick continuous bone. However, in many old specimens, trabeculisation of the rim had taken place and a rim was hardly recognisable. This would partly explain the reduced radiodensity of the rim seen in old individuals.

The above description concerns the changes that occur in trabecular bone architecture during aging and in osteoporosis. However, if trabecular thinning can be considered as a first sign of age changes, it was first observed around the region of the entry of the basivertebral vessels to the vertebral body. It has been reported that the basivertebral vein becomes enlarged in advanced age (Williams et al. 1989). Therefore, it is open to question whether this thinning occurs in response to enlarging veins or as a truly independent age change.

3.3.5 Microfractures and micocallus

An increase in trabecular microfractures and free ends was also observed with increasing age. However, microcallus formation was seen only in individuals above 50 years of age (Figure 20). This is in agreement with the results of Vernon-Roberts and Pirie (1973) who also reported the incidence of microcallus to be higher in 4th lumbar vertebra than in the rest of the lumbar

spine. Hahn et al. (1989) observed microcallus formation in cases over 45 years of age. Microcallus can be detected even at the low magnification seen in Figures 13,14,15 and 18.

Microcallus was seen in vertical, horizontal and even in oblique trabeculae in later life (Figure 13). It has been reported that microfractures most frequently occur in the upper and lower thirds of the vertebral body (Vernon–Roberts and Pirie 1973, Hansson 1977). This was confirmed by the present study (Figure 18). This finding may be associated with the fact that there are more, fine, rod–like trabeculae in these regions which are more vulnerable to fracture than the thick plates at the centre. Microcallus formation was present, however, in all regions of the vertebral body and even in the mid–horizontal trabeculae described earlier.

The morphology of the callus was dependent upon the diameter of the trabeculae on which it was formed. When it occurred on thin trabeculae (these were usually horizontal or oblique as in Figure 20), it presented as small nodes or fusiform lesions and angulated excrescences as described by Vernon–Roberts and Pirie (1973). When examined at high magnification, canals large enough for blood vessels could clearly be identified on the surface of the nodes.

Alternatively, when callus appeared on thick vertical trabeculae it had the "cauliflower" appearance seen in Figure 15. Higher magnification showed a large number of perforations on such microcallus. On very thick vertical trabeculae, it presented as mineral aggregates on one surface only, which may sometimes mark the beginnings of the formation of microcallus. In a sample where collapse of the vertebral body had occurred, callus formation was found across the section – the so called bridge callus formation. The callus in this instance linked several trabeculae around the region. However, bridge callus formation was not observed even in severe osteoporotics unless collapse or wedging of the vertebra had taken place. Therefore, the bridge callus formation may have occurred as a result of a collapse, and, whilst, as Hahn et al. (1989) have suggested, the microcallus formation may show the compensatory possibilities of the bone that is still intact, bridge callus formation should not be taken uncritically as an architectural reform. The formation of fine trabecular networks around existing thick trabeculae was also observed in several old samples. These may be the beginnings of formation of microcallus. However, it is doubtful if bridge callus formation and formation of fine trabecular elements would form a functionally effective structure which would replace the complex architecture that existed earlier.

When partially formed microcallus was examined under high magnification, it was not possible to detect microfractures on the trabeculae on which the callus was forming. The evidence for a microfracture may perhaps have been covered, or difficult to detect if no displacement had occurred. On the other hand, microfracture may not be the only stimulus for the formation of microcallus. Hahn et al. (1989) suggested that the appearance of microcallus may be an indication of changed stability of the vertebral body through loss of structure and quality of bone. It could be that the loss of connectivity which would result in greater fragility (Heany, 1988) and accumulation of microdamage (Frost, 1973, 1985) may play a significant role in the formation of new bone.

3.3.6 Changes in the length of horizontal trabeculae.

Figures 21–23 present the values for lengths of horizontal trabeculae calculated at three zones for different age groups. Long horizontal trabeculae at the middle zone are clearly evident in the normal samples (Figures 21A and B). In the male sample, the range of mid horizontal trabeculae was from 0.67 to 1.21mm and at the peripheral zones it was from 0.47 to 0.78mm. In the female sample, the length at the middle zone varied from 0.44 to 1.24mm, and at the periphery from 0.28 to 0.90mm.

When an old, clinically non–osteoporotic male was considered (Figure 22A), the general pattern of the normal bone was maintained, but the overall length of the trabeculae had markedly increased (the range at the middle zone was from 0.70 to 1.83mm and at the periphery from 0.54 to 1.4mm). However, a clinically non–osteoporotic woman (Figure 22B), presented a completely different picture: the length of the horizontal trabeculae of the middle zone ranged from 0.73 to 1.33mm, and at the peripheral zones from 0.63 to 1.78mm. In this case not only has the normal pattern changed, but the inferior zone consists of very long horizontal trabeculae when compared with the other two zones.

Similar changes were also observed in both male and female, clinically confirmed, osteoporotics (Figures 23A and B). In the osteoporotic male, horizontal trabeculae at the middle zone ranged from 0.65 to 1.78mm and at the periphery from 0.76 to 2.67mm, with the inferior zone having the longest trabeculae. In the female osteoporotic, the middle zone trabeculae ranged from 0.98 to 1.83mm and the peripheral zones from 0.86 to 2.40mm. The superior and inferior zones in this case had very long horizontal trabeculae compared with that of the middle zone. The above analysis confirms the earlier observations in this study on the sizes of horizontal trabeculae at different zones and their changes with age and osteoporosis.

A measure of length of horizontal trabeculae is the same as a measure of distance between the vertical trabeculae. Previous studies using different methods have demonstrated a highly significant age–related increase in this distance (Mosekilde 1988). In samples used for the analysis in figures 21–23, increase in the horizontal trabecular lengths was calculated. Table I presents ratios of the mean length of horizontal trabeculae in old and osteoporotic samples divided by the mean length in young samples at different zones in both males and females.

ZONE	OLD/YOUNG		OSTEOPOROTICS/YOUNG	
	MALE	FEMALE	MALE	FEMALE
SUP.	1.36	1.48	1.57	2.70
MID.	1.15	1.17	1.29	1.63
INF.	1.44	2.33	2.56	2.83

TABLE I

*The increase in vertical trabecular spacing at different zones of old (non-osteoporotic) and osteoporotic samples
(The ratio of mean length of horizontal trabeculae in old and osteoporotic samples divided by mean length in young samples).*

These data indicate an increased vertical trabecular spacing at superior and inferior zones compared to the middle zone, confirming the architectural changes described earlier.

Irrespective of vertebral body size, very long horizontal trabeculae could usually be observed in old and osteoporotic samples. However, no correlation was detected between vertebral body size and the length of the horizontal trabeculae in normal samples of younger age. The decisive factor of the length of the horizontal trabeculae is the spacing among vertical trabeculae. The number and the size of the vertical trabeculae are determined by the original pattern of ossification which in turn depends on the pattern of the vasculature of the vertebral body. Therefore, different patterns of vascularisation during development would give rise to different sizes and numbers of vertical trabeculae, which would in turn vary the sizes and lengths of the horizontal trabeculae irrespective of vertebral body size. However, barely any research has been carried out to relate the different patterns of vasculature during development to the differences in trabecular bone architecture of the vertebral body. More extensive work will be necessary to understand this process completely and its significance for the competence of the bony structure at advanced age.

3.3.7 Changes in the number of vertical and horizontal trabeculae with age

Figures 24–27 show the relationship between age and the number of horizontal and vertical trabeculae per centimetre of the section. The horizontal trabeculae were counted along the central axis of the vertebral body (plane G–H of Figure 1). There was a highly significant decrease in the number of horizontal trabeculae with age in both males and females ($r=-0.873$, $p<0.002$ and $r=-0.865$, $p<0.002$ respectively)(Figures 24A and B).

A highly significant decrease in vertical trabeculae was observed in the superior zone (plane A–B of Figure 1) in both males and females ($r=-0.816$, $p<0.002$ and $r=-0.865$, $p<0.002$ respectively: Figures 25A and B).

A highly significant decrease was also apparent in the inferior zone (plane E–F, Figure 1) in both sexes ($r=-0.809$, $p<0.002$ and $r=-0.859$, $p<0.002$ respectively) (Figures 27A and B).

In the middle zone (plane C–D of Figure 1), the decrease in vertical trabeculae with age is more and more significant in females than males ($r=-0.817$, $p<0.002$ and $r=-0.662$ $p<0.01$ respectively: Figures 26B and 26A). Within the male group, the decrease in the middle zone is less pronounced than in the other two zones.

3.3.8 Biconcavity index

When the relationship between the biconcavity index and age was considered, a significant decrease in the index was observed in male samples ($r=-0.596$, $p<0.01$) (Figure 28A). This decrease was not statistically significant in females ($r=-0.262$: Figure 28B) even though there was a negative correlation between the biconcavity index and age. This suggests that the decrease in trabecular elements and the change in architecture in a vertebral body is more advanced than would be indicated by its biconcavity index. A vertebral body with a normal biconcavity index could already be advanced in the process of removal of trabecular elements and a body with a slight decrease in the index may be in an advanced stage of osteoporosis. Therefore, biconcavity index is not a reliable method of assessing architectural changes in the vertebral body. This is in agreement with Arnold (1973), who found that biconcavity appears to increase if there is a decrease in trabecular bone, but is not related to whether or not collapse fractures are present. He proposed that biconcavity develops progressively once bone loss has occurred and is, therefore, a measure of the duration of osteoporotic state rather than an index of its presence.

3.3.9 Osteoporotic state

Clinically, osteoporosis means that the subject has a lower bone mass than might be expected from age and sex norms and an increased risk of fractures (Woolf and Dixon 1988). The disease state is usually identified by spontaneous fractures of the vertebrae or long bones.

Arnold (1973), in a study of trabecular bone density, concluded that below 0.07 g ash/cm³ of medullary tissue represents a pathologic level that can be termed the osteoporotic state. However, he observed that not all patients below the osteoporotic threshold had fractures. Therefore, some factor other than decreased bone mass must be responsible for the development of fractures in clinical osteoporosis. Further, he deduced that in the presence of a single fracture in the lower spine, there is a 50 per cent chance that the vertebral mineral content is normal. Arnold also suggested that physical exertion and trauma may play a role in male vertebral collapse cases where trabecular bone concentration is above the threshold value.

At the present time, bone mass measurements are used to diagnose the osteoporotic state. There is an extensive overlap in bone mass values between normal and osteoporotic persons and this overlap is found for all of the bone mass measurement technologies (Heaney 1989). Further, it

is not always possible to find the expected correlation between severity of osteoporosis and the degree of bone loss (Pødenphant et al. 1987).

Cummings (1987) reported similar results in hip fracture patients. He suggested that factors besides decreased bone mineral density must also play an important role in hip fractures and he attributed the increased risk of fractures with aging to the increased risk of falling and patterns of falling.

Heaney (1989) concluded that a 10–40% reduction in bone mass, as is commonly found in osteoporosis, is insufficient to explain the fragility which osteoporotic bone typically exhibits. While reviewing the discrepancies in this mass-based theory of osteoporosis he composed a hypothesis including fatigue damage and trabecular connectivity as two important factors that contribute to the increased bone fragility. Heaney (1987) also presented a detailed discussion on the role of bone quality and fatigue damage as important factors in developing osteoporotic fractures.

Kleerekoper et al. (1987) concluded that the age-related decline in cancellous bone mass is associated with age-related changes in the overall architecture of cancellous bone. The age-related decline in mechanical competence of cancellous bone is greater than can be accounted for by the age-related decline in mass alone, but can be more completely accounted for by the decline in mass combined with the alteration in architecture. Thus they proposed that the limited ability of bone mass measurements to distinguish between patients with and without osteoporotic fractures can in part be accounted for by an alteration in cancellous bone architecture that cannot be detected by simple measurements of cancellous bone mass. Kleerekoper et al. (1987) also noted that an increased separation and decreased connectivity with reduction in the number of trabecular bars and plates is the major structural change in cancellous bone architecture with age. Heaney (1989) grouped compression fractures of the spine as those with low values for mass and a high degree of trabecular disconnection, and femoral neck fractures as those with low bone mass and accumulated fatigue damage.

Although all these recent research findings emphasise the importance of changing trabecular bone architecture during aging and osteoporosis, the exact nature of these changes has not been clearly understood.

Arnold (1970) observed that the pattern and number of trabeculae in osteoporosis produced by steroid therapy is apparently normal and the reduction in bone mass is produced by a uniform narrowing of the individual trabeculae to a thread-like appearance. In contrast to this, a progressive loss of individual trabeculae or bone structure was encountered with aging and was seen as the end product of postmenopausal or senile osteoporosis.

From the results of both histological and biochemical studies it has been postulated that age-related bone loss in women is predominantly due to increased bone resorption (Nordin et al. 1981, Hodgkinson et al. 1982), while decreased bone formation is responsible for bone loss in men (Hodgkinson et al. 1982). Aaron et al. (1987) confirming these results, have also shown that age-related bone loss in women is associated with a reduction in trabecular number without change in trabecular width: in men trabecular width reduced with age with no loss in trabecular number.

Similar results have been obtained by Compston et al. (1987). Based on the above results, it has been assumed that the structural integrity of trabecular bone is preserved in men, but not in women (Francis 1987).

Contrary to the above views, uniform thinning without removal of trabecular elements was observed in the present study in both old men and women. Both thinning and removal of trabeculae were observed in both sexes in osteoporotic cases (Figures 13, 19). It has to be borne in mind that Aaron et al. (1987) derived their conclusions from histomorphometric analyses of iliac crest biopsies and by comparing only limited areas of vertebral body sections. It is doubtful how far it is possible to understand a complex three dimensional structure of trabecular bone by two dimensional histomorphometric analysis. Hahn et al. (1989) developed a new technique which allowed simultaneous observation of the two dimensional surface and the three dimensional structure underneath: they showed that the surface picture can be misleading as to the nature of the three dimensional structure. When trabeculae with similar dimensions and patterns were encountered in two dimensional sections, their underlying structure could be quite different; one being plate-like in form as in normal bone and the other rod-like as in osteoporotic bone. Consequently, it will often be incorrect to relate the results derived from thin sections of trabecular bone to its three dimensional architecture.

As noted earlier, extensive regional variations exist in mid-sagittal sections of a vertebral body. It is often not too difficult to find a region which is plate or tube-like (which we usually term normal bone) and a region of rod or needle-like elements (as in "osteoporotic" bone) in the same vertebral section. In a comparative study, therefore, a reasonable assumption can be made only if the same region is compared in different specimens. This is also true for the superior and inferior zones of the vertebral body. Due to extensive developmental variations, the normal regional structure will vary most widely in the middle zone. This degree of developmental variation also implies that the result may still be far from satisfactory even if an histomorphometric analysis is performed on the whole vertebral section.

It should be further noted that the pattern of trabecular bone architecture at any one site may be very different from an other. Development, the mechanical loading history and functional importance may be some of the factors that decide this pattern. With aging the effect of systemically acting factors may be uniform on all these sites, but locally acting factors could be very different and the architectural change that occurs with aging and osteoporosis would therefore be different from site to site. While bone mass (TBV) measurement at a site such as the iliac crest might give some indication about bone loss in the spine, architectural changes such as trabecular thinning and loss of connectivity in the iliac crest might consequently not give correct information about analogous changes in the spine. In an analysis of trabecular bone architecture of the vertebral body therefore, it could be stated that only a three dimensional analysis of whole sections would produce results with a reasonable accuracy and reliability.

It is generally accepted at the present time that bone loss occurs by conversion of plates to rods followed by complete removal of the trabecular elements. However, Vogel et al. (1989) showed that the bone volume depends almost entirely on the number of plates, whereas there is no

(or even an inverse) relation between bone volume and the number of rods. Hahn et al. (1989) also found that the number of rod-like trabeculae is constant in every decade. They also considered the appearance of perforations as the main mechanism for conversion of plates to rods.

Reduction in the number of plates can easily be observed with increasing age. However, no method has yet been developed to quantify this reduction because of the extensive variations in the form of trabecular plates in different samples. Plates of different sizes usually exist in normal bone and it is virtually impossible to draw a line which will distinguish plates and rods. Furthermore, different numbers of horizontal plates usually exist and they appear as rods in sagittal sections. They are commonly encountered under the vertebral end plates. Due to non-uniformity in loss of rods, it is also impossible to quantify their disappearance. Similar reasons also make it difficult to quantify the appearance and progression of perforations on the plates and rods.

All this suggests the need for an analysis of three dimensional architecture or connectedness; it may be pointless to quantify bits and pieces of trabecular bone unless they are seen in context. Again, the answer lies with a complete three dimensional analysis.

From the present study, it could be suggested that the total removal of trabeculae during osteoporosis may preceded by generalised thinning of trabeculae in both sexes. This could be true of the Type II osteoporotic cases (Riggs and Melton 1983) that were examined. Nevertheless, in Type I osteoporotics it may be possible to see the complete removal of trabecular elements due to the high rate of bone resorption at a much younger age than in normal females. In this instance it will be hardly possible to see uniform thinning prior to complete removal. It could be that failure to make this distinction may have led to the belief that the main mode of bone loss in females is by complete removal of trabecular elements.

What are the possible mechanisms responsible for selective removal of trabeculae? Arnold (1970) pointed out that the action of a local factor may be more important for the focal excessive resorption than systemically acting factors and mechanical loading. The effect of systemically acting endocrine and nutritional factors may be diffuse (if close proximity of a piece of bone to a blood vessel is not considered) on all the surfaces of trabecular bone. The role of decreased mechanical stress in explaining the excessive resorption appears to be more likely secondary rather than primary. The local factors that change the micro-environment of the trabeculae could be changes in vascularity, changes in pressure, or the production of different agents (such as cytokines) by the local cell community. Resorption relating to increased pressure has usually been observed in cases with bone tumours. However, the focal effect of changing vascularity with age is not well known.

3.3.10 Implications of changing vascularity of lumbar vertebral bodies with age

According to Ratcliffe (1982) there is a very extensive intra-osseous arterial anastomotic network in the vertebral body in infants. In normal adults and adolescents the intra-osseous arteries are end arteries. The virtual absence of vertebral osteomyelitis in children under the age of nine has been correlated with the occurrence of extensive intra-osseous arterial anastomosis. A

septic embolus in adults will result in infarction of a wedge of bone in the metaphysis and vertebral osteomyelitis may therefore be segmental.

Ratcliffe (1986) also carried out extensive work on arterial changes in the vertebral body associated with aging. He reported that two types of intra-osseous arteries are found in the adult, peripheral and central, whereas in children only central arteries are found. The number of peripheral arteries in the vertebral bodies increases with age, and this alters the direction of blood flow from centrifugal to centripetal in the aged vertebral bodies. He suggested that the reversal of the direction of the flow may alter the surface charge on the vertebral body, which might have implications for the mineralisation of the vertebral body and possibly for the distribution of collagen fibres. Further, the central arteries in aging vertebral bodies become very tortuous and coiled and this results in an alteration of the intra-osseous haemodynamics. The increased resistance to flow results in ischaemia, which in turn may be a stimulus for the growth of new arteries that would grow in from the periosteal arteries. The coiled arteries lie enclosed within a delicate connective tissue sheath which varies with the degree of distension of the arteries. The coils and their sheaths will modify the height of the pulse wave within the artery, and in effect transfer kinetic energy from the artery wall to the surrounding extracellular fluid within the vertebral body. This causes agitation of the extracellular fluid, which is more marked in the elderly (Ratcliffe 1986). Such changes will undoubtedly alter the micro-environment around the trabeculae, but it is still not clear what effect this would have on bone turnover and the selective removal of trabeculae during osteoporosis.

Batson (1957) classified the veins of the human body into two principal groups: those within the pressure chamber of the thoraco-abdominal cavity, and those outside this cavity. The "vertebral vein system of Batson" lies outside the cavity. This system parallels, joins, and at the same time bypasses, the cavity veins. Like the azygos vein, it unites the superior vena cava to the inferior vena cava, but lies outside the pressure cavity. With every rise of pressure in the trunk, as during lifting, coughing, sneezing, bending or any rotational manipulation of firmness, venous blood is not only prevented from entering the thoraco-abdominal cavity but is actually shunted to the vertebral vein system.

Farfan (1975) suggested that a combination of raised intra-abdominal pressure and the presence of the posterior longitudinal ligament together impede the rate of outflow of blood from the vertebral body, and thereby increase its crush strength. The pressure within the vertebral body therefore varies with the activity status of the person.

The patterns of veins at the middle zone of the vertebrae vary extensively even within the normal specimens used during this study. The basivertebral vein was not always present as a nutrient vessel, but sometimes as an emissary vein draining through the vertebral body. The direction of blood flow is not always constant because these veins do not have valves. Venous engorgement and thinning of walls of the veins is a common finding with aging. Matsuo (1985) observed total circumferential thinning of the anterior internal vertebral vein with age. Macnab (1971) related the occurrence of venous engorgement and stasis of venous blood in the aging vertebral bodies to the back pain experienced in osteoporosis. Macnab (1977) also observed that

the size of the unwedged vertebral body is unchanged while the bone mass is markedly diminished so that the volume of its contents must be greater. Since the fat content of the vertebral body usually does not change, the amount of blood, and therefore venous stasis, is increased. The results of the present study also support this view. It was observed that the walls of the vertebral body had not collapsed even when mass destruction of trabeculae within the vertebral body had taken place with a resultant increase in inter-trabecular spacing. The analysis of the biconcavity index also confirms this conclusion.

Macnab (1977) also found that the intra-osseous venous pressure of a normal vertebra is about 28 mm Hg (3.73 kPa) and that of an osteoporotic vertebra is about 40 mm Hg (5.33 kPa). This increase in intra-osseous hypertension could be a reason for low back pain in osteoporosis. Arnoldi (1976) suggested that intra-osseous hypertension plays a significant role in osteoarthritis of the extremities and the spine. Degenerative changes in the intervertebral disc may also be caused by arteriolar thrombosis and venous obstruction in the vessels supplying cancellous bone deep to the end plates (Helfet et al. 1978).

It is interesting to see what structural changes in trabecular bone would be brought about by the vascular changes of aging. In their studies of osteoarthritis of the hip, Arnoldi et al. (1972) reported that circulatory derangement may be responsible for structural changes of trabecular bone such as the necrosis, signs of osteogenesis, cyst formation and interstitial oedema that are found in this condition. Further, they also showed that intermittent intramedullary hypertension may lead to changes in trabecular and cortical bone in the ankle region. The changes they observed were apposition of new layers of periosteal bone as osteophytes and a mixture of rarefaction and sclerosis of the lamellae of trabecular bone. There is also evidence from other sites such as the patella (Darracott and Vernon-Roberts 1971) where osteoporosis was most marked in the region of the major vascular supply. In animal experiments, Brookes and Helal (1968) were able to produce structural changes in the trabecular bone of the femur of adult rats by ligation of the major veins of the limb.

This evidence suggests that the vascular changes that take place during the process of aging and the development of osteoporosis may contribute to the observed structural changes in trabecular bone. Intra-osseous hypertension may perhaps be a major factor contributing to the resorption of trabeculae at the focal level. It is also possible that the collapse of the already weakened trabecular network within the vertebral body could take place during a sudden rise in intra-osseous venous pressure without a collapse of the walls of the vertebral body. Future research into structural changes of trabecular bone should therefore also give proper attention to the effect of changing vascularity on the vertebral body.

In experiments with rat tails, Kery et al. (1971) found that lesions of bone and cartilage following venous stasis were more severe than those produced by arterial ischaemia of the same duration. The potential of the tissues to repair was also more depressed by venous stasis than by arterial ischaemia. This suggests that more emphasis should be placed on venous than arterial aspects of the circulation in future work.

Finally, the status of the general circulation also may play a part in the pathogenesis of

spinal osteoporosis. A significant positive relationship between the degree of aortic calcification and frequency of spinal fractures was found in a study of 281, 70 year-old females (Jensen et al. 1986). These authors suggested that local vascular factors partly determine the occurrence of osteoporosis and that spinal osteoporosis might accelerate due to atherosclerosis in the regional nourishing vessels. However, confirmation of these results also demands more extensive research on changes in vascularisation with aging and during osteoporosis.

3.4 CONCLUSION

In an analysis of the three dimensional architecture of trabecular bone, two dimensional techniques including the limited reconstructions of the third dimension from data so far obtained from such techniques are of limited value. A simple technique employing stereophotographs of whole sections of lumbar vertebrae provided an excellent method of dealing with this problem.

The method enabled a detailed description of the three dimensional structure of the normal 4th lumbar vertebral body and its changes with aging and osteoporosis. The normal structure varied from sample to sample especially in the central zone, possibly depending upon the prior history of vascularisation and patterns of ossification during development.

Long horizontal trabeculae differing from those of the peripheral zones were observed in the middle zone of the vertebral body. The parallax measuring facility of the stereoscope enabled the calculation of real lengths of horizontal trabeculae from stereophotographs. A highly significant, age related decrease in the number of both vertical and horizontal trabeculae was also observed in both sexes. The results of this morphometric analysis also supported the observed architectural change with aging and in osteoporosis.

A different pattern was produced in osteoporotic samples by the removal of horizontal and selected vertical trabeculae followed by a thickening of the remaining vertical trabeculae in the peripheral zones. Very long, thin horizontal trabeculae were formed in all three zones during this process.

The observation of osteoporotic architecture in both non-osteoporotic old specimens and clinically confirmed osteoporotic specimens points out the inadequacy of the clinical criterion of the occurrence of a fracture in judging the osteoporotic state.

Osteoporosis has an architectural face. A patient can be judged as osteoporotic by bone mass measurements, but the architecture of the vertebral body can be normal and it is unlikely that the patient will develop a crush fracture due to the greater stability of this structure. Similarly, a patient can be normal according to bone mass measurement, but may have already developed osteoporotic architecture in a vertebral body, so that a crush fracture would be inevitable. Such contradictions would probably explain the overlap usually seen in bone mass measurements and the incidence of spontaneous crush fractures of the spine. While treatment of osteoporosis can increase the bone mass, no known treatment can restore the normal architecture once it is destroyed. This again emphasises the importance of prevention of osteoporosis over its treatment.

Attention is drawn to the influence of development on normal architecture of the vertebral body. To understand this process, different patterns of vascularisation and ossification during

Brooks M, Helal B (1968) Primary Osteoarthritis, venous engorgement and osteogenesis. *J Bone Joint Surg.* **50B**:493-504.

development should be studied thoroughly to relate these differences to the differences in the normal architecture of the vertebral body.

It is also important to investigate changing vascularisation during old age to understand the influence of these changes on the development of osteoporotic bone architecture. Intra-osseous hypertension and venous stasis could have especially important influences on trabecular bone remodelling during osteoporosis.

3.5 REFERENCES

- Aaron JE, Makins NB, Sagreiya K (1987) The microanatomy of trabecular bone loss in normal aging men and women. *Clin Orthop Rel Res* **215**:260–271.
- Amstutz HC, Sissons HA (1969) The structure of the vertebral spongiosa. *J Bone Joint Surg* **51B/III**:540–550.
- Arnold JS, Bartley MH, Tont SA, Jenkin DP (1966) Skeletal changes in aging and disease. *Clin Orthop Rel Res* **49**:17–38.
- Arnold JS (1968) External and trabecular morphologic changes in lumbar vertebrae in aging. In: *Progress in methods of bone mineral measurement*. Whedon GD, Cameron JR (eds) pp. 352–411.
- Arnold JS (1970) Focal excessive endosteal resorption in aging and senile osteoporosis. In: *Osteoporosis*. Brazel US (eds) Grune and Stratton, New York, pp 80–100.
- Arnold JS (1973) Amount and quality of trabecular bone in osteoporotic vertebral fractures. *Clin Endo Metab* **2**:221–238.
- Arnoldi CC, Linderholm H, Mussbichler H (1972) Venous engorgement and intraosseous hypertension in osteoarthritis of the hip. *J bone joint surg* **54B/III**:409–421.
- Arnoldi CC (1976) Intraosseous hypertension. *Clin Orthop Rel Res* **115**:30–34.
- Atkinson PJ (1967) Variation in trabecular structure of vertebrae with age. *Calcif Tissue Res* **1**:24–36.
- Batson OV (1956) The vertebral vein system. *Am J Roent* **78**:/II195–212.
- Bell GH, Dunbar O, Beck JS (1967) Variation in strength of vertebrae with age and their relation to osteoporosis. *Calcif Tissue Res* **1**:75–80.
- Bergot C, Preteux F, Laval-Jeantet AM (1987) Quantitative image analysis of thin sagittal and transversal slices from autopsy specimens of L3 vertebrae. In: *Osteoporosis 1987*. Christiansen C, Johansen JS, Riis BJ (eds) Virborg Denmark : Nohaven A/S pp 338–340.
- Bergot C, Laval-Jeantet AM, Preteux F, Meunier A (1988) Measurement of anisotropic vertebral trabecular bone loss during aging by quantitative image analysis. *Calcif Tissue Res* **43**:143–149.
- Bick EM, Copel W (1950) Longitudinal growth of the human vertebra. *J bone joint surg* **32A**:/IV803–813.
- Birkenhager-Frenkel DH, Courpron P, Hupscher EA, Clermonts E, Coutinho MF, Schmitz PIM, Meunier PJ (1988) Age-related changes in cancellous bone structure. *Bone and Mineral* **4**:197–216.
- Bullough PG, Boachie-Adjei O, (1988) *Atlas of spinal disease*. Gower Medical Publishing, New York London.
- Cann CE, Genant HK, Kolb FO, Ettinger B (1985) Quantitative computed tomography for prediction of vertebral fracture risk. *Bone* **6**:1–7.
- Cohen J, Curraino G, Nerhauserr EBD (1956) A significant variant in the ossification centres of the vertebral bodies. *Am J Roent* **76**:469–475.
- Compston JE, Mellish RWE, Garrahan, NJ (1987) Age related changes in iliac crest trabecular microanatomic bone structure in man. *Bone* **8**:289–292.
- Crock HV, Yoshizawa H, Kame, SK (1973) Observations on the venous drainage of the human vertebral body. *J bone joint surg* **55B**:/III528–533.
- Crock HV, Yoshizawa H (1976) The blood supply of the vertebral column. *Clin Orthop Rel Res* **115**:6–21.
- Crock HV, Yoshizawa H (1977) *The blood supply of the vertebral column and spinal cord in man*. Springer-Verlag, New York Wien.
- Cummings SR (1987) Epidemiology of hip fractures. In: *Osteoporosis 1987*. Christiansen C,

Martin DB (1966) Stereoscope with optical means of measuring parallax. *Int. Arch. Photogrammetry.* **16:III** 37-44.

- Johansen JS, Riis BJ (eds) Virborg Denmark : Nohaven A/S pp 40–44.
- Delling VG (1989) Neuere Vorstellungen zu Bau und Struktur der menschlichen Spongiosa–Ergebnisse einer kombinierten zwei–und dreidimensionalen Analyse. *Z gesamte inn Med*, Jahrg 44:Heft 18 536–540.
- Dunnill MS, Anderson JA, Whitehead R (1967) Quantitative histological studies on age changes in bone. *J Path Bact* 94:275–291.
- Farfan HF (1975) Muscular mechanisms of the lumbar spine and the position of power and efficiency. *Orth Clin N Amer* 6:135.
- Feldkamp LA, Goldstein SA, Parfitt AM, Jesion G, Kleerekoper M (1989) The direct examination of three dimensional bone architecture in vitro by computed tomography. *Bone* 4:13–11.
- Francois RJ, Dhem A (1974) Microradiographic study of the normal human vertebral body. *Acta Anat* 89:251–265.
- Frost HM (1963) Bone remodelling dynamics. Charles C Thomas Publishers USA.
- Frost HM (1964) The laws of bone structure. Charles C Thomas Publishers USA.
- Frost HM (1973) The spinal osteoporosis. *Clin Endo Metab* 2:II257–275.
- Frost HM (1985) Pathomechanics of osteoporosis. *Clin Orthop* 200:198–225.
- Galante J, Rostoker W, Ray RD (1970) Physical properties of trabecular bone. *Calcif Tissue Res* 5:236–246.
- Garrahan NJ, Mellish RWE, Compston JE (1986) A new method for the two dimensional analysis of bone structure in human iliac crest biopsies. *J Micros* 142:III341–349.
- Hahn M, Vogel M, Pompesius Kempa M, Delling G (1989) Kombinierte zwei–und dreidimensionale Analyse der Wirbelsäule als Grundlage für das Verständnis endokriner Knochenmassenverlust– Syndrome. Quintessenz Verlags GmbH Berlin.
- Hansson T (1977) The bone mineral content and biomechanical properties of lumbar vertebrae. Monograph, Dept. Orthopaedic Surgery, University of Göteborg, Sweden.
- Heaney RP (1987) Qualitative factors in osteoporotic fracture: the state of the question. In: Osteoporosis. 1987 Christiansen C, Johansen JS, Riis BJ (eds) Viborg Denmark : Norhaven A/S 281–287.
- Heaney RP (1989) Osteoporotic fracture space: an hypothesis. *Bone Mineral* 6:1–13.
- Helfet AJ, Grubel Lee DM, (1978) Disorders of the lumbar spine. JB Lippincott Co Philadelphia Toronto.
- Jensen GF, Boesen J, Transbol I (1986) Spinal osteoporosis: a local vascular disease? XIX European symposium on calcified tissues. Stockholm Sweden Abs–107.
- Kery L, Vizkelety T, Woutters HW (1971) Recherches experimentales a' propos de l'effect de la stase veineuse sur los, le cartilage et le disque intervertebral. *Rev de Chir Orthop* 57:8.
- Kleerekoper M, Villanueva AR, Staneiu J, Sudhaker Rao D, Parfitt AM (1985) The role of three dimensional trabecular microstructure in the pathogenesis of vertebral compression fractures. *Calcif Tissue Int* 37:594–597.
- Kleerekoper M, Feldkamp LA, Goldstein SA, Flynn MJ, Parfitt AM (1987) Cancellous bone architecture and bone strength. In: Osteoporosis 1987. Christiansen C, Johansen JS, Riis BJ (eds) Viborg Denmark : Norhaven A/S 294–300.
- Lindahl O, Lindgren GH, (1962) Grading of osteoporosis in autopsy specimens. *Acat Orthop Scand* 32:85–100.
- Macnab I (1971) The mechanism of spondylogenic pain. In: Hirsh C, Zotterman Y eds. Cervical Pain, Pregman press, Oxford.
- Macnab I (1977) Backache. William and Wilkins, Baltimore.
- Matsuo H (1985) Venographic findings on changes in the lumbar anterior internal vertebral vein with regard to age. *Nippon Ika Daigakuzasshi* 52:VI633–641.
- Mosekilde L (1988) Age–related changes in vertebral trabecular bone architecture – Assessed by a new method. *Bone* 9:247–250.
- Mosekilde Li, Mosekilde Le, Danielsen CC (1987) Biomechanical competence of vertebral trabecular bone in relation to ash density and age in normal individuals. *Bone* 8:79–85.
- Parfitt AM, Mathews CHE, Villanueva AR, Kleerekoper M, Frame B, Rao DS (1983) Relationship between surface, volume, and thickness of iliac trabecular bone on aging and in osteoporosis: implications for the microanatomic and cellular mechanism of of bone loss. *J Clin Invest* 72:1396–1409.
- Pesch HJ, Henschke F, Seibold H (1977) Einfluss von Mechanik und Alter auf den Spongiosumbau in Lendenwirbelkörpern und im Schenkelhals. *Virchows Arch A Path Anat and Histol* 377:27–42.
- Pødenphant J, Heress Nielsen VA, Riis BJ, Gotfredsen A, Christiansen C (1987) Bone mass, bone

Twomey L, Taylor J, Furniss B (1983) Age changes in the bone density and structure of the lumbar vertebral column. *J Anat* **136**:115-25.

- sturcture and vertebral fractures in osteoporotic patients. *Bone* **8**:127–130.
- Pompsius–Kempa M, Hahn M, Vogel M, Delling G (1989) Neue Untersuchungen zur Mikroarchitektur der Spongiosa bei Osteopathien im Vergleich zu altersbedingten Veränderungen. Willert HG, Heuck FHW (Hrsg) *Neuere Ergebnisse in Osteologie*. Springer–Verlag, Heidelberg.
- Pugh JW, Rose RM, Radin EL (1973) Elastic and viscoelastic properties of trabecular bone: dependence on sturcture. *J Biomech* **6**:475–485.
- Ratcliffe JF (1980) The arterial anatomy of the adult human lumbar vertebral body *J Anat* **131**:/I57–79.
- Ratcliffe JF (1982) An evaluation of the intra–osseous arterial anastomoses in the human vertebral body at different ages. A microarteriographic study. *J Anat* **134**:373–382.
- Ratcliffe JF (1986) Arterial changes in the human vertebral body associated with aging. *Spine* **11**:/III235–240.
- Riggs BL, Melton LJ (1983) Evidence for two distinct syndromes of involuntional osteoporosis. *Am J Med* **75**:899–901.
- Schinz HR, Tondury G (1942) Zur Entwicklung der menschlichen Wirbelsäule; die FrÜhossifikation der Wirbelkörper. *Fortschr a d Geb d RÖntgenstrahlen* **66**:253–289.
- Schmorl G, Junghanns H (1975) *The human spine in health and disease*. Grune and Stratton, NewYork and London.
- Singh I (1978) The architecture of the cancellous bone. *J Anat* **127**:/II305–310.
- Tanaka T, Uhthoff HK (1981) The pathogenesis of congenital vertebral malformations. *Acata Orthop Scand* **52**:413–425.
- Tanaka T, Uhthoff HK (1983) Coronal cleft of vertebrae, A varient of normal endochondral ossification. *Acta Orthop Scand* **54**:389–395.
- Vernon–Roberts B, Pirie CJ (1973) Healing trabecular microfractures in the bodies of lumbar vertebrae. *Ann Rheum Dis* **32**:406–412.
- Vesterby A, Gundersen HJG, Melsen F (1989) Star volume of marrow space and trabeculae of the first lumbar vertebra : Sampling efficiency and biological variation. *Bone* **10**:7–13.
- Vogel M, Hahn M, Pompesius–Kempa M, Delling G (1989) Trabecular microarchitecture of the human spine. *Neuere Ergebnisse in der Osteologie*. Springer–verlag, Heidelberg, 449–455.
- Wakamatsu E, Sissons HA (1969) The cancellous bone of the iliac crest. *Calc Tissue Res* **4**:147–161.
- Whitehouse WJ, Dyson ED, Jackson CK (1971) The scanning electron microscope in studies of trabecular bone from a human vertebral body. *J Anat* **108**:/III481–496.
- Wiley AM, Trueta J (1959) The vascular anatomy of the spine and its relationship to pyogenic vertebral osteomyelities. *J Bone Joint Surg* **41B**:796–809.
- Williams PL, Warwick R, Dyson M eds. (1989) *Gray's Anatomy* (37th edition) Churchill Livingstone, Edinburgh, London, Melbourne, NewYork.
- Willis TA (1949) Nutrient arteries of the vertebral bodies. *J Bone Joint Surg* **31A**:/III538–540.
- Woolf AD, Dixon A St John (1988) *Osteoporosis – A clinical guide*. Martin Dunitz, London.

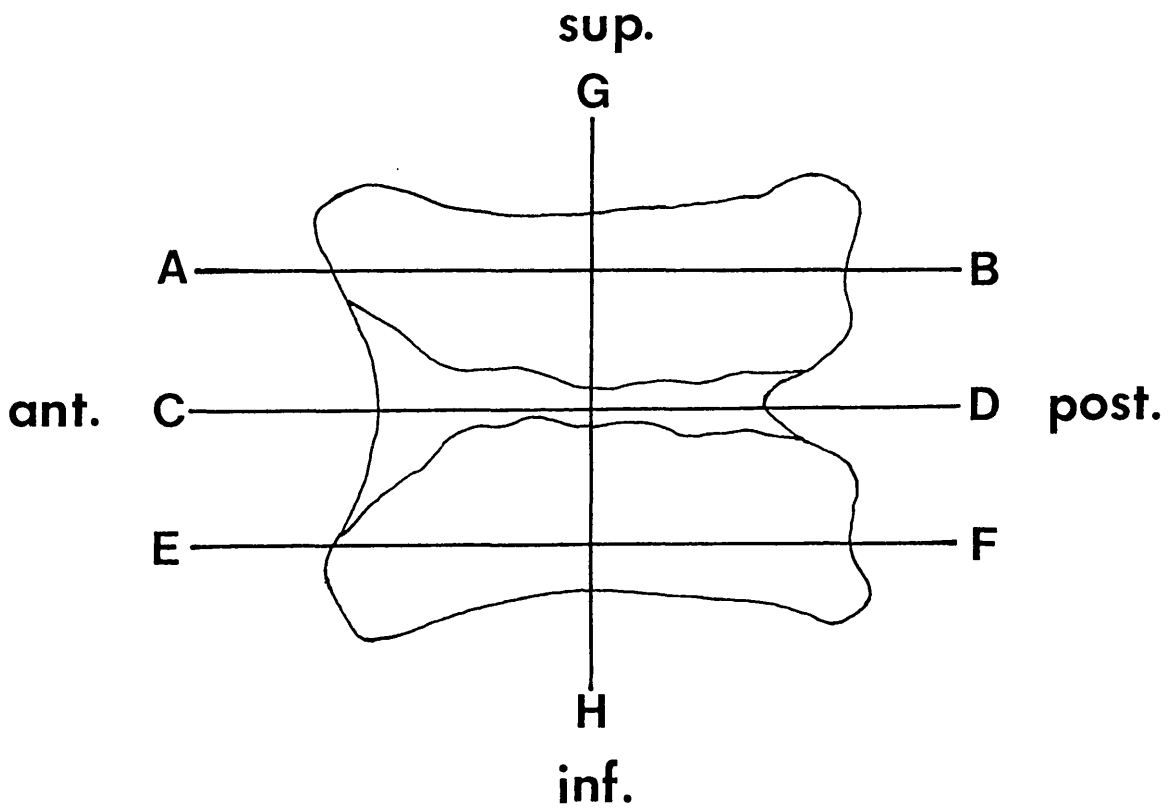


Fig. 1 A drawing of a Mid-sagittal section of a 4th lumbar vertebra showing planes at which trabeculae were counted.

Fig. 2 31 yr male. Mid-sagittal section. The three zonal distribution of trabeculae is apparent in this section. The middle zone is composed of vertically oriented cylinders, while the peripheral zones are dominated by a more rod like, cross-braced structure. The rod shaped trabeculae are longer at the middle zone compared with peripheral zones. Note that vertical trabeculae arise from respective walls (anterior or posterior) at extreme corners of the section. x3.8

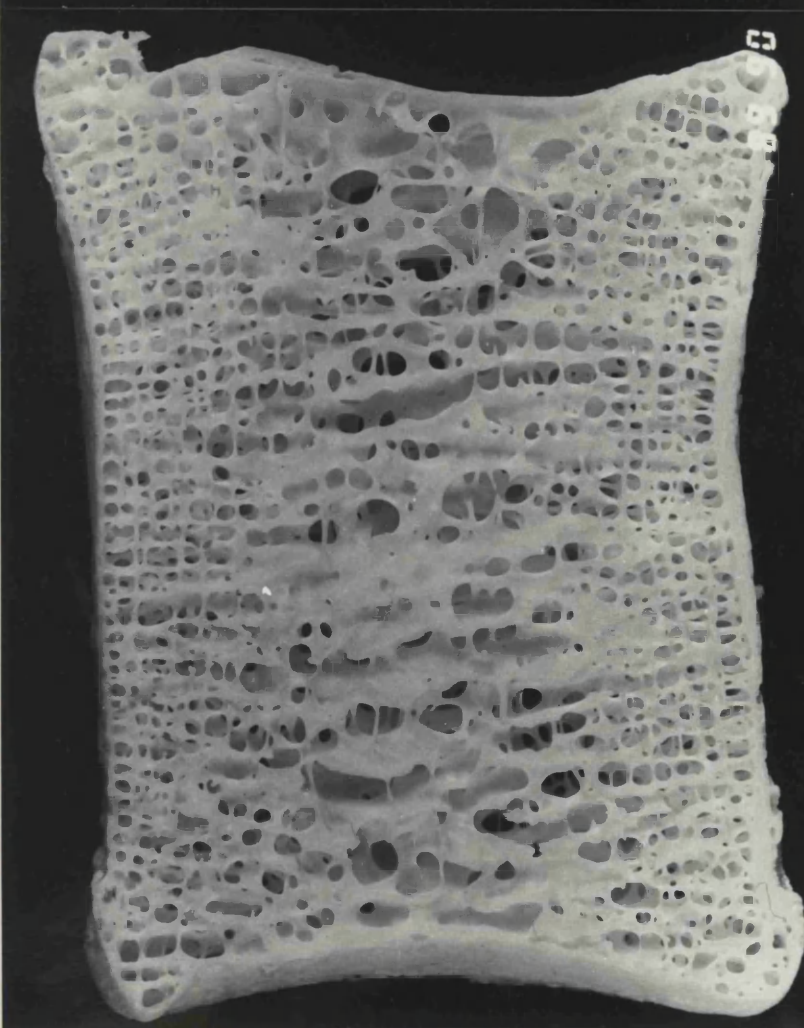
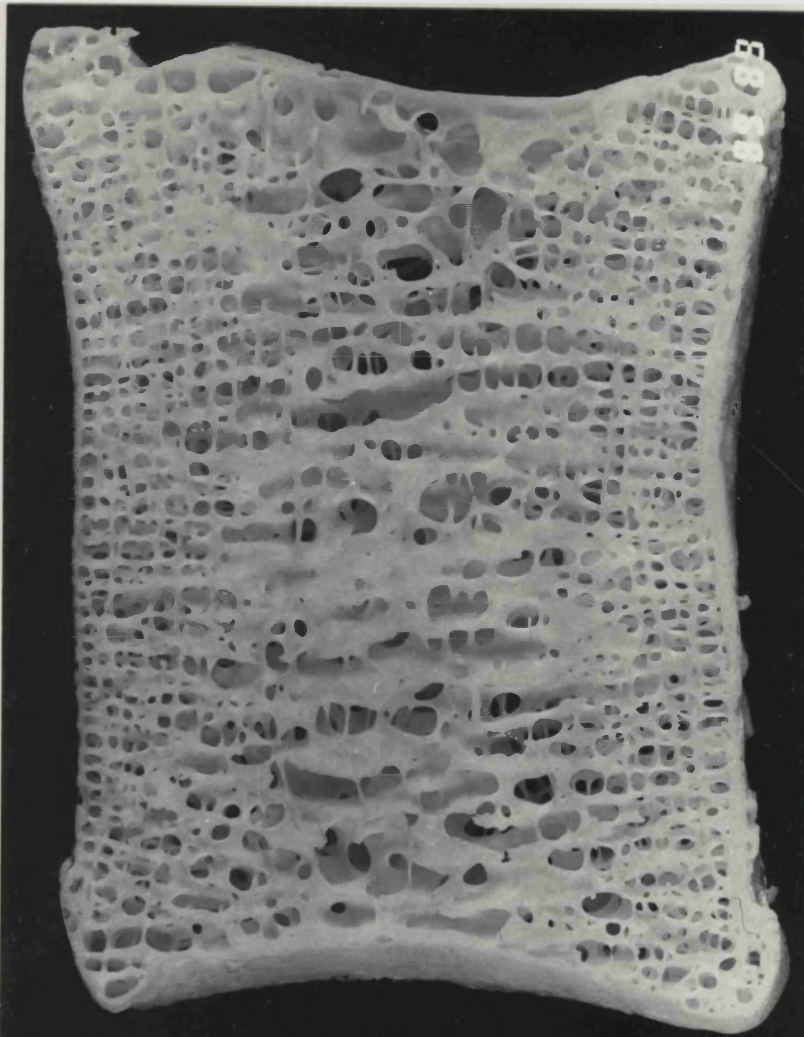
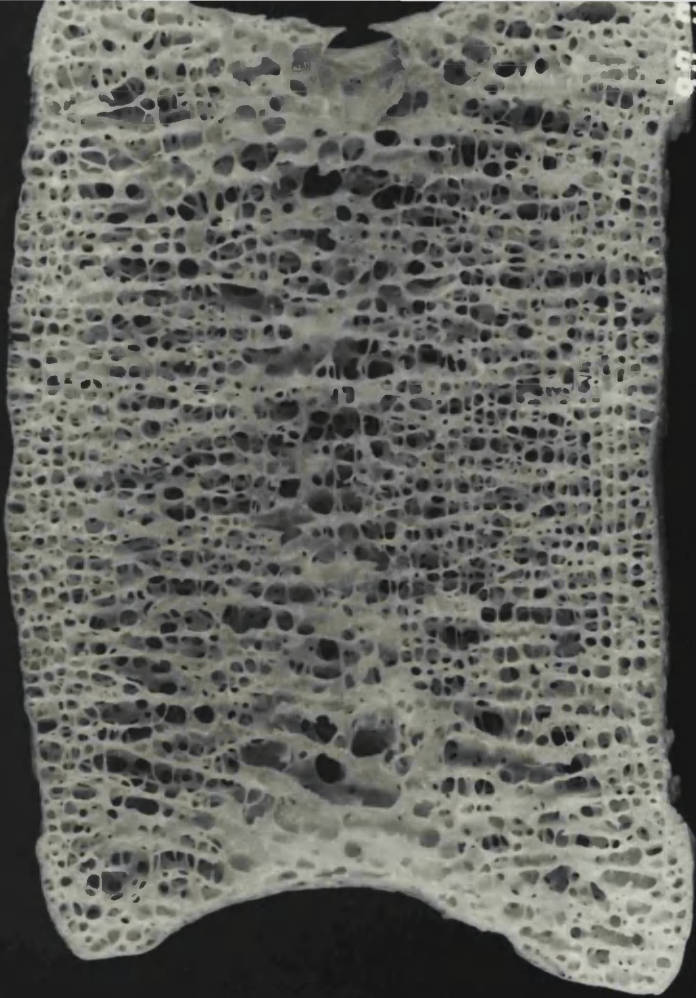
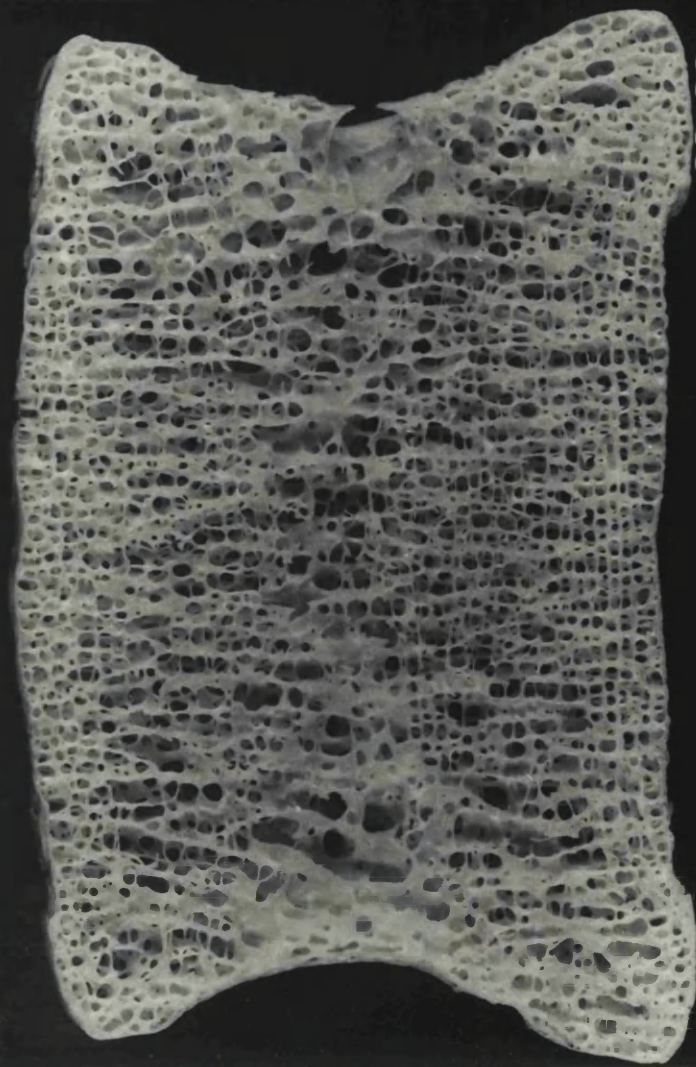


Fig. 3 30 yr female. Coronal section through midpoint of the vertebral body. A narrow central zone with several antero-posteriorly directed canals for blood vessels can be recognised in this section. The peripheral zones show an approximately uniform cross-braced structure. The vertical trabeculae arise from lateral walls at extreme corners. Note that cortical bone is virtually absent in this section. x3.3



20 05



20 05

Fig. 4 30 yr female. Horizontal section through the middle zone. Large diameter holes resembling horizontally cut cylinders and long horizontal trabeculae can be recognised at anterior and lateral regions of the section. At the centre, small diameter holes are bounded by more or less rod shaped trabeculae. The trabeculae are gradually thickened postero-laterally towards the vertebral arch region. Note two canals for blood vessels are directed centrally and posteriorly from lateral walls. x3.2.

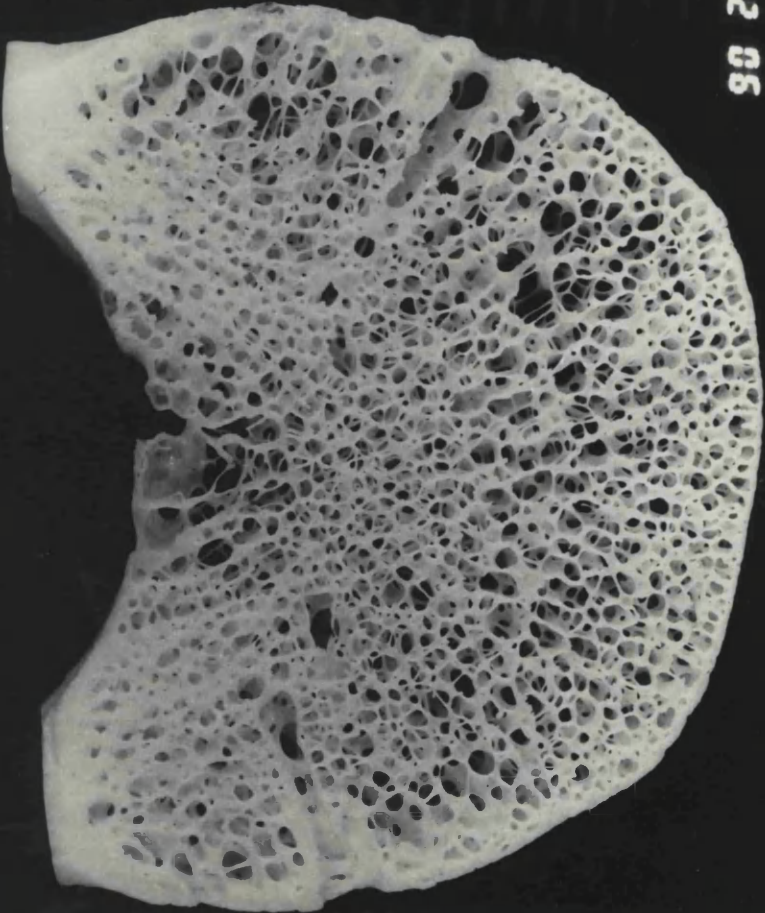


Fig. 5 30 yr female. Horizontal section through the superior zone of the same vertebral body in the figure 5. Unlike the mid–horizontal plane (figure 5), a large number of smaller diameter cylinders can be seen at this plane. Horizontal trabeculae are also shorter, and the middle zone cylinders are even smaller than that from the rest of the section. x3.2

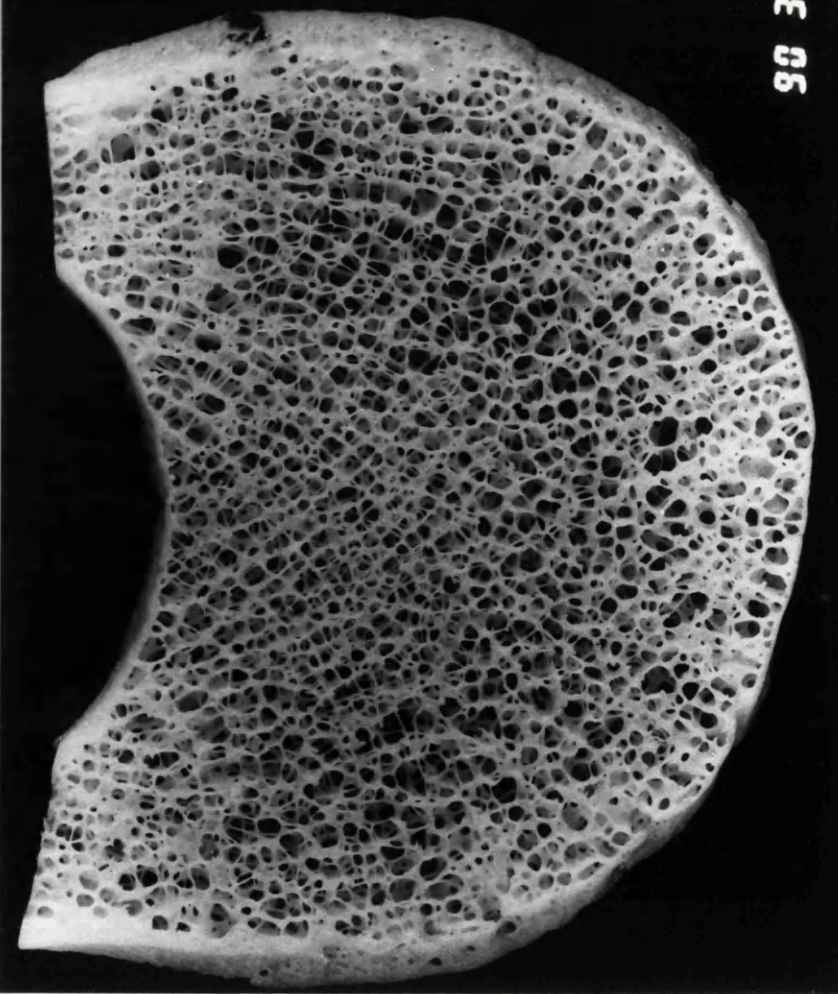
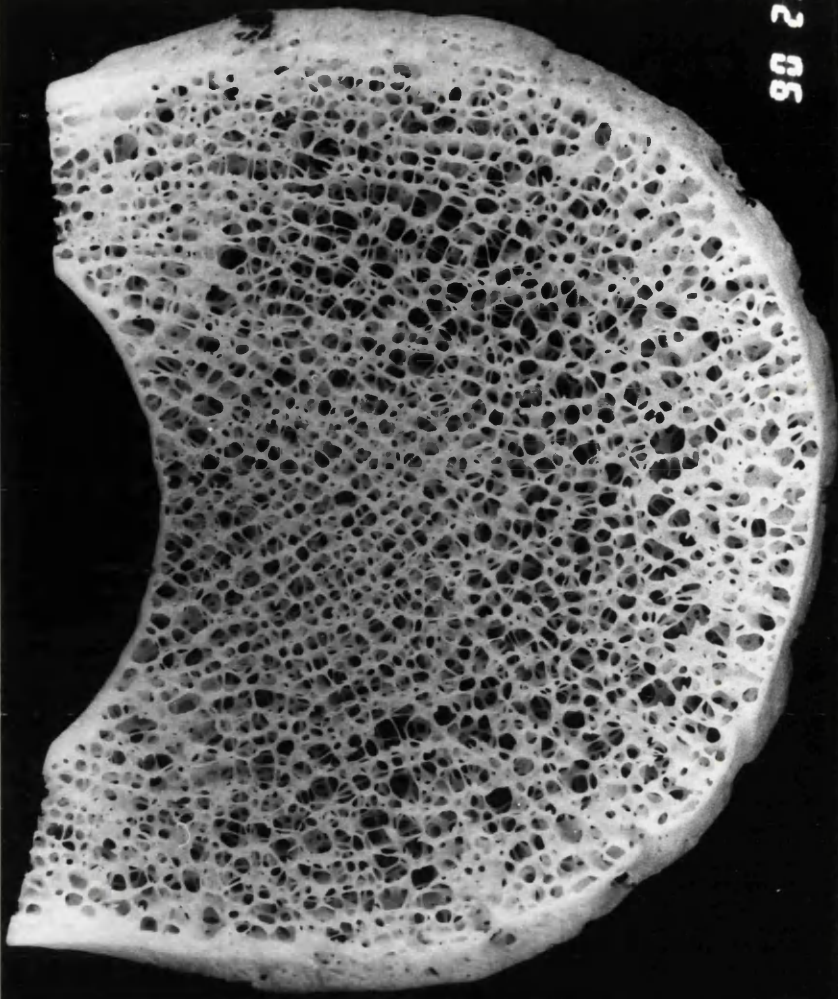
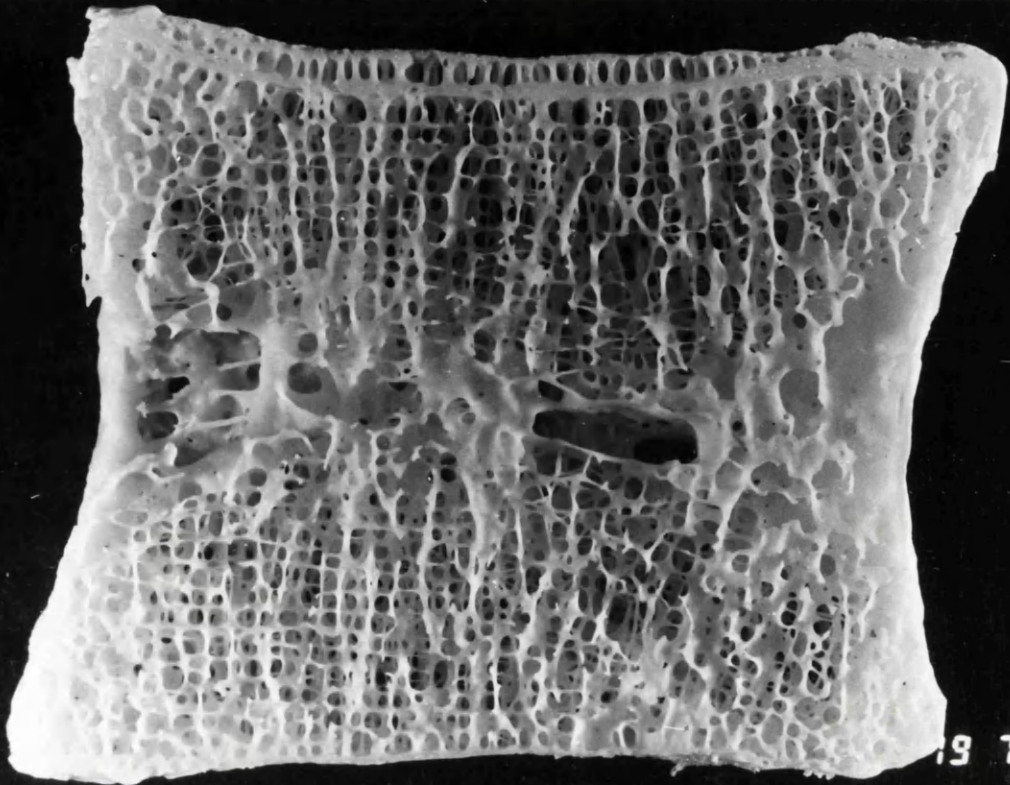
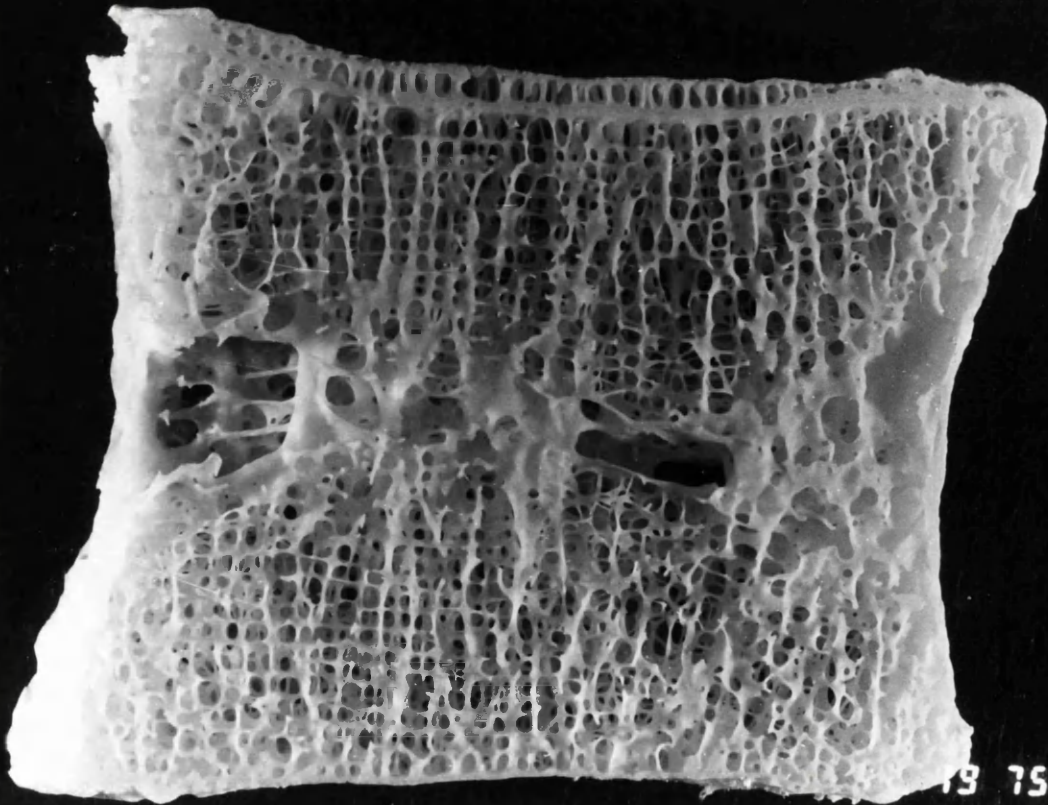


Fig. 6 50 yr male. Mid-sagittal section. Large canals for blood vessels can be recognised at the middle zone of this section. A triangular arrangement of plates can be seen anteriorly in the middle zone and a large vertical trabeculum has branched out posteriorly to give rise to vertical trabeculae at the peripheral zones. Note that double vertebral end plates are present at the superior end of the section. x3.5



19 76



19 75

Fig. 7 64 yr male. Mid-sagittal section. Thinning and removal of trabeculae are apparent in this vertebral section. The horizontal trabeculae are thinner, longer, and there is an increase in the spacing among vertical trabeculae. The deficiency at the posterior side represents the entry of basivertebral vessels. A canal for a large vessel can also be seen traversing the middle zone. x3.3

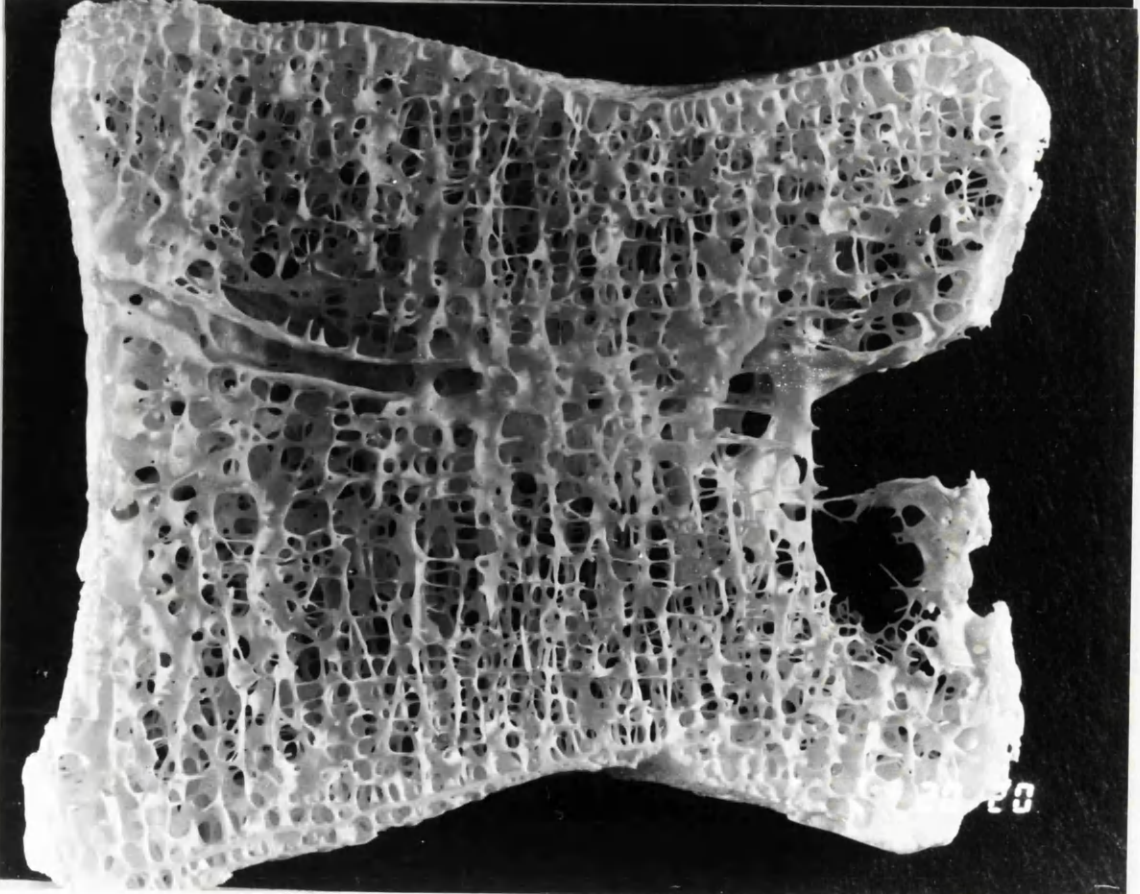
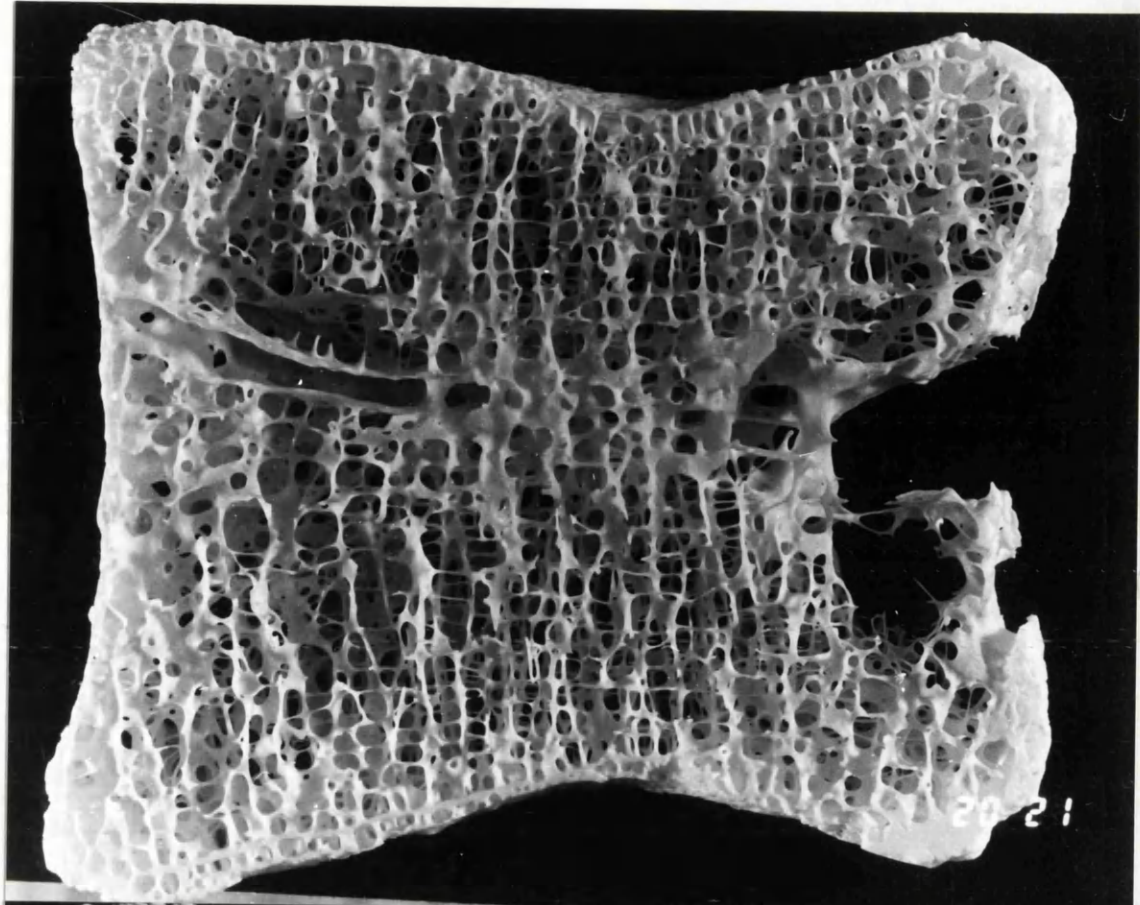


Fig. 8 30 yr female. Coronal section through the most anterior part of the vertebral body. The different trabecular bone structure of the middle zone becomes apparent when compared with the peripheral zones. The structure in the middle zone resembles antero-posteriorly oriented tubes. Note that some of these are opened to outside and are possibly canals for blood vessels. x3.4

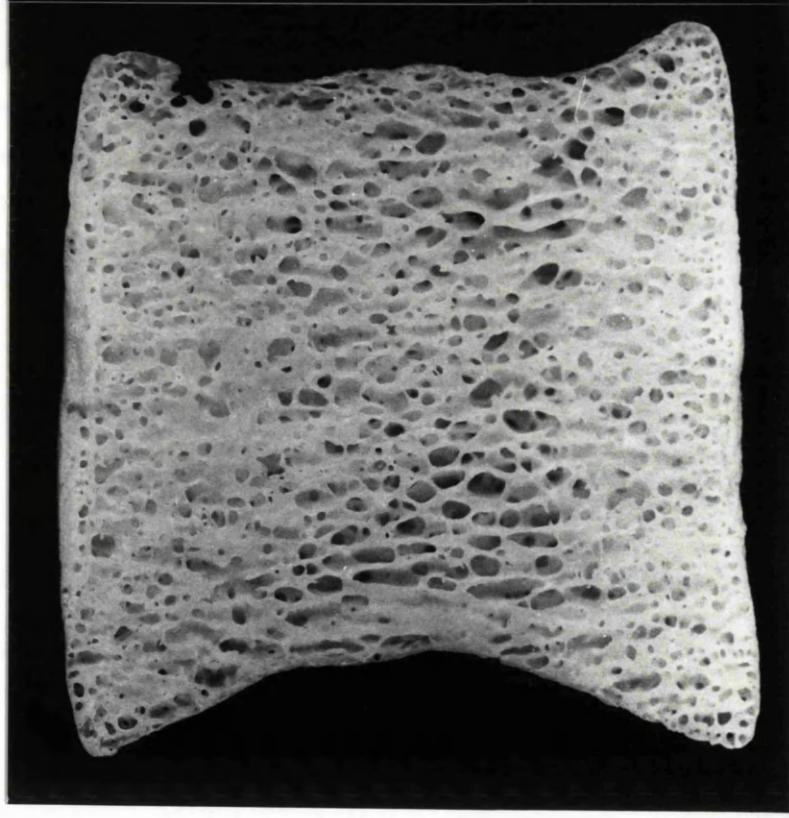
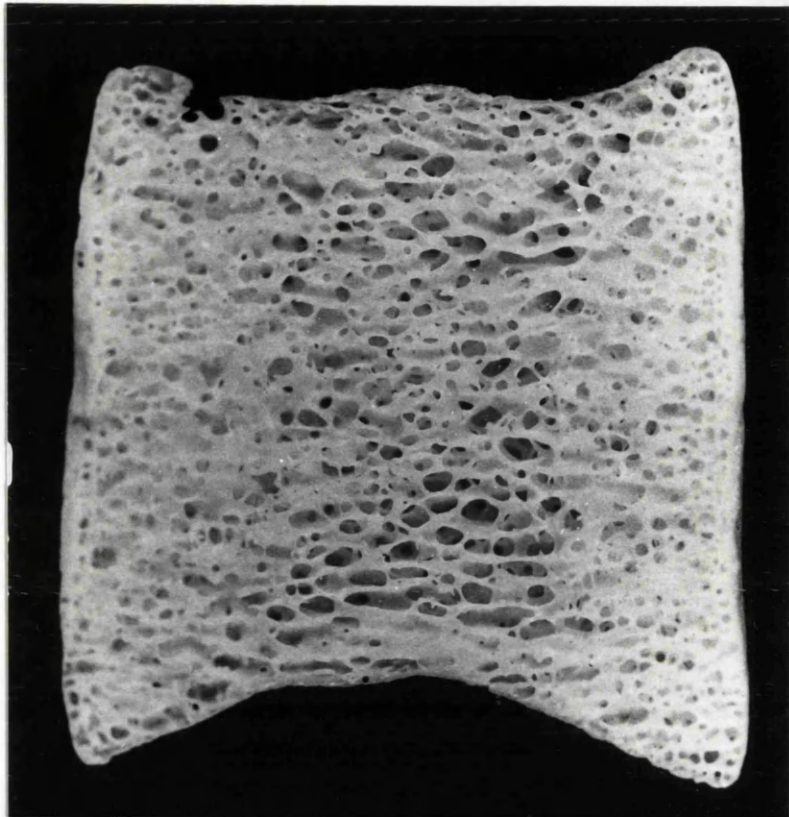


Fig. 9 30 year female. Coronal section through the posterior most part of the vertebral body. The central hole bounded by plates represents the entry of the basivertebral vessels. The arrangement of trabeculae is approximately similar throughout the section. However, a thickened structure can be recognised at the upper lateral regions where vertebral arches are attached. x3.4

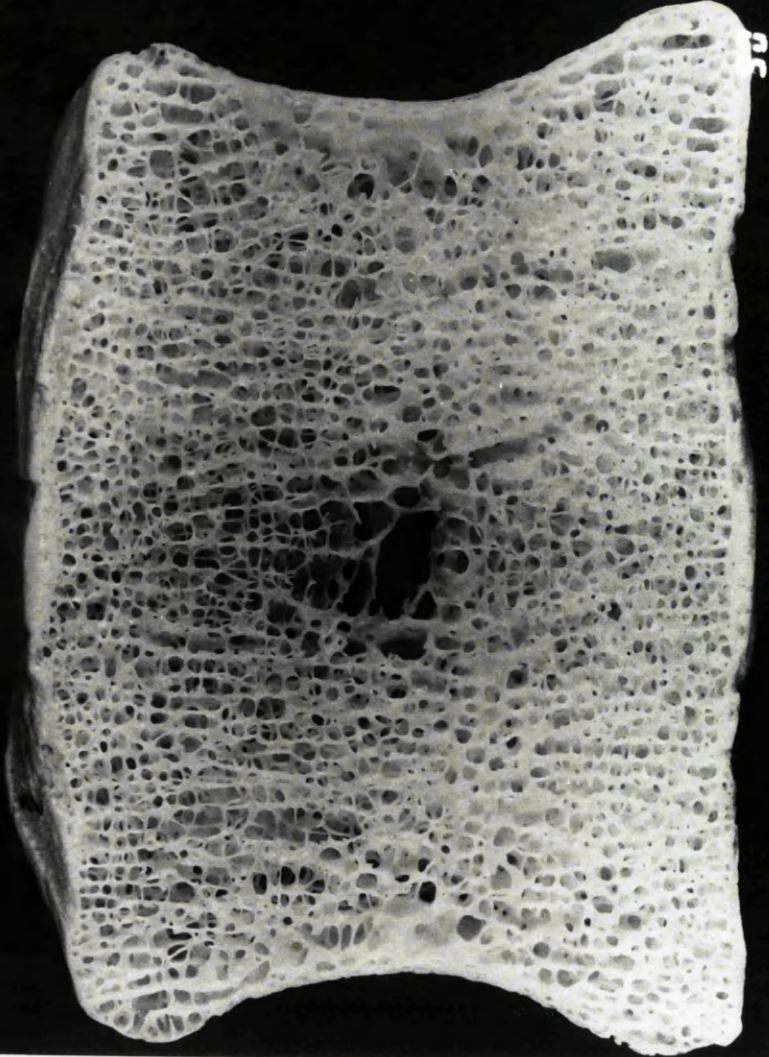
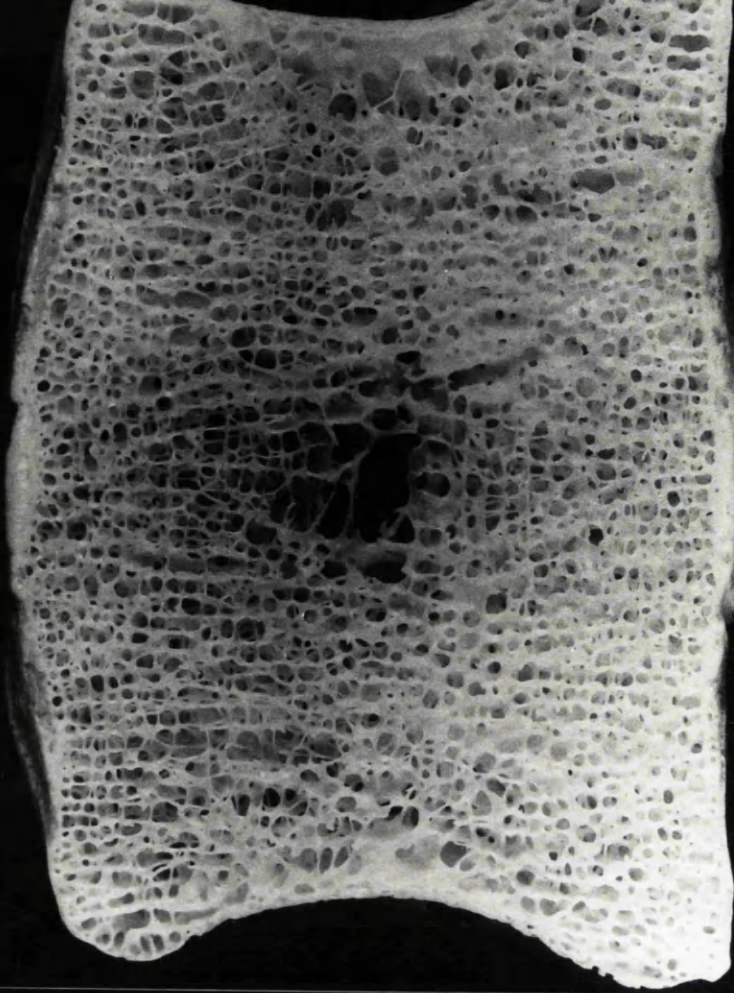
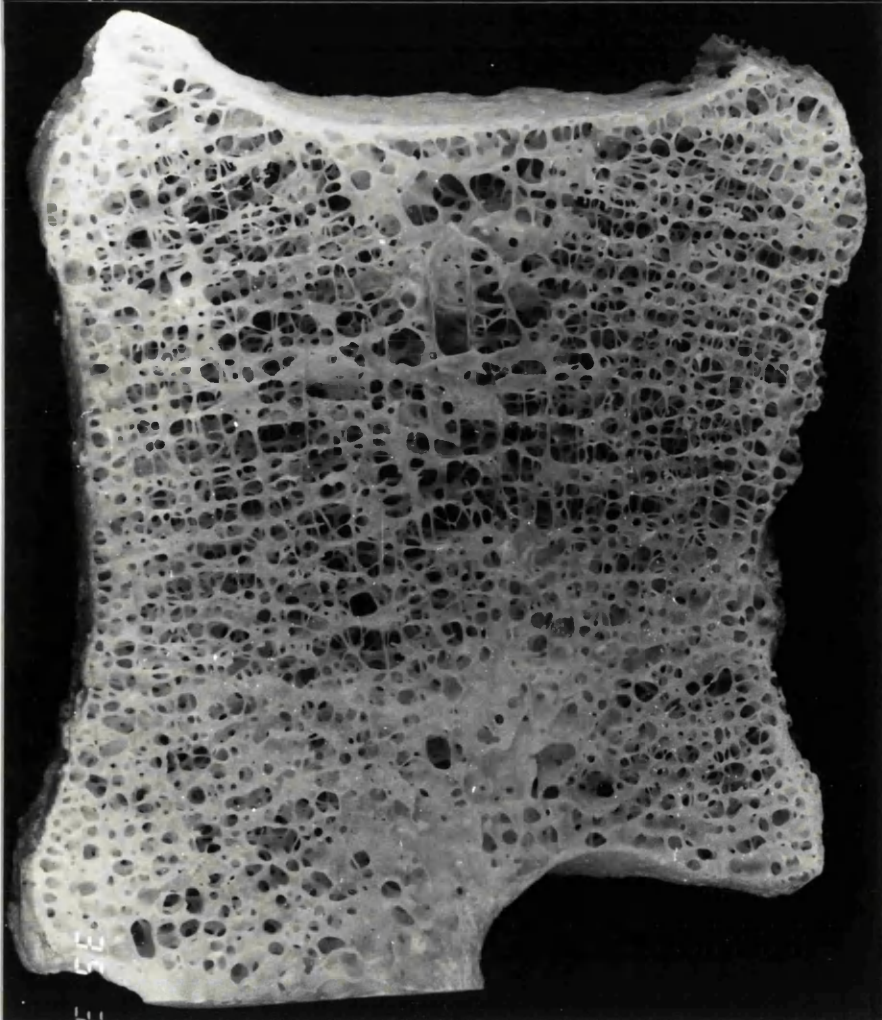
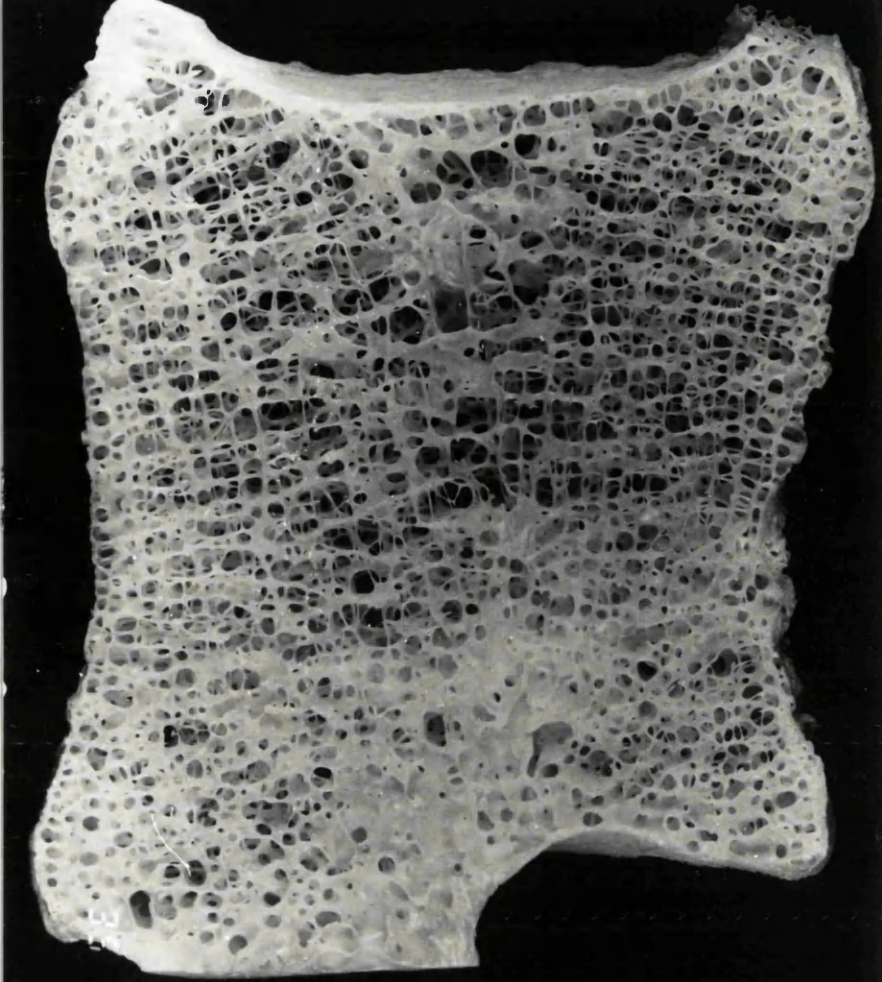


Fig. 10 69 yr male. Para-sagittal section. A true zonal arrangement of trabeculae is not visible in this section. However, a canal for blood vessel can be seen anteriorly at the middle region. Note that the trabeculae are thicker posteriorly where the body is attached to the vertebral arches. x3.6



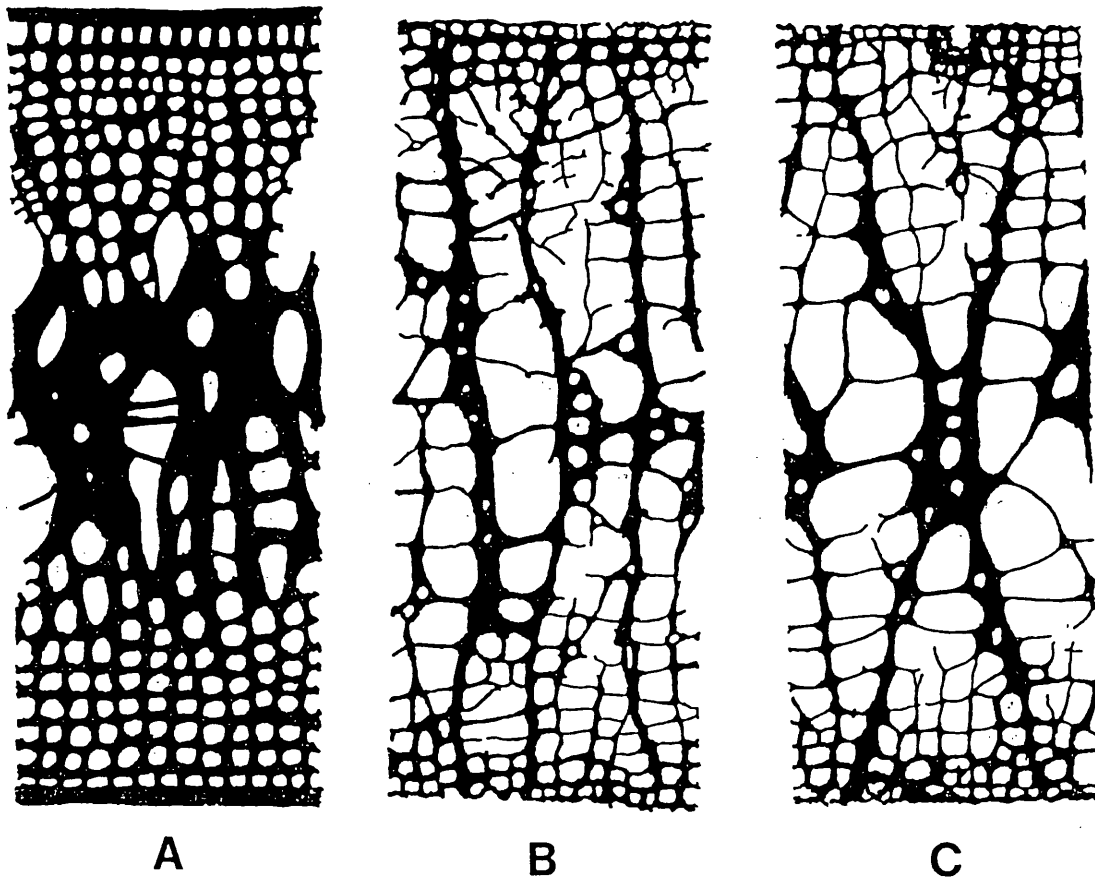


Fig. 11 The proposed two dimensional models for trabecular bone architecture at the mid-sagittal plane of normal (Fig. 11A) and osteoporotic (Figs. 11B and 11C) 4th lumbar vertebral body. In the normal model (Fig. 11A), large cylindrical trabeculae at the middle zone branch off to give rise to an approximately uniform cross-braced structure at the peripheral zones. The rod-shaped horizontal trabeculae are longer in the middle zone; while at the periphery, they are shorter, thicker, and sturdy. The osteoporotic model is composed of thick, widely spaced vertical trabeculae extending from one end plate to the other. These are connected by long, thin, horizontal or oblique trabeculae throughout the section. Trabecular collapse, perforations, microfractures and microcallus are all common features in osteoporotic sections.

Fig. 12 71 yr male. Mid-sagittal section. Trabecular thinning can be observed all over this section. However, it is more marked around the area of entry of basivertebral vessels. Very long horizontal trabeculae can be seen (arrow) at the middle zone. x3.5

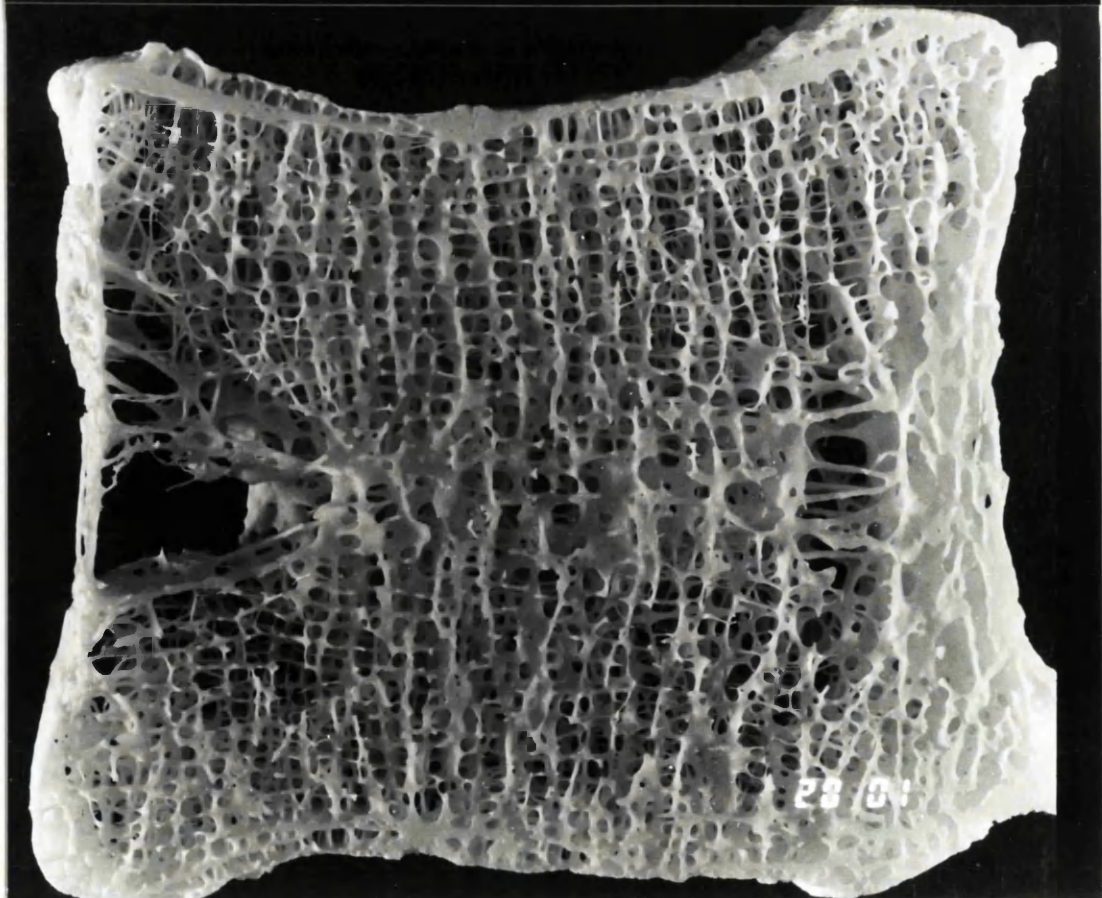
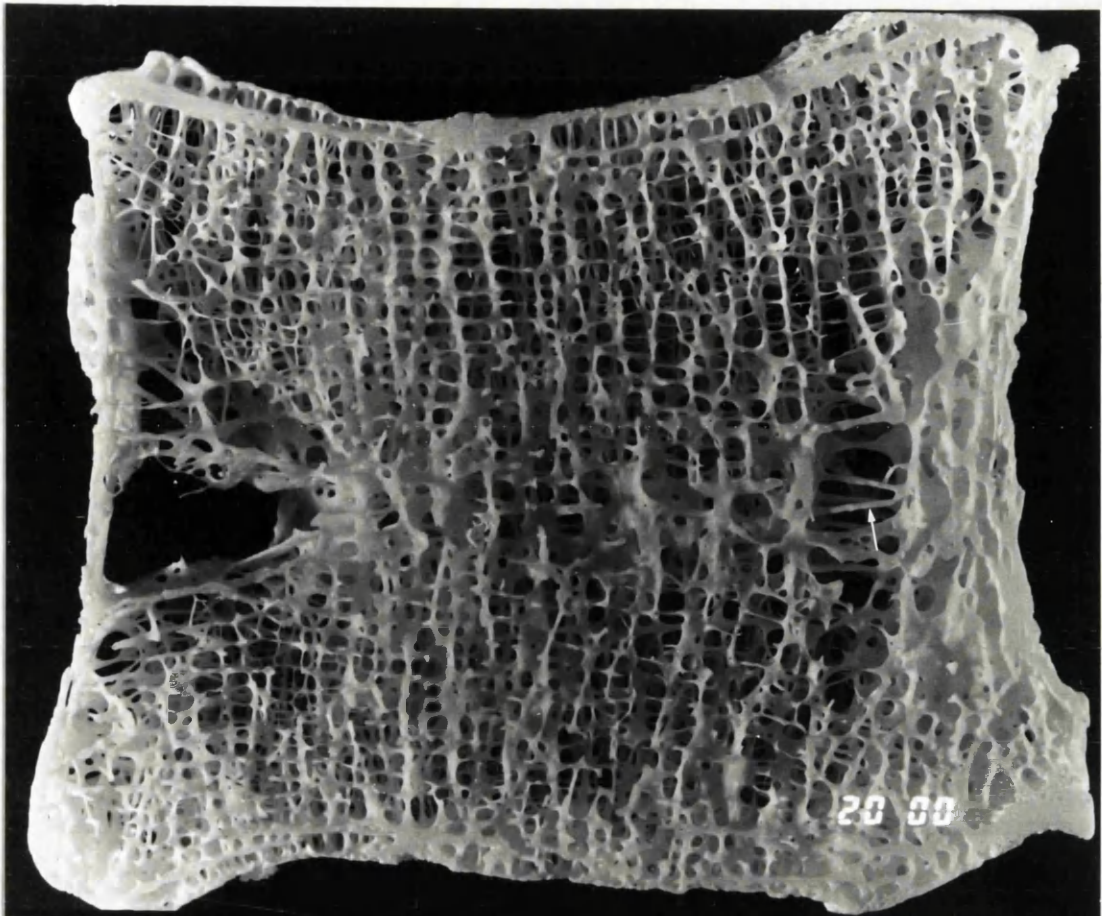


Fig. 13 89 yr osteoporotic female. Mid-sagittal section. Complete loss of normal architectural pattern is apparent in this section. Both vertical and horizontal trabeculae have been reduced in number and the vertical trabeculae can be traced from one end plate to the other. The remaining horizontal trabeculae are long, thin, and frail compared with normal sections. Oblique trabeculae, trabecular collapse, microfractures, perforations and microcallus can also be identified. The break at one corner of the section has occurred during sample preparation. x3.6

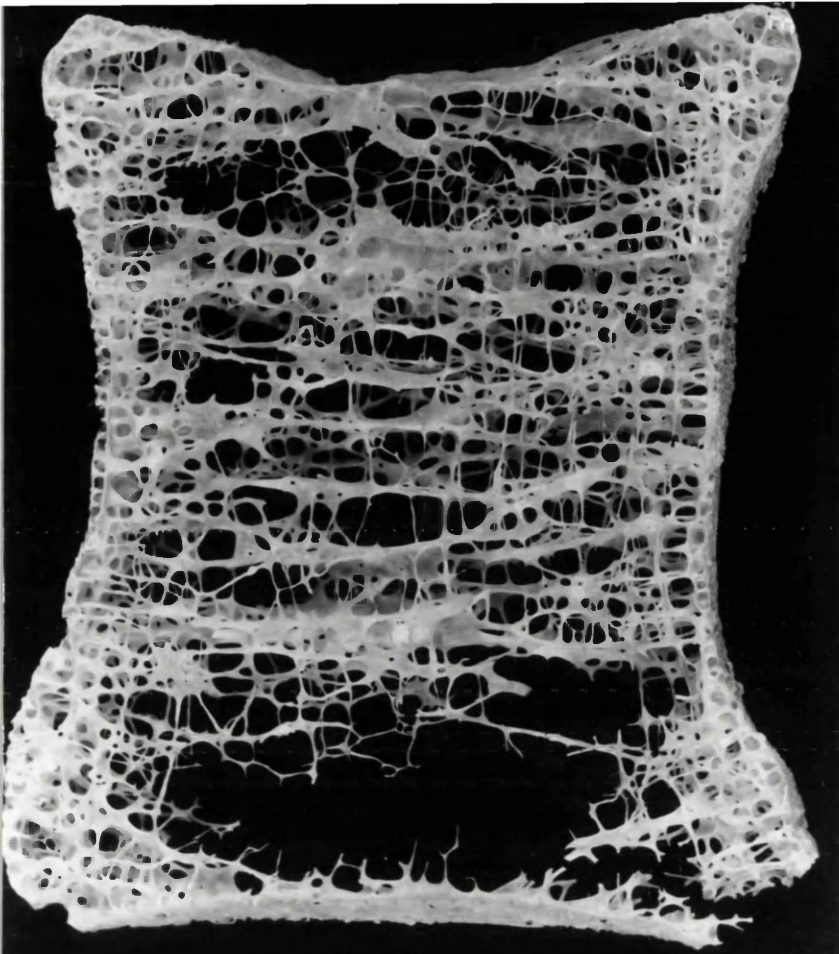


Fig. 14 89 yr male. Mid-sagittal section. Bone loss due to generalised thinning is evident in this section from an old vertebral body, but the architectural pattern is normal for a patient of this age. Thus, a greater stability could be anticipated in this vertebral body compared with one with an osteoporotic architecture.
x3.4

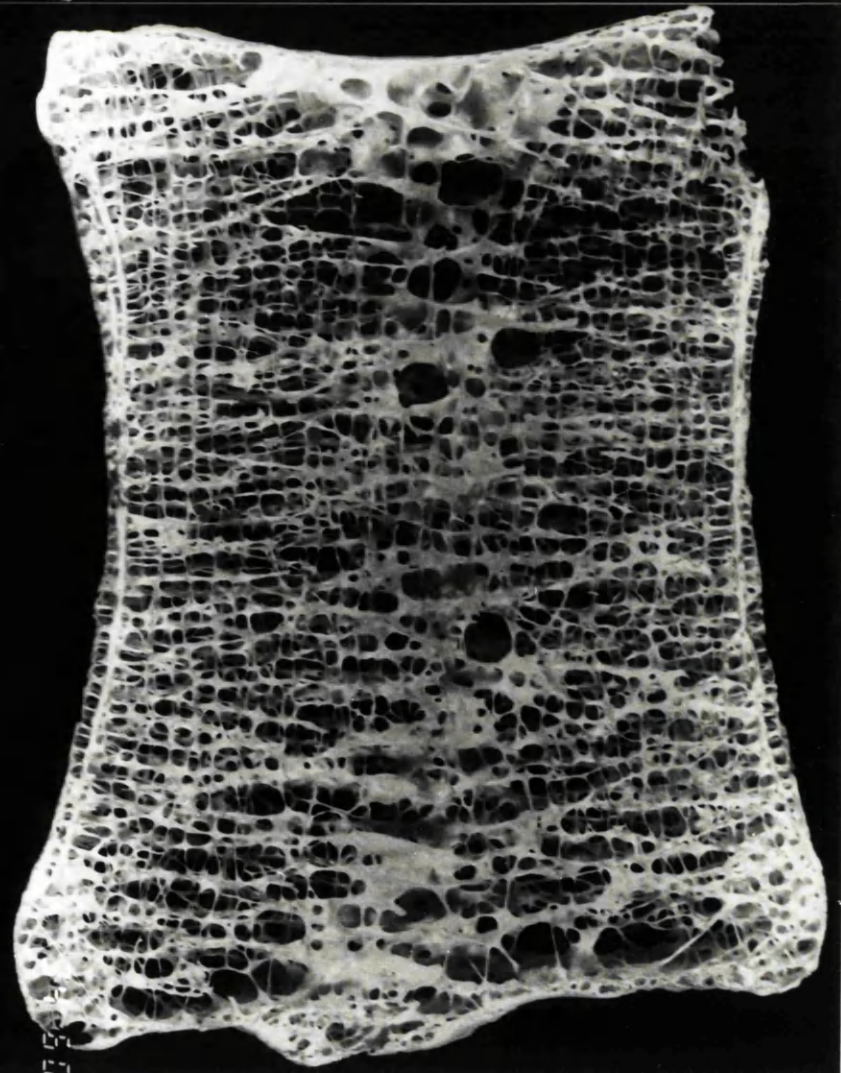
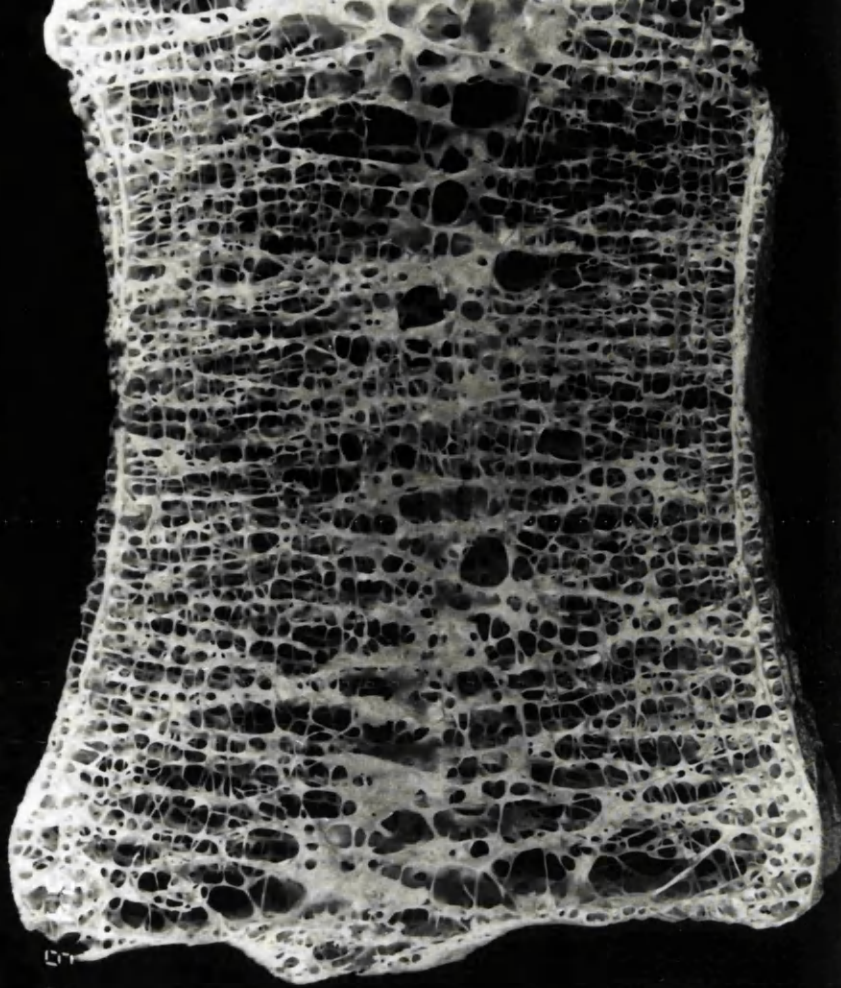


Fig. 15 88 yr female. Mid-sagittal section. This section illustrates a classical osteoporotic architecture. Some vertical trabeculae can be seen arising from anterior and posterior walls at extreme corners of the vertebral body. Although not clinically confirmed, this vertebral body can be said to be osteoporotic from its architectural pattern alone. A microcallus (arrow) can also be identified.
x3.6

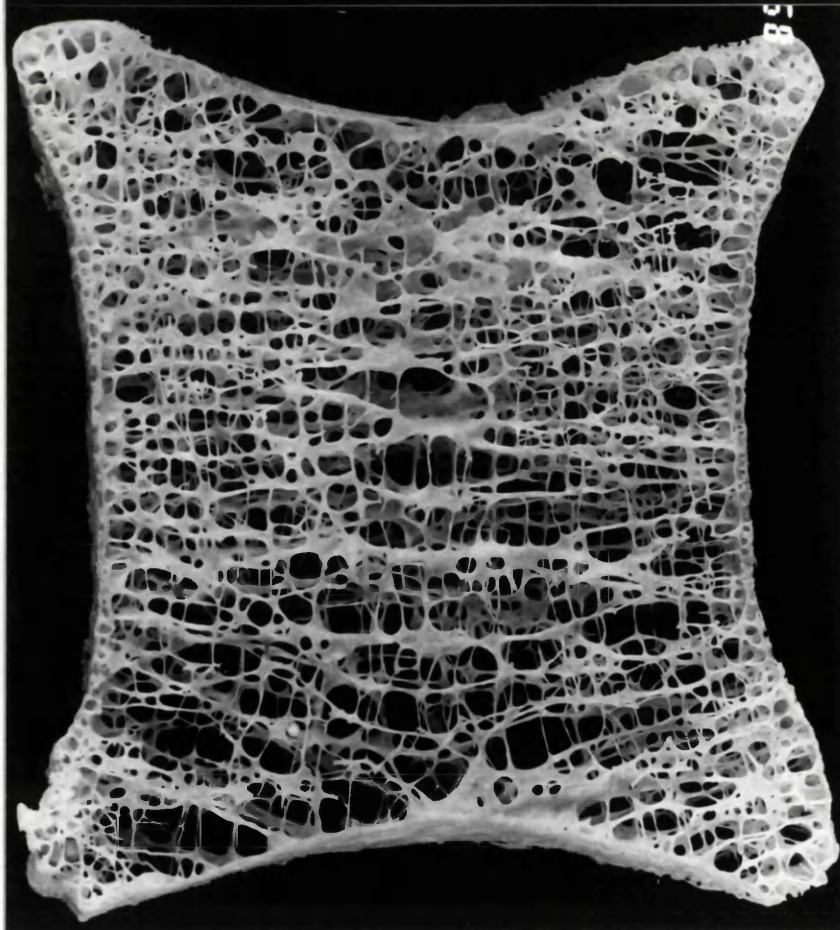
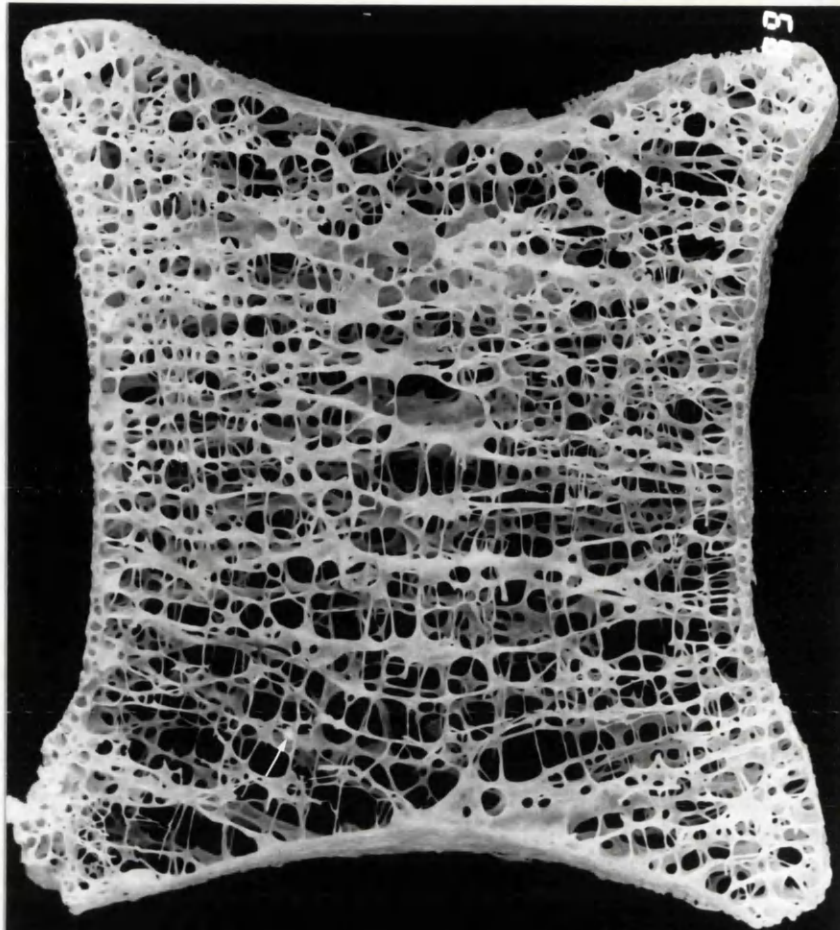


Fig. 16 88 yr female. Coronal section through the middle of the vertebral body. The normal architectural pattern has been maintained in this section irrespective of thinning of trabeculae in many regions. Several depressions can be identified on end plates and the trabeculae have thickened beneath some of these depressions. At extreme corners, trabeculae can be seen arising from corresponding lateral walls. x3

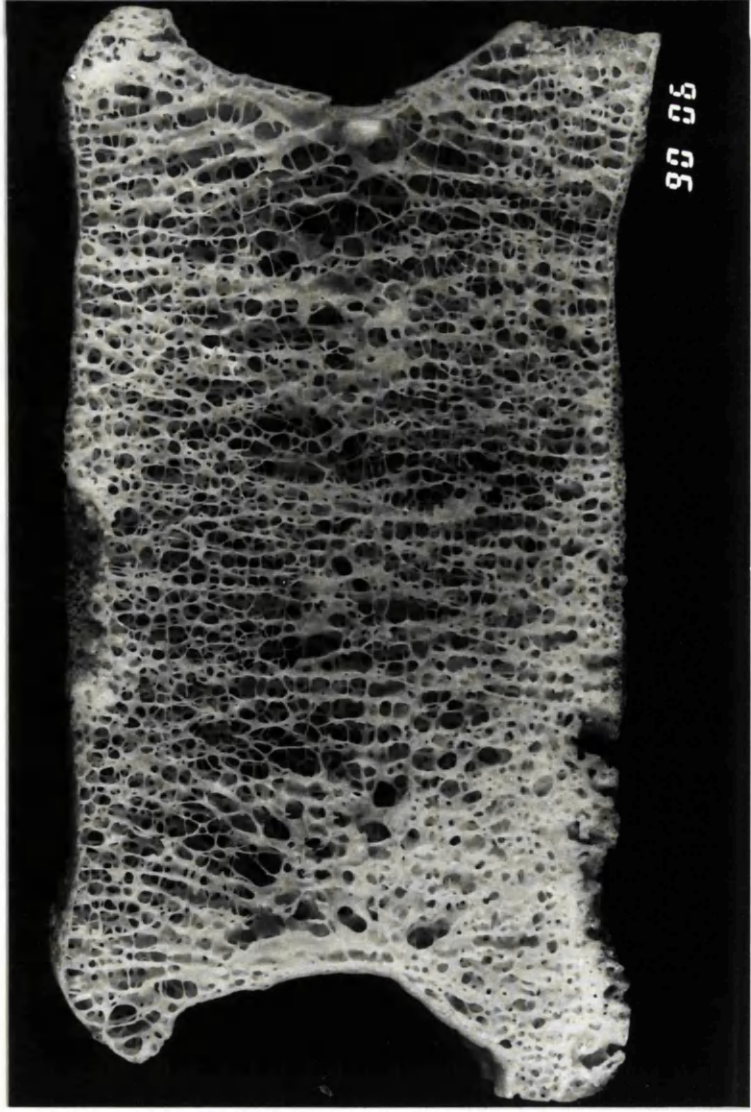
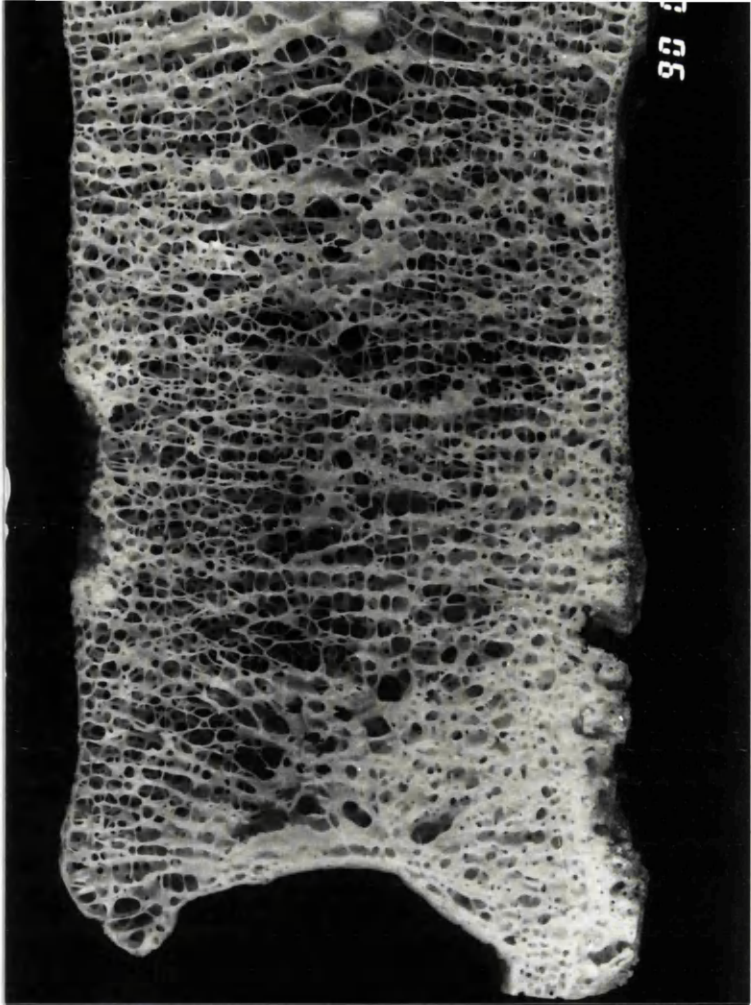


Fig. 17 88 yr female. Mid-horizontal section. At this plane, thinning of trabeculae ("cylinders") can be observed in many regions except at the attachment of the vertebral body to the arch where thick trabeculae are still maintained. x3.2

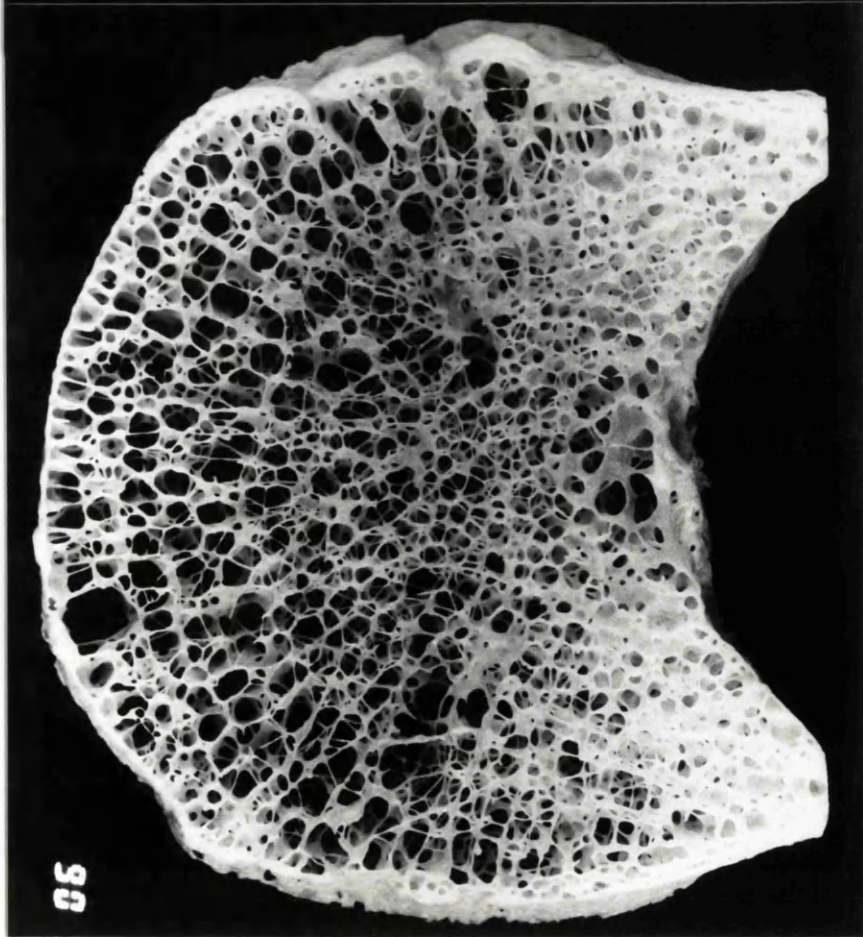
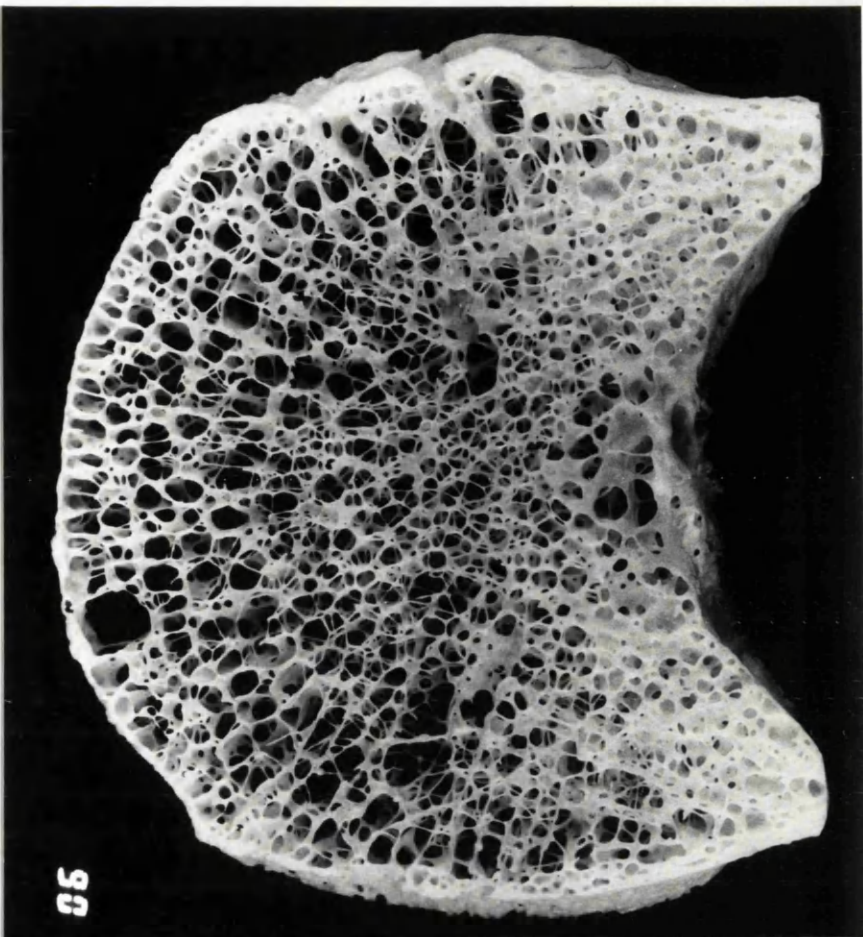
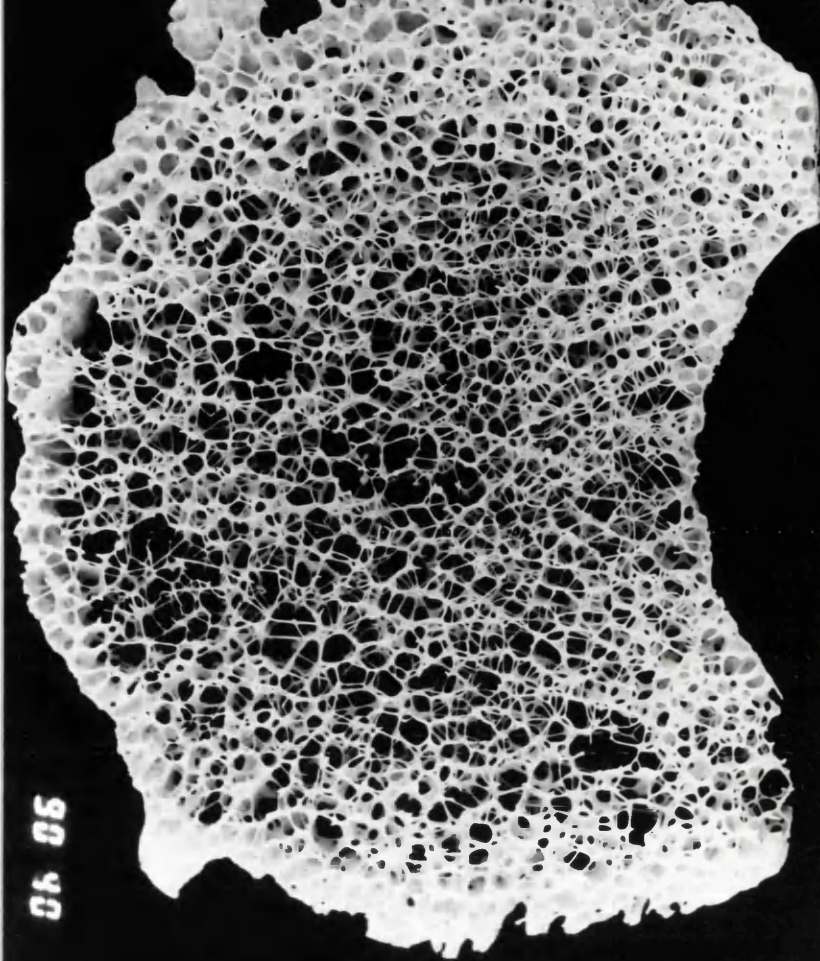
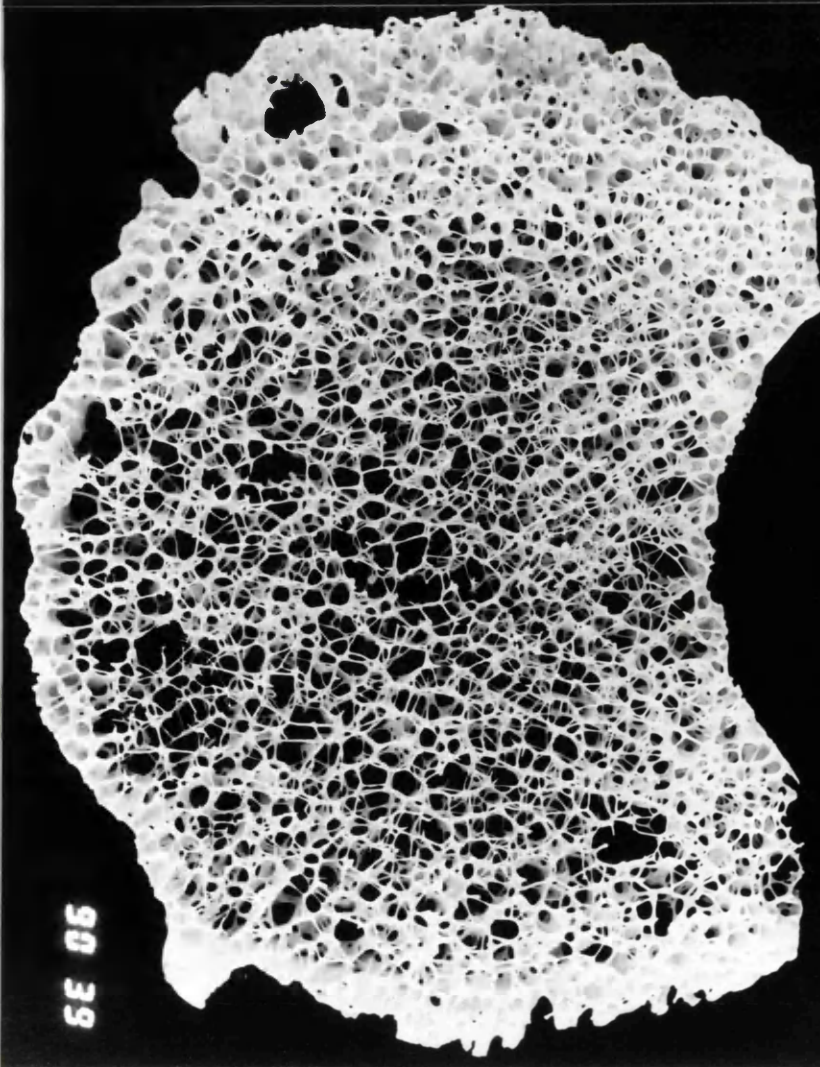


Fig. 18 88 yr female. Horizontal section through the superior zone of the vertebral body in Fig. 17. Thinning and collapse of trabeculae are especially evident at the central region of the section. The shape of the holes bears more resemblance to pentagons bounded by rods rather than to cylinders. The irregular outline of the section was brought about by the formation of osteophytes. Several microcallus can also be identified. x3.2

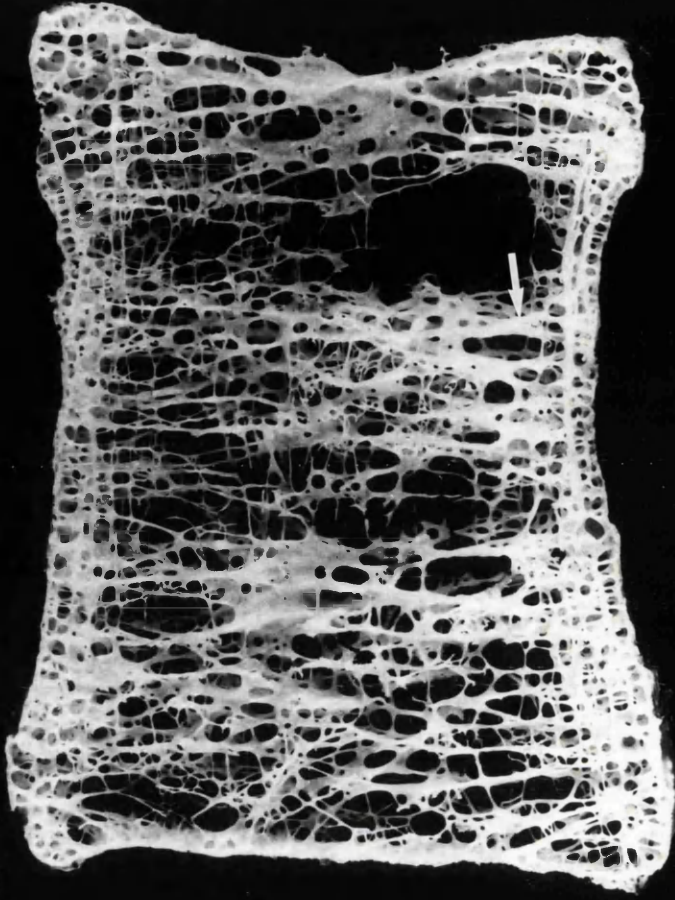


06 05



05 06

Fig. 19 89 yr osteoporotic male. Mid-sagittal section. Thickened vertical trabeculae can be seen at the superior zone (arrow). Collapsed regions are apparent in this section as is the loss of vertical and horizontal elements. The area below the arrow shows a type of fine trabeculae that are different from rest in the section. x3.1

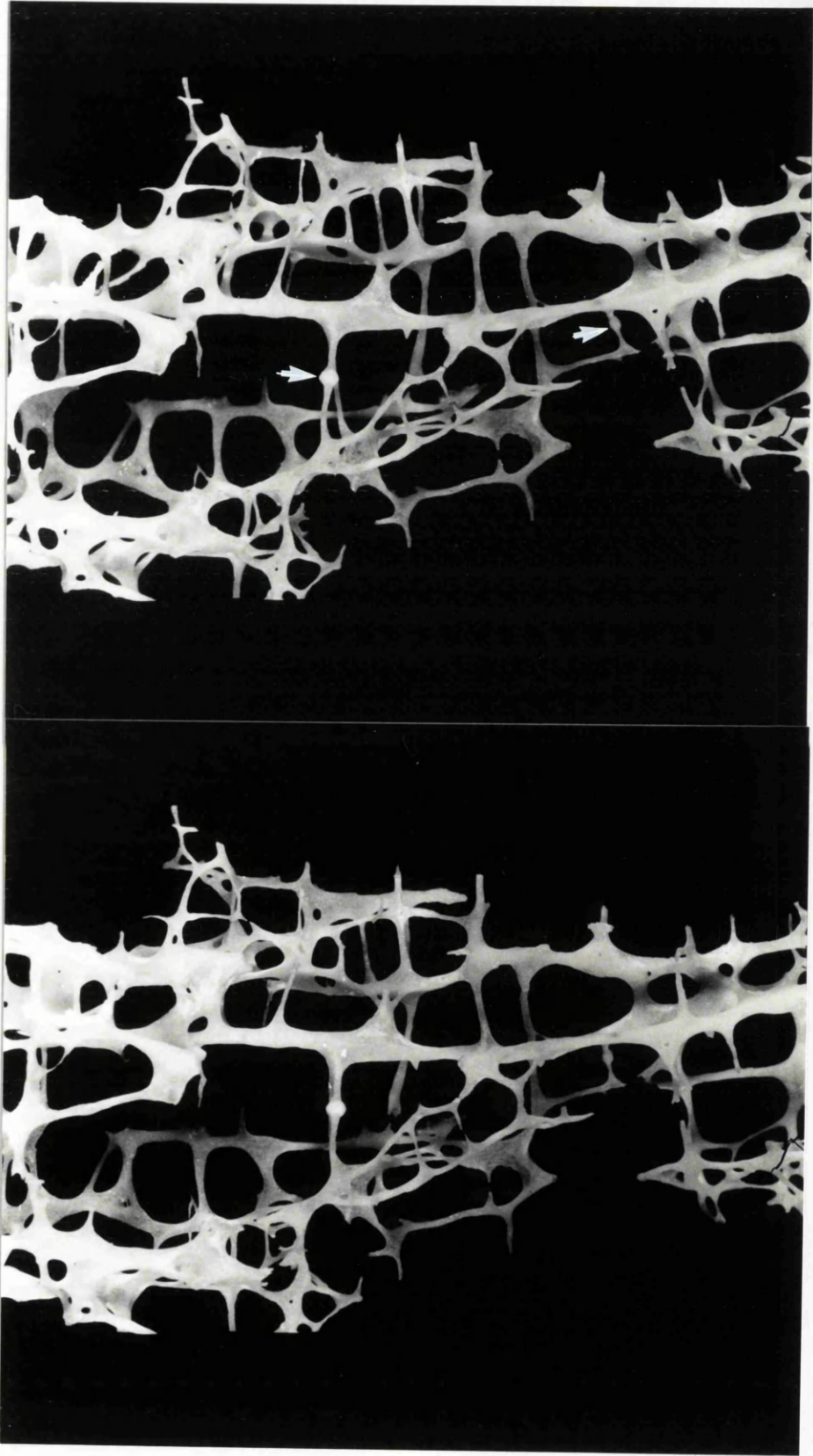


95



95

Fig. 20 89 yr osteoporotic female. A segment of trabecular bone from a mid-sagittal section showing two microcallus (arrows) on horizontal trabeculae. Usually, microcallus showed a similar nodular appearance when they occurred on horizontal trabeculae. x10



Figs. 21–23 A graphical comparison of horizontal trabecular lengths in different zones of mid–sagittal sections of the 4th lumbar vertebral body obtained from young, old and osteoporotic patients of both sexes.

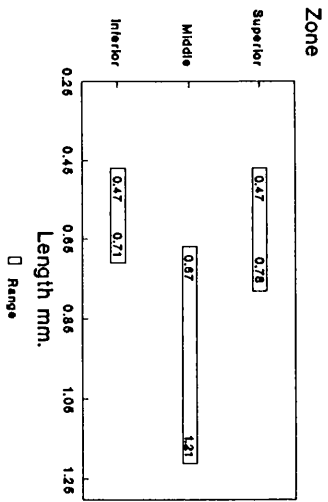


Fig. 21 A - 31 yr, Male

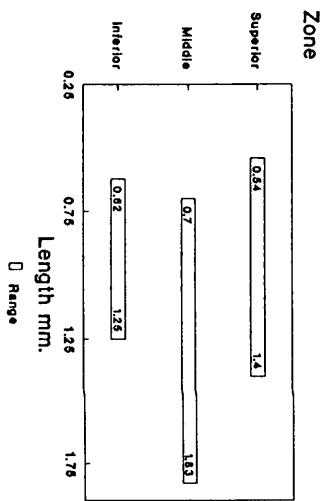


Fig. 22 A - 77 yr, Male

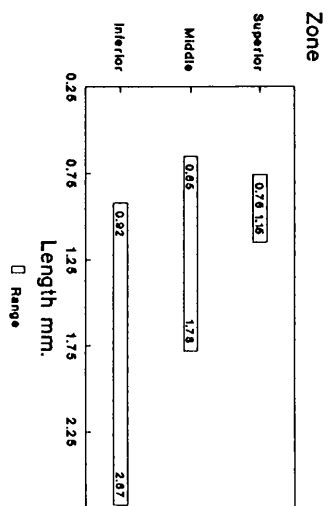


Fig. 23 A - 89 yr, Male (Osteoporotic)

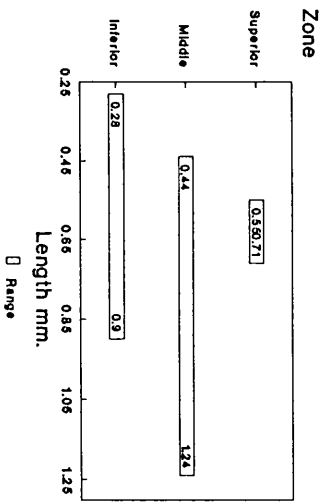


Fig. 21 B - 30 yr, Female

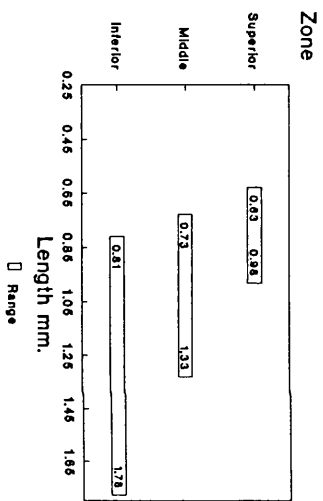


Fig. 22 B - 91 yr, Female

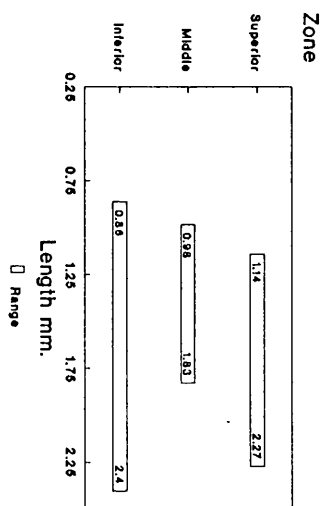


Fig. 23 B - 89 yr, Female (Osteoporotic)

Fig. 24 Changes in the number of horizontal trabeculae at mid-sagittal plane of the 4th lumbar vertebral body with age in males (Fig. 24 A) and in females (Fig. 24 B).

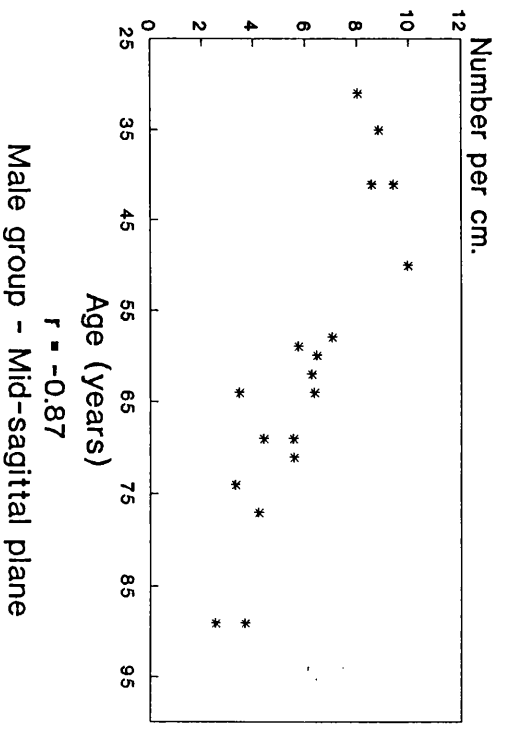


Fig. 24 A

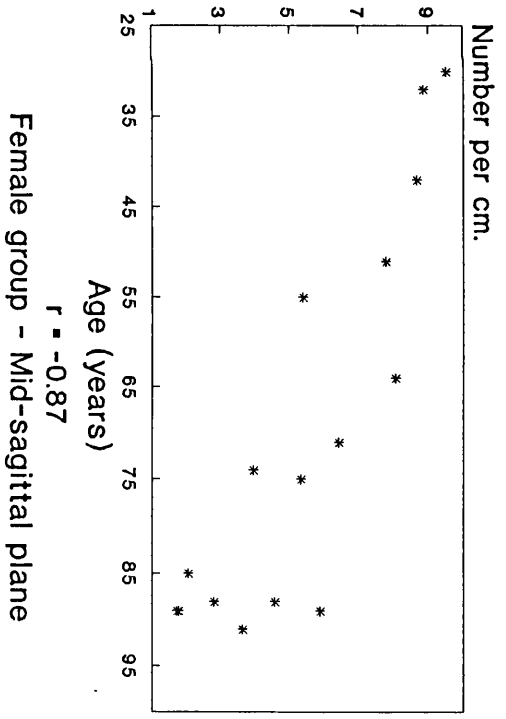


Fig.24 B

Figs. 25–27 Changes in the number of vertical trabeculae at different zones of mid-sagittal plane of the 4th lumbar vertebral body with age in both sexes.

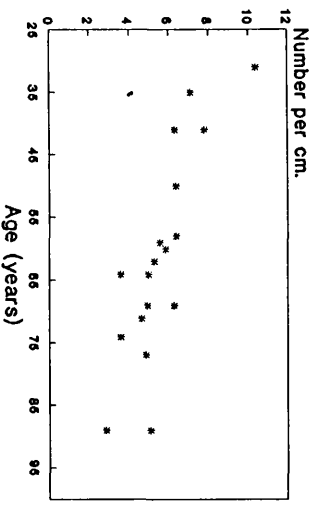


Fig. 25 A - Male group - Superior zone

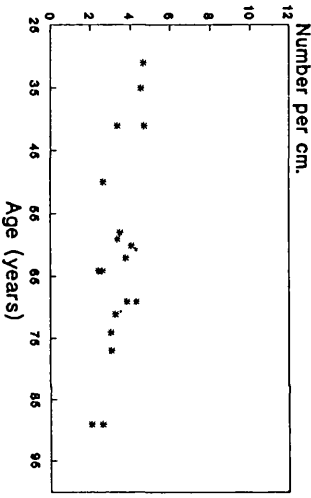


Fig. 26 A - Male group - Middle zone

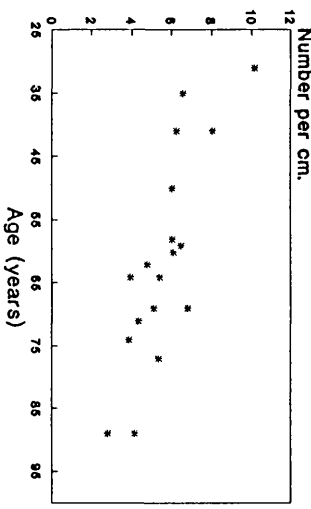


Fig. 27 A - Male group - Inferior zone

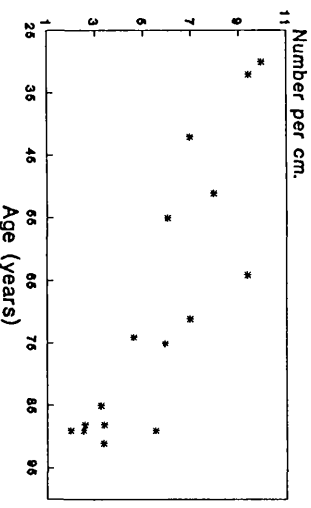


Fig. 25 B - Female group - Superior zone

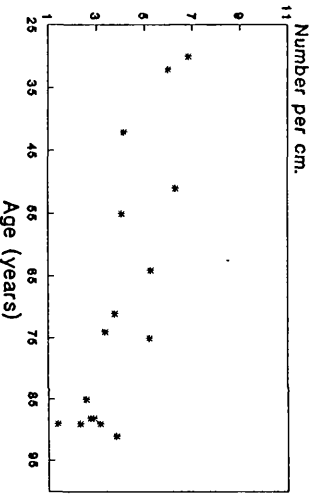


Fig. 26 B - Female group - Middle zone

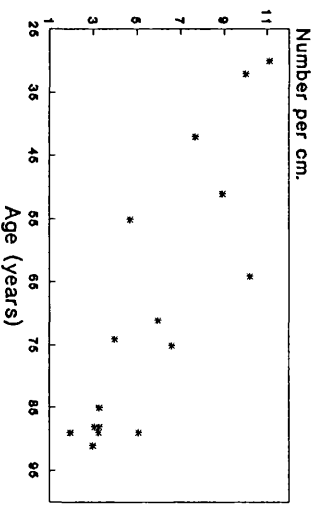


Fig. 27 B - Female group - Inferior zone

Fig. 28 Changes in the biconcavity index of the 4th lumbar vertebral body with age both in males (Fig. 28 A) and in females (Fig. 28 B).

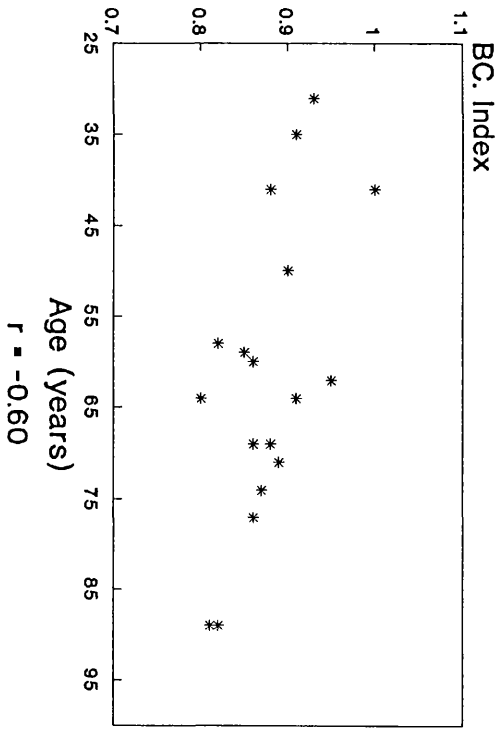


Fig. 28 A - Male group

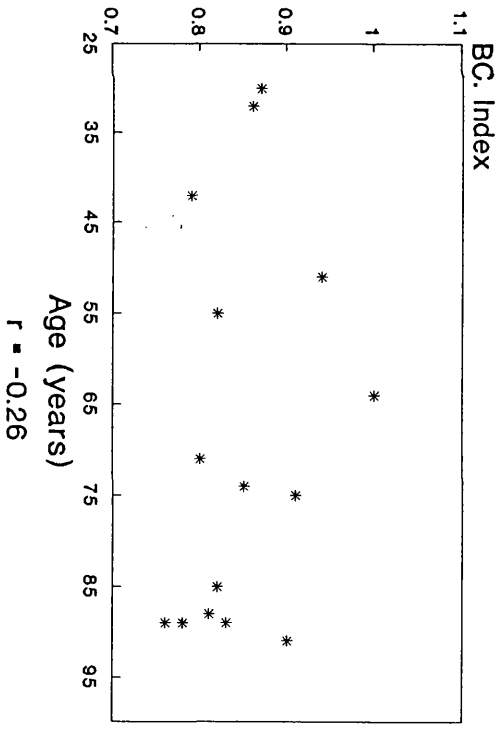


Fig. 28 B - Female group

CHAPTER 4

THE ANALYSIS OF TRABECULAR BONE IN THE FREQUENCY DOMAIN

4.1 INTRODUCTION

4.1.1 Image processing in the frequency domain

4.1.1.1 Frequency methods

In digital image processing, the term "spatial methods" refers to methods that concentrate on working with the grey level at each point in the picture. An alternative to the spatial method is to examine the composition of the image in terms of the way that it can be made up from a series of periodic functions. Such methods are referred to as frequency methods.

The spatial frequency is essentially the rate at which the brightness of an image changes with distance. High spatial frequencies correspond to rapidly varying detail and low frequencies correspond to slowly changing brightness.

The most powerful techniques for digital image processing in the frequency domain are those that involve Fourier analysis. The basis for Fourier techniques is the *Fourier transform*, which is a mathematical operation based on a theorem that states that any harmonic function can be represented by a series of sine and cosine functions. These functions differ only in frequency, amplitude, and phase (Walter and Berns 1986).

For example, a square wave can be considered to be made up of a sum of sine waves of frequency $1v, 3v, 5v, \dots$, where v is the frequency of the square wave. As the number of component sine waves reaches infinity, their sum converges to a perfect square wave. Similarly, any other waveform can be regarded as being made up of a mixture of sine waves.

A graph showing the decomposition of a waveform into its frequency components is called its *spectrum*. A complete spectrum specifies the amount of each frequency, its amplitude and how much the sine wave has to be shifted with respect to the others (phase). A waveform and its spectrum are related to each other in such a manner that a waveform can be deduced from its spectrum and vice versa. This means that the spectrum is interchangeable with the waveform.

The spectrum contains the same information as the waveform, but in a different arrangement. However this duality only holds when the spectrum contains information about the amplitude and phase at each frequency (James 1987).

The square of the amplitude is proportional to the power (energy) at a given frequency. A plot of the square of the amplitude versus the frequency is therefore called the *power spectrum*.

4.1.1.2 Fourier transformation of an image

The real data of an image exists as a two-dimensional array where the data consist of x and y co-ordinates together with the intensity at each point. The Fourier transform of such a two-dimensional signal can be performed as two separate one-dimensional transforms i.e. the two-dimensional Fourier transform is separable.

4.1.1.3 The discrete Fourier transform

The usual theory of the Fourier transform applies to functions defined on a continuous interval, but the images which are processed by computer are defined on a discrete set of points: a corresponding theory involving the use of the discrete Fourier transform applies in this case.

The two-dimensional discrete Fourier transform is also separable and can be computed by first taking the discrete Fourier transform of the rows, and then taking the discrete Fourier transform of the columns of the matrix representation.

4.1.1.4 The fast Fourier transform

To calculate the discrete Fourier transform directly using the equation is very time consuming. However, this problem was solved by Cooley and Tukey (1965) who introduced an algorithm for the computation of Fourier coefficients which requires much less computational effort. This method is now widely known as the "*Fast Fourier Transform*". The fast Fourier transform (FFT) algorithm is a method for computing the finite Fourier transform of a series of N complex data points in approximately $N \log_2 N$ operations (Cochran et al. 1967). The history of this technique has been summarised by Cooley, Lewis and Welch (1967).

4.1.2 Applications of the Fourier transform

Fourier analysis is a widely utilised technique employed primarily in engineering and physics. The discrete Fourier transform with or without computational algorithm has long been used for signal analysis (Cooley et al. 1967). Fourier transform methods have also widely been utilised for image coding (Andrews et al. 1968a, 1968b and 1968c). Examples for many earlier uses of these techniques include improvement of pictures taken by artificial satellites (Andrews 1970), in holographic and photographic investigations (Holeman 1968) and in recognising writing or finger prints (Duda and Hart 1973).

Spatial filtering involving Fourier techniques had been a very useful way of manipulating images. Since the Fourier transform of an image contains as much information as the original image, any problems that can be tackled by spatial methods can also be tackled by frequency methods. Removal of noise from images by the spatial method could be carried out by employing any sort of local smoothing (Walker 1982). Isolated dark and light spots can effectively be removed using an appropriate filter this way. In Fourier techniques, for example, high or low spatial frequency information can be deleted from an image by designing a Fourier filter that is nontransmitting where these frequencies appear in the Fourier transform. It is especially useful in removing harmonic noise such as the dark and light bands sometimes seen in video images. As this noise is harmonic, it can be located in localised discrete parts of the Fourier transform. When these local areas are removed from the transform, the reconstructed image is virtually unaltered except that the noise is gone.

Generally, the choice of approach (spatial or frequency) to use depends on the nature of the problem. The spatial viewpoint seems to favour problems with local structure and the frequency

viewpoint helps with problems with global or periodic structure (James 1987).

The development of frequency techniques was originally related to problems of image enhancement, that is, to produce an image in an improved form or to visualise features previously barely detectable (Shulman 1970, Becker et al. 1969, Madsen and Park 1985).

Oxnard (1973) described research (by Davies, geology, Univ. of Kansas) where these techniques were modified to be analytical in nature in studying pore and particle status in thin sections of oil bearing rocks. Contoured power spectra from two different rocks were compared. The two sections and their power spectra were extremely similar in appearance, but contoured power spectrum from one section demonstrated that a certain contour was oriented in one direction, showing that particles of that size in the original picture had a preferred orientation. Frequency techniques can thus be employed to detect differences between images that are superficially similar. Since our eye catches bigger particles first and a judgment is made depending on the characteristics of these particles, it may be difficult to observe differences in smaller ones. Frequency methods may be useful in solving problems of this nature. By filtering away bigger elements, smaller elements can be exposed for visual assessment or frequency analysis. Alternatively, contoured power spectra can provide quantitative and qualitative information directly.

4.1.3 Use of Fourier techniques in biological sciences

Fourier techniques have been used in many branches of the biological sciences. For example, similarities and differences in wing shape among 127 species of mosquitoes from north America were analysed quantitatively by Rohlf et al (1984). Fourier techniques have also been used to study shells of the mussel 'Mytilus edulis' (Scott Ferson 1985). Fourier transforms have mostly been very useful in analysing biological patterns and shapes. The fast Fourier transform has been employed to study the outline of the face (Lu 1965). Fourier analysis has been considered to be well suited for studies of longitudinal growth since the method permits the accurate measurement of irregular morphological shapes. Lestrel et al. (1976) employed Fourier analysis to study adolescent growth of the cranial vault using lateral cephalometric radiographs.

The efficacy of Fourier analysis in discriminating between groups of primates on the basis of shape of the lateral cranial projection has been tested (O'Higgins, et al. 1987). The pattern of discrimination was consistent with current taxonomic classification of the extant species. It has also been suggested that Fourier analysis can occasionally offer advantages over more traditional methods of shape measurement, especially because of its relative independence of the need to define "homologous landmarks" (O'Higgins et al. 1987). O'Higgins et al. (1986) have also employed Fourier analysis to investigate vertebral column development in allophenic mice, while Lestrel et al. (1977) have provided a quantitative description of the shape of the hominid distal femur using Fourier analysis. A recent review of methods of shape description including Fourier methods has been presented by O'Higgins and Johnson (1988). Fourier techniques have also been used in other areas of biology such as paleobiology. It has been utilised as an objective descriptor of Ostracode margins (Kaester et al. 1972) and to characterise chamber shapes of fossil tubular

bryozoons (Anstey et al. 1972).

In biological microscopy these techniques have been applied to enhance images or to analyse microscopical patterns. Optical Fourier transform methods were utilised to analyse exfoliated cervical cytological samples to detect the occurrence of malignant cells (Kopp et al. 1976). It has also been used extensively in enhancing information retrieval from electron micrographs (e.g. Taylor et al. 1974) and to improve the quality of tomographic images (Madsen et al. 1985).

4.1.4 Applications of Fourier techniques to trabecular patterns

in bone

Oxnard (1972, 1973) pioneered the investigation of trabecular patterns using Fourier techniques. He employed laser diffraction techniques to study the gross microscopic trabecular bone structure of the lumbar vertebrae. Trabecular patterns in sagittal sections of third and fifth lumbar vertebrae are markedly different. Oxnard was able to relate these differences to the differences in their power spectra. In contrast, trabecular patterns in second and fourth lumbar vertebra look similar, but their power spectra still showed clear differences. By contouring these power spectra he was able to describe these differences, their position and orientation.

Oxnard also showed how the power spectrum of a bone image can be used to obtain useful information. The power spectrum can be a "finger print" of the trabecular pattern for the purpose of comparison. It can also be employed as a hypothesis testing mechanism. For example, it may be useful in testing similarity between observed power spectra and those expected from a particular model as to the nature of trabecular structure. The trabecular elements were believed to be aligned in the same way as the stresses that they resisted. This trajectorial theory of bone architecture (Meyer 1867, Wolff 1870) has been subjected to many criticisms during the past century. Fourier techniques may be another tool to test this type of theory.

In later work Oxnard (1980, 1981, 1984) described further applications of these techniques, using filters to screen out some of the data in a transform, thereby allowing other information in the picture to reveal itself more readily. Radiographic images can be improved by removing shadows that mask important information. In trabecular bone, more prominent trabecular elements can be filtered away, allowing smaller, less obvious elements to be studied. In a study of radiographs of the bodies of lumbar vertebrae from chimpanzees, orangutan, gorilla and human, Oxnard showed that even though the radiographs are similar in appearance, the transform of the orangutan vertebrae was star shaped while the others were cruciate in shape implying that the trabecular pattern in the latter are chiefly vertical and horizontal. Examination of the orangutan vertebrae showed that the trabeculae existed as a honeycomb pattern with elements lying at many angles.

Based on the above work, Fourier techniques were utilised during this study to investigate trabecular patterns in human bone in order to develop efficient methods to analyse age changes and changes occurring during disease states such as osteoporosis both qualitatively and quantitatively. A TN-8500 image analysis system (Tracor Northern, Inc.) was employed for this

purpose.

4.2 PRELIMINARY, EXPERIMENTAL WORK

4.2.1 Analysis of simulated trabecular patterns

In vertebrae the main arrangement of trabecular elements are vertical and horizontal (Schmorl and Junghans 1975, Amstutz and Sissons 1969). During age related bone loss, the normal adult trabecular structure of thick plates and rods is converted to a structure with predominantly thin rods. There is also removal of entire trabecular elements. This process is initiated by the perforation of trabecular plates, progressive enlargement of the perforation leading to the conversion of plates to rods (Parfitt et al. 1983). The extreme of this process can be seen in severe osteoporotic patients.

It is interesting to know whether at any stage of this process the trabecular structure is represented by any distinctive pattern. Prior to testing of vertebral patterns therefore, it was decided to study different known patterns using Fourier transform package of the image analysis system. In addition to recognition of trabecular patterns, this would also help to understand the Fourier transform procedure itself.

4.2.1.1 Method

Regular 1cm square grids and patterns simulating trabecular bone in different locations and conditions were drawn on white paper with black ink. These images were acquired into the image analyser using a Cohu 4710 solid state CCD camera (Cohu Inc., San Diego CA). The screen of the monitor was calibrated using a 1cm grid acquired under identical conditions. A pyramid aperture function was applied during the fast Fourier transform process to dampen effect of the edges of the source image. The power spectra were compared with the original images.

4.2.1.2 Results

Studying the power spectra of simulated patterns is useful in interpreting the real power spectra of real images of different trabecular patterns. Some simple points are driven home: an image with no preferential orientation of the elements gives a circular power spectrum. Departure from circularity reflects an orientation in the elements of the image. Using spatial frequency, the periodicity and orientation of these elements can be derived. The size of the power spectrum is related to the size of the components in the image: the larger the elements of an image, the smaller the power spectrum.

One would expect a power spectrum of a simple grid at the extreme, if generalised thinning occurred during age related bone loss. If preferential removal of trabeculae took place, this could also be recognised in the different power spectra. However, in reality, regular patterns rarely exist in trabecular bone. Nevertheless, power spectra of simulated patterns were useful as models to test against observed power spectra from trabecular bone images.

4.2.2. Preliminary studies with trabecular bone patterns

The first practical problem to be addressed in an analysis of trabecular patterns using fast Fourier transforms is to compromise to reach a decision on the optimum image input. The thin histological sections usually used for routine histomorphometrical analysis are unsuitable for this purpose. First, there are insufficient projections from the three dimensional structure to establish a reasonable pattern. Second, it is also necessary to average reasonably large areas of bone for the Fourier analysis and this is rarely possible with histological sections. The poor resolution of routine radiographs and any other clinical images also precludes their use.

It is critical to have an image with a reasonable resolution of the trabecular pattern for a study of this nature. This will exclude the use of conventional incident light micrographs which will always have out of focus features in the image and sample deeper layers non-uniformly according to the chances of obscuration by more superficial layers. Candidates would include contact (high resolution) radiographs and images from beam scanning confocal microscopes. In contact radiographs, the three dimensional structure of the whole thickness is projected on to the film. Using the extended focus facility in confocal optical microscopes it is possible to make optical sections to the required thickness by through focussing whilst capturing the image. Xerox radiographs also offer an alternative due to the quality of the edge enhancement produced, but they were not used in the present study.

What would be the optimum thickness to analyse? The differences between the power spectra of normal and osteoporotic sections would be expected to disappear beyond a certain thickness due to anisotropic nature of trabecular bone. At the other extreme, thin sections would be meaningless in terms of describing trabecular patterns because too little volume is sampled. There is also another problem with osteoporotic samples in that it is impossible to make sections below a certain thickness without disrupting the trabecular pattern. Fortunately, confocal microscopy offers solutions to this aspect of the problem.

A pilot study was carried out to examine possible image inputs and the section thickness required prior to applying fast Fourier transform methods in studying the changing spatial frequency of trabecular bone with age.

4.2.2.1 Materials and methods

(a) Femoral head samples – Femoral heads were obtained at post mortem examination from eight clinically normal premenopausal and osteoporotic postmenopausal females (Age range 30–89 years). These samples were cleaned and frozen immediately. Approximately 5mm thick mid vertical sections of the femoral heads were cut using a band saw and contact radiographs of these specimens were made using a 40 kV X-ray source. The tube–film distance was kept constant during the procedure. The films were hand developed using standard solutions.

(b) Lumbar vertebral body samples – 4th lumbar vertebral bodies were also removed from the premenopausal and postmenopausal cases mentioned above. They were cleaned and stored in 70% ethanol. Using a low speed diamond saw (Isomet–11–1180) with minimum added weight, plane

parallel, precision 3mm thick sagittal sections were cut from these samples. They were then treated with 3% Hydrogen Peroxide (10 fold volume dilution of stock concentrate) at 37°C for 24 hours. After this period the samples were cleaned carefully with a jet of water and defatted in a solution of 50:50 chloroform and methanol for few hours. They were then air dried.

A scientific X-ray machine (ANDREY-Radiation product AS Copenhagen Denmark) was used to produce contact radiographs of these samples on KODAK direct exposure diagnostic films. The exposure time was 2 minutes with 45KV (2ma current) X-ray output.

A beam scanning confocal microscope (Bio-Rad MRC Lasersharp 500) was employed to produce the optical images from these same samples. The microscope was focused on to the topmost layer of the sample, and using the motorised stage, 100 micron extended focus reflected light images were recorded using a Nikon 2/0.08 Planapo objective lens. A Kalman filter was applied to average 20 frames per image plane.

Even with the 2 X objective lens only a maximum area of 24mm² of the sample could be scanned. Therefore several images were recorded from different regions of the same specimen. These images were then normalised (by histogram expansion) and photographed on 35mm film (Ilford FP4).

4.2.2.2. Image input

A uniform, diffused light source with a stabilised power supply was used to illuminate the X-rays and the negatives. All the images were acquired into the TN8500 image analysis computer using a Cohu 4710 solid state CCD camera (Cohu Inc., San Diego CA). During the capture period 30 frames were averaged for an image. In the case of the X-rays only the maximum square of the sample excluding any edges was acquired. The screen was calibrated using a millimetre grid and the 512² pixels by 256 grey level images were stored in the computer. The exact conditions for the video set-up could be recorded in computer memory and recalled on successive occasions to eliminate any problems introduced in acquiring images under different conditions. In the case of 35mm negatives from the BioRad MRC 500 laser confocal microscope, the images were negated prior to storage to produce positive images.

4.2.2.3. Image analysis

The X-ray images of approximately 5mm thick femoral head whole sections showed the poorest resolution. The vertebral body images from the laser confocal microscope had a better resolution, but a disturbing high intensity patch from reflection at optical component surface was present at the centre of every image. It was not possible to avoid this pattern in this microscope at this low magnification. Radiographs of precisely 3mm thick, cleaned vertebral gave reasonably good resolution.

Power spectra of all these images were obtained using the fast Fourier transform package in the TN8500 image analyser. Different aperture functions were experimented with during this procedure and it was decided to use a pyramid window because of its property of dampening the edges of the source image. When power spectra obtained from femoral head sections were

examined, different patterns could be seen in osteoporotics and normals. However, due to poor resolution in the source image, these differences could not be correlated with possible origin in the original image. It was therefore decided to exclude the femoral head radiographs from this pilot study.

Unlike the regular synthetic patterns, power spectra from both types of images of vertebral specimens were dominated by a cloud of intensities around the centre. The asymmetries in power spectra from osteoporotic samples differed from those from normals. However, it was not possible to pick out interesting frequencies from these images. It was necessary to apply some sort of editing to these images to facilitate quantitative analysis and comparison with other images. An assessment of different methods for displaying, highlighting and analysing the data contained in these power spectra was consequently carried out.

Colour coding the digitised power spectrum was found to be useful in highlighting different groups of intensities. Highest intensities at the centre decreased towards the periphery of the power spectrum. Even after applying the standard topo ramp, however, the image was still far from satisfactory for an easy assessment. It was therefore decided to apply a filtering function to improve the image. The "smooth median", size = 3 being selected as the most suitable. This filter sorts the intensities in a 3x3 area, ranking them from lowest to highest, and then places the median value in the centre pixel of the area. The filter was usually applied five times. Images were contoured to simplify the smoothed power spectra. Maps were drawn using different contour intervals to select a suitable value. The contoured power spectra were compared with the original images and with other spectra from different regions of both normal and osteoporotic bone, recording the frequencies at different intensities and angles.

To study different orientations of trabeculae separately, template images were created. Figures 1A to 1C show binary templates that permit the selection of the vertically, horizontally and diagonally oriented elements of an image. The edge of the binary mask was smoothed to reduce edge effects. For analysis, therefore, the images were forward transformed, the template applied to the transform, and the reverse transform process carried out to reconstruct the desired image. It was found that an image with improved resolution could be obtained by creating an image of unwanted elements by the reverse transform and using image mathematics to subtract this image from the original image.

4.2.2.4 Results

The methodological study was beneficial in many respects. It helped in understanding the effects of different routines in the image analysis system, which was important because no extensive published work of this nature could be found in the literature. By examining the CSLM images, it was possible to relate frequency information to original image features. This knowledge was useful in analysing images with poor resolution. The reproducibility and the reliability of the results were both more satisfactory with images of contact radiographs of 3mm vertebral sections (compared with the 100 micron extended focus CSLM images and with the radiographs of 5mm femoral head sections).

Regarding the section thickness, a 100 micron section would be ideal (and would equate roughly with plate/rod thickness), but could not be produced by physical sectioning of unembedded samples. An alternative lies with optical sectioning, but there were many disadvantages with the confocal images that were used during this study. An artifactual reflection at the centre has already been mentioned. Some CSLM images also had "pseudo-zero" areas given by the imaging system. The high frequencies introduced by such breaks are not real and complicate the analysis. It was also found that a large regional variation in trabecular arrangement exists within the same sample, so that images from the whole section should be used. This was not possible with the confocal microscope used during this study as it could only scan a maximum area of 24^2 mm with a 2x objective lens. No confocal microscopes which could produce images from a bigger area than this have been built to date. Scanning the object instead of the light beam may be one of the ways of producing images from such a bigger area. An ideal image for a this kind of analysis might derive from a specially designed, object scanning confocal microscope.

It was also evident from the above study that osteoporotic bone is more polarised than normal bone yet osteoporotic bone contains trabeculae that are oriented at angles other than vertical and horizontal. In normal bone, however, true trabeculae are mainly orthogonal, but the two groups have elements that resist stress at other angles.

The image for analysis of changing spatial frequency of trabecular bone with age should therefore derive from a thin whole section of a vertebral body. The contact radiographs of precise 3mm sections were best suited for this purpose.

4.3 A STUDY OF CHANGES IN VERTEBRAL TRABECULAR BONE WITH AGE USING FREQUENCY DOMAIN ANALYSIS

4.3.1 Method

Post mortem samples of 4th lumbar vertebral bodies were obtained from 13 female and 19 male (Age range 30–91 years) patients. Three females and one male had suffered fractures at the femoral neck and were confirmed osteoporotics.

Plane parallel precision 3mm mid–sagittal sections were cut from these samples using a low speed diamond saw. The sample preparation, image input and analysis were as described above. The power spectra were contoured using an interval of 2, at intensities 2, 4, 6, 8 and 10. For the purpose of the analysis of changing spatial frequency with age, only frequencies at intensities 4, 6 and 8 of the power spectra of clinically normal bone images were used, thereby excluding extreme high and low frequencies. The frequencies in one half of the power spectrum were recorded at 45, 90, 135, 180 degrees. Since one half of the spectrum contains all the information in the original image, the recorded frequencies represent all the frequencies in the vertical, horizontal and diagonal axes of the original image.

4.3.2 Results

4.3.2.1 The comparison of contoured power spectra

Figure 2A is an X-ray image of a 4th lumbar vertebral body mid-sagittal section from a 30 year old female. The image contains all three major zones of the vertebral body (superior, middle and inferior) but excludes cortical bone. Note that the plate like structures of the mid-anterior region and canals for blood vessels can also be seen in the X-ray image. Figure 2B is a contour map of the power spectrum of this image. The contours represent intensities of 8, 6, 4 and 2 respectively from centre towards periphery. The cursor has been placed on contour 6 in all the contoured power spectra that will be discussed in this section.

The high frequency (low intensity) contours of the figure 2B are approximately circular indicating random orientation at these frequencies. Towards the centre, the contours become increasingly polarised and the contour at intensity 6 suggests that the average periodicities in the original image are vertically and horizontally oriented. The intense central contour is horizontally oriented. This means that the orientation of features with the largest periodicities are vertical in the image. The vertical arrangement of thick trabeculae can be clearly seen in the original image.

Figure 3A is a similar X-ray image from a 55 year old female L4. The power spectrum (Figure 3B) shows the predominantly vertical and horizontal arrangement of all the frequencies. Loss of bone is clearly evident in this post menopausal sample. However, as the shape of the contours of the power spectrum suggests, the increase in spacing has mainly occurred in the diagonal directions. This would be predicted from generalised thinning of the "trabeculae" prior to complete removal of elements. Thus as plates convert to rods by the increasing enlargement of perforations the resulting true trabeculae become more and more polarised and the increase in spacing is therefore more marked in diagonal planes.

The extent of the frequencies from the centre is nearly equal in both the vertical and horizontal axes, suggesting that the vertical and horizontal periodicities are nearly equal in this sample. The central contour is highly polarised indicating the almost vertical and horizontal orientations of larger elements in the image. The appearance of thick horizontal elements could have resulted both from the thinning of the large plates and laminae at the central zone, giving rise to horizontally oriented elements, and from the exposure of the walls of the horizontally running blood vessel canals at the centre.

When a the X-ray image of a 4th lumbar vertebral section from a 71 year old female is examined (Figure 4A), bone loss is evident in several regions of the sample, but the overall impression is of normality. However, it is difficult to understand the complex arrangement of the trabeculae by examining the image. The power spectrum (Figure 4B) shows the orthogonal arrangement of all the groups, but the vertical axis is shorter than the horizontal axis, showing an increase in the spacing of horizontal elements. Thus the contoured power spectrum shows the loss of horizontal trabeculae more clearly than the raw image.

The X-ray image of a 4th lumbar vertebral section from a 74 year old female in figure 5A shows a different circumstance. Extensive bone loss is visible in many regions of this sample and the power spectrum (Figure 5B) indicates that the loss has occurred to the same extent in both

vertical and horizontal trabeculae. The contour at intensity 6 suggests that there is a greater increase in the spacing in the diagonal directions. The central contour shows the vertical orientation of the thickest trabeculae in the sample.

Figure 6A is an X-ray image of a 4th lumbar vertebral section from a 89 year old clinically confirmed osteoporotic female showing severe loss and collapse of trabeculae. The main arrangement of the trabeculae is orthogonal, but many fine trabecular elements with oblique orientations can be encountered within the image. The contoured power spectrum (Figure 6B) reflects these features. The orthogonal arrangement dominates the spectrum, but the irregular contours indicate the many other orientations of the elements in the image.

The images from the female group showed no significant differences to that of the male group when followed through increasing age.

Again, features not apparent in the images could be deduced by examining the power spectra. For example, Figure 7A is an X-ray image of a 4th lumbar vertebral section from a 50 year old man. The image the walls of the blood vessel canals appear as intense horizontal elements at the centre: some bone loss can be seen in the peripheral zones. The power spectrum (Figure 7B) indicates an orthogonal arrangement. However, the contour at intensity 6 (green contour) shows an eccentricity between the 45° and 135° directions, indicating an increased spacing in 45° direction.

As an example of how size of the power spectrum may indicate some characteristics of an image, Figure 8A is an X-ray image of a vertebral section from an 89 year old clinically confirmed osteoporotic male showing extensive loss of bone. The power spectrum (Figure 8B) is comparatively small, indicating the presence of fewer, larger elements. It is also stretched horizontally, and the frequencies are very low (spacing large) in the vertical axis.

4.3.2.2 The analysis of changing spatial frequency with age

Frequencies were determined for both the male and female groups and the following statistical analyses carried out.

(a) The histograms

Two random samples of frequencies were taken from each group and their histograms were drawn to observe the shape of the curve. As none of the expected curves (Bell or Skewed) were observed it was concluded that there is no linear relationship within frequencies in each group.

(b) The distribution of frequencies

To test the assumption that the frequencies are approximately normally distributed, the t-test of significance for the point biserial coefficient was carried out and normal plots of frequencies of each group were drawn. Approximately "S" shaped curves were obtained, implying that the samples were approximately normally distributed.

It is therefore possible to use the above test to examine the correlation between male and female samples (or to verify $r=0$; r = Correlation Coefficient between samples).

(c) The relationship between frequencies of male and female groups

The Correlation Coefficient (r) was calculated.

$$r(\text{RSM}, \text{RSF}) = -0.095$$

RSM = Random sample male

RSF = Random sample female

$$t = r \sqrt{(n-2)/\sqrt{(1-r^2)}}$$

Where r = Correlation Coefficient

$$n = 50$$

Null hypothesis; $H_0 : r \neq 0$

Alternative hypothesis $H_1 : r = 0$

The significance level of $\alpha = 0.01$ was used and the critical region is given by

$$r \leq -r_{n, 2\alpha}, \text{ for this test.}$$

Where n = 50

$$\alpha = 0.01$$

r = Calculated value of Correlation Coefficient

This tabulated value was -0.427

$$\text{But } r = -0.095$$

This implies that the H_0 is rejected at the 1% level. Alternatively this suggests that $r = 0$, and there exists strong evidence (99%) to say that there is no association between these two groups of frequencies. This suggests that when building up a regression model to express these frequencies, the two groups should be considered separately.

(d) The relationship between frequency and age within each group

The χ^2 test was employed to examine the relationship between frequency and age within the male and female groups.

$$\chi^2_{k-1} = \frac{(n_1-3)Z_1^2 + (n_2-3)Z_2^2 - [(n_1-3)Z_1 + (n_2-3)Z_2]^2 / (n_1-3 + n_2-3)}{(n_1-3) + (n_2-3)} \text{-----(1)}$$

Where k = Number of samples

n_1 = Sample size of the male group

n_2 = Sample size of the female group

Z_1 and Z_2 are obtained from the Fisher Z transformation

$$Z_r = 1/2 [\log_e(1+r) - \log_e(1-r)]$$

Where r = Correlation Coefficient

Now the Correlation Coefficient of the two samples were obtained

Let $r_1 = \text{Corr}(f,a)$, $n_1 = 15$ for male random sample

Let $r_2 = \text{Corr}(f,a)$, $n_2 = 10$ for female random sample

f = Frequency and a = Age

$H_0 : r_1 \neq r_2$; $n_1 = 15, n_2 = 10$

The observed values for r_1 and r_2 were

$$r_1 = -0.925$$

$$r_2 = -0.174$$

The values for $Z_1 = -0.1758$, $n_1 = 15$

$$Z_2 = -0.16225$$
, $n_2 = 10$

$$k = 2$$

Therefore from (1) $\chi^2_1 = 14.5$

The tabulated value of $\chi^2_{v,a} = 0.9995$

Where v (degree of freedom) = 1

$$a \text{ (significance level)} = 0.01$$

This suggests that there is strong evidence supporting $r_1 = r_2$ at the 0.01 significance level. Alternatively, there exists strong evidence to say that the relationship between frequency and age is similar within each group.

The above analysis suggests the building of a model to express frequency in terms of other parameters and to investigate the association between frequency and age separately within male and female groups.

(e) The multiple regression analysis

The following variables were employed during this analysis.

Dependent variable = f

Co-variables = $a, l, i, al, ai, li, a^2, l^2, i^2$.

f = frequency, a = age

l = angle, i = intensity

To determine whether log co-variables are appropriate in building up a model, a common transformation was given to each co-variable.

$$X = \exp(L \log x)$$

x = given co-variable

$$L \in [-2, +2]$$

The calculated values for L and R^2 from a computer statistical programme (Minitab) are given in the Appendix II.

(i) The stepwise multiple regression of the male sample

Using the nine above mentioned co-variables, stepwise regression was carried out to determine the appropriate model.

The selected model among these co-variables is

$$f = 4.60 - 0.994i + 0.0000431i^2 + 0.0402i^2 - 0.000561a^2 + 0.0627a - 0.000624li \text{-----} (2)$$

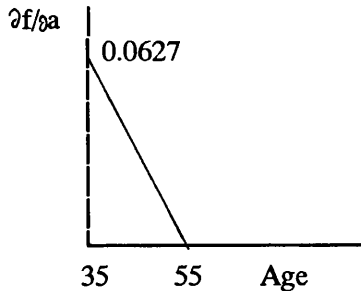
The R^2 of this model = 91.0%

This value is greater than the value given by the log co-variables. Hence, log co-variables are inappropriate and the appropriate model should be (2).

Next the partial derivative of the frequency with respect to age was determined.

$$\partial f / \partial a = -0.001122a + 0.0627$$

When plotted



From these results the following conclusions could be deduced.

When the angle and the intensity are constant, the maximum incremental rate of the frequency with respect to age in the male sample occurred within the earlier age group studied.

The increment rate continuously decreased from 35–55 years (but the frequency continuously increased). The increment rate decreased beyond 55 years (e.g. The frequency decreased with increasing age).

Figure 9 is a plot of the frequency against age in the male sample.

(ii) The stepwise multiple regression of the female sample

The same co-variables as used in the male sample were utilised to carry out stepwise regression on the female sample.

The selected model among these co-variables is

$$f = 6.40 - 0.921i + 0.0000411l + 0.00280ii - 0.000053al \text{-----} (3)$$

This model specifies that the $\partial f / \partial a$ is constant.

Thus in the case of the female sample, the rate of change of frequency with respect to age is a positive constant provided the angle and the intensity are constant.

Figure 10 illustrates the plot of frequency against age in the female sample.

(f) The test of significance for the coefficients of the model

The two sided t-test at 0.002 significance level was employed for this purpose.

(i) For the male data set

$$t_{(273, 0.002)} = 3.145$$

From the ANOVA table the absolute values of the t-ratio of the coefficients are >3.14 except for LI. For the coefficient of LI the absolute value of the t-ratio >2.601 ($t_{273, 0.01}$).

This means the coefficient of LI is significant only at the 99% level whereas the others are significant at the 99.9% level.

The significance of the total variation :

$$\text{Mean square ratio (M.S.R.)} \approx F_{6, 273}$$

But the calculated value of M.S.R. (From the ANOVA table) is 445.

This implies $F_{(6, 273)}(.001) \ll 445$.

There is therefore strong evidence to say that this regression equation exhibits a significant

part of the total variation.

(ii) The same procedure was repeated for the female data set.

$$t_{(152, 0.002)} = 3.14.$$

The ANOVA table shows that all the coefficients are significant at the 0.002 level (e.g., 99.9%).

The significance of the total variation :

$$M.S.R \propto F_{4, 152}$$

The calculated value for M.S.R. = 284.6

This implies $F_{(4, 152)}(0.001) \ll 284.6$

The female regression model also therefore exhibits a significant part of the total variation.

(g) The increase in trabecular spacing with age

The reciprocal of the frequency in the power spectrum provides the periodicity of the elements in the image at right angle to the direction of the frequency. In power spectra of the trabecular bone images, the periodicities were calculated in this way at different ages at 45⁰, 90⁰, 135⁰ and 180⁰. Tables I and II show periodicities at three intensities (4, 6, 8) at each angle for male and female groups respectively.

For both male and female groups, the lowest and the highest periodicities were encountered in the majority of cases at around 35 year and 89 year of age. The increase in periodicity and therefore the increase in trabecular spacing was higher at high intensity levels. Low intensity levels represent smaller periodicities in the image. Thinning of trabeculae could give rise to the small elements which in turn would be responsible for small periodicities on aging. This would be the reason for the comparatively less well marked increase in periodicities at low intensity levels. By contrast, the increase in higher periodicities was not affected by such a phenomenon and is therefore depicted accurately at high intensity levels.

Considering the increase in trabecular spacing at different angles, the increase at 45⁰, 90⁰, 135⁰ and 180⁰ in males was by factors of roughly 2.23, 2.5, 2.30 and 1.60 and in females by factors 3.01, 1.72, 3.14 and 1.68. This shows that in females the increase is most marked at the diagonals (45⁰ and 135⁰). However, the overall mean increase in trabecular spacing was by a factor 2.10 in males and 2.39 in females.

4.3.2.3 The volume density of radiographs and the study of individual groups of trabeculae using templated images

(a) The significance of net radiodensity of 3mm plane parallel sections

In a radiograph, the radio opacity of a region depends on the volume fraction of bone in that region of the sample. Therefore, if the bone composition, section thickness, image recording and transfer functions were constant, pixel intensities would (roughly) index mass/area of the section. Since plane parallel, precise 3mm sections were used in this study and all the other conditions were constant, mapping these intensities provides information with respect to the packing density (porosity) of bone in different regions of the vertebral section. This is therefore

another approach of analysing volume density of radiographic images.

In Figure 11 A–D the images were mapped using the colour scheme used on topographical maps (see ramp at top of figure). Figure 11A is an image from a 4th lumbar vertebral section from a 30 year old female. Generally the colours represent the higher intensity part of the scale indicating the dense nature of the normal bone. The walls of the section are white (=peak white), the colour band corresponding to the highest (X–ray) optical density in the original bone slice – the least optical density in the negative radiographic image, because there is minimal pore space in the compact cortex. In Figure 11A, the next lower density band lies immediately underneath the walls. The core of the section is generally comparatively less dense, but thick vertical and horizontal components (red in colour) representing parts of vertical and horizontal trabeculae can be seen throughout the section. Nevertheless, none of these "trabeculae" can be traced from one end to the other (It must be remembered that these summation images reflects the addition of layers of trabeculae/plates/tubes in the 3mm section thickness – the only true single trabecular elements are represented by elements of thickness blue! Even thickness green means a plate like element on edge!). Canals for blood vessels can also be identified at the centre of the section.

Figure 11B is a similar digitised radiographic image of a 3mm section of L4 from a 31 year old man. The features described above can also be seen in this section. However, the intensities are low around the entry of the basivertebral vessels, and this is indicated by the cartons from the lower end of the colour scale (shown in Fig.11B). Lower intensities can also be encountered at the most anterior part of the middle third of the section where the structure normally consists of huge plates oriented in vertical direction. Hence the volume density of bone is less when the structure is almost plate–like and the plates (or walls of tubes) are imaged face on, and in regions where large blood vessels are present and bone is correspondingly absent. Immediately beneath the superior end–plate of the section, a second horizontally oriented plate can be seen at the centre of the section. These double end plates are a normal occurrence in vertebral bodies. Such plates are peak white indicating that they are as compact as the cortex proper.

Figure 11C is the digitised radiograph, again of a 3mm plane parallel section, of L4 from a clinically non–osteoporotic 89 year old female. Four less dense regions are located at anterior and posterior ends of the superior and inferior zones of the section. The vertical "trabeculae" in these regions are "more dense" (i.e. thicker and more massive, having a greater volume) than the horizontal and can almost be traced from one end plate to the other at the anterior region of the section. Further, all the density bins from black to peak white are represented in this section.

Figure 11D is an image of a radiograph of L4 colour coded for (volume) density from a 89 year old osteoporotic female. Even though some dense regions can be seen in the cortical shell of the section, the majority of the trabecular bone is at the lowest end of the density scale, and most intermediate density bins are absent in this image. This reflects the fact that the trabecular spacing is so increased that only single trabecular elements are imaged in the 3mm thickness of the section. An approximate indication of the colour scale is that each of the 16 colour bins represents 3/16 mm, taking all bone to have a standard density. The dark and light blue bands thus cover net thicknesses (optical paths) of 3/16 and 3/8 mm respectively.

Returning to consideration of the factors that would contribute to the density of different regions in the contact radiograph of the plane parallel section of a vertebral body: in the case of the cortical shell, it is merely the thickness that determines the radiographic optical density. In trabecular bone, the thickness of the individual elements, and their morphology, by influencing the number of overlapping trabeculae, also contributes to the image density. Where large blood vessels are present, the radiographic density is low, since the vessel space effectively excludes bone tissue and the walls of the canals for these vessels are thin compared with the thick sturdy trabeculae elsewhere. In regions where huge vertically oriented plates are present (as in the mid anterior region) the plate are actually walls of cylinders running vertically in the vertebral body. The diameter of these cylinders is large in the middle zone of the body and this therefore makes the number of overlapping elements less in the section making the region less dense.

Different numbers of vertical and horizontal trabeculae may contribute to the different densities seen. One way to understand this is to "dissect" vertically, horizontally and diagonally oriented elements using binary templated reverse FFT transformation and thus study them separately to observe the changes that occur with aging and during osteoporosis.

(b) The study of trabecular groups using templated FFT routine

Figure 12 shows four images of a mid-sagittal vertebral section from a 30 year old female. The first is the whole image and the others are images of vertically, horizontally and diagonally oriented trabeculae respectively. These "dissected" images, representing as they do only discrete fractions of the total density, show generally lower intensities, as can be seen by reference to the standard colour coding scale.

As indicated by the changing colour along the course, both vertical and horizontal elements have different densities when traced from one end to the other. Beneath the end plates of the vertebral bodies, the fraction represented by the vertical trabeculae is less significant than that of the horizontal trabeculae. i.e. horizontal trabeculae contribute more to the net density under the end plates. As shown by the lower right image in Figure 12, the diagonally oriented "elements" are more evenly distributed.

Figure 13 shows similar four images derived from a vertebral section of a 50 year old man. The central zone has a very dense region while the superior zone and the anterior part of the inferior zone are comparatively less dense. The "dissected" images show that all three components contribute to the density of the denser region in the central zone. In less dense regions however, it is the horizontal component that is missing to a greater extent. The "horizontal image" emphasises the canal for the large blood vessel which is denser than the rest of the trabecular elements.

Figure 14 derives from similar binary templated reverse FFT transformation of the contact radiograph of a 3mm section of the L4 body of a 71 year old, clinically non-osteoporotic man. Compared with the 30 year old female (Figure 12) there are less high intensity regions, indicating the decreasing density with age. Comparing the whole image with the dissected images, it is again apparent that it is the horizontal trabeculae that are mostly missing in the less dense regions, which are in the same locations as observed in Figure 13.

It is presently well accepted that the horizontal trabeculae are lost first during age related bone loss in the vertebral body. However, it is not clear in which region this process of removal begins. From the examination of a series of dissected images from the ages of 30 to 91, it was found that this process first appears at the regions noted (in the horizontal trabecular images of) in Figures 13 and 14. In other words, with age, thinning and loss of horizontal trabeculae in the mid-sagittal plane occurs first at anterior and posterior regions of the superior and inferior zones. Thinning was also observed with age around the region of the entry of the basivertebral vessels. However, this component could be in response to changes in vasculature with age rather than to generalised bony changes.

Figure 15 is a similar image from a 89 year old, clinically confirmed osteoporotic female patient. Most of the intermediate intensity bins are missing indicating that section consists of high density cortical shells enclosing low density trabecular cores. However, unlike the core in normal bone, some prominent vertical features are as dense as the surrounding cortical shell.

When the dissected images are compared, it is obvious that most of the remaining bone of this sample is vertically oriented. Horizontal and diagonally oriented elements are either almost absent or confined only to discrete regions. Double vertebral end plates were not encountered in osteoporotic sections.

The diagonally oriented trabecular elements in younger samples appeared as short bits distributed evenly all over the section. This agrees with the impression that they are pieces of huge plates and rods oriented in other directions. However, in some old and osteoporotic samples, several real trabeculae oriented in these directions could be readily identified.

The technique of studying separated groups of trabeculae in the vertebral body might also be useful in studying pathological conditions other than osteoporosis. In the Figure 16 the first image is a vertebral section from a 75 year old female. A big Schmorl's node is present at the superior aspect of this section. Very high intensities show denser bone tissue around the node. When "dissected" images are examined, it is clear that the horizontal trabeculae have mostly contributed to this thickness. Thickened vertical trabeculae can only be seen on the side walls of the nodes. Further, there are few thickened trabeculae in diagonal directions as indicated by the lower right image of the figure 16.

When these changes of different groups of trabeculae were compared between sexes, no significant differences could be observed.

4.4.3 Discussion

4.4.3.1 Contoured power spectra

The power spectra can be used to obtain valuable information from vertebral sections. By examining different contours of the contour map of the spectrum it was possible to provide measures of size and orientation of elements in the original image. The main orientations of trabeculae in both young and old samples are vertical and horizontal, but the large elements are more polarised than the smaller ones in young samples.

The increase in trabecular periodicity with age related bone loss first occurs at the diagonals. This could happen as a result of generalised thinning of all the trabecular elements. Horizontal spacing increases secondarily. Spacing of vertical increases with age but to a lesser degree than in horizontal and diagonal directions.

It was possible to gain some information from the power spectrum that cannot be obtained by looking at the image alone. Figure 4 showed one such example. Even though the image looked quite normal, the power spectrum revealed an increase in horizontal spacing (loss of horizontal trabecular elements). The occurrence of different orientations in trabecular groups of osteoporotic bone can be judged accurately from the power spectra. It is simple to see if the bone is osteoporotic by looking at the power spectrum alone. The extent of bone loss can easily be identified from the power spectrum rather than the image. Even when an image with poor resolution is examined the power spectrum can still provide valuable information that is not apparent from the image.

The size of the power spectrum is an index of the range of the sizes of elements in the image. The smaller area covered by the significant central elements in spectra from porotic samples reflects the fewer, larger trabecular groups. The power spectrum can therefore be used effectively to analyse trabecular bone patterns and their changes with age as well as in osteoporosis. Power spectra might be useful in "fingerprinting" different structural patterns.

4.4.3.2 The analysis of changing spatial frequency with age

One objective of this work was to seek an efficient method to derive quantitative information from trabecular bone. The analysis of spatial frequency offered a superior technique for this purpose.

The random samples that were used for the statistical analysis were approximately normally distributed, but there was no linear relationship of the frequencies within each group. When probable relationships between spacing and age were tested, they were found to be similar within both male and female groups.

The data used in the trabecular frequency analysis were selected from clinically normal and histologically non-osteoporotic samples. The clinical criteria of the occurrence of a fracture to distinguish between normal and osteoporotic bone was not satisfactory. Some clinically non-osteoporotic samples showed severe osteoporosis on sectioning, but were excluded from the frequency analysis.

The multiple regression analysis revealed interesting results regarding the relationship of trabecular spacing to age. In both males and females the frequency generally decreased with age. In males, this decrease occurred only after the middle of the sixth decade and the annual increment continuously decreased. Up to this point the frequency actually increased with a decreasing incremental rate. However, this increase in frequency was negligible compared with the decrease afterwards. In females, however, the frequency continuously decreased throughout life with a more or less constant incremental rate.

Decrease in frequency means increase in trabecular spacing. This is therefore another method of expressing age related bone loss.

The data obtained from different histological and densitometric techniques for age related bone loss in the spine are conflicting (Riggs and Melton 1986). For example, Madsen (1977) reported that the bone mineral content in women did not change until the sixth decade, while others found an onset of bone loss as early as the third or fourth decades in both males and females (Bell et al, 1967; Havivi et al, 1971; Arnold 1973; Riggs et al (1981). Many studies have also reported a linear reduction of bone from young adulthood throughout life in both sexes (See. Mazess 1982). However, others have reported an accelerated phase of bone loss during the decade following menopause (Krønlner and Nielsen 1982; Meunier et al, 1973).

There can be many reasons for the diversity of results obtained from different techniques. Both invasive and noninvasive techniques have their own disadvantages. For example, tomographic measurements may over-estimate the extent of bone loss because they are greatly influenced by the fat content of the marrow. Most histological studies use a small volume of bone and are not representative of the extent of the regional variations within the vertebral body. Further, the anatomical site of measurement may also be important in understanding the differences between studies. Bone loss in one site is influenced not only by generalised factors, but by local factors such as changes in mechanical stress and vascular supply. Consequently, as predicted by some studies, measurements from iliac crest biopsies would not provide a correct impression about changes in the spine. Biological variations between subjects will be possibly the most important of all origins of discrepancies. It has also been pointed out that sample sizes encountered in most studies are insufficient for a reasonable assessment of onset and rate of bone loss (Mazess 1982). The present study is also lacking in this respect: one can only point to the difficulties involved in obtaining and processing samples!

Most existing techniques measure the amount of trabecular bone rather than providing any analysis of arrangement or architecture. Techniques that have measured arrangement – such as counting different groups of trabeculae – suffer from the same disadvantages as the histological studies; they are unwieldy and inefficient in dealing with large groups of samples.

The spatial domain techniques considered here offer several advantages over most previous methods. The samples used are cleaned and defatted sections, so that the results are not influenced by tissues other than bone. Furthermore, the use of whole sections minimises the effects of regional variations in trabecular structure on the analysis. The use of whole sections in other techniques would be very time consuming. However, once a radiographic image has been acquired and digitised in the image analyser, it takes only a few minutes to acquire necessary results. The technique involves no counting or measurements by the examiner; frequencies can be directly recorded by moving the cursor over the relevant region of the power spectrum. Therefore, examiner variation as such is absolutely minimal with the frequency analysis.

There are also additional advantages with this technique. Since frequencies can be recorded at different angles, the trabecular spacing can be derived as a function of orientation. This can further widen our knowledge about the mechanism of bone loss and permits comparisons and correlations of the pattern of bone loss with other factors such as location in the spine, morphology of the individual vertebra and the influence of direction of mechanical stress.

The present study suggests that there is a minimum trabecular spacing at approximately 35 years and a maximum at approximately 89 years. In other words, trabecular spacing increases with age and the overall increase was two fold (linear) over the age range examined.

It was also possible to calculate the average increase in spacing in separate vertical, horizontal and diagonal directions. In females this increase was more marked in diagonal directions, while males showed no such preference. The increase in spacing is more prominent among the larger elements of the trabecular bone image. Complete removal, rather than thinning of the bigger trabeculae, may be responsible for the increase in trabecular spacing.

More extensive studies using a larger number of samples will be necessary to confirm these results.

Frequency analysis does not measure the amount of bone in a sample. A measure of frequency or the trabecular spacing is a measure of two dimensional arrangement of features in an image of trabecular bone, and may not necessarily correlate with independent measurements of bone mass or density. In old age it may be possible to find a correlation between falling bone mass and increasing trabecular spacing, but, this may not necessarily be the case at a younger age. It is possible that a considerable amount of bone may already have been lost when the first signs of increased trabecular spacing are apparent.

The measurement of trabecular spacing with increasing age should play an important role in an assessment of age related bone loss. It is now well known that the measurement of bone mass alone is not sufficient to explain the fragility of bone that osteoporotic patients usually exhibit. Failure to measure bone architectural changes has been given as one reason for this. However, there are no simple methods to describe and quantify architectural changes in a complex three dimensional structure such as trabecular bone. A two dimensional technique such as frequency analysis can never totally fulfil this requirement, but, combined with other techniques, could produce more reliable results than possible with other techniques alone.

4.4.3.3 The study of trabecular groups using templated images

"Density" in the radiographic images can be derived directly by digitising, and could be made reasonably quantitative if, for example, an aluminium step wedge standards was used to calibrate the densities of plane parallel sections . Using pseudo-colours to grade different intensity levels, it was already possible to identify regions with matching net densities in the vertebral sections. For example, regions composed mainly of plate like trabeculae or regions with vascular channels are less dense than the more rod like regions.

The results were more remarkable when different groups of trabeculae were separated using binary templated reverse FFT transformation. Firstly, it was possible to identify which group of trabeculae makes the major contribution towards the net density within a particular region. Secondly, the age series showed which trabecular orientations are thinned out first and in which regions this thinning first takes place. Accordingly, horizontal trabeculae were found to be the first to go and the thinning initiated in anterior and posterior regions of the peripheral zones of mid-sagittal sections of 4th lumbar vertebral bodies. No other technique allows the simple study of

different trabecular groups separately. The results are reliable, obtained automatically and are independent of examiner bias.

This technique also provided additional information about the changing architecture of vertebral trabecular bone with age. In younger samples, the cortical shell showed the highest density. "Trabeculae" traced from one end to the other showed varying densities along this course and there were many variations in densities over the field of the section. By contrast, some of the remaining "trabeculae" in osteoporotic bone were as dense as the cortical shell. The overall density of osteoporotic sections did not vary much: – either there were very dense regions or very porous regions. All this suggests the existence of a very simple architecture in osteoporotic bone compared with the normal complex trabecular architecture.

The use of intensity mapping to study density and the study of different groups of trabeculae will be very useful techniques in analysing trabecular bone changes with age and during osteoporosis. They may also be applicable to other pathological conditions of bone.

4.5 CONCLUSION – FREQUENCY DOMAIN ANALYSIS

The objective of this project was to experiment with the powerful capabilities of the Fourier transform routines of the "state of the art" image analysis techniques to find a possible way of investigating human vertebral trabecular bone patterns, with particular reference to the study of age and osteoporotic changes, both qualitatively and quantitatively.

Since no prior published work was available for reference, the reliability and reproducibility of any proposed routines had therefore to be tested at each and every step.

Several important conclusions can be drawn from this preliminary study. Firstly, this is a new tool to analyse trabecular patterns and their age and osteoporotic changes, which offers several advantages over more traditional methods. Secondly, the use of contoured power spectra to compare different images provides an accurate and efficient method of analysing different trabecular patterns. The technique of studying separated groups of trabeculae using templated images is quite new and new information concerning differences in the disposition, arrangement and density of various groups of trabeculae at various regions can be derived using this technique. Techniques based on the separation of features ("particles") in standard image analysis routine would need a great deal of operator involvement and judgment in deciding where to "cut" trabeculae.

Finally, frequency domain analysis also permits the quantitative analysis of trabecular bone. Not only the changes in trabecular spacing with age could be assessed more efficiently and accurately, but the technique could also be used to obtain more descriptive information that cannot yet be derived from any other technique. For example, it is possible to measure the increase in spacing in different directions of the vertebral body and then to correlate these results with the results obtained from other indirect techniques. Hopefully, it might also be possible to relate such findings with changes in mechanical strain in different directions.

When developing a proper frequency domain technique, one of the most important considerations is the image input. The images of contact radiographs of 3mm thick vertebral

sections used during this study are not the best for this purpose. Producing plane parallel sections of 3mm sections and contact radiographs with a stable exposure and standard development is very difficult and time consuming, especially when the samples are severely osteoporotic. One potential solution to this problem lies with confocal microscopes, if a method could be developed to produce images from larger areas of bone: existing commercially available instrument systems and lenses are not suited.

4.6 REFERENCES

- Amstutz HC, Sissons HA (1969) The structure of vertebral spongiosa. *J Bone Joint Surg* **51B**:/III540–550.
- Andrews HC (1968) A high speed algorithm for the computer generation of Fourier transforms. *IEEE Trans Comp C*–17/IV373.
- Andrews HC, Pratt WK (1968a) Fourier transform coding of images. *Int Conf System Sci, Hawaii*. pp 677–679.
- Andrews HC, Pratt WK (1968b) Television bandwidth reduction by encoding spatial frequencies. *Soc Motion Pic Tele Eng* **77**:1279–1281.
- Andrews HC, et al. (1970) *Computer techniques in image processing*. Academic press NewYork London
- Arnold JS (1973) Amount and quality of trabecular bone in osteoporotic vertebral fractures. *Clin Endo Metab* **2**:221.
- Becker HC, Meyers PH, Nice CM (1969) Laser light diffraction, spatial filtering and reconstruction of medical radiographic images. *Ann NY Acad Sci* **157**:465–486.
- Bell GH, Dunbar O, Beck JS (1967) Variations in strength of vertebrae with age and their relation to osteoporosis. *Calcif Tissue Res* **1**:75.
- Bookstein FL, Straus RE, Humphries JM, Chernoff B, Elder RL, Smith GR (1982) A comment upon the use of Fourier methods in systematics. *Syst Zoo* **31**/I85–92.
- Cochran WT, Cooley JW, Favini DL, Helms HD, Kaenel RA, Lang WW, Maling GC, Nelson DE, Rader CM, Welch PD (1967) What is the fast Fourier transform? *Proc IEEE* **55**:/X1664–1674.
- Cooley JW, Tukey JW (1965) An algorithm for the machine calculation of complex Fourier series. *Math Comp* **19**:297–301.
- Cooley JW, Lewis PAW, Welch PD (1967) Historical notes on the fast Fourier transform. *Proc IEEE* **55**:/X1675–1677.
- Duda RO, Hart PE (1973) *Pattern classification and scene analysis*. Wiley Interscience NewYork.
- Erlich R, Banter Pharr R, Healy–Williams N (1983) Comments on the validity of Fourier descriptors in systematics: a reply to Bookstein et al. *Syst Zoo* **32**:/II202
- Ferson SF, Rohlf J, Koehn RK (1985) Measuring shape variation of two dimensional outlines. *Syst Zool* **34**:/I59–68.
- Goodman JW (1968) *Introduction to Fourier optics*. McGraw–Hill NewYork.
- Greenfield GB, Hubbard LB (1984) *Computers in Radiology*. Churchill Livingstone NewYork.
- Havivi E, Reshef A, Schwartz A, Guggenheim K, Bernstein DS, Hegsted DM, Stare FJ (1971) Comparison of metacarpal bone loss with physical and chemical characteristics of vertebrae and ribs. *Israel J Med Sci* **7**:1055.
- Holeman JM (1968) Holographic character reader. In: *Pattern recognition*. Kanal LN (ed) Thompson Book Co. Washington 63–78.
- James M (1987) *Pattern recognition*. BSP Professional Books.
- Kopp RE, Lisa J, Mendelsohn J, Pernick B, Stone H, Wohlers R (1976) Coherent optical processing of cervical cytological samples. *J Histochem Cytochem* **24**:122–137.
- Krølnær B, Pors Nielsen S (1982) Bone mineral content of the lumbar spine in normal and osteoporotic women: cross–sectional and longitudinal studies. *Clin Sci* **62**:329–336.
- Lestrel PE, Brown HD (1976) Fourier analysis of adolescent growth of the cranial vault: a longitudinal study. *Hum Biol* **48**:517–528.
- Lestrel PE, Kimbel WH, Prior FW, Fleischmann ML (1977) Size and shape of the hominoid distal femur: Fourier analysis. *Am J Phys Anthropol* **46**:281–290.
- Lu KH (1965) Harmonic analysis of the human face. *Biometrics* **21**:491–505.

- Madsen M (1977) Vertebral and peripheral bone mineral content by photon absorptiometry. *Invest Radiol* **12**:185-188.
- Madsen MT, Park CH (1985) Enhancement of SPECT images by Fourier filtering the projection image set. *J Nucl Med* **26**:395-402.
- Mazess RB (1982) On aging bone loss. *Clin Orthop Rel Res* **165**:239-252.
- Meunier P, Courpron P, Edouard C, Bernard J, Bringuier J, Vignon G (1973) Physiological senile involution and pathological rarefaction of bone: quantitative and comparative histological data. *Clin Endo Metab* **2**:239-256.
- Meyer GH (1867) Die Architectur der Spongiosa. *Arch Anat Physiol Wiss Med* 615-628.
- O'Higgins P, Johnson DR, McAndrew TJ (1986) The clonal model of vertebral column development: a reinvestigation of vertebral shape using Fourier analysis. *J Embryo Exp Morph* **96**:171-182.
- O'Higgins P, Williams N (1987) An investigation into the use of Fourier coefficients in characterizing cranial shape in primates. *J Zool Lond* **211**:409-430.
- O'Higgins P, Johnson DR (1988) The quantitative description and comparison of biological forms. *CRC critical reviews in anatomical sciences* **1**:/III149-170.
- Oxnard CE (1972) The use of optical data analysis in functional morphology: investigation of vertebral trabecular patterns. In: *The functional and evolutionary biology of primates*. Tuttle R (ed) Aldine Atherton, Chicago New York 337-347.
- Oxnard CE (1973) *Form and pattern in human evolution*. The university of Chicago press, Chicago London.
- Oxnard CE (1980) The analysis of form: without measurement and without computers. *Amer Zool* **20**:695-705.
- Oxnard CE (1984) *The order of man. A biomathematical anatomy of the primates*. Yale university press, New Haven London.
- Riggs BL, Melton LJ (1986) Involutional osteoporosis. *New Eng J Med* **314**:1676-1686.
- Riggs BL, Wahner HW, Dunn WL, Mazess RB, Offord KP, Melton LJ (1981) Differential changes in bone mineral density of the appendicular and axial skeleton with aging. Relationship to spinal osteoporosis. *J Clin Invest* **67**:328-335.
- Rohlf FJ, Archie JW (1984) A comparison of Fourier methods for the description of wing shape in Mosquitoes (Diptera: Culicidae). *Sys Zool* **33**:/III302-317.
- Schmorl G, Junghanns H (1975) *The human spine in health and disease*. Grune and Stratton, New York and London.
- Shulman AR (1970) *Optical data processing*. Wiley, New York.
- Taylor CA, Ranniko JK (1974) Problems in the use of selective optical spatial filtering to obtain enhanced information from electron microscopy. *J Microscopy* **103**:/III307-314.
- Walker J (1982) Simple optical experiments in which spatial filtering removes the "noise" from pictures. *Sci Am* **247**:/V194-206.
- Walter RJ, Berns MW (1986) *Digital image processing and analysis*. In: *Video Microscopy*, Inoue S Plenum press New York and London pp 327-392.
- Wolff J (1870) Ueber die innere Architektur der Knochen und ihre Bedeutung fuer die Frage vom Knochenwachstum. *Virchows Arch Path Anat Physiol* **50**:389-453.

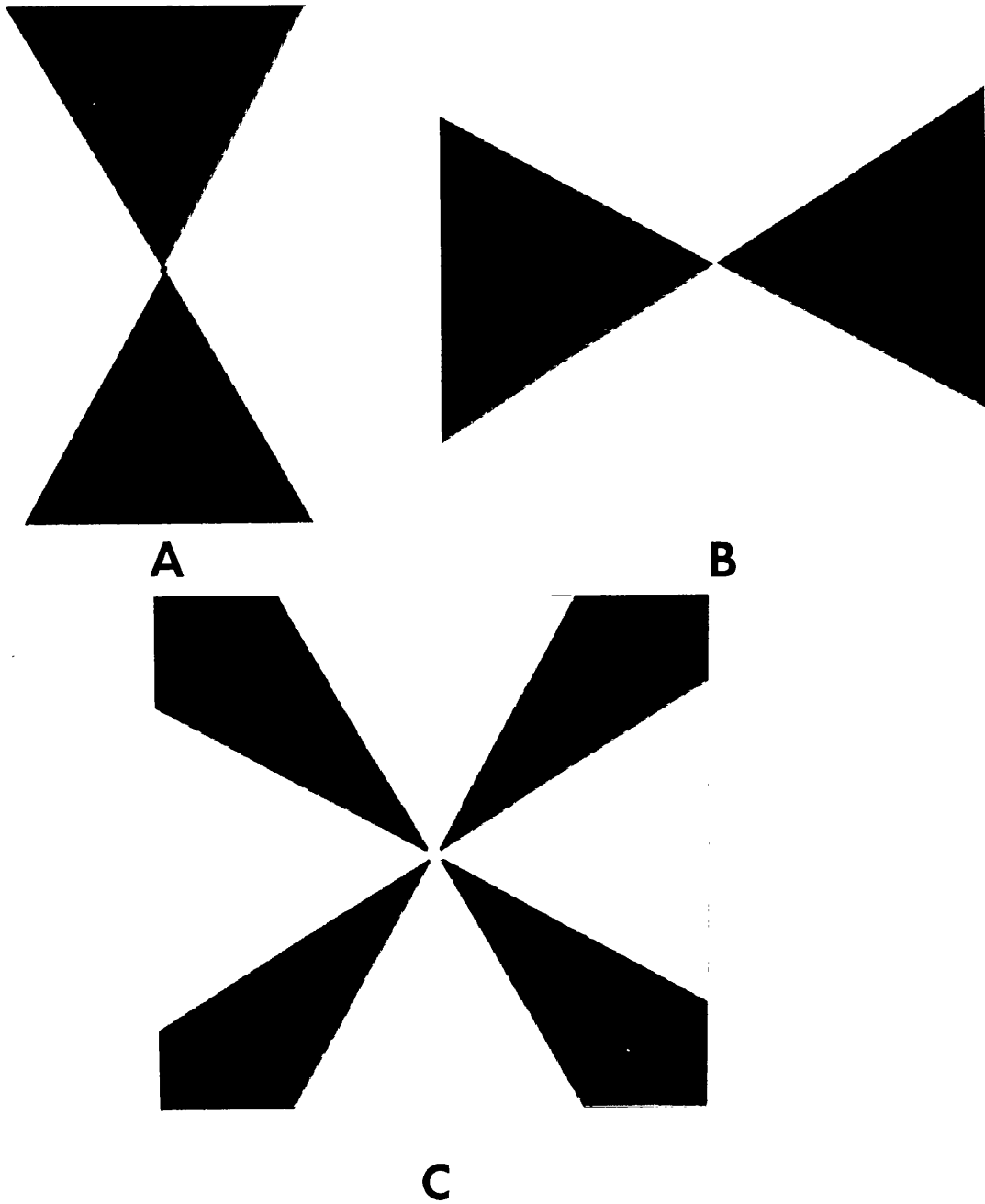


Fig. 1 Template images used for individual analysis of vertically (A), horizontally (B) and diagonally (C) oriented elements in trabecular bone images. These templates were applied to forward transformed images and the reverse transform process was carried out to reconstruct the desired image.



A



B

The trabecular bone images of all the figures in this chapter are derived from X-ray images of 3mm mid-sagittal sections of 4th lumbar vertebral bodies.

Fig. 2 An image from a 30 year old female (A) and its contoured power spectrum (B).

The contours represent intensities 8, 6, 4 and 2 from the centre towards the periphery. All the power spectra in this chapter were contoured using an interval of 2.



A



B

Fig. 3 A trabecular bone X-ray image from a 55 year old female (A) and its contoured power spectrum (B). The power spectrum shows prominent vertical and horizontal arrangements of all the frequencies.



A



B

Fig. 4 A trabecular bone X-ray image from a 71 year old female (A).The contoured power spectrum (B) is normal for a patient of this age, but the vertical axis is shorter indicating an increase in the spacing of elements horizontal in this image.

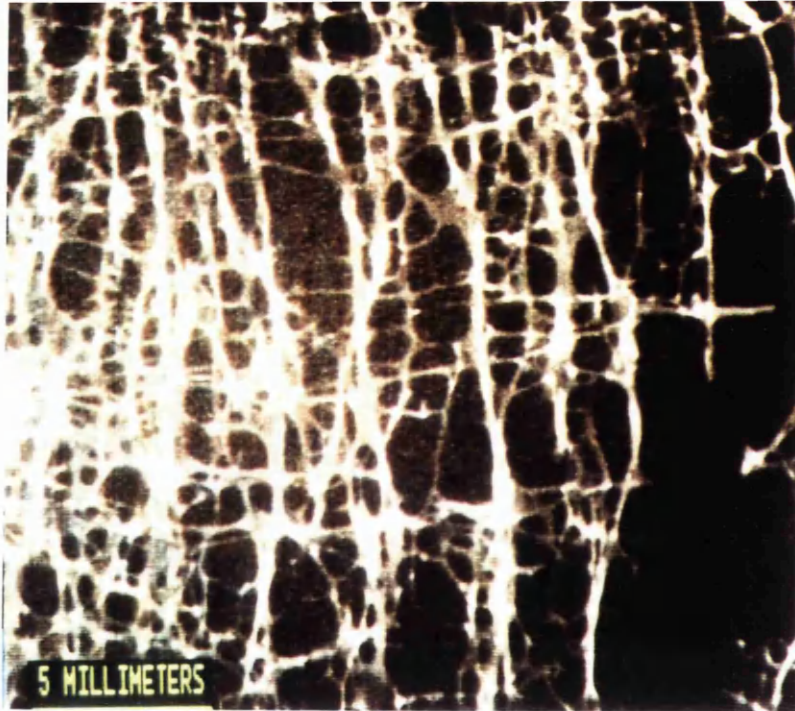


A



B

Fig. 5 A trabecular bone X-ray image from a 74 year old female (A) and its power spectrum (B). Bone loss is evident from both the image and the power spectrum. However, the power spectrum shows that the loss has occurred to the same extent in both vertical and horizontal elements.



A



B

Fig. 6 A trabecular bone X-ray image from an 89 year old osteoporotic female (A). The power spectrum (B) reflects the severe bone loss seen in the image. The vertical and horizontal arrangements dominate the spectrum, but the irregular contours indicate many other orientations in the image.



A



B

Fig. 7 A trabecular bone X-ray image from a 50 year old male (A). The power spectrum (B) reflects orthogonal arrangements of elements in the image. However, the green contour (intensity = 6) shows a diagonal deficiency indicating an increased spacing in 45° direction.



A



B

Fig. 8 A trabecular bone X-ray image from an 89 year old osteoporotic male (A). The smaller power spectrum (B) reflects the presence of fewer, larger elements in the image. The shorter vertical axis of the spectrum indicates an increased spacing among horizontal elements in the image.

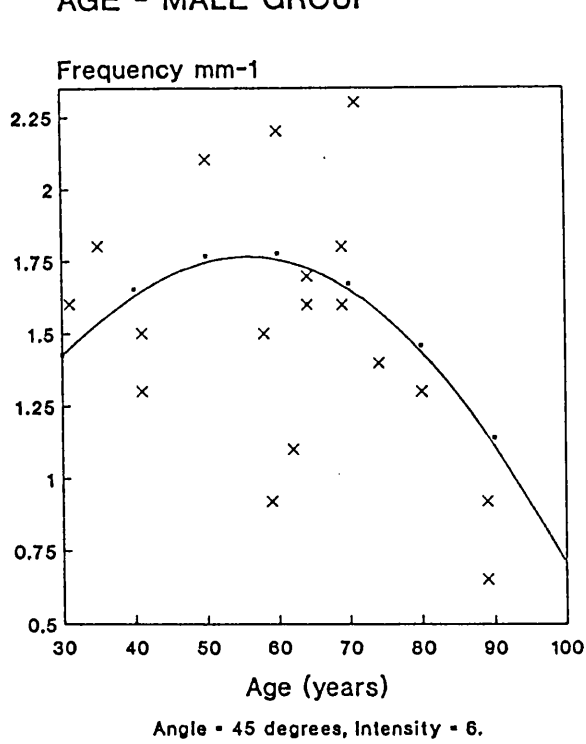


FIG.10 CHANGES IN FREQUENCY WITH AGE - FEMALE GROUP

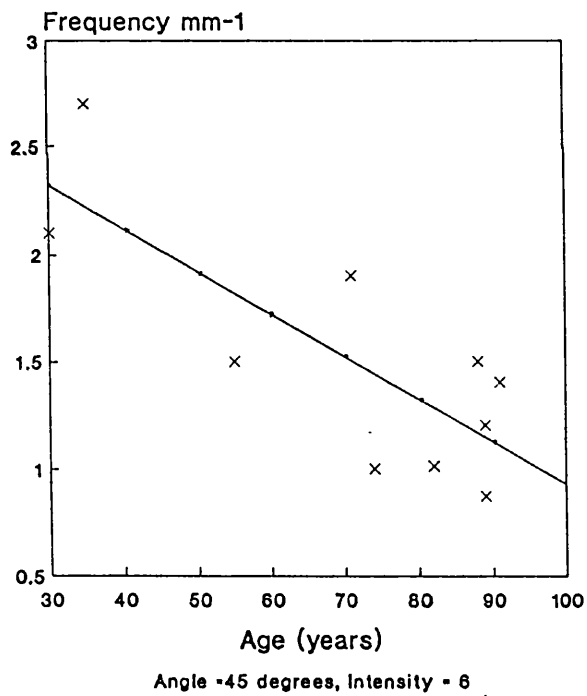


Fig. 9 The change in trabecular spatial frequency with age in the male group. The frequency increased until mid sixth decade and decreased afterwards.

Fig. 10 The change in trabecular spatial frequency with age in the female group. There was a continuous decrease in the frequency with age.

ANGLE	INTENSITY	LOWEST PERIODICITY (L) & AGE	HIGHEST PERIODICITY (H) & AGE	INCREASE IN TRABECULAR SPACING (H/L)	INCREASE IN DIFFERENT ANGLES
45°	4	0.32(35Y)	0.50(89Y)	1.55	
	6	0.56(35Y)	1.54(89Y)	2.77	2.23
	8	1.92(35Y)	4.55(89Y)	2.36	
90°	4	0.25(35Y)	0.31(80Y)	1.25	
	6	0.34(35Y)	0.56(80Y)	1.61	1.60
	8	0.63(35Y)	1.20(80Y)	1.93	
135°	4	0.34(35Y)	0.50(89Y)	1.45	
	6	0.59(31Y)	1.79(89Y)	3.04	2.30
	8	1.89(35Y)	4.55(74Y)	2.41	
180°	4	0.27(35Y)	0.40(89Y)	1.48	
	6	0.40(35Y)	0.67(89Y)	1.67	2.50
	8	0.59(35Y)	2.56(89Y)	4.36	

The increase in trabecular spacing at different angles and intensities in the male group. The overall increase was 2.1 times.

TABLE-I

ANGLE	INTENSITY	LOWEST PERIODICITY (L) & AGE	HIGHEST PERIODICITY (H) & AGE	INCREASE IN TRABECULAR SPACING (H/L)	INCREASE IN DIFFERENT ANGLES
45°	4	0.27(35Y)	0.42(89Y)	1.54	
	6	0.37(35Y)	1.00(89Y)	2.70	3.01
	8	0.83(35Y)	4.00(89Y)	4.8	
90°	4	0.24(35Y)	0.33(89Y)	1.4	
	6	0.32(35Y)	0.67(89Y)	2.67	1.72
	8	0.59(35Y)	1.00(91Y)	1.7	
135°	4	0.26(35Y)	0.43(89Y)	1.70	
	6	0.37(35Y)	1.01(74Y)	2.73	3.14
	8	0.91(35Y)	4.55(91Y)	5.00	
180°	4	0.22(35Y)	0.29(89Y)	1.29	
	6	0.30(35Y)	0.48(88Y)	1.57	1.68
	8	0.48(35Y)	1.04(88Y)	2.19	

The increase in trabecular spacing at different angles and intensities in the female group. The overall increase was 2.4 times.

TABLE-II

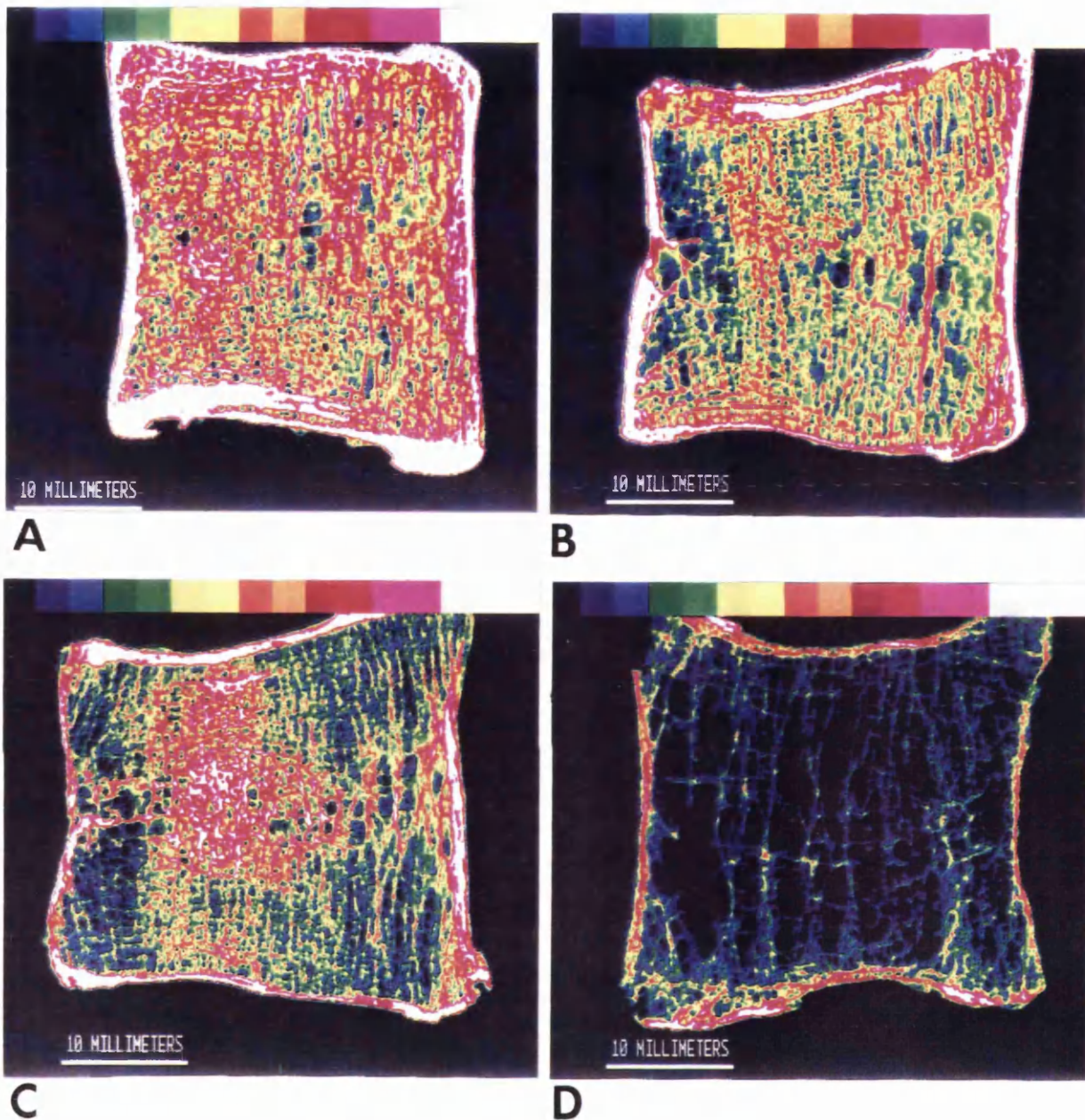


Fig. 11A An X-ray image of a trabecular bone section from a 30 year old female, mapped using the colour scheme used on topographical maps. In the ramp at the top of the figure, peak white indicates the highest and the black the lowest optical density of the X-ray image. In the rest of the figures in this chapter, this scheme was used to map optical densities of similar X-ray images.

Fig. 11B-D Intensity mapped X-ray images from a 31 year old male, an 89 year old female and an osteoporotic 89 year old female respectively.

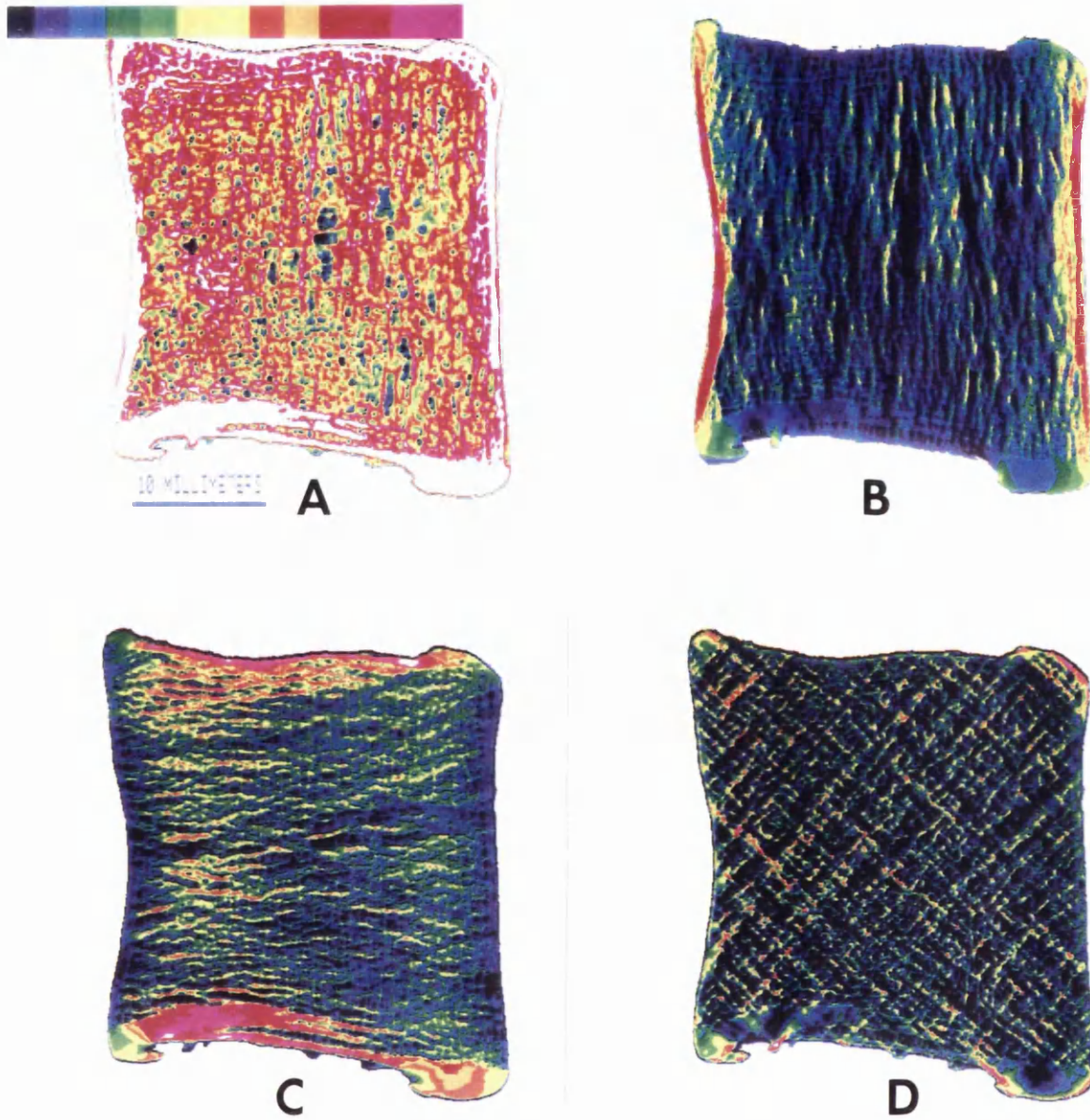


Fig. 12 An intensity mapped X-ray image (A) from a 30 year old female and dissected images of vertically (B), horizontally (C) and diagonally (D) oriented trabecular elements.

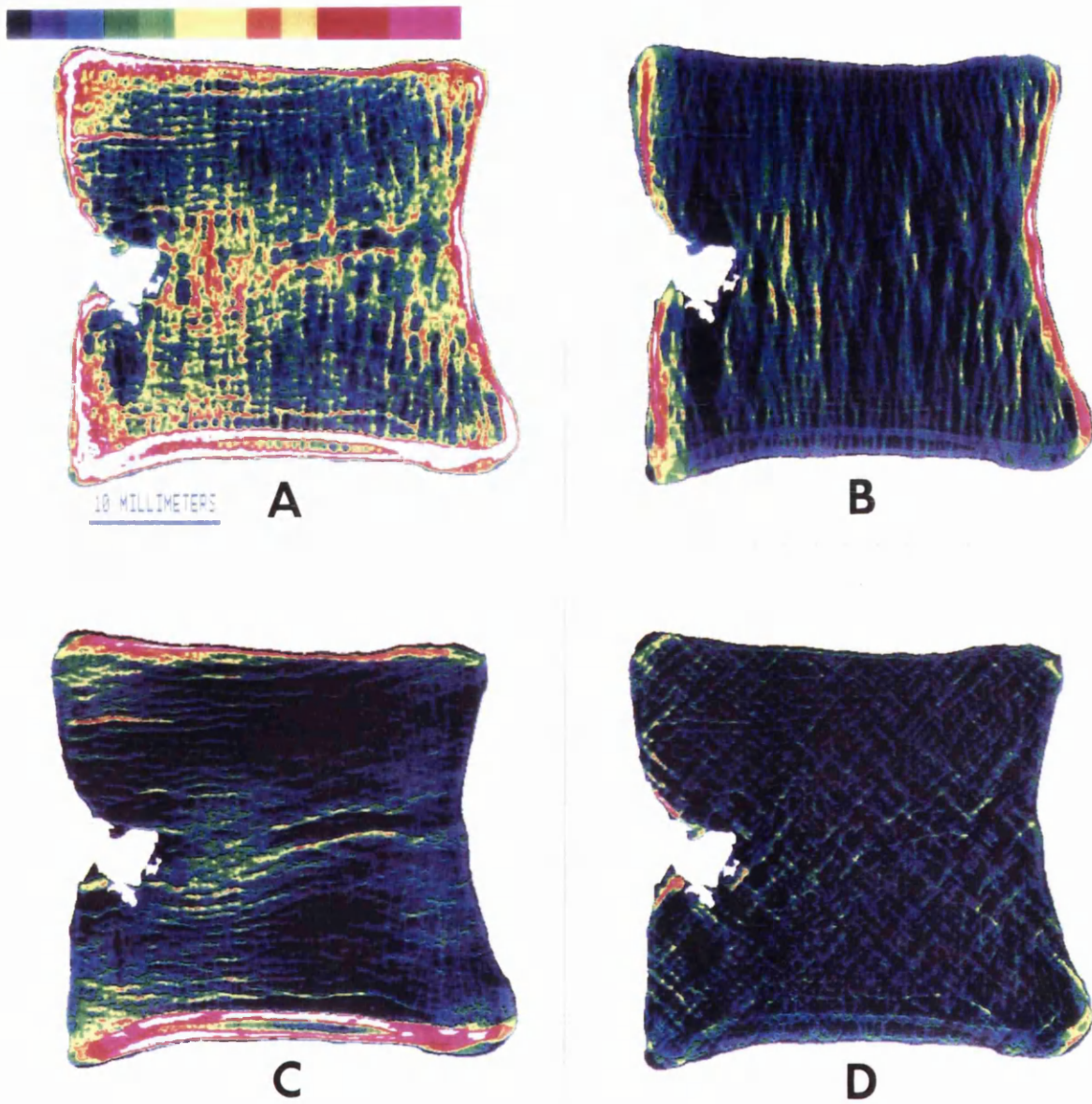


Fig. 13 An intensity mapped X-ray image (A) from a 50 year old male and dissected images of vertically (B), horizontally (C) and diagonally (D) oriented trabecular elements.

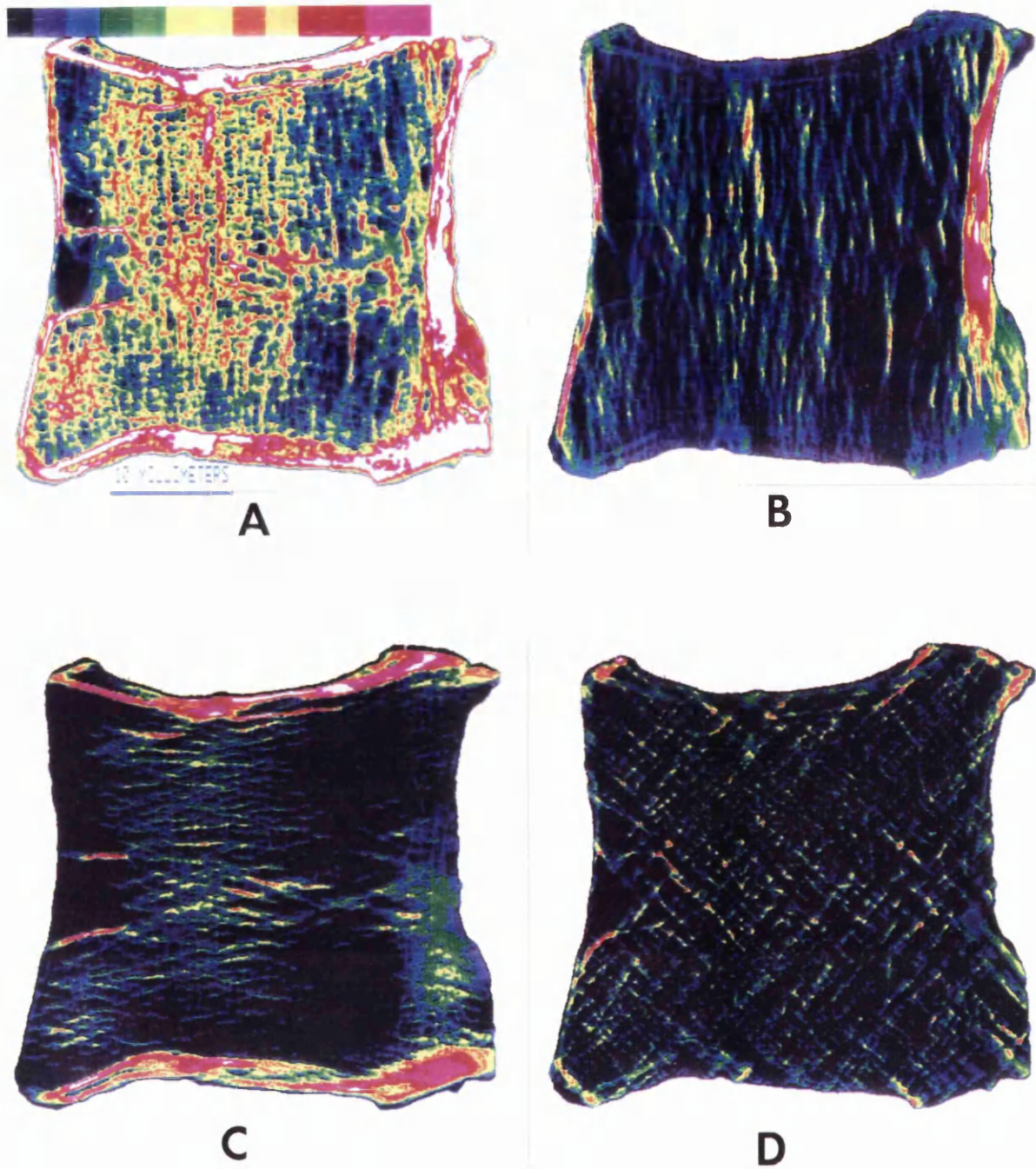


Fig. 14 An intensity mapped X-ray image (A) from a 71 year old male and dissected images of vertically (B), horizontally (C) and diagonally (D) oriented trabecular elements.

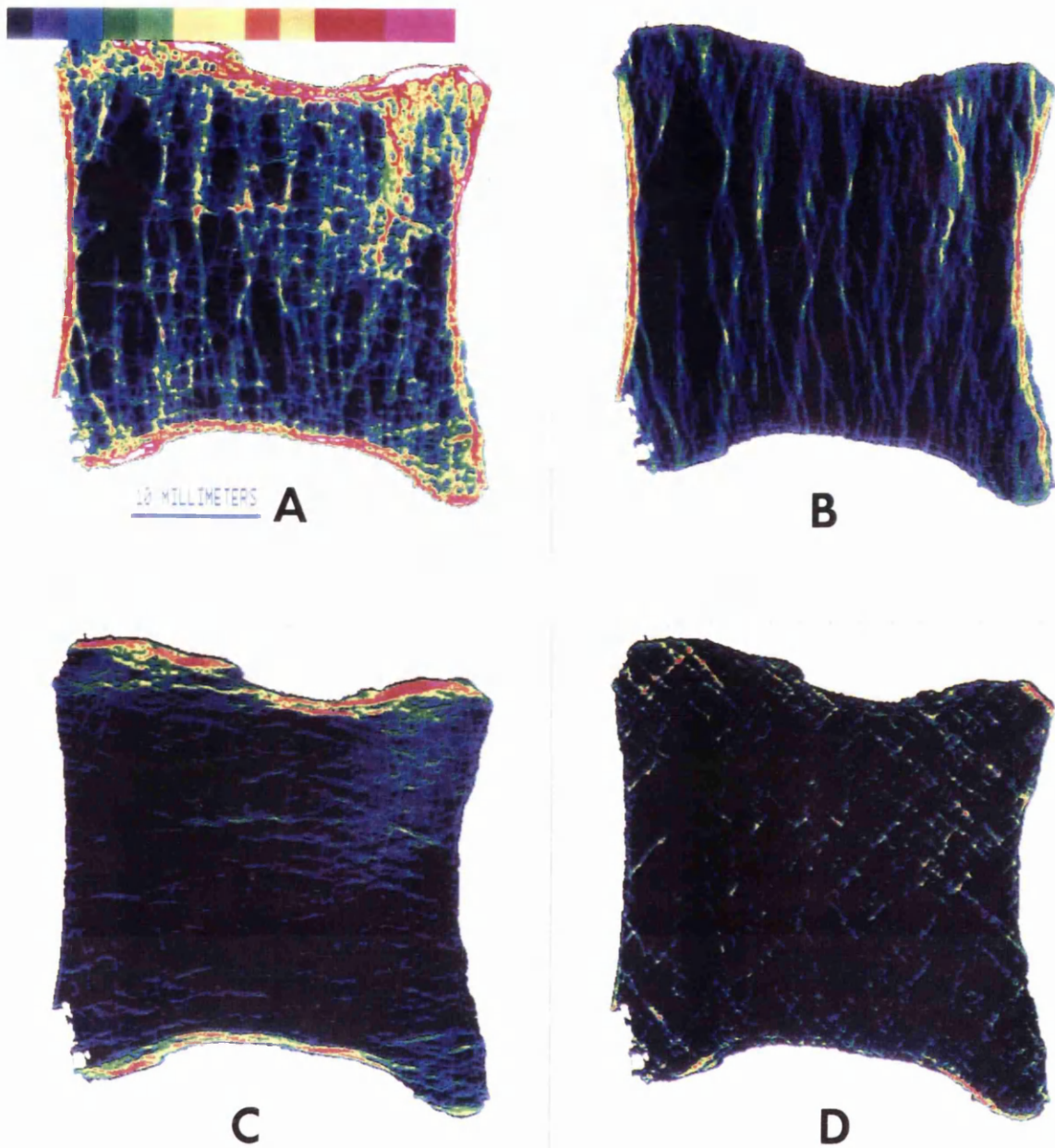


Fig. 15 An intensity mapped X-ray image (A) from an 89 year old osteoporotic female and dissected images of vertically (B), horizontally (C) and diagonally (D) oriented trabecular elements.

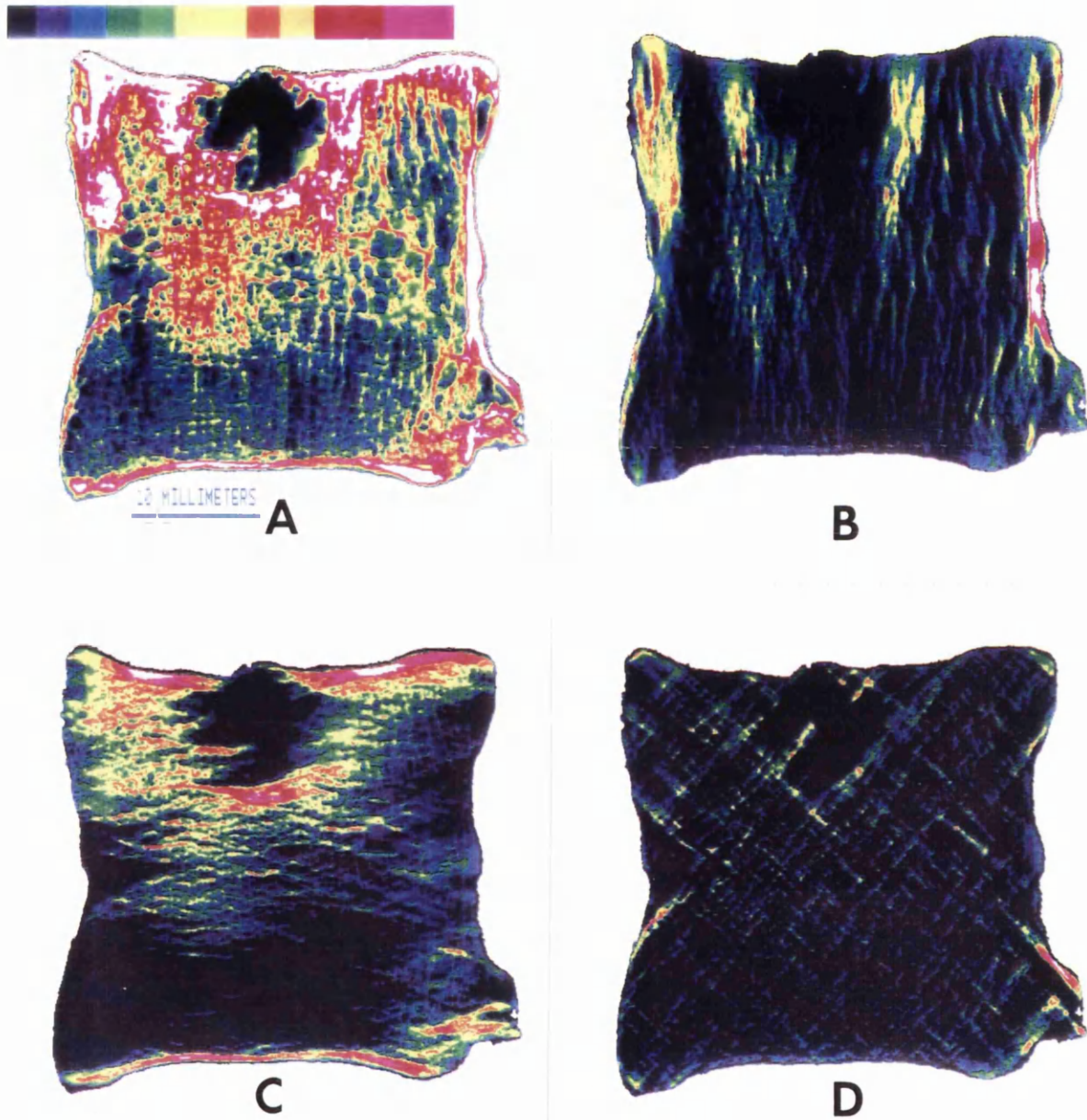


Fig. 16 An intensity mapped X-ray image (A) from a 75 year old female. A schmorl's node is present at the superior aspect of the section. The images in figures 16B, 16C and 16D show vertically, horizontally and diagonally oriented trabecular elements respectively.

CHAPTER 5

CHANGES IN QUALITY OF TRABECULAR BONE ON AGING AND IN OSTEOPOROSIS AND THE CONSEQUENCES OF THESE CHANGES ON BONE STRENGTH.

5.1 INTRODUCTION

It has been widely believed that the quality of bone does not change during age related bone loss, the loss being only in quantity (Albright and Reifenshtein 1948). However, many studies have shown changes in various qualities of bone both on aging and in disease (reviewed by Grynepas and Holmyard 1988). Frost (1985) expressed a more comprehensive view of osteoporosis as a manifestation of osteopenia and mechanical incompetence.

The clinically most important condition manifested by changes in the quality of bone is osteomalacia, which consists of several disorders in which there is a defect in, or failure of, bone mineralisation. Chalmers et al. (1967) reported that osteomalacia is not uncommon in elderly women and that it could be confused with senile osteoporosis. In describing 93 cases of osteomalacia Chalmers (1968) found that most of the cases with no apparent cause were over 70 years old. Many studies have also shown that osteomalacia is commoner in elderly women than in men (Chalmers et al. 1967, Rosin 1970, Exton-Smith 1971, Dent 1974, Aaron et al. 1974a, Campbell et al. 1984).

The association between osteomalacia and fractures of the femur has been demonstrated mainly in western countries (Jenkins et al. 1973, O'Driscoll 1973, Aaron et al. 1974b and 1974c, Lund et al. 1975, Faccini et al. 1976, Johnston et al. 1987). A high incidence of osteomalacia among hip fracture patients has also been reported in South Africa (Solomon 1973) and in India (Vaishnava and Rizvi 1974).

The causes of an increased incidence of osteomalacia in the elderly population are not clear. Conflicting results have been obtained regarding vitamin D deficiency in elderly patients. Some studies have reported normal values for 25-hydroxy vitamin D (Lund et al. 1975, Weisman et al. 1978, Wootton et al. 1979), while others have shown low serum concentrations (Brown et al. 1976, Baker et al. 1979). Webster et al. 1975 found that the response of elderly patients with osteomalacia to intravenous administration of vitamin D₃ was poor, and it was therefore suggested that impaired metabolism of vitamin D, rather than its deficiency, may be responsible for the disease. It has also been suggested that the cause of osteomalacia in elderly people is often multifactorial: both impaired renal function (Webster et al. 1976) and insufficient exposure to sunlight (Baker et al. 1979) could also contribute to the occurrence of this condition.

In most of these studies, a histological diagnosis of osteomalacia is accomplished by the stereological measurement of the proportion of osteoid covered surfaces in iliac crest biopsies. Further, most of the work has been carried out on patients with femoral neck fractures (Jenkins et

al. 1973, Solomon 1973, Aaron et al. 1974b and 1974c, Vaishnava and Rizvi 1974, Lund et al. 1975, Faccini et al. 1976, Weisman et al. 1978, Baker et al. 1979) rather than with vertebral or other age-related fractures. It is not clear how well data obtained from iliac crest biopsies correlate with real fracture sites.

The status of bone mineralisation in the spine of the elderly and in patients with osteoporosis and vertebral crush fractures has not been subjected to extensive studies. The contribution of spinal osteomalacia to diminishing mechanical competence of the vertebrae is thus not known. Another important question concerns whether mineralised bone in elderly and osteoporotic patients is "normal" in quality. Techniques that measure unmineralised bone do not provide an answer to this question.

The present study was carried out to investigate the status of mineralisation of vertebral trabecular bone on aging and in osteoporosis. The mechanical competence of the trabecular bone before and after removal of unmineralised matrix was tested in order to observe the effect of the removal on total bone strength.

5.2 METHODS

5.2.1 Sample preparation

Plane parallel, precise 4mm thick para-sagittal sections were cut from fourth lumbar vertebral bodies obtained at autopsy from 16 male and 8 female individuals (age range 30 to 89 years) using a slow speed diamond saw (Isomet 11-1180). Mid-sagittal sections from most of these samples were used during the study in chapter 4 and these para-sagittal sections were cut from the left side adjacent to the mid-sagittal sections. The cortical bone from all four sides of the sections was removed by carefully cutting across at the peripheries of the samples with the diamond saw to produce approximately square beams consisting entirely of trabecular bone.

The samples were treated at 50°C with a 5% solution of an enzyme detergent (TERG-A-ZYME) for 24 hours to remove marrow and soft tissues. This procedure removes all soft tissue, but leaves unmineralised osteoid intact. At the end of the digestion the samples were cleaned with a jet of water and extracted with a 50:50 solution of chloroform and methanol. They were then air dried.

5.2.2 Measurements of the apparent density

The thickness of the samples was measured by taking the mean value of several measurements from different regions and the mean area was taken as the average of the area measurements from tracings of both sides of the samples. The weight of each sample was measured using an accurate microbalance (SARTORIUS 2024 MP). The apparent density of trabecular bone was taken as the mass of bone tissue divided by the bulk volume of the sample, including mineralised bone and bone marrow spaces (Carter and Hayes 1977, Hayes and Gerhart 1985). From the above measurements, the apparent density values were calculated for all the samples.

5.2.3 Mechanical testing

The type of mechanical testing employed was three line bending of the samples using a universal testing machine (Hounsfield H25K). A special three line testing rig was constructed so that the sample would rest on two parallel rods and be compressed by a third, central rod attached to the upper portion of the device (Fig.1). The objective of the testing was to record the force required to cause a constant deformation before and after removal of the osteoid. It was not necessary to calculate the actual stresses and strains produced during testing.

The speed of advance employed during testing was 0.1 mm per minute. Both the force and the extension of the rod could be directly recorded from the display of the machine and the load–deformation curve was drawn on graph paper by a device attached to the testing machine. It was important not to cause any permanent damage to the samples during testing before the removal of osteoid. Therefore, it was imperative to stay within the elastic region of the load–deformation curve during loading. Consequently, before testing, several trial samples were loaded up to the yield point and the average extent of the elastic region was determined. The load was kept well clear of that which would damage the samples during testing. Further, once the load was withdrawn in the elastic region, both the load and the extension display should drop back to zero and this could also be observed in the load–deformation curve recorded on the graph paper. Before taking any readings therefore, the same load was applied several times and the uniformity of the curve was confirmed.

After the first testing, the samples were treated with 3% hydrogen peroxide solution for 24 hours to remove all unmineralised bone. They were then carefully washed, dehydrated and defatted with 50:50 chloroform:methanol, and air dried. The samples were then weighed again and the testing procedure repeated. The orientation of both the testing rig and the samples were marked after the first testing procedure so that the second testing was done in the same orientation i.e. the three lines to which the load was applied were the same before and after the removal of unmineralised bone matrix.

5.2.4 Study of trabecular fractures

During the second testing, after the removal of osteoid, some of the samples fractured. After the second testing, all the remaining samples were also loaded until they fractured and collapsed. Stereo photographs of these samples were produced by tilting the sample under a 35mm camera with a 80mm macro lens as described in Chapter 3 and the fracture plane was examined under a stereoscope. A conductive coating of gold was given to some of these samples and the fractured trabeculae were examined by SEM at 10kv.

5.3 RESULTS

5.3.1 Mechanical behaviour of trabecular bone

Tables 1 and 2 show calculated values for apparent density, loss of tissue after treatment with hydrogen peroxide and force required to cause a constant deformation (i.e. to deform samples by 1mm) before and after treatment in both female and male groups. In the female group (Table 1),

two of the osteoporotic samples (aged 85 and 89 years) cracked under the testing rig after removal of unmineralised bone before applying any force by the testing machine. These two samples also showed the highest loss of tissue with hydrogen peroxide treatment. The load required to cause a constant deformation was in all cases reduced to a varying degree after the removal of unmineralised bone matrix, indicating a reduction in stiffness after the treatment.

Figure 2 shows load deformation curves for three of the samples (35 year old male and 55 and 89 years old females) tested during the study. Curves marked with letters "A" show deformation before treatment with hydrogen peroxide. Load was applied up to the points indicated by the arrows marked with "X" and the deformation was recorded. The load was maintained for a few seconds and was gradually withdrawn at the points marked with arrows "Y".

Load deformation curves after treatment are marked with letters "B". The sample from the 35 years old male (Fig. 2.1B) showed a complete curve similar to that before treatment. In the two other samples shown in Figures 2.2B and 2.3B, trabeculae began to break before reaching the originally applied maximum load. In all the samples above the age of 50 years, at least a few trabeculae cracked before reaching the load applied before removal of unmineralised bone matrix. In most of younger samples no further breaks occurred until the original force was exceeded. In several older samples trabeculae continued to break until the samples totally collapsed at less than the original applied load. In such samples, it was never possible to apply the original maximum load before the collapse. The load deformation curves dropped when trabecular groups broke and in Figures 2.2B and 2.3B such breaks have been indicated by short arrows. For the purpose of this study the recorded force and the deformation just before the first break occurred was used.

The curves for young samples were also steeper (Fig. 2.1) compared with old samples, indicating a greater stiffness in younger bone.

The apparent density distribution showed diverse values at different ages (Figure 3), but the general trend was a drop in apparent density with increasing age. The two osteoporotic female samples aged 85 and 89 years showed the lowest values. Generally, the male group had higher apparent densities.

When the load needed to cause the same deformation before and after treatment with hydrogen peroxide in each individual sample was compared (Figures 4 and 5), a highly significant correlation was observed between the load before and after treatment in both females ($r=0.954$, $p<0.001$) and males ($r=0.915$, $p<0.001$). Most of the old samples required considerably less force to cause the same deformation as compared with young samples which required much higher loads. This was especially seen in the male group (Fig. 5), although they were still stiffer than the female group. Two osteoporotic female samples that collapsed after hydrogen peroxide treatment were very much less stiff before treatment.

Possible relationships between apparent density, age and the load required to cause a constant deformation before removal of unmineralised bone matrix were also looked for. (Figures 6 and 7). In both females (Fig. 6) and males (Fig. 7), the load required correlated with the apparent densities of the samples. This correlation was more marked above the ages of 75 years in females and 60 years in males.

No correlation was observed in either sex between the reduction in load necessary to cause a constant deformation after treatment with hydrogen peroxide and the loss of bone during the treatment (Figures 8 and 9).

5.3.2 Fracture behaviour of the samples

The three line bending technique employed during this study (Fig. 1) produces different types of stresses within different regions of the sample. Since the samples were loaded at the centre of the top surface, the trabeculae around the upper part were loaded in compression while around the lower part they were loaded in tension. Trabeculae fractured where they were loaded in tension and there was a strong relationship between the nature of the fracture and the structure of the trabeculae in the sample. Figure 10 is a stereopair of a sample in which thick plates and tube like trabecular structures dominate throughout the section. Fracture lines in such strong sections were more or less straight – as in solid materials – and both vertical and horizontal components fractured without any preference. However, the trabeculae on the compressive side (top) side of the sample did not fracture and the fracture line extended through only about half the thickness of the sample.

Figure 11 is a stereopair of a sample in which the structure of the trabeculae is different from that in the Figure 11. In the central third of this sample, more plate-like trabeculae are present, compared with a rod-based, more open structure in the outer thirds. The horizontal trabeculae in the outer thirds are predominantly thin and rod-shaped and, when the fracture line (indicated by arrows) was examined, it was the horizontal trabeculae that had fractured most. Most of the horizontal trabeculae had also fractured at their centres, indicating that this was the weakest location. In the majority of the samples, the fracture lines were irregular and leapt from one weak trabecular group to another, breaking through some vertical trabeculae on their way. Vertical trabeculae fractured in a similar fashion in all regions in young samples, but horizontal trabecular fractures dominated at the peripheral regions in old samples whilst most of the vertical trabecular fractures were seen at the central region.

When a sample such as that in the Figure 11 was examined from the superior or inferior aspect of the vertebra the trabeculae appear as large tubes at the central third branching to form several tubes in the peripheral thirds (See chapter 3 for details of this structure). When fracture lines were examined from this direction it was observed that the fractures involved one large tube at the centre and several tubes at the periphery. However, the extent of the fractures across the samples was more or less the same in all regions.

The fracture behaviour of some of the old samples was very different from that was seen with the sample in Figure 11. Figure 12 shows a stereopair of such a sample from a 74 year old female. Other than the thick plates forming the canal for the basivertebral vessels at the centre, the structure of the trabeculae is similar to that observed at the periphery of the sample in Figure 11. However, after initial cracking of a few trabeculae at the lower part (that loaded in tension), the sample immediately cracked into two pieces. This shows that trabeculae had become very brittle after treatment with hydrogen peroxide. The fracture lines were roughly straight, with both vertical

and horizontal trabeculae breaking without any preference.

Some osteoporotic samples were also very brittle and collapsed under the testing rig before applying any added load! (Figure 13). Most of such samples cracked in many places: the dislodged bits of trabeculae could be easily crushed between the fingers to form a fine powder.

The SEM revealed different characteristics of fracture lines. Most of the huge plates at the middle zone of vertebral sections cracked right across without even involving round or oval openings that are around the crack (Figure 14), but this was through the thinnest part of the plate. The plate was thicker around these openings, some having strong bony rims around them. When the fracture face was examined (Figure 15), it was apparent that different lamellae had fractured at different levels thus creating an irregular face.

On most occasions, thick rods attached to plates separated at their junctions (Figure 16). This was especially seen in younger samples.

Most frequently, the rods fractured at right angle to their longitudinal axes and the fracture plane had propagated more or less straight across different layers of collagen fibre bundles (Figure 17).

Figure 18 shows a long horizontal trabeculum from an osteoporotic sample. Such long trabeculae are a common feature in vertebrae from old individuals. It can be seen that this trabeculum has fractured where thinnest. Figure 19 shows this fracture at a higher magnification. The surface around the fracture is formative with a mineralising front with large mineral particle clusters. Perhaps, after a resorptive phase bone is forming around this weakest region of the trabeculum. In this instance also, the fracture line has gone across the trabeculum without separating lamellae.

5.4 DISCUSSION

The main objectives of this study were to determine whether the quality of mineralised bone in old and osteoporotic individuals differs from that of young individuals and whether the removal of unmineralised bone would affect the mechanical strength of the vertebral trabecular bone. No attempt was made to investigate the occurrence or severity of osteomalacia in the samples using classical histological methods such as the measurement of the amount of osteoid tissue. Further, it was recognised that (a) it was not necessary to calculate the compressive or tensile strength or modulus of elasticity as the intention was only to determine the existence of possible changes in stiffness after removal of unmineralised bone: and (b) that it would be almost impossible to give formal meaning to values determine for an undefined volume of an undetermined, porous structure. Comparing the loads necessary to cause about a constant deformation sufficed for the present purpose.

The strength and stiffness of a material such as trabecular bone is determined not only by the amount of mineralised tissue present, but by factors such as bone ultrastructure, mineralisation status and trabecular orientation or anisotropy. Carter et al. (1977) pointed out that porosity, ash density and apparent density are all reasonable measures of the amount of mineralised tissue. According to Galante et al. (1970) the apparent density is more important than real density in

determining the strength of trabecular bone.

An age related decrease in total ash density of human vertebrae was reported by Bell et al. (1967), who also demonstrated a significant correlation between compressive strength and relative ash content in whole lumbar vertebrae. A decrease in apparent density with increasing age was found in the present study (Figure 3). The lowest values for the apparent density were recorded in osteoporotic samples revealing the highly porous nature of these samples. The load required to bring about a given deformation also decreased with increasing age. However, when required loads were compared with apparent densities (Figures 6 and 7), no correlation was observed in young samples and old samples exhibited only a slight correlation. Consequently, factors other than the apparent density should also be responsible for the changes in stiffness with age.

Galante et al. (1970) observed that vertebral bone specimens loaded in the superior-inferior direction were stronger than those loaded along the two other directions. They also found that the strength also depended on the rate of loading, with those samples deformed at a rate of 1 cm per minute having significantly higher strength than those deformed at a rate of 0.01 cm per minute.

The samples used during this study were taken from identical positions in all vertebrae and were loaded in the same direction under similar conditions. The deformation rate was also constant (0.1 mm per minute) when testing before and after treatment with hydrogen peroxide. Therefore, trabecular anisotropy and the rate of loading could be excluded as factors affecting results of this study. This leaves us to consider different structural features in the arrangement of the tissue in different samples, their ultrastructure and mineralisation status at different ages.

The size, the shape and the structural arrangement of trabeculae varied extensively among the young samples. In some, plate- or tube-like structures dominated, while others had more rod shaped trabeculae. In addition, the trabecular structure varied from region to region in the same section and these variations were not constant from section to section. It is possible that developmental history, vascularisation and exposure to different mechanical loading patterns may be responsible for these differences in young samples. With such variations it is not surprising that different samples exhibit different strengths when tested under similar conditions.

By contrast, the trabecular structure in older samples was less complex. Prominent rod shaped elements, fewer plates, and an increased spacing with long horizontal trabeculae were all common features in most of the old and osteoporotic sections. The structure did not vary significantly among different samples. This would perhaps explain the approximate correlation observed between apparent density and tissue stiffness in old age.

When the vertebral sections were treated with hydrogen peroxide and retested, it was found that the stiffness had reduced in all sections irrespective of age (Figures 4 and 5). This reduction was very much less in very young samples, however, and different samples exhibited differing degrees of reduction in strength which had no correlation with age.

Comparing the load needed to bring about the same deformation before and after treatment with hydrogen peroxide, a highly significant correlation was seen in both male and female groups (Figures 4 and 5). This means that hydrogen peroxide treatment had not changed the architectural

arrangement of trabeculae in these sections. It could therefore be concluded that only the loss of non-mineralised tissue had influenced the changes in stiffness in the samples used during this study.

An increased amount of osteoid in trabecular bone from old individuals has been demonstrated in a few studies. For example, Faccini et al. (1976) concluded that osteomalacia was an important factor in the pathogenesis of fracture of the femoral neck, but such conclusions have been objected to on the basis that the increase in osteoid may possibly have occurred between the fracture event and the removal of the biopsy or the fractured fragment. Treatment with hydrogen peroxide removes osteoid and all other non-mineralised collagen matrix from bone. One would therefore expect that the hydrogen peroxide treatment would remove more tissue from old samples than young ones. However, Tables 1 and 2 show that this is not always the case. Even though the highest values for tissue loss were recorded in osteoporotic and older samples, there was no linear relationship between age and the hydrogen peroxide induced tissue loss. Furthermore, when the drop in the required load after treatment was compared with tissue loss (Figures 8 and 9), there was no correlation between these two variables. Thus, factors other than amount of osteoid per se should be responsible for these observations.

When samples were loaded until they fractured after dissolving the unmineralised collagen, the results were more complicated. Only a few of the younger adult samples could be loaded to the originally applied load without fracturing any of the trabecular elements. Most of the samples from individuals below the age of 50 years and some samples above this age fractured a few trabeculae at the beginning of loading, but could be loaded normally afterwards. In the majority of the samples over the age of 50, and in some below this age, the trabeculae continued to break after initial cracking until total collapse occurred. When fractures were examined after collapse (in all the above instances) it was found that only the lower part loaded in tension has fractured while the upper or compressive side remained connected.

In contrast to the above, some old samples cracked right across and separated into two pieces after an initial break involving a few trabeculae, indicating that they had become brittle after the treatment with hydrogen peroxide. The two osteoporotic samples were also brittle, collapsed under minimal load and could not even be tested after treatment.

The above observations suggest that hydrogen peroxide treatment changes the material properties of trabecular bone in a different manner in different samples (especially in old samples), perhaps indicating variations in mineralisation patterns among them. It is possible that the trabecular bone of the osteoporotic and other old samples that had turned brittle had not been mineralised properly, but had unmineralised areas within the mineralised tissue. In such instances, hydrogen peroxide would remove unmineralised areas thereby weakening the remaining network of mineralised bone.

It is also possible for long rods of osteoporotic bone to be attached via blocks of "osteoid" ("mini Looser's zones" analogous to Looser's zones in osteomalacic patients). If such regions are present, removal of non-mineralised zones would actually disconnect some trabeculae and weaken the samples further. If more and more such regions persist, especially in thin and frail osteoporotic

bone, there is also a possibility for some of the trabecular pieces to dislodge from the samples. This means that the data presented in this study for the loss of bone (Table I and II), particularly for old specimens, may not necessarily represent simply the amount of osteoid tissue lost, but could also include small chunks of mineralised tissues lost in this way.

This study clearly indicates that the quality of trabecular bone is not always the same in old age. Differing degrees of mineralisation can occur in different individuals and would perhaps have major implications for the occurrence of vertebral crush fractures.

It is not clear how far the standard histological techniques used for the analysis of osteoid tissue (such as the Eosin : von Kossa technique) would be able to detect different degrees of mineralisation within mineralised trabecular bone. Density measurements, such from, for example, backscattered electron imaging in the scanning electron microscope, would probably provide more useful information for this purpose.

When the two sexes were compared, higher values for both apparent density and stiffness were recorded in male samples, especially below the age of sixty years. However, the before and after hydrogen peroxide behaviour of the old samples (as described above), was similar in both males and females. This suggests that the change in mineralisation patterns in old age takes place in both sexes.

The analysis of the artificial fractures produced during this study proved that the trabeculae are weaker in tension than in compression. Furthermore, the fracture itself was related to the architectural arrangement of the trabeculae within the vertebral section. In young, less porous samples with thick trabecular elements, the fracture planes were approximately straight indicating that such samples are more close to solid materials. However, some old peroxide-treated sections also fractured in approximately straight "lines". These were the samples that turned brittle after the hydrogen peroxide removal of non-mineralised collagen. In other sections, fracture planes were irregular and passed through weak regions depending on the arrangement of the trabeculae within the sections. The orientation of the samples during testing was such that the bending forces were predominantly applied to the horizontal trabecular elements. The changes in stiffness therefore mainly reflect the distribution of the horizontal elements rather than the vertical. This is important, because the major structural changes take place in horizontal trabeculae rather than the in vertical ones during aging.

The majority of the rod-shaped horizontal trabeculae also fractured at their centres, which therefore seem to be the weakest position. Examination of the fracture faces in the SEM showed a relationship between the fractured profile of the surface and the organisation of the collagen lamellae. In plates, collagen bundles were arranged in different layers orientated in different directions. When plates fractured right across and when rods attached to plates separated at their junctions, the fracture travelled in between differently oriented lamellae. In thin rods, the collagen layers are mainly arranged along the long axis of the rods. Such elements fractured at right angles to the direction of the these layers.

These observations show that the characteristics of the fractures are dependent not only upon the size, shape and spatial arrangement of the trabecular elements, but also on the

5.5 CONCLUSION

The results of this study have demonstrated, firstly, that unmineralised bone matrix also contributes to the stiffness of lumbar vertebrae, irrespective of age, and in both males and females. This is shown by the reduction in stiffness after treatment with hydrogen peroxide in all age groups.

Secondly, the quality of mineralised trabecular bone is different among different individuals in old age. Some very old individuals had properly mineralised bone while other younger samples showed poor quality bone. The two clinically confirmed osteoporotics showed the poorest quality. This signifies the importance of poor mineralisation as a contributory factor in pathogenesis of osteoporotic fractures. This may perhaps explain why only some patients with loss of bone below a certain mass or volume/volume threshold level develop fractures. It could therefore be concluded that not only loss of quantity, but both osteomalacia and the poor quality of mineralised bone also contribute in different degrees in different individuals, to the occurrence of fractures such as crush fractures of the vertebrae. No sex differences were noted in this study in the defects in mineralisation in old age .

The trabeculae are weaker in tension than in compression. The trabecular fractures were related not only to the size, shape and morphology of different elements and to their architectural arrangement inside the vertebral body, but also to the organisation of collagen within the trabeculae.

5.6 REFERENCES

- Aaron JE, Gallagher JC, Anderson J, Stasiak L, Longton EB, Nordin BEC, Nicholson, M (1974) Frequency of osteomalacia and osteoporosis in fractures of the proximal femur. *Lancet* 229–233.
- Aaron JE, Gallagher JC, Nordin BEC (1974a) Osteomalacia and femoral fractures. *Lancet* 572.
- Aaron JE, Gallagher JC, Nordin BEC (1974b) Seasonal variation of histological osteomalacia in femoral neck fractures. *Lancet* 84–85.
- Albright F, Reifenstein EC (1948) The parathyroid glands and metabolic bone disease. Williams and Wilkins, Baltimore, MD. pp.393.
- Baker MR, McDonnell H, Peacock M, Nordin BEC (1979) Plasma 25-hydroxy vitamin D concentration with fractures of the femoral neck. *B M J* 589.
- Bell GH, Dunbar O, Beck JS (1967) Variations in strength of vertebrae with age and their relation to osteoporosis. *Calcif Tissue Res* 1:75–80.
- Brown IRF, Bakowska A, Millard PH (1976) Vitamin D status of patients with femoral neck fractures. *Age Aging* (1976) 5:127–131.
- Campbell GA, Kemm JR, Hosking DJ, Boyd RV (1984) How common is osteomalacia in the elderly? *Lancet* 386–388.
- Carter DR, Hayes WC (1977) The compressive behaviour of bone as a two-phase porous structure. *J Bone Joint Surg* 59A/VII:954–962.
- Chalmers J (1968) Osteomalacia: a review of 93 cases. *J Roy Col Surg Edin* 13:255–275.
- Chalmers J, Conacher WDH, Gardner DL, Scott PJ (1967) Osteomalacia – A common disease in elderly women. *J Bone Joint Surg* 49B/III:403–423.
- Dent CE (1974) Definition of osteomalacia. *Lancet* 805.
- Exton-Smith N (1971) Nutrition in the elderly. *Br J Hos Med* 5:639–646.
- Faccini JM, Exton-Smith AN, Boyde A (1976) Disorders of bone and fractures of the femoral neck. *Lancet* 1089–1092.

- Frost HM (1985) The pathomechanics of osteoporosis. *Clin Orthop Rel Res* **200**:198–225.
- Galante J, Rostoker W, Ray RD (1970) Physical properties of trabecular bone. *Calcif Tissue Res* **5**:236–246.
- Grynepas MD, Holmyard D (1988) Changes in quality of bone mineral on aging and in disease. *Scanning Microscopy* **2/II**:1045–1054.
- Hayes WC, Gerhart TN (1985) Biomechanics of bone : Applications for assessment of bone strength. *Bone Min Res/III*, William A Peck eds. 259–294.
- Jenkins DHR, Roberts JG, Webster D, Williams EO (1973) Osteomalacia in elderly patients with fracture of the femoral neck *J Bone Joint Surg* **55B/III**:575–580.
- Johnston CC, Peacock M, Meunier PJ (1987) Osteomalacia as a risk factor for hip fractures in the USA. *Osteoporosis 1987. Pro Int Sym Osteoporosis*. Christiansen C, Johansen JS, Riis BJ eds. 317–319.
- Lund B, Sørensen OH, Christensen AB (1975) 25-Hydroxycholecalciferol and fractures of the proximal femur. *Lancet* 300–302.
- O'Driscoll M (1973) Subcapital fracture types and osteomalacia and vitamin D deficiency. *J Bone Joint Surg* **55B/IV**:882.
- Rosin AJ (1970) Clinical features of osteomalacia in the elderly. *Post Med J* **46**:131–136.
- Solomon L (1973) Fracture of the femoral neck in the elderly : Bone aging or disease? *S Afr J Surg* **11/IV**:269–278.
- Vaishnava H, Rizvi SNA (1974) Frequency of osteomalacia and osteoporosis in fractures of proximal femur. *Lancet* 676–677.
- Webster SGP, Leeming JT, Whittaker JS, Wilkinson M (1975) An evaluation of the intravenous vit D test in geriatric patients with suspected osteomalacia. *Age aging* **4**:69–72.
- Weisman Y, Salama R, Harell A, Edelstein S (1978) Serum 24,25-dihydroxy vitamin D and 25-hydroxy vitamin D concentrations in femoral neck fracture. *B M J* 1196–1197.
- Wootton R, Brereton PJ, Clark MB (1979) Fractured neck of femur in the elderly : an attempt to identify patients at risk. *Clin Sci* **57**:93–101.

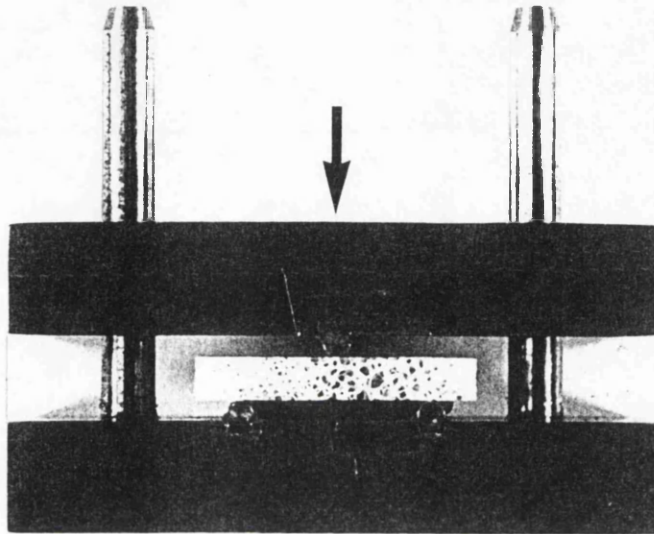


Fig. 1 The three line rig used for mechanical testing. The sample rests on two parallel rods and was compressed by a third, central rod from the top surface. The arrow indicates the direction of load.

TABLE 1 - DENSITY, LOSS OF TISSUE AND STIFFNESS
FEMALE GROUP

Age	Apparent Density g/cm ³	Force necessary to deform a sample by 1 mm before H ₂ O ₂ (Newton)	Force necessary to deform a sample by 1 mm after H ₂ O ₂ (Newton)	Drop in Force %	Loss of tissue after treatment with H ₂ O ₂ mg/g
30	0.21	60.17	57.36	4.67	62.85
55	0.16	38.16	29.09	23.77	60.33
71	0.18	14.52	4.91	66.12	43.93
74	0.16	12.78	6.22	51.25	91.16
75	0.17	35.78	22.28	37.73	42.54
85	0.08	11.11	*	100	142.42
89	0.07	4.61	*	100	252.06
89	0.18	34.44	14.35	58.33	79.40

* Data not available as samples collapsed after treatment.

TABLE 2 - DENSITY, LOSS OF TISSUE AND STIFFNESS
MALE GROUP

Age	Apparent Density g/cm ³	Force necessary to deform a sample by 1 mm Before H ₂ O ₂ (Newton)	Force necessary to deform a sample by 1 mm after H ₂ O ₂ (Newton)	Drop in Force %	Loss of tissue after treatment with H ₂ O ₂ mg/g
35	0.21	96.67	96.43	0.25	61.39
41	0.21	67.41	24.28	63.97	45.10
41	0.25	105.76	87.50	17.27	54.92
45	0.25	62.07	51.67	16.76	57.46
50	0.23	76.15	73.55	3.41	35.95
58	0.19	56.30	53.33	5.26	68.57
59	0.24	47.04	34.55	26.55	61.86
60	0.24	93.56	61.96	33.78	63.60
62	0.18	45.64	35.81	21.56	52.58
64	0.18	49.50	42.22	14.71	38.41
64	0.15	40.17	29.19	27.33	40.99
69	0.16	12.20	7.97	34.75	43.54
69	0.16	44.17	9.00	79.62	162.07
71	0.20	7.10	5.20	26.76	37.08
74	0.14	4.33	2.60	39.95	29.49
89	0.12	5.34	1.30	75.66	72.62

Fig. 2 The load deformation curves for samples from a 35 year male (Fig. 2.1), a 55 year female (Fig. 2.2) and 89 year female (Fig. 2.3). The curves "A" and "B" show the deformation before and after treatment with hydrogen peroxide. The load was applied up to the points marked with "X" and was maintained for a few seconds until points marked with "Y" when it was gradually withdrawn. A greater stiffness in the younger bone is evident from the steeper curves of the young sample: these curves were similar in shape both before and after treatment with hydrogen peroxide (Fig. 2.1). In the other two samples, trabeculae began to break after treatment with hydrogen peroxide before reaching the maximum load applied before treatment. The points of trabecular fractures have been indicated by short arrows in Figures 2.2B and 2.3B.

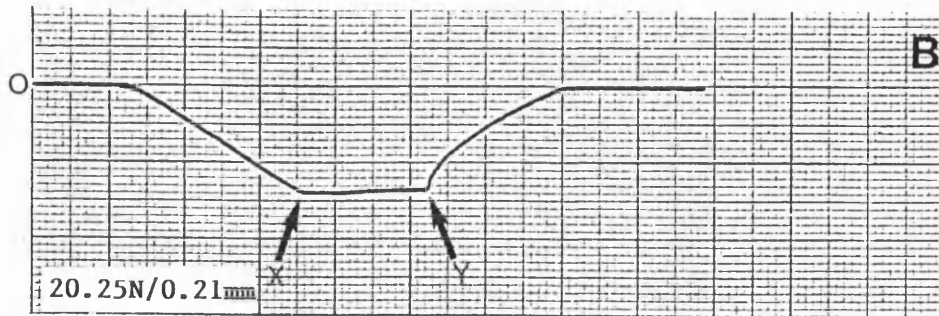
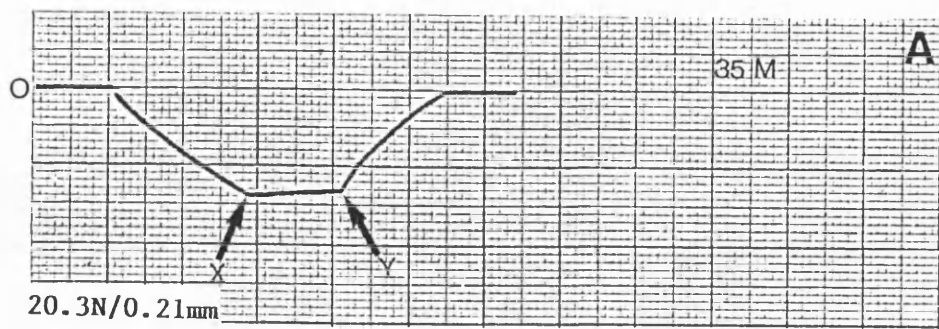


FIG. 2.1

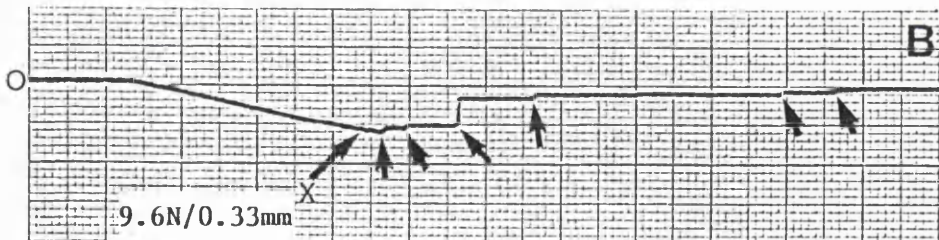
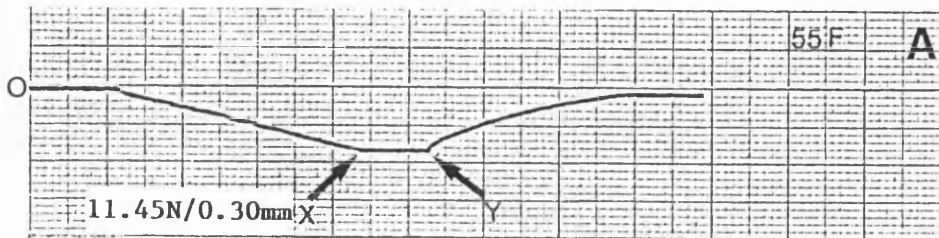


FIG. 2.2

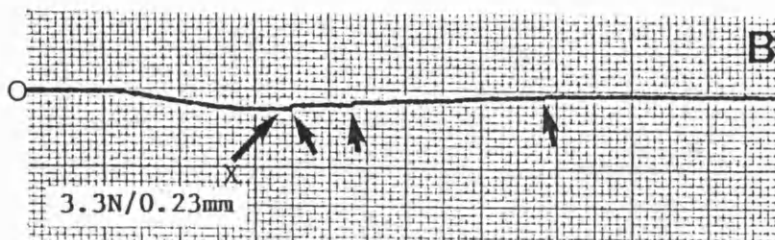
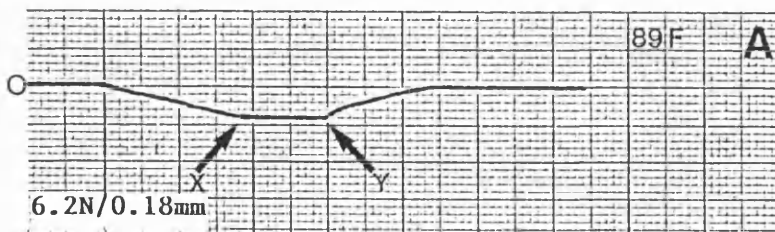


FIG. 2.3

Apparent density distribution

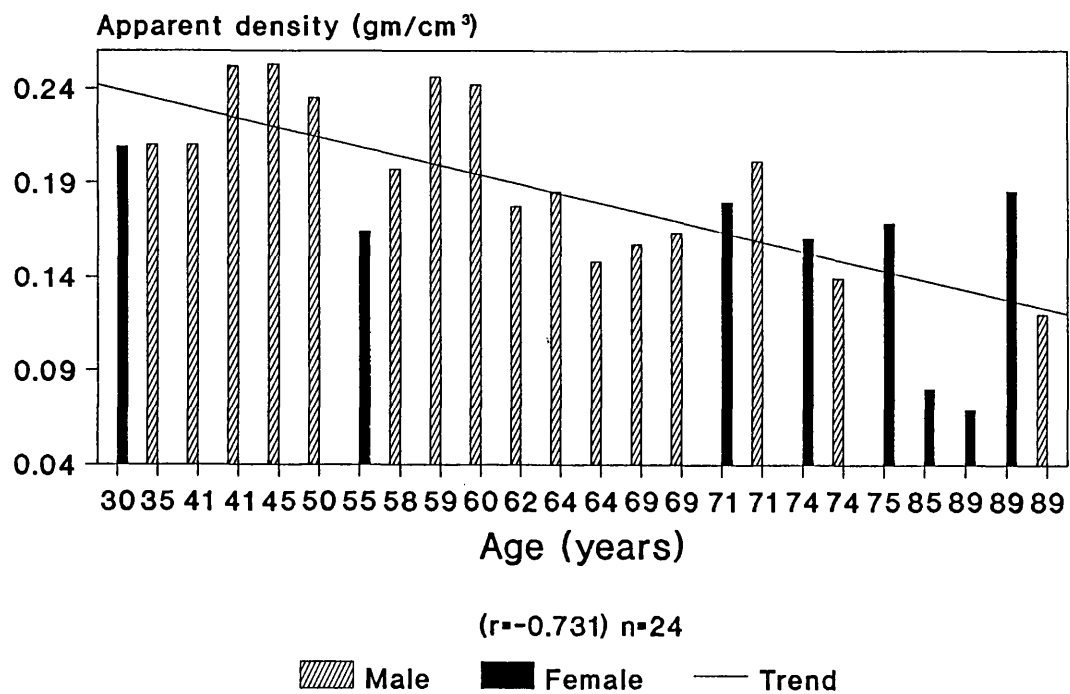


Fig. 3

Force required to deform samples by 1mm before and after removal of osteoid.

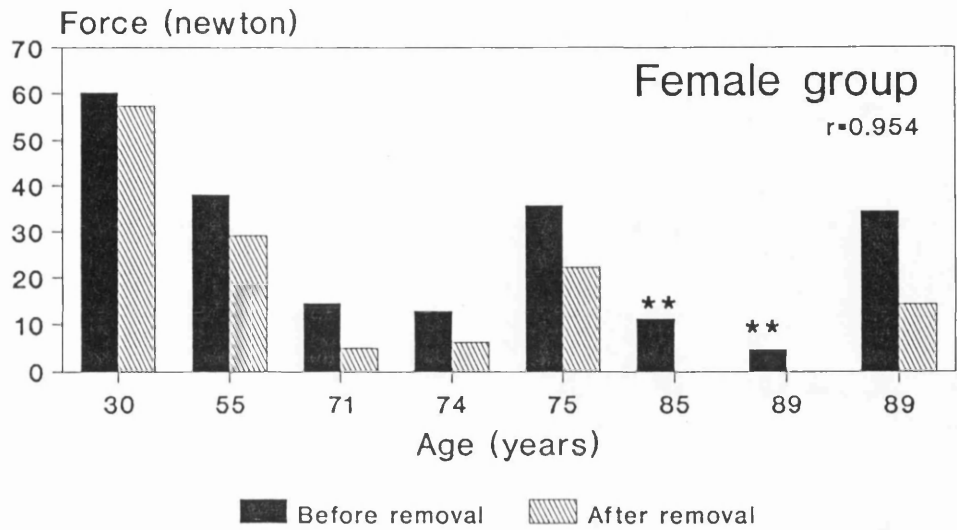


FIG. 4

• • These two osteoporotic samples collapsed after removal of osteoid

Force required to deform samples by 1mm before and after removal of osteoid.

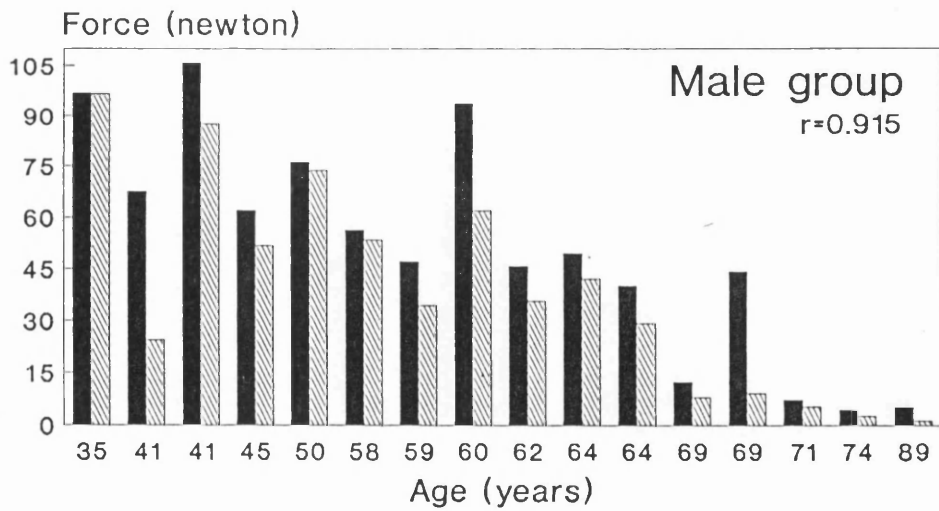


FIG. 5

Before removal After removal

The relationship between apparent density and force needed to cause a constant deformation - Female group.

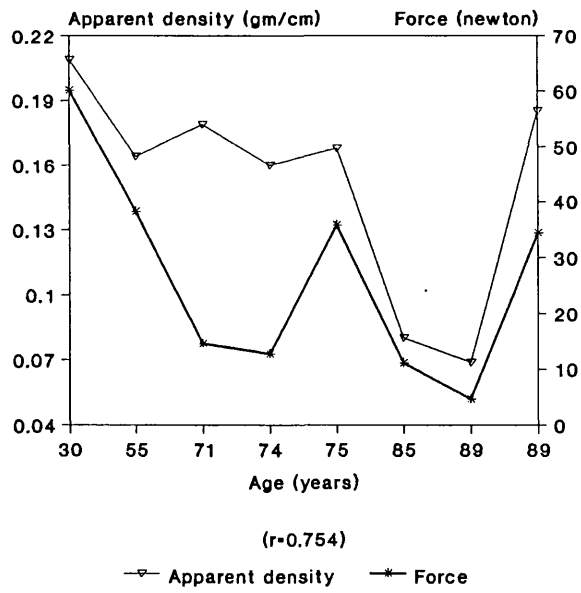


Fig.6

The relationship between apparent density and force needed to cause a constant deformation - Male group.

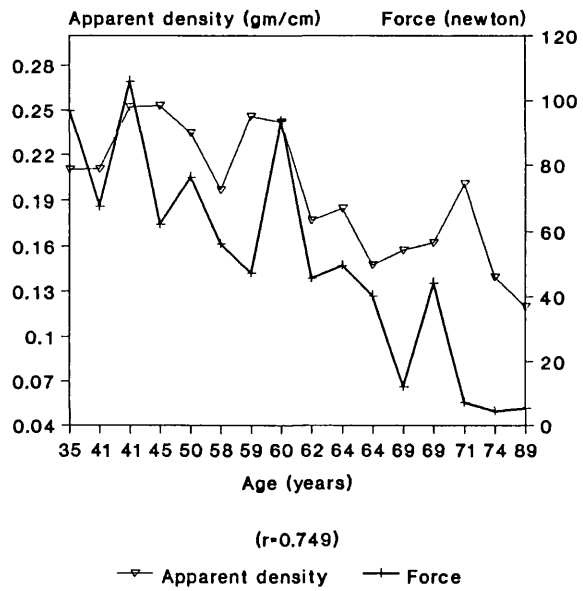


Fig. 7

The relationship between reduction of required force and loss of bone after treatment - Female group

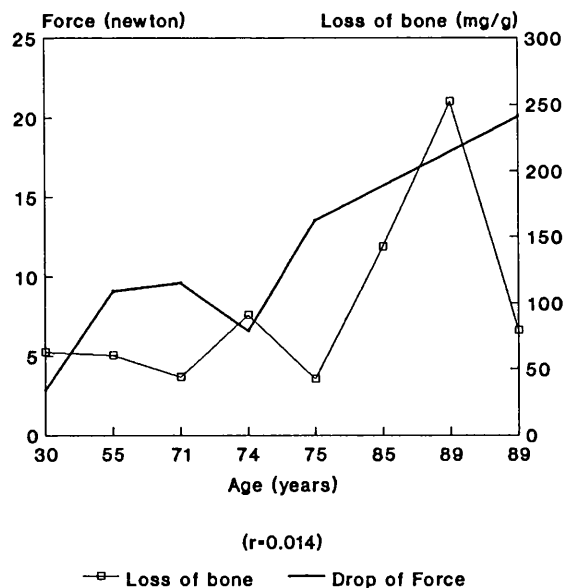


Fig. 8

The relationship between reduction of required force and loss of bone after treatment - Male group

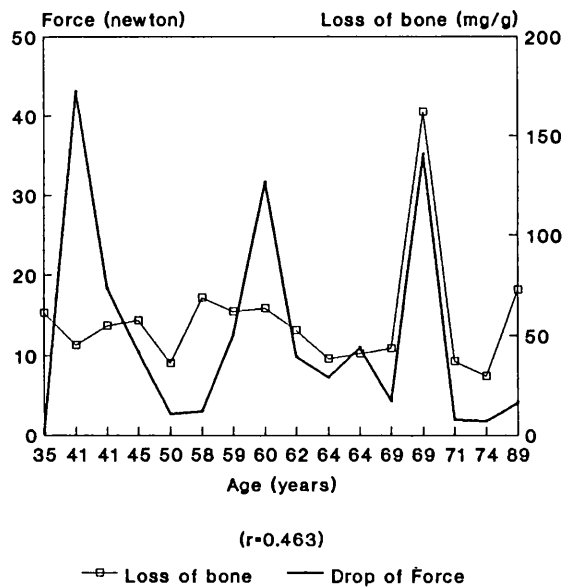


Fig. 9

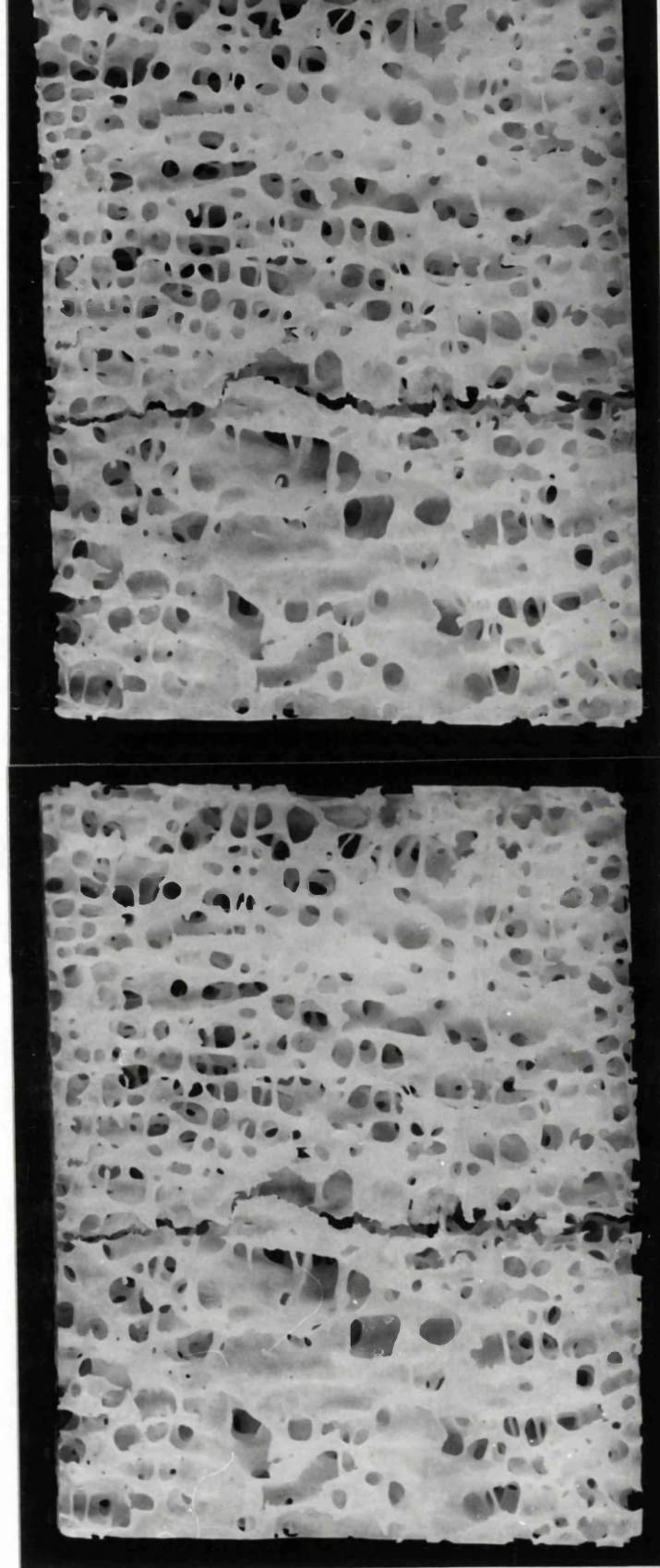


Fig. 10 A stereopair of fractured trabecular bone specimen from a 60 year old male. The trabecular structure is dominated by thick plates and tubes. The fracture line is approximately straight with both vertical and horizontal elements fracturing without preference.

Fig. 11 A stereopair of fractured trabecular bone specimen from a 62 year old male. At the middle third of the sample trabecular elements are more plate like, while at outer thirds a dominant rod shaped structure is apparent. Most of the fractured trabeculae are horizontal and they are mostly rod shaped. The irregular fracture line (arrows) has gone through the weakest parts fracturing some vertical elements on its way.

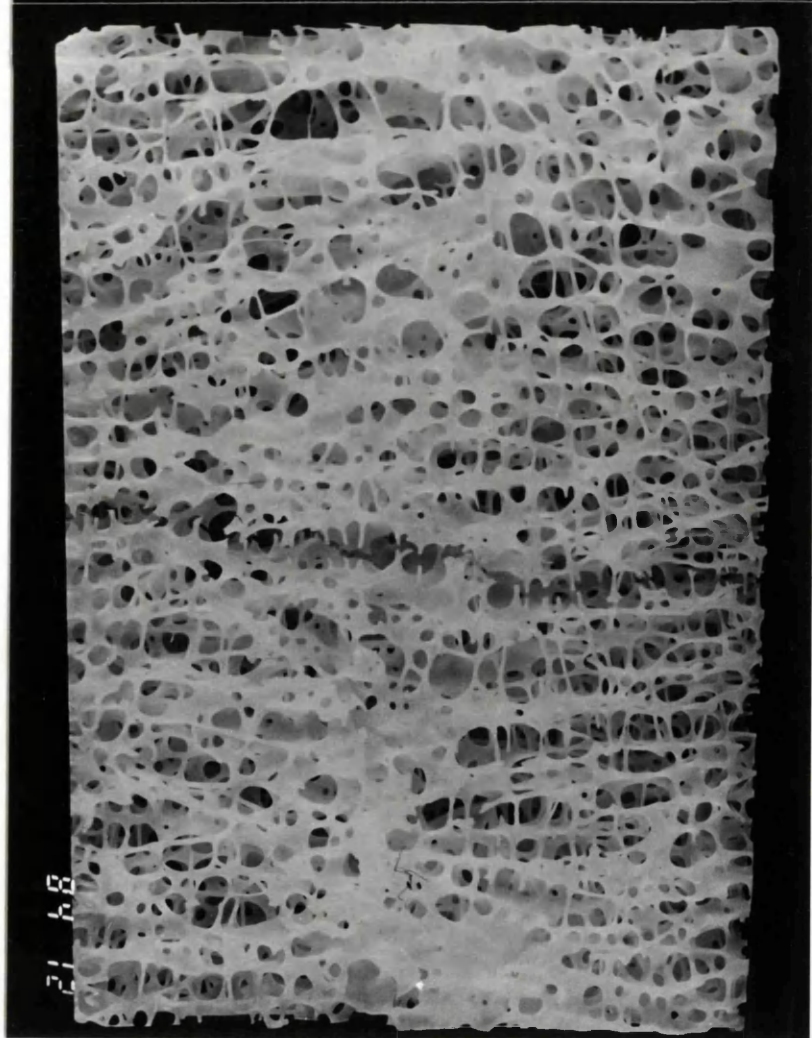


Fig. 12 A stereopair of a fractured trabecular bone specimen from a 74 year old female.

This sample had become brittle after treatment with hydrogen peroxide and cracked into two pieces with a load that was less than that applied before treatment. The fracture line is approximately straight with all the elements fracturing without any preference.

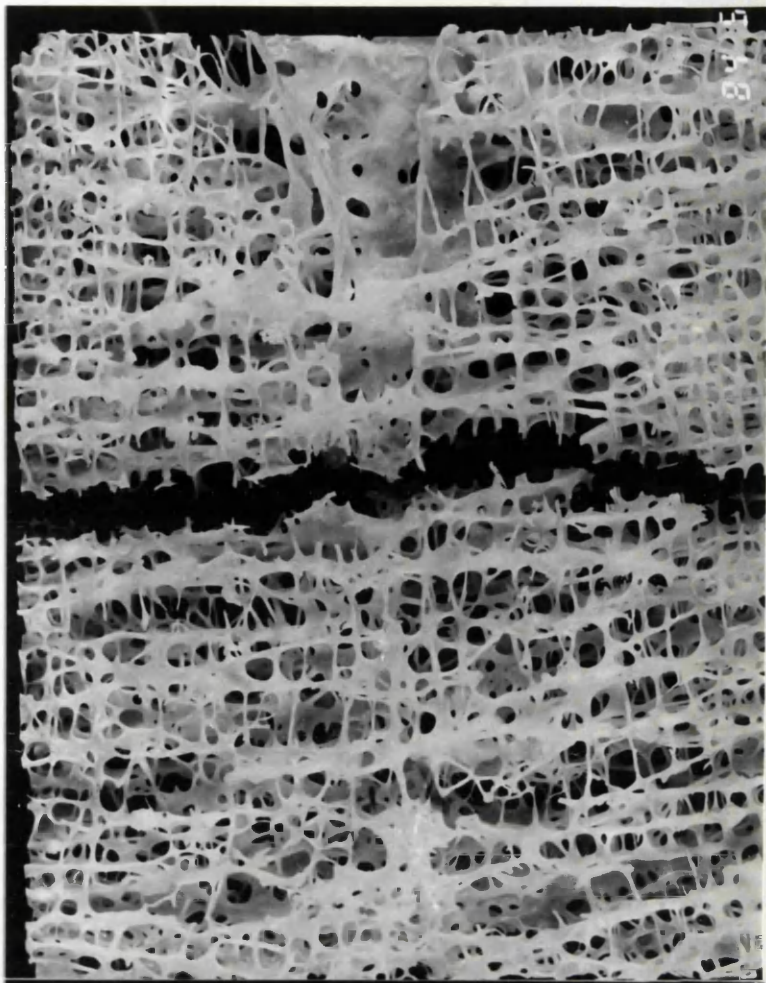
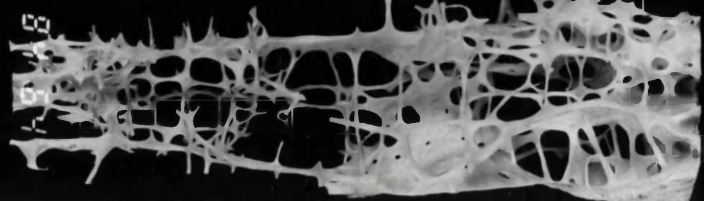
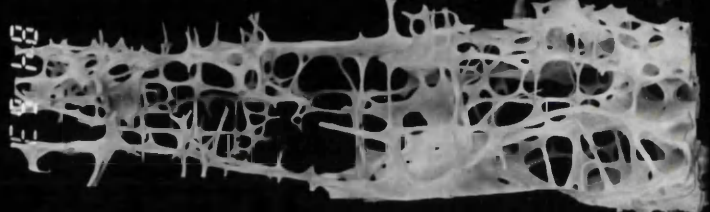
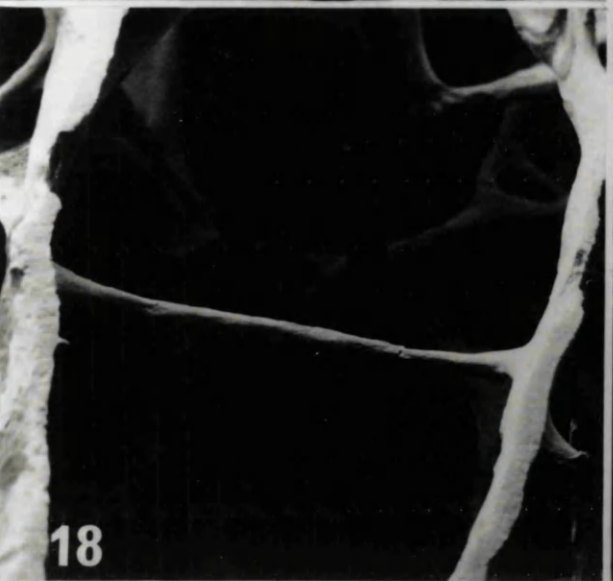
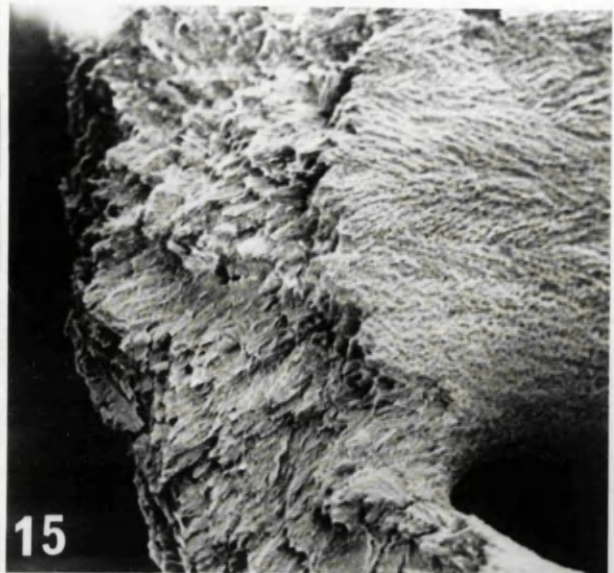


Fig. 13 A stereopair of fractured trabecular bone specimen from an 89 year old osteoporotic female. After treatment with hydrogen peroxide this sample was very brittle and collapsed under the testing rig before applying any load. The sample cracked in many places and could easily be ground into a fine powder.



- Fig. 14** An SEM micrograph of a fractured plate region from the middle third of a vertebral section from a 58 year old male. Fieldwidth 2mm.
- Fig. 15** A fracture face of a plate from the specimen in the figure 14. The fracture line has exposed lamellae at different levels. Fieldwidth 230 μm .
- Fig. 16** An SEM micrograph showing fracture line in a vertebral section from a 30 year old female. Thick rods have separated at their junction with the plate. Fieldwidth 955 μm .
- Fig. 17** A fractured rod from an 89 year old female. The fracture line has severed collagen bundles and is perpendicular to the long axis of the rod. Fieldwidth 205 μm .
- Fig. 18** A long horizontal trabeculum in a vertebral section from an 89 year old osteoporotic female. The trabeculum has fractured where thinnest. Fieldwidth 2mm.
- Fig. 19** High power view of the fracture of the trabeculum in the figure 18. The fracture line has gone right across collagen bundles. Note that the surface of the trabeculum appears to be formative with a mineralising front with large nodules. Fieldwidth 105 μm .



CHAPTER 6

AN INVESTIGATION OF THE MICROMORPHOLOGY OF HUMAN LUMBAR VERTEBRAL TRABECULAR BONE SURFACES USING SCANNING ELECTRON MICROSCOPE.

6.1 INTRODUCTION

The SEM has contributed immensely to our understanding of bone structure and function. Using the SEM, morphological appearances of bone surfaces can be characterised and both microscopic structure and in vivo cellular activities can readily be studied (Boyde and Hobdell 1969, Boyde 1972). Some well documented studies include the description of lamellar bone and primary membrane bone and their mineralising fronts (Boyde and Hobdell 1969a and 1969b, Boyde 1980, Boyde et al. 1982), osteocyte lacunae (Marotti 1981), osteocyte orientation and canaliculi (Marotti et al. 1985 and Marotti et al. 1985), bone endosteal surfaces (Krempien 1979, Reid 1987), cell–matrix interface (a review by Jones et al. 1986) resorbing surfaces (Krempien and Klimpel 1981 and a review by Boyde and Jones 1987) and study of fossil bone (Bromage 1987).

Many pathological conditions of bone have also been studied using the SEM (Sela 1977 and a review by Boyde et al. 1986). Paget's disease of bone (Munzenberg et al. 1971, Chappard et al. 1984), osteoporosis (Dempster et al 1986), renal osteodystrophy (Krempien et al. (1977), hyperparathyroidism (Krempien et al. 1975), familial hypophosphataemia (Steendijk and Boyde 1973) and osteogenesis imperfecta (Lindenfelser et al. 1972, Reid and Boyde 1983) are some pathologies where SEM has been a useful microscopic method.

Whitehouse et al. (1971) described the structural arrangement of trabeculae within a vertebral body using low power SEM micrographs. However, trabecular bone surfaces from lumbar vertebral bodies have rarely been subjected to SEM studies. During aging, trabecular bone at this site undergoes considerable changes. The structure changes from one with prominent plate-like trabeculae to one dominated by rods or needle-like features. Further, perforations and the removal of trabecular elements are commonly seen with aging (Parfitt 1987), but the mechanisms responsible for such changes are not well understood. Microfractures have also been frequently observed in old and osteoporotic patients, but have not been adequately investigated. The occurrence of vertebral crush fractures in old age also emphasises the importance of micromorphological studies of trabecular bone surfaces.

In the present study, SEM was employed to characterise trabecular bone surfaces of fourth lumbar vertebral bodies derived from young adult, old and osteoporotic subjects. The objective of the study was to understand the micromorphology of these surfaces and relate them to already described changes that occur during aging and in osteoporosis.

6.2 MATERIALS AND METHODS

At the time of routine autopsies, fourth lumbar vertebral bodies were removed from 30 subjects (18 male and 12 females) aged from 30 to 91 years. Cleaned samples were stored in 70% ethanol until required.

Using a low speed diamond saw (Isomet-11-1180), plane parallel mid sagittal sections of 4mm in thickness were cut from each vertebral body and treated with a solution of 2% hydrogen peroxide at 37°C for 24 hours to remove marrow and soft tissues. Afterwards, the samples were cleaned with a jet of water; defatted in a 50:50 solution of chloroform and methanol for a few hours and were air dried.

A Cambridge Stereoscan (S4-10) SEM was used for the study. The samples were coated with gold by sputtering and examined in the SEM at 10kV (for SE), or at 20kV (for BSE, using an annular, 4-segment, solid-state BSE detector). Stereopair micrographs were recorded with a tilt angle difference of 10°.

6.3 RESULTS

6.3.1 Identification and distribution of activities

The three main morphologies which characterise the different activity states of bone surfaces (Boyde 1972) could readily be identified on various components of trabecular bone. There were marked differences in the amount, morphology and the distribution of these activities in different age groups.

Fully mineralised collagen bundles characterising resting surfaces were evident mainly in young adult samples (Figure 2). In old samples the proportion of resting surfaces was reduced, while in osteoporotics the majority of the surfaces exhibited one or the other cellular activity (e.g. resorption or formation). "Prolonged resting surfaces" identified by the extension of mineralisation into the ground substance thus obscuring collagen fibre detail – together with fusion of collagen bundles to form more larger bundles – were seen only in younger adult samples (Figures 1 and 4).

The greatest diversity in activity with age was observed in resorbing surfaces identified by the presence of excavation bays or "snail tracks" (Boyde and Jones 1979) on trabecular surface. These will be discussed later. Forming or mineralising surfaces were evident from the presence of mineral aggregates or interrupted collagen fibre bundles. In any one trabecular element a formative front was observed adjacent to a resorbing area indicating a proper coupling between these two processes in younger samples (Figure 3). However, in most occasions in old and osteoporotic samples, one type of activity dominated in one area or sometimes in one trabecular element. These changes were related to structural changes such as perforations, thinning and removal of trabecular elements that take place with age and in osteoporosis.

6.3.2 Collagen organisation

The organisation of collagen in trabecular bone was dependent upon the shape and morphology of different elements. In rod shaped trabeculae, the collagen fibre bundles were mainly

aligned along the long axis (Figure 1). However, overlapping domains (Boyde and Hobdell 1969) showed distinctive angles to each other whilst still more parallel than perpendicular to the rod (Figure 2).

Plate-like trabeculae were usually encountered in the middle zone of mid sagittal sections of the vertebrae and contained several round or oval openings (Figure 6). No definite overall alignment of the collagen fibre bundles was apparent on the surface of the plates. However, at the margins of the plates they were aligned approximately parallel to the margins. At the junction between a plate and a rod, the bundles converged towards each other to form the rod (Figure 8). At the boundary of the openings, the domains were very short and each domain was partially overlapped by a differently oriented domain (Figure 7) giving rise to the smooth appearance of the boundary.

At surfaces where recent resorption had occurred, prominent collagen fibre bundles could be observed in the floors of resorption bays and the different orientations within lamellae was evident at the various depths exposed (Figure 21 and 38). At forming surfaces, parts of incompletely mineralised collagen bundles presented as aligned mineral residues representing the mineralised lengths of individual collagen fibrils (Figures 5 and 18). In young adult specimens, the structural organisation of collagen was not very different from that previously reported for cortical bone (Boyde 1972, Reid 1987).

In some old and osteoporotic samples, irregular collagen organisation was evident on trabecular surfaces (Figure 36) and even though not organised into extensive domains, these collagen bundles were completely mineralised (Figure 37). However, such irregular collagen orientation seems to be a surface phenomenon since normal lamellar organisation could be observed in deeper layers (Figure 38). Atypical collagen patches were also observed in many old and osteoporotic samples, sometimes related to micro-cracks present on these surfaces (Figure 39). A different organisation of collagen bundles was also seen in areas of healing microfractures (Figure 44) and in regions where microcallus was forming.

6.3.3 Resorption

The characteristics of the resorbing surfaces showed considerable variability both within the same age group and at different ages. These variations were related to the structural changes of trabecular bone that occur with age, such as thinning, perforation and removal of different elements. The size, shape and morphology of resorption bays varied from very long, shallow elongated furrows ("snail track resorption bays": Boyde and Jones 1979) to small, rounded deep lacunae (Figures 14, 29 and 34). The snail tracks were usually aligned with their neighbours and followed the orientation of collagen in adjacent areas (Figures 3 and 11: Reid 1987). Around openings on the plates, resorption bays followed the circumference of the opening suggesting that they also track the collagen orientation here (Figure 9). The amount of bone removed by resorption varied from superficial "licking" of surfaces (Figures 12 and 13) to complete perforation or disconnection of trabecular elements (Figure 42).

In young specimens, resorption was dominantly superficial (Figure 4) and involved

extensive areas over the trabecular surface. Such resorption was followed by formation to cover up the area resorbed (Figure 10). In most instances, resorption seemed to have been initiated at a node and had advanced towards surrounding rods and plates (Figure 12). This type of resorption can be considered as a part of normal remodelling process where bone mass is maintained through a proper coupling of the two processes.

The removal of trabeculae seemed to be initiated by the appearance of perforations on different elements simultaneously and was most often seen in old and osteoporotic specimens. Occasional perforations were also observed in younger specimens (Figure 19). They frequently appeared at a node (Figure 19) or at the centre of a plate (Figure 20) and were always preceded by superficial resorption. It appeared that after removal of the top-most layer, a group of osteoclasts cut across collagen bundles to dig deep into bone (Figure 21). Such perforations sometimes commenced from the base of a previously formed groove (Figure 26): this was mostly seen during resorption of rods (Figure 24). As figure 27 suggests, a single osteoclast might be capable of initiating the process of perforation by tunnelling deep into bone.

Many different types of resorption patterns were observed in rods. The thinning of rods seemed to have been brought about by several successive episodes of osteoclastic resorption from one node to the other (Figure 34 B). The snail track type of resorption, with parts of remaining tracks from a previous episode, was frequently seen on such surfaces (Figure 11). Sometimes a mixture of both morphological types of resorption bay was evident on the same trabeculum (Figure 14).

When direct removal of a rod rather than thinning was the result, three distinct resorption types were observed. Firstly, without any superficial resorption, osteoclasts seemed to have made short but deep excavations (Figure 15) to cut right across a trabeculum. However, appearances were seen in some specimens which suggested that before a complete separation, the trabeculum may have been broken away, perhaps by a minimal load *in vivo* or during the preparation of the specimens (Figure 29). This type of resorption was usually observed at one end of a rod where it was connected to a node or a plate (Figure 28). Secondly, after a superficial resorption characterised by the snail track type of bay, some rods were deeply grooved by what appeared to be a more aggressive type of osteoclastic activity (Figures 32 and 33). Such grooves seemed to have deepened gradually and or extended along the rod towards the other end. Perforations sometimes appeared to have commenced on the floors of these grooves (Figure 24) and may have then progressed to pierce the whole thickness of the trabeculum. Thirdly, appearances were seen which suggested that groups of osteoclasts grooving a rod may have "tunnelled in" while moving along it (Figure 30). Sometimes several such tunnels could be seen around one trabeculum (Figure 31). It was also observed that if the rod had not broken while the resorption was occurring, the osteoclasts appeared to have actually "eaten away" until it was disconnected (Figures 34A and 42). This was especially evident with the last two types of resorption described.

The floors of resorption bays showed several microscopic textures. Smooth floors were evident where the surface was resting after an initial resorption event (Figures 4 and 34). The "snail tracks" usually displayed this texture. In areas of active resorption, collagen fibre bundles with

various orientations were observed depending on the exposed lamellae at different depths (Figures 21 and 29), while mineral nodules of varying sizes were apparent on the floors where active bone formation had begun (Figure 31). Osteocytic lacunar profiles of different sizes were also frequently observed within resorption bays (Figure 34B).

Another interesting feature that was reported long ago (Boyde 1968, Boyde and Hobdell 1969) and also observed during the present study was the resorption of osteoid by osteoclasts. This was widely seen both in young and old specimens (Figures 15,29 and 34B) suggesting that osteoclasts do not selectively resorb fully mineralised surfaces, but that un-mineralised or mineralising fronts are also involved.

6.3.4 Mineralising surfaces

The specimens used during this study were made anorganic by treating them with hydrogen peroxide to remove the un-mineralised organic matrix.

Different stages of mineralisation could be recognised from the texture of mineralised surfaces, from those which showed mineral nodules which were less well aligned with each other (Figures 3 and 23) and in which it was more difficult to see the direction of the collagen fibres, to those where the nodules were well aligned, which may represent a later stage in the completion of mineralisation. Mineralised lengths of individual collagen fibrils indicate a looser packing of fibrils (Figure 5). The active mineralisation seemed to have ceased on some surfaces and a progressive mineralisation of the remaining osteoid was evident.

In the young adult specimens, appearances suggested that the amount of bone formed was more or less equivalent to the amount resorbed (Figure 10). This may reflect not only a maintenance of bone mass, but a lesser change in size and shape of the individual trabecular elements. Contrary to this, in old and osteoporotic specimens, vast areas of mineralising front covering several generations of resorption bays were observed (Figures 16, 17 and 23). In plates, such fronts appeared to have advanced from two sides towards each other (Figure 16), while in rods, signs of mineralisation (indicating new formation) sometimes surrounded a trabeculum (Figure 28). This process would undoubtedly change the size and shape of trabecular elements and would account for the compensatory thickening and structural changes of trabeculae seen in old age. It was also observed that the morphological type of mineralisation was not constant in old age. This may explain the rugged appearance of trabeculae seen especially in osteoporotic specimens (Figure 35).

An interesting finding was that repair was not dependent upon resorbing patterns in old specimens. Mineralisation (new formation) was observed not only in shallow resorption bays but even in deep tunnelling grooves (Figure 31). Further, it was often seen that the surrounding surface was still mineralising when the result of deep resorption had been to disconnect a trabeculum (Figure 29). Mineralisation was also observed on disconnected trabeculae. This, and the fact that resorption disregards the texture of the resorbing surface, shows that these two processes may be quite independent of each other, indicating an uncoupling of resorption and formation in old age.

6.3.5 Osteocyte lacunae

Osteocyte lacunae showed several morphological differences depending on the activity status of the surface. Generally, they were elongated with their long axes aligned with the surrounding collagen fibre bundles (Jones 1973). Examples of half-formed lacunae in resting or forming surfaces can be seen in figures 4, 5 and 6. Resorption also has exposed lacunae at different depths, forming profiles of various shapes on the surface (Figure 34B). The walls of the osteocyte lacunae were proud of the resorbed surface (Figure 25) indicating a degree of protection offered by the surviving osteocyte in vivo (Boyde 1980).

The walls of osteocyte lacunae were smooth (ie. the collagen was completely mineralised) in resting and resorbed surfaces. Sometimes, the thick, mineralised collagen bundles of the underlying lamellae were evident (Figure 25): and in some forming surfaces, the lacunar wall showed a pattern of randomly oriented fine fibrils (Figure 5). The mineralising lacunar floor showed the same characteristics as the surrounding surface in actively forming surfaces (Figure 18).

The lacunar walls were penetrated by a variable number of canalicular openings (Figures 25 and 34B). These were also widely observed on resorbed surfaces and were sometimes crowded together indicating the whereabouts of underlying osteocyte lacunae (Figures 22 and 34B).

6.3.6 Microfractures

In most of the old, and especially in the osteoporotic specimens, trabecular disconnections were widely observed. These disconnected trabeculae were most often rod shaped, but were thin, long and frail compared with the thick, sturdy rods in young specimens. The disconnections were also seen at any distance along the rods. As previously noted, such discontinuities were not always microfractures, but many had resulted from the resorption of whole thickness of the trabeculae by osteoclasts (Figures 34A and 42).

Microfractures were usually noted at the centre, or the thinnest and therefore weakest, part of a trabeculum. It appeared that they were always preceded by (in any case, associated with) some degree of resorption on the surface. A trabeculum could break with a minimum of resorption on one side (Figure 40) or with different degrees of resorption (Figures 28 and 41) depending on the load to which it had been subjected.

Once a trabeculum had become disconnected and was therefore no longer subjected to mechanical force, both resorption and formation appeared to have continued for sometime, then later ceased and the broken ends were left "ignored" (Figure 43). Occasionally, the tips of these ends were "bandaged" or "wrapped" by the laying down of collagen bundles around them (Figures 44 and 45).

6.4 DISCUSSION

The results of this study show that the basic micro-organisation of vertebral trabecular bone is not significantly different from that previously described for other sites (Boyde and Hobdell 1969, Boyde 1972, Reid 1987). For example, mineralised collagen bundles were organised as domains on trabecular surfaces. Further, resorption bays, mineralising fronts and osteocyte lacunae showed the same characteristics as described in the above mentioned studies. The differences however, reflected the structural variations in trabecular elements. In rods, the main alignment of the collagen bundles is along the main axis. In plates, various collagen orientations are possible, depending on their shapes. Resorption follows collagen orientation. Accordingly, in oval or round openings of the plates, resorption bays are arranged around their circumference (Figure 9).

The most interesting results of the present study concern the incidence of the different surface activity states. In the young age group, a normal remodelling process with a morphological coupling of resorption and formation was observed. However, in the older age group, and especially in the osteoporotic subjects, many changes were evident in conformity with the structural changes in trabecular elements occurring with advancing age.

The trabecular bone structure consists of a complex three dimensional network of plates and rods (Whitehouse et al. 1971). During age related bone loss, thinning and perforation of trabeculae leads to a conversion of plates to rods with the end result of removal of entire structural elements (Parfitt et al. 1983). In describing the mechanisms involved in this process, a quantum concept has been proposed (Parfitt 1979), according to which bone loss occurs either because osteoclasts erode cavities that are too deep, or osteoblasts deposit new layers of bone that are too thin. The former process has been attributed to the rapid loss of trabecular bone resulting from complete removal of structural elements, while the latter to a slow loss with progressive trabecular thinning (Parfitt 1984).

Such conclusions have been reached from studies made on thin histological sections and by measurements of quantities such as mean trabecular wall thickness. Arnold (1970,1981), using macrophotographs of trabecular bone specimens, first proposed the occurrence of perforations due to focal excessive resorption which led to thinning and loss of structural elements. During the present study with the SEM, it was possible to study such perforations. They usually appear at the centre of a node or a plate (Figures 19 and 20). The fact that their appearance is preceded by superficial resorption indicates the presence of two distinct types of osteoclastic activity. Similar differences were also observed in rods, where successive superficial resorption led to thinning of rods (Figure 34B), while deep grooving, tunnelling or perforation (Figures 24,28, 32) were responsible for their disconnection. The two patterns of resorption could be interpreted as indicating different movement patterns of the osteoclasts. The superficial planing of the surface suggests lateral movements during resorptive phases – a wave of resorption passing over the surface (lateral resorption). The deep or vertical resorption could be static, and may be related to cytokine producing cells. New bone formation was observed on most of the surfaces and even on the floors of deep excavations made by osteoclasts (Figure 31). However, it appeared that such

formation was often insufficient to fill the resorption bays. The results of this study therefore confirm the quantum concept of bone loss, but also emphasise the importance of the location of aggressive resorptive activity.

The evidence for uncoupling between formation and resorption seen in the present study would be explained by a delay in the recruitment of osteoblasts after an episode of resorption, such that formation began only after several successive resorption events and sometimes only after the appearance of perforations (Figure 16). Further, mineralising fronts were disproportionately extreme and common when compared with the situation in the younger age group. Mineralising fronts (i.e. new bone formation) sometimes covered a whole trabeculum. If the interpretation that these are mineralising rather than arrested fronts is correct, these appearances would indicate the conversion of the trabeculum to a different size and shape. Apart from microcallus formation, this would perhaps explain the compensatory increase in trabecular thickness observed in previous studies (Atkinson 1967, Siffert 1967, Pesch et al. 1977). The present study also demonstrated and supported the view that osteoclasts may resorb mineralising osteoid (Boyde 1968, Boyde and Hobdell 1969, Reid 1987).

Abnormalities in both formation and mineralisation were also seen especially in very old and osteoporotic subjects. Randomly arranged collagen bundles were sometimes observed on the surface (Figure 37). If the different morphological types of mineralising front represent different rates of mineralisation and if this in turn reflects different rates of formation, then these would be an explanation for the irregular surface of the rods (Figure 35). Even though the conversion of plates to rods has been generally regarded as a phenomenon of age-related bone loss, it should be noted that these long, slender rods do not necessarily resemble the rods seen in younger specimens.

The observation that fractured trabeculae were frequently partially resorbed indicates that microfractures may occur when resorption weakens the trabeculae to an extent that they are no longer able to withstand the mechanical stress. However, if they do not break, the resorption may continue until complete trabecular cleavage. The mineralisation and different resorptive activities seen on disconnected trabeculae were most probably activities that occurred before the disconnection. The slowdown of these activities seen after disconnection may reflect the lost effect of mechanical stress on the disconnected elements. The dramatic reduction in the number of trabecular elements with age indicates that such disconnected elements are ultimately removed by complete resorption. However, some evidence for a degree of repair of disconnected elements was also observed during the present study.

6.5 CONCLUSIONS

The characteristics and activities of trabecular bone surfaces are not significantly different from that of cortical bone. In the younger age group studied, a proper coupling of formation and resorption maintained both the bone mass and the structural integrity of the trabecular elements. In old individuals and in osteoporotics, irregularities and uncoupling of these activities brought about a loss of bone and a disruption of trabecular structure. Different resorption patterns were observed in old age and two distinct resorption types (lateral and vertical) that are responsible for trabecular

thinning and removal of structural elements were identified. Previously proposed resorptive mechanisms were also confirmed by this SEM study. Irregularities in the formative process in old age may account for the compensatory thickening and changes in shape and texture of trabecular elements. The mechanisms involved in the occurrence of microfractures and the fate of disconnected elements were also identified.

6.6 REFERENCES

- Arnold JS (1970) Focal excessive endosteal resorption in aging and senile osteoporosis. In: Barzell US ed. Osteoporosis. Grune and Stratton, New York, 80.
- Arnold JS (1981) Trabecular pattern and shapes in aging and osteoporosis. In: Jee WSS, Parfitt AM eds. Bone histomorphometry. Third international workshop. Armour Montagu, Paris, 297–308.
- Atkinson PJ (1967) Variation in trabecular structure of vertebrae with age. *Calcif Tissue Res* 1:24–32.
- Boyde A (1968) Height measurements from stereopair scanning electron micrographs. *Beitrage zur Elektronenmikroskopische Direktabbildung von Oberflächen*. 1:97–105.
- Boyde A (1972) Scanning electron microscopic studies of bone. In: Biochemistry and physiology of bone. Bourne GH ed. volume I, Academic press, New York, 259–310.
- Boyde A (1980) Electron microscopy of the mineralising front. *Metab Bone Dis Rel Res* 2S:69–78.
- Boyde A, Hobdell MH (1969a) Scanning electron microscopy of lamellar bone. *Z. Zellforsch. Mikros Anat.* 93:213–231.
- Boyde A, Hobdell MH (1969b) Scanning electron microscopy of primary membrane bone. *Z. Zellforsch. Mikros Anat.* 99:98–108.
- Boyde A, Jones SJ (1979) Estimation of the size of resorption lacunae in mammalian calcified tissues using SEM stereophotogrammetry. *Scanning electron microscopy /1979/II SEM Inc. AMF O'Hare, Il 60666*, 393–402.
- Boyde A, Jones SJ (1987) Early scanning electron microscopic studies of hard tissue resorption: their relation to current concepts reviewed. *Scanning Microscopy* 1/I:369–381.
- Boyde A, Jones SJ, Ashford J (1982) Scanning electron microscope observations and the question of possible osteocytic bone mini- (re-) modelling. In: Current advances in skeletogenesis. Silbermann M, Slavkin HC eds. International Congress Series No. 589. Elsevier, Amsterdam. 305–314.
- Boyde A, Maconnachie E, Reid SA, Delling G, Mundy GR (1986) Scanning electron microscopy in bone pathology: review of methods, potential and applications. *Scan Elect Micros* 4:1537–1554.
- Bromage TG (1987) The scanning electron microscopy/Replica technique and recent applications to the study of fossil bone. *Scanning Microscopy* 1/II:607–613.
- Chappard D, Alexandre C, Laborier JC, Robert JM, Riffat G (1984) Paget's disease of bone. A scanning electron microscopic study. *J submicrosc Cytol* 16:341–348.
- Dempster DW, Shane E, Horbert W, Lindsay R (1986) A simple method for correlative light and scanning electron microscopy of human iliac crest bone biopsy: qualitative observations in normal and osteoporotic subjects. *J Bone Min Res* 1:15–21.
- Jones SJ (1973) Morphological and experimental observations on bony tissues using the scanning electron microscope. Ph D thesis, University of London.
- Jones SJ, Boyde A, Ali NN (1986) The interface of cells and their matrices in mineralised tissues: A review. *Scan Elect Micros* 4:1555–1569.
- Krempien B (1979) Bone modelling processes at the endosteal surface of human femora. Scanning electron microscopical studies in normal bone and in renal osteodystrophy. *Virchows Arch A Path Anat Histol.* 382:73–88.
- Krempien B, Geiger G, Ritz E (1975) Alteration of bone tissue in secondary hyperparathyroidism. A scanning electron microscopical study. In: Vitamin D and problems related to Uremic Bone Disease. Norman AW, Schaefer K, Grigoleit HG, von Herrath D, Ritz E eds. Walter de Gruyter, Berlin. 157–161.
- Krempien B, Friedrich G, Geiger G, Ritz E (1977) Renal osteodystrophy studies with scanning and transmission electron microscopy. *Adv Exp Med Biol* 81:493–505.

- Krempien B, Klimpel F (1981) Scanning electron microscopical studies of resorbing surfaces. In: Bone Histomorphometry. Jee WSS, Parfitt AM eds. Armour Montagu, Paris. 45–51.
- Lindenfelser R, Hasselkus W, Haubert P, Kronert W (1972) Osteogenesis imperfecta congenita. Scanning electron microscopic studies. *Virchows Arch B Cell Pathol* **11**:80–89.
- Marotti G (1981) Three dimensional study of osteocyte lacunae. In: Bone Histomorphometry. Jee WSS, Parfitt AM eds. Armour Montagu, Paris. 223–229.
- Marotti G (1985) A SEM study of osteocyte orientation in alternately structured osteones. *Bone* **6**:331–334.
- Marotti G (1985) Quantitative investigation on osteocyte canaliculi in human compact and spongy bone. *Bone* **6**:335–337.
- Munzenberg KJ, Flajs G, Roggatz J (1971) Scanning electron microscopy studies on diseased bone structures, especially in Paget's disease of bone. *Orthop Z* **109**:760–768.
- Parfitt AM (1979) The quantum concept of bone remodelling and turnover. Implications for the pathogenesis of osteoporosis. *Calcif Tissue Int* **28**:1–5.
- Parfitt AM, Mathews CHE, Villanueva AR, Kleerekoper M, Frame B, Rao DS (1983) Relationship between surface, volume, and thickness of iliac trabecular bone on aging and in osteoporosis: implications for the microanatomic and cellular mechanism of of bone loss. *J Clin Invest* **72**:1396–1409.
- Parfitt AM (1984) Age-related structural changes in trabecular and cortical bone: cellular mechanisms and biomechanical consequences. *Calcif Tissue Int* **36**:S123–S128.
- Parfitt AM (1987) Trabecular bone architecture in the pathogenesis and prevention of fracture. *Am J Med* **82(suppl1B)**:68–72.
- Pesch H–J, Henschke F, Seibold H (1977) The influence of mechanical forces and age on the remodelling of the spongy bone in lumbar vertebrae and in the neck of the femur. A structural analysis. *Virchows Arch (Pathol Anat)* **377**:27–42.
- Reid SA (1987) Micromorphological characterisation of normal human bone surfaces as a function of age. *Scanning Microscopy* **1/II**:579–597.
- Reid SA, Boyde A (1983) SEM and osteogenesis imperfecta. *Proc Symp Osteogenesis imperfecta*. Oxford, August 29–31, 1983.
- Sela J (1977) Bone remodelling in pathologic conditions. A scanning electron microscopic study. *Calcif Tissue Res* **23**:229–234.
- Siffert RS (1967) Trabecular patterns in bone. *Am J Roentgenol* **99/III**:746–755.
- Steendijk R, Boyde A (1973) SEM observations on bone from patients with hypophosphataemic (vitamin D resistant) rickets. *Calcif Tissue Res* **11**:242–250.
- Whitehouse WJ, Dyson ED, Jackson CK (1971) The scanning electron microscope in studies of trabecular bone from a human vertebral body. *J Anat* **108/III**:481–496.

All figures in this chapter are SEM micrographs of anorganic mid-sagittal sections of 4th lumbar vertebral bodies.

Fig. 1 35 yr male. Surface of a rod-shaped trabeculum. More or less fully mineralised collagen bundles aligned along the long axis of the rod. Note the usual branching bundle pattern of bone collagen. Fieldwidth 95 μm .

Fig. 2 35 yr male. Surface of a rod-shaped trabeculum showing arrangement of collagen bundles into domains. Overlapping domains show distinctive collagen orientations at angles to each other along the long axis of the rod. Fieldwidth 95 μm .

Fig. 3 30 yr female. A mineralising (left) and a resorbing surface (right) on a rod shaped trabeculum. The resorption bays ("snail tracks") were aligned along the long axis of the rod. Fieldwidth 95 μm .

Fig. 4 35 yr male. Superficial resorption of surface of a rod (top) and resting surface (bottom). The half formed osteocyte lacunar back wall was completely mineralised. Fieldwidth 185 μm .

Fig. 5 30 yr female. Forming surface of a rod. Mineralised lengths of individual collagen fibrils were evident in mineralised parts of collagen bundles. In the osteocyte lacunar back wall, mineralised fibrils have not been organised in to bundles. Fieldwidth 50 μm .

Fig. 6 30 yr female. An area dominated by plates from the middle region of a mid-sagittal section of a 4th lumbar vertebral body. Such plates usually contain round or oval openings. Fieldwidth 955 μm .

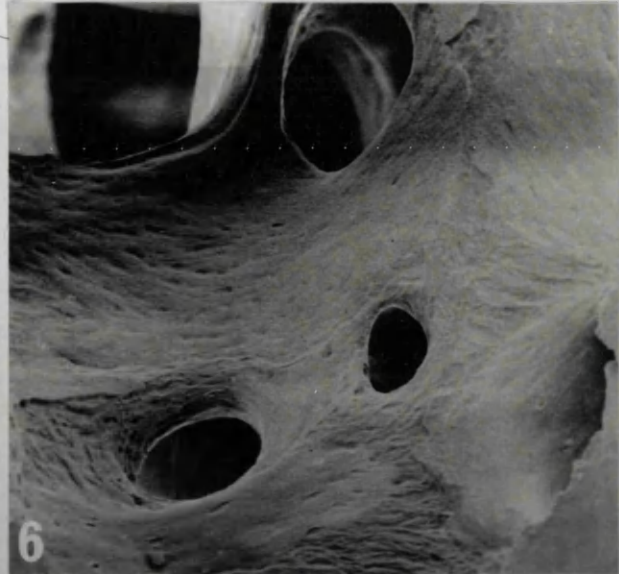
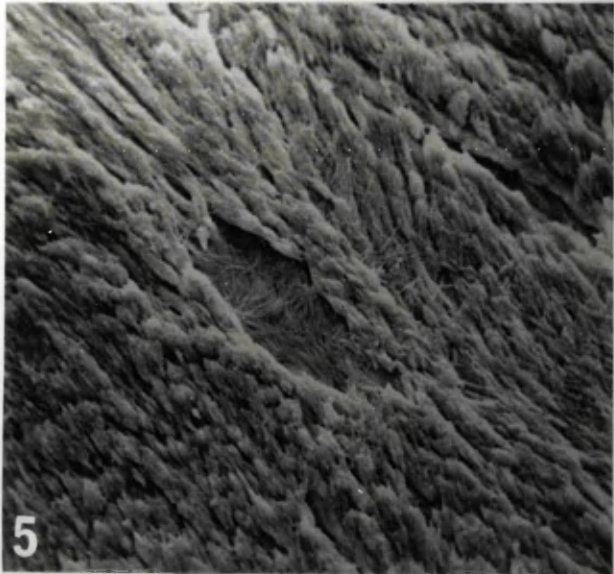
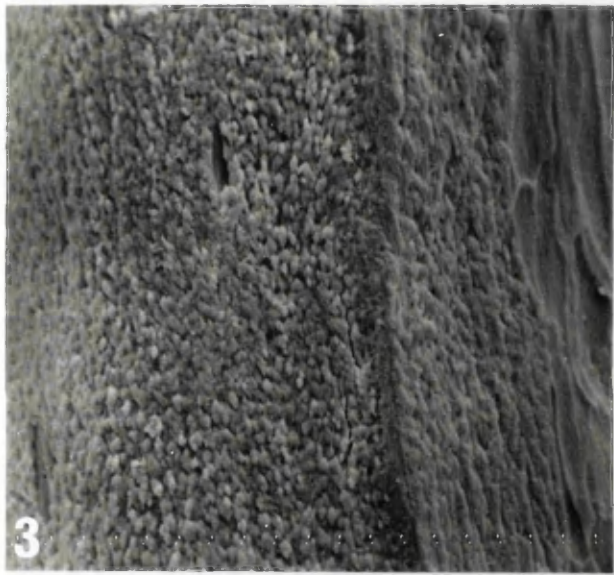
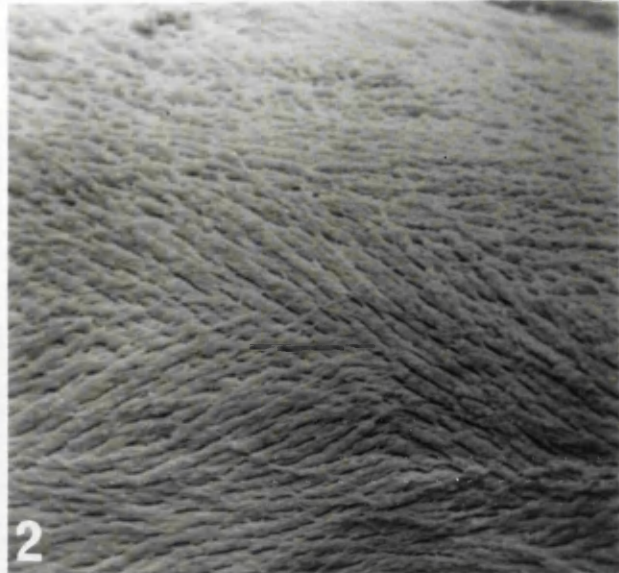
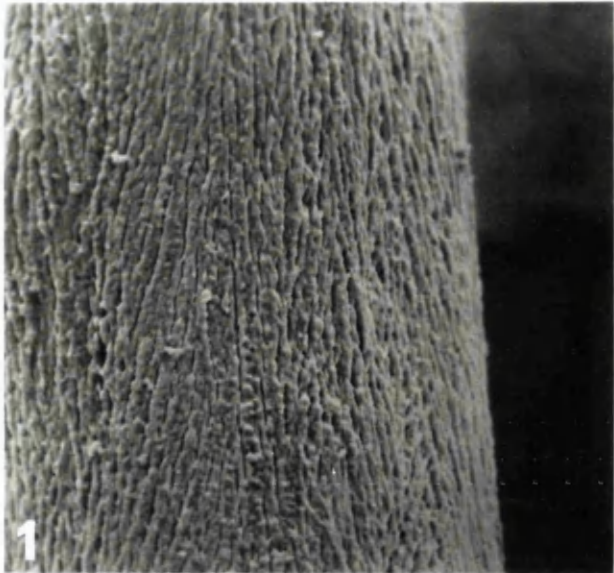


Fig. 7 64 yr male. Boundary of a round opening in a plate. Short collagen domains at the boundary partially overlap each other giving rise to a smoother appearance at the opening. Fieldwidth 60 μm .

Fig. 8 75 yr female. A stereopair showing fracture face of the junction between a rod and a plate. Collagen bundles from sides of plate converge towards each other to form the rod. A fractured osteocyte lacunar profile can also be seen on the fracture face. Fieldwidth 95 μm .

Fig. 9 41 yr male. A round opening from a plate showing "snail track" type resorption bays tracking collagen orientation around the circumference of the opening. Fieldwidth 180 μm .

Fig. 10 30 yr female. Superficial resorption on trabeculae was followed by formation, indicating a proper coupling between these two processes in this younger specimen. Fieldwidth 470 μm .

Fig. 11 41 yr male. "Snail track" type superficial resorption on a trabeculum. Remaining parts of tracks from previous resorption indicates, that several episodes of resorption had taken place on this surface. Fieldwidth 205 μm .

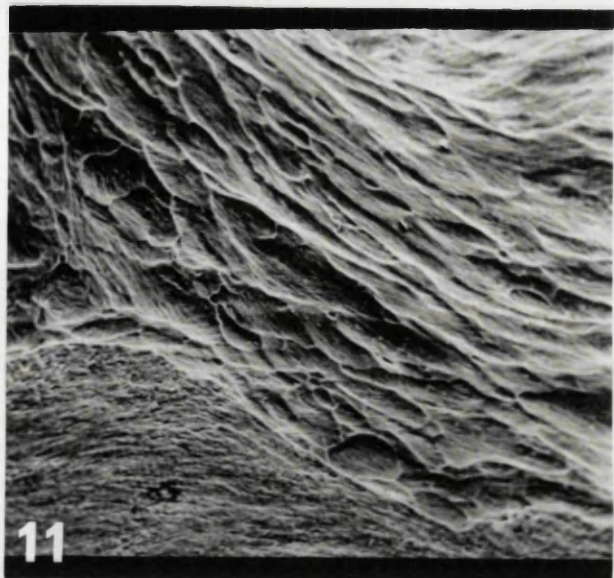
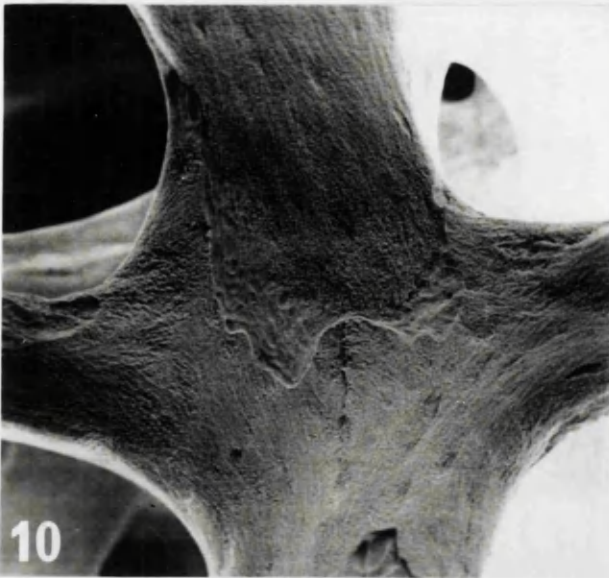
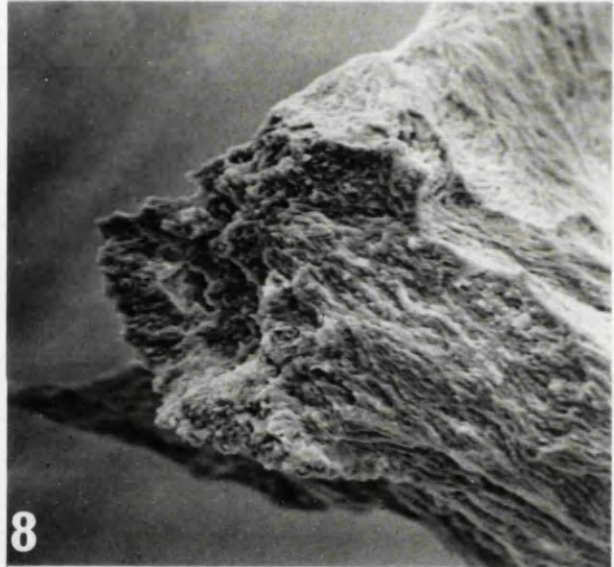
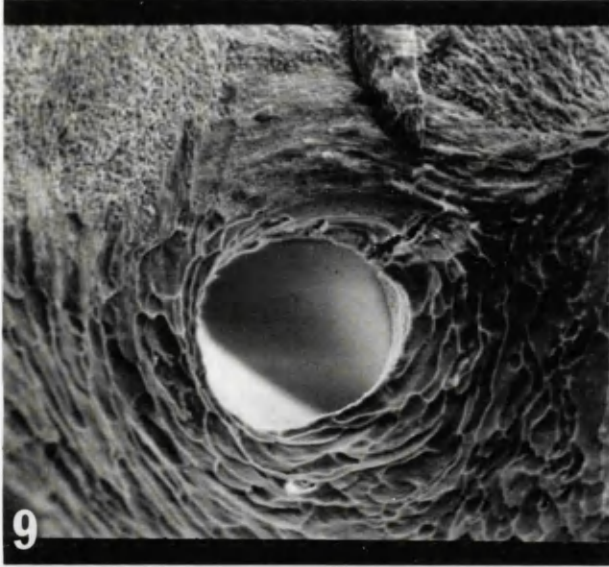
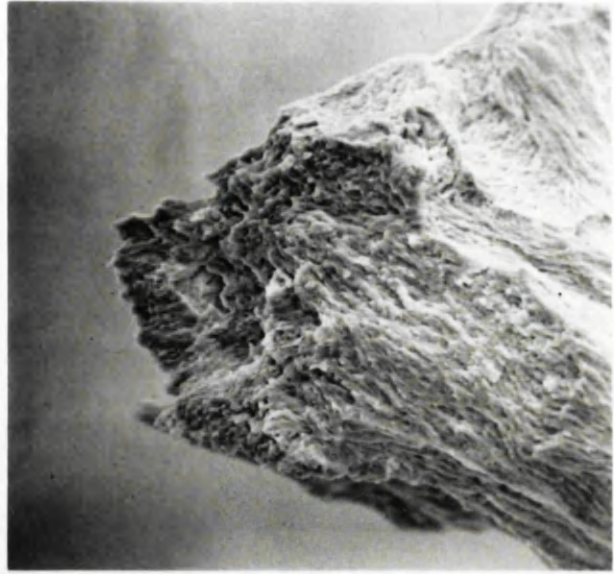
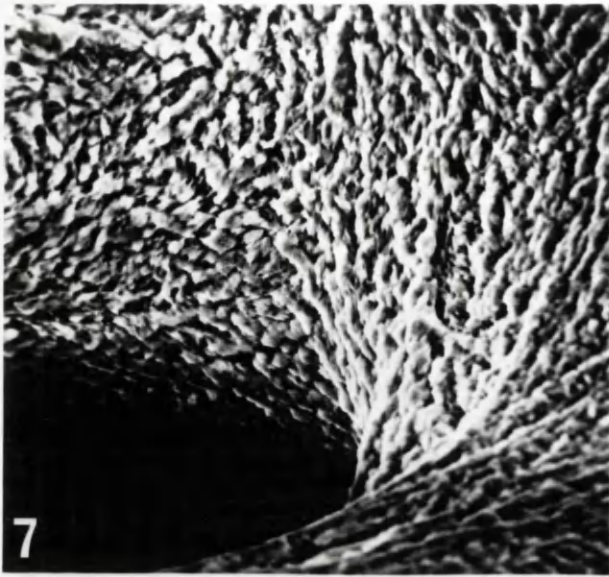


Fig. 12 41 yr male. Resorption initiated at a node and advanced towards surrounding rods and plates. This is typical of the younger specimens. Fieldwidth 470 μm .

Fig. 13 69 yr male. Initiation of resorption on a trabeculum. Superficial shallow resorption. Fieldwidth 205 μm .

Fig. 14 69 yr male. A trabeculum showing different morphological types of resorption bays. A long snail track is evident on the upper part of the trabeculum, while the lower part shows many different shapes. Fieldwidth 215 μm .

Fig. 15 89 yr osteoporotic female. Deep resorption at the junction between a rod and a plate. The result of such resorption seemed to be complete disconnection of the two elements. Surface of the trabeculum shows the morphology of a mineralising surface indicating that resorption of osteoid has taken place. Fieldwidth 95 μm .

Fig. 16 75 yr female. Two disproportionately large mineralising fronts (forming new bone packets or parts of the same packet) approaching each other from two sides to cover several generations of resorption bays. A deep pit at the centre of the plate might indicate an early state of progress to perforation. Resorption of this nature was commonly seen in old specimens. Fieldwidth 470 μm .

Fig. 17 75 yr female. Higher magnification showing detail of a mineralising front from figure 16. New formation has partially covered fully mineralised collagen bundles at the upper part of the surface, with resorption in the lower part of the field. Fieldwidth 85 μm .

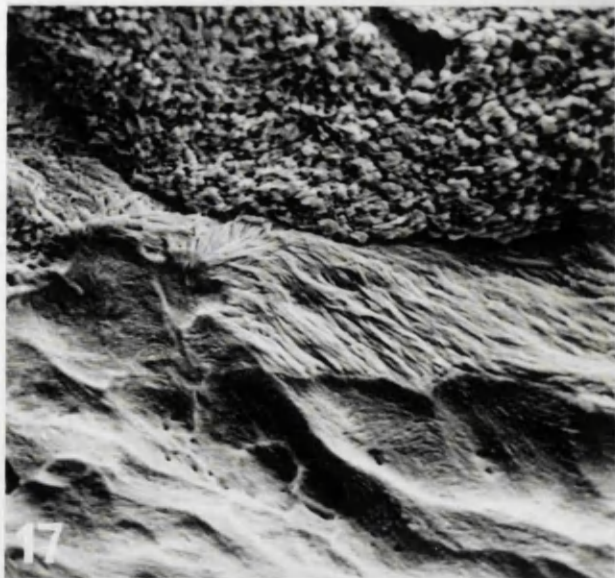
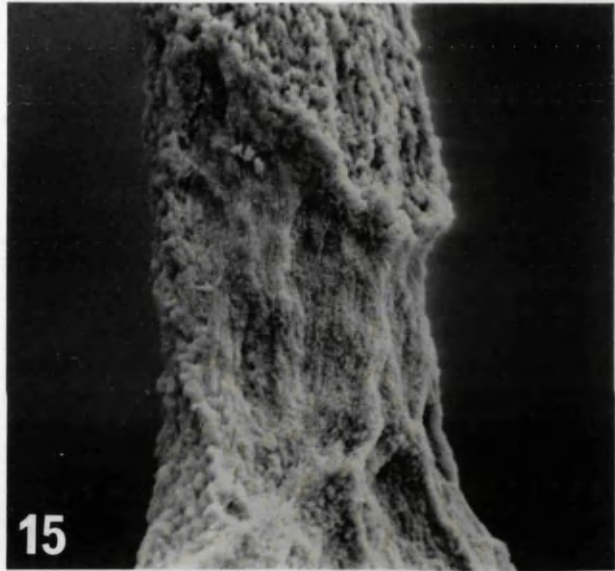
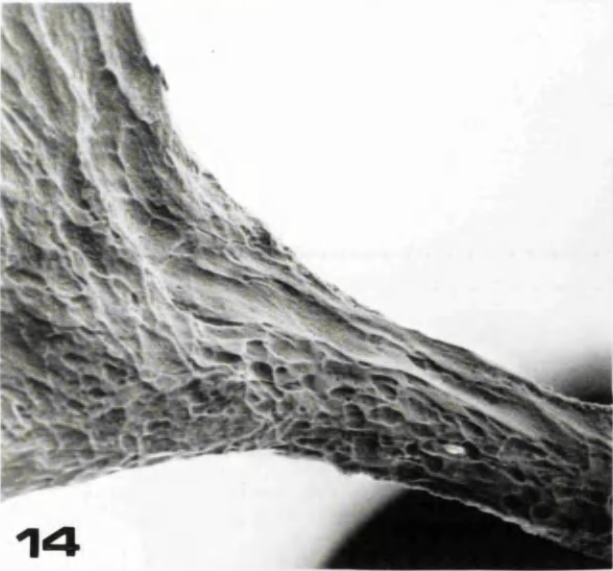
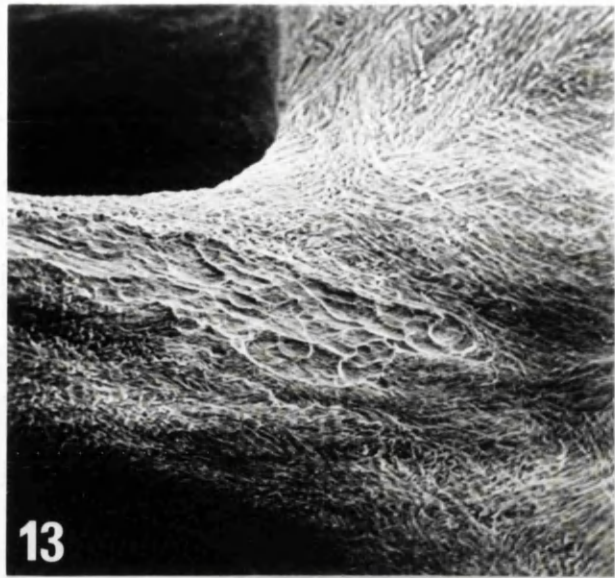
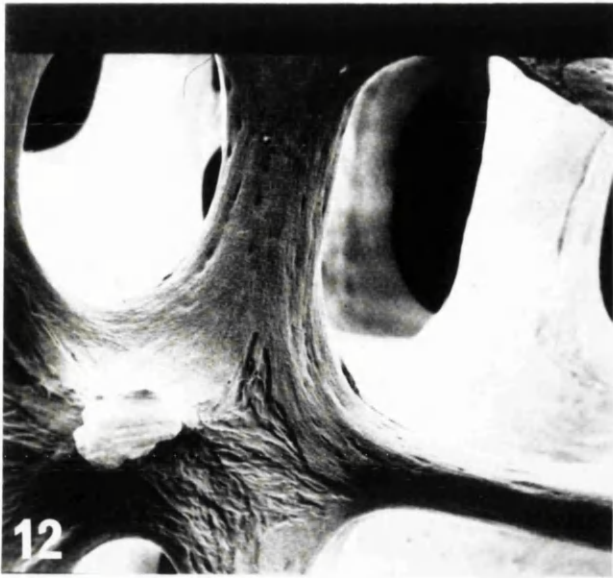


Fig. 18 75 yr female. A half-formed osteocyte lacuna from the mineralising front shown in figure 17. The back wall of the lacuna showed the same characteristics as the surface, indicating that this is an actively forming front. Fieldwidth 20 μm .

Fig. 19 41 yr male. Stereopair showing deep resorption at the centre of a node. Fieldwidth 905 μm .

Fig. 20 75 yr female. Most of the surface of this area has been superficially resorbed. A patch of resting surface and a forming front can be seen on the left side, with deep resorption appearing at the centre. Fieldwidth 470 μm .



Fig.21 75 yr female. Stereopair showing deep resorption at central region of figure 20.

Different orientations of collagen bundles can be seen in different lamellae exposed by deep osteoclasts. Fieldwidth 50 μm .

Fig. 22 75 yr female. Superficially resorbed trabecular surface showing many canaliculi. In some regions canaliculi were grouped together indicating osteocyte lacunae immediately underneath. Fieldwidth 190 μm .

Fig. 23 75 yr female. A superficially resorbed trabecular surface (below) being covered by a massive mineralising front (left), resting surface right. Fieldwidth 190 μm .

Fig. 24 91 yr female. Stereopair showing a deeply grooved trabeculum. Fieldwidth 190 μm .

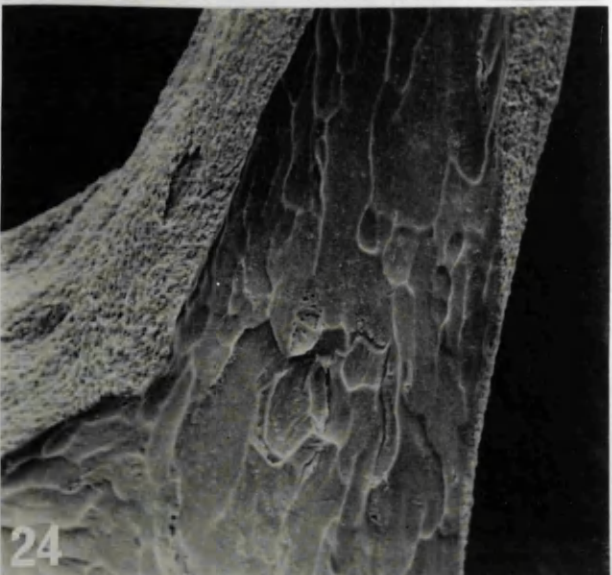
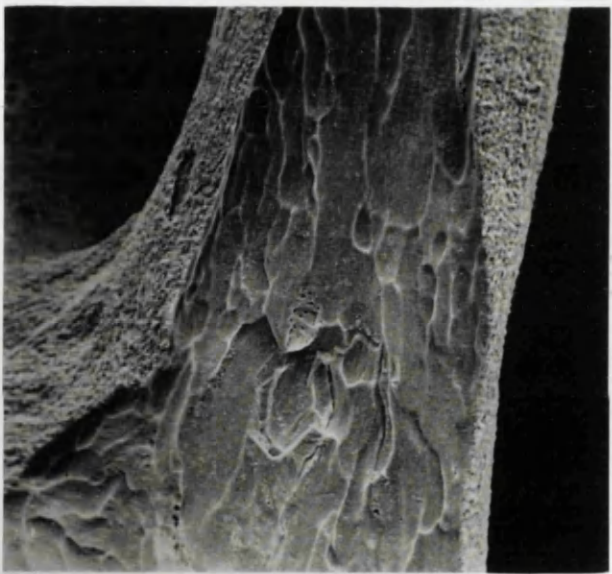
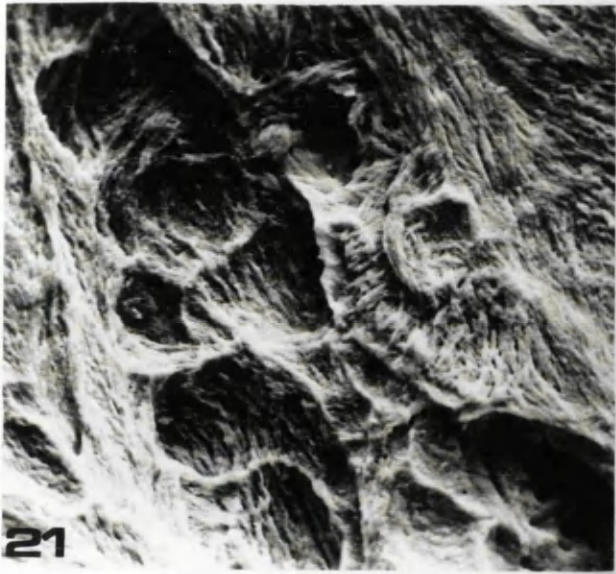
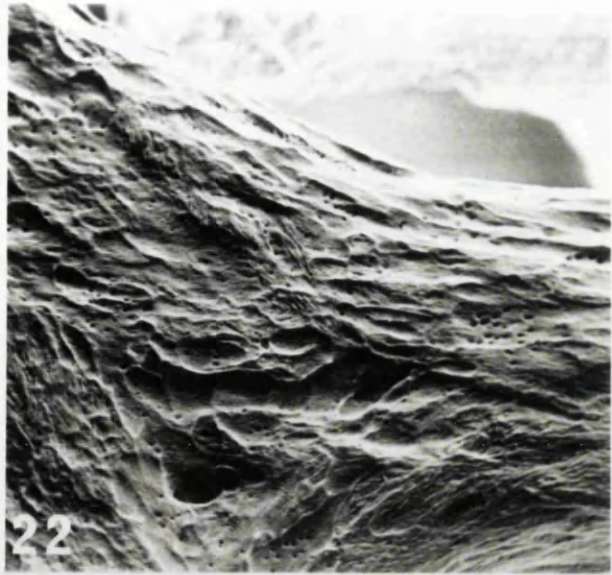
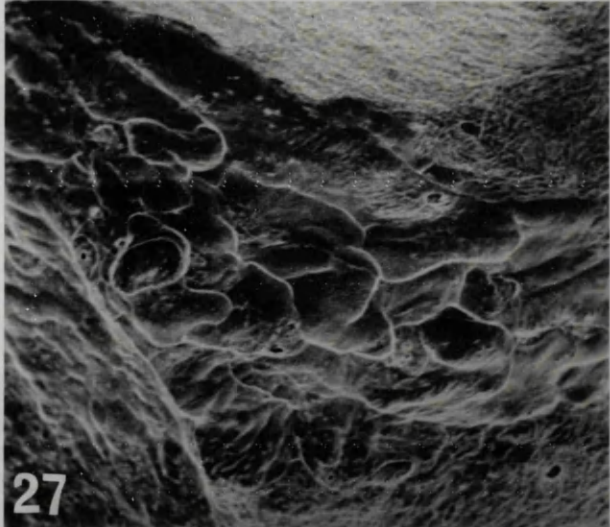
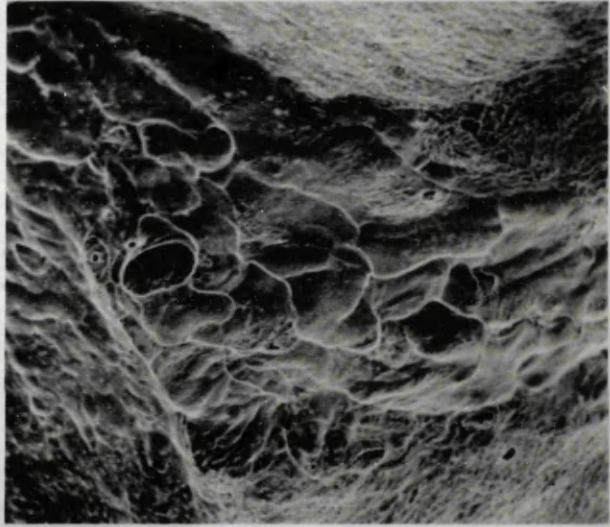
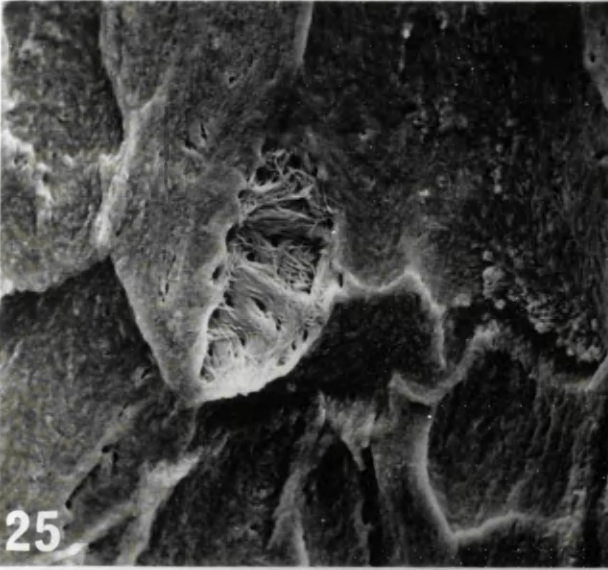
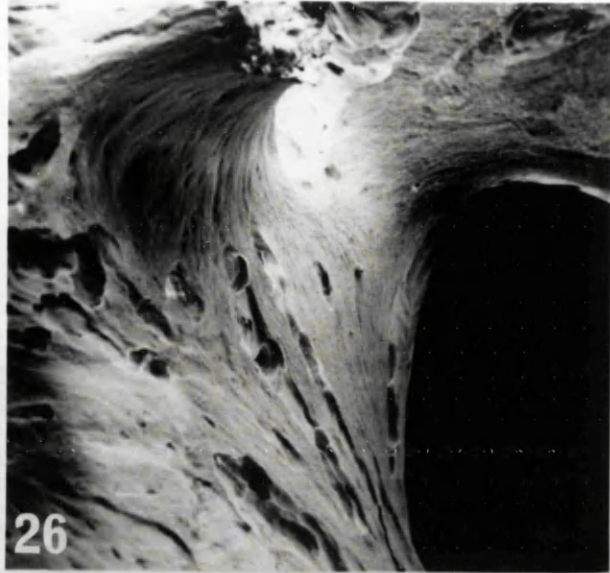


Fig. 25 91 yr female. Stereopair showing detail from the floor of the groove from figure 24. Note collagen fibres organised into thick bundles in the wall of the osteocyte lacuna, which has been untouched by resorption. Fieldwidth 50 μm .

Fig. 26 60 yr male. Surface of a plate showing appearance of several deep resorption patches (? future perforations) in the floor of grooves. Fieldwidth 570 μm .

Fig. 27 74 yr male. Stereopair showing superficial resorption of a plate surface. The deep pit at centre suggesting a single osteoclast resorbing deep into bone. Fieldwidth 260 μm .

Fig 28 89 yr osteoporotic female. A rod shaped trabeculum has almost been cut away at its base by deep, aggressive resorption of osteoclasts (The disconnection of the rod may have occurred during specimen preparation). No superficial resorption can be seen on surrounding mineralising front surface. The trabeculum in the upper part of the figure has been completely surrounded by formation. Fieldwidth 470 μm .



26

25

27

28

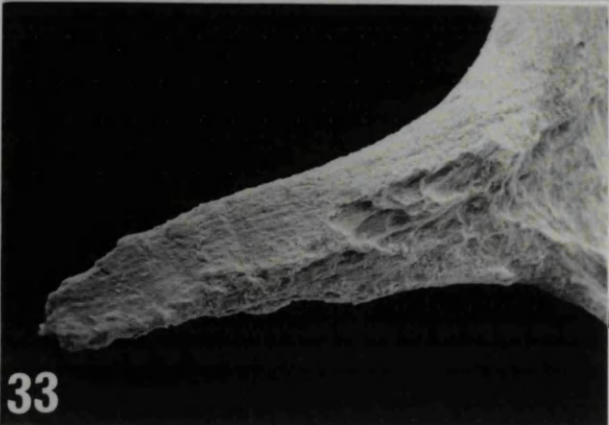
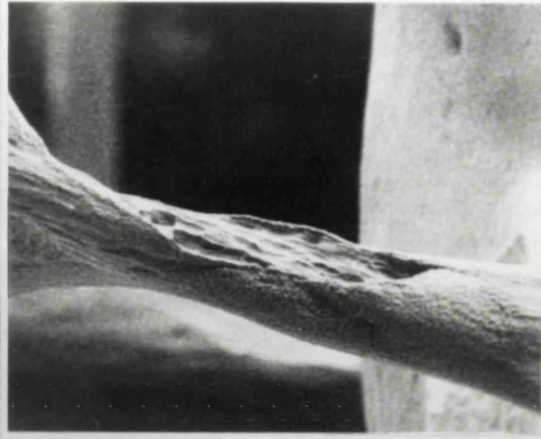
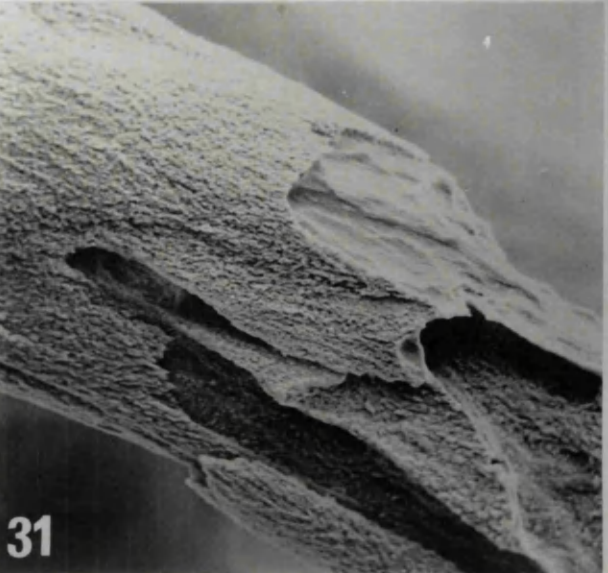
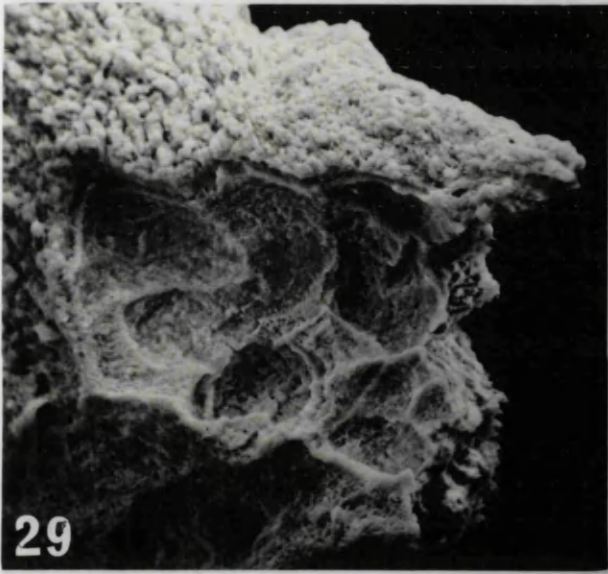
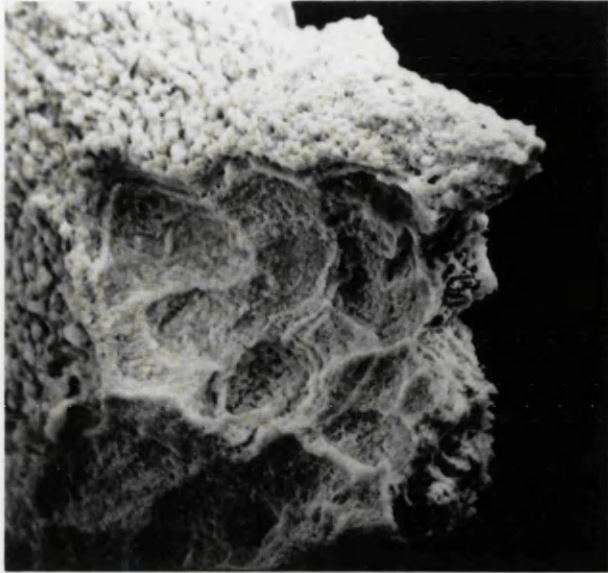
Fig. 29 89 years osteoporotic female. Stereopair showing detail of resorption lacunae in figure 28. Double margins of the lacunae suggest that several episodes of resorption had taken place, while the surrounding mineralising surface indicates that resorption has occurred on a forming surface. The remaining part of the trabeculum has been fractured. Fieldwidth 95 μm .

Fig. 30 75 yr female. Stereopair showing a grooved trabeculum. The osteoclasts seemed to have "tunnelled" into the rod while resorbing along it. Fieldwidth 500 μm .

Fig. 31 91 yr female. Several "tunnelled" grooves on a single rod. The surface of the rod is mineralising while mineralising fronts can also be seen on the floor of some grooves. Fieldwidth 190 μm .

Fig. 32 89 yr osteoporotic female. After superficial resorption, a deep groove is progressing along the long axis of this trabeculum. Fieldwidth 470 μm .

Fig. 33 89 yr osteoporotic female. A sectioned trabeculum along a groove similar to that of in figure 32. The appearance of resorption bays suggests that the groove is deepening while moving along the rod. Fieldwidth 470 μm .



29

30

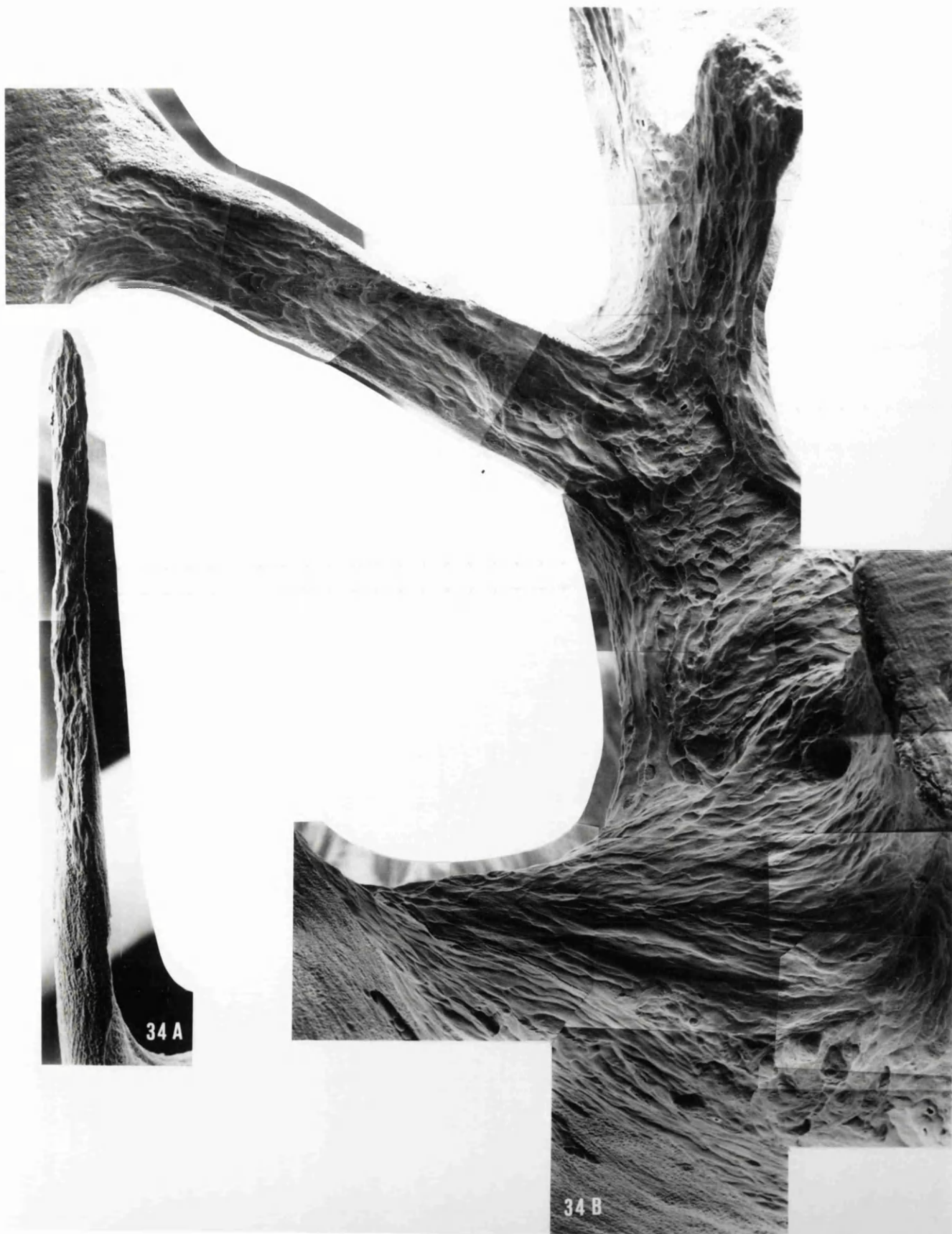
32

31

33

Fig. 34 A 69 yr male. A trabecular disconnection brought about by osteoclastic resorption. Montage x475.

Fig. 34 B 75 yr female. Extensive resorption on trabecular surfaces. Many morphological types of resorption bays can be recognised. Note the long "snail tracks" at the bottom of the figure. At top left, the rod shaped trabeculum appeared to have been thinned down by several successive episodes of resorption. Osteocyte lacunar profiles of different shapes and canalicular openings can also be observed on resorbed surfaces. Unresorbed surfaces show characteristics of mineralising fronts. Montage x500.



34 A

34 B

Fig. 35 89 yr osteoporotic female. Typical surface appearance of long, slender rod shaped trabeculae seen in old and osteoporotic specimens. Uneven mineralising surface may indicate disparate mineralisation rate or pattern. Fieldwidth 95 μm .

Fig. 36 75 yr female. Junction between a plate and a rod showing superficial resorption (top) and irregular arrangement of collagen bundles (bottom). Fieldwidth 205 μm .

Fig. 37 75 yr female. Irregular but completely mineralised surface from figure 36. Fieldwidth 50 μm .

Fig. 38 75 yr female. Detail of deep, round resorption bays from figure 36. Different orientations of collagen bundles are apparent at various depths exposed by osteoclastic resorption, suggesting that only the most superficial bone showed the unusual collagen fibre orientation pattern. Fieldwidth 105 μm .

Fig. 39 71 yr osteoporotic male. A rod shaped trabeculum showing irregular collagen organisation in relation to possibly non-artifactual micro-cracks at the surface. Fieldwidth 190 μm .

Fig. 40 89 yr osteoporotic female. A fractured rod showing shallow resorption on one side, which may have weakened it. Rest of the surface is mineralising while the back wall of the half formed osteocyte lacuna has been completely mineralised. Fieldwidth 95 μm .

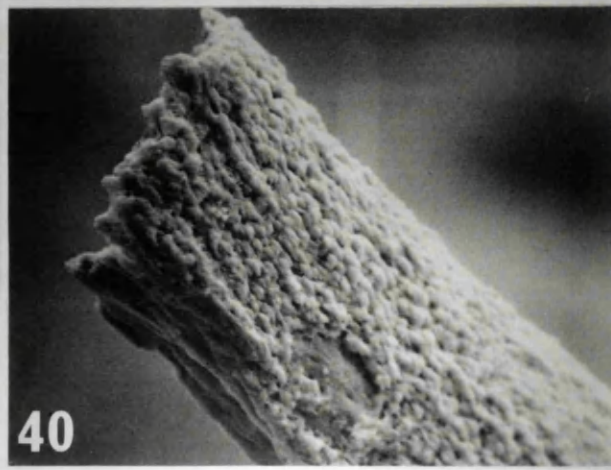
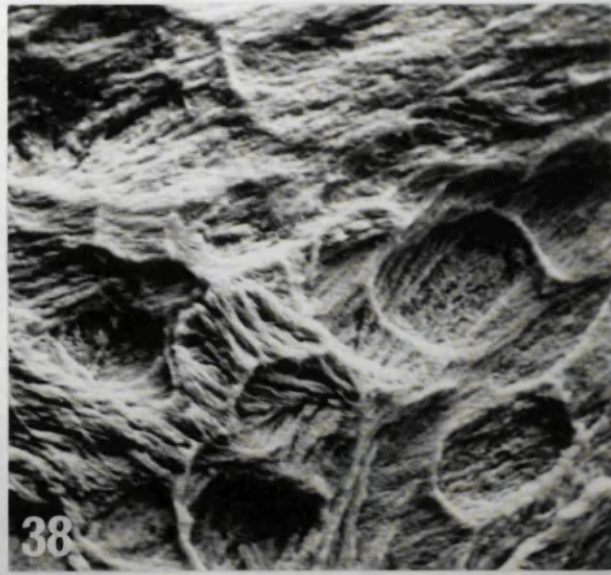


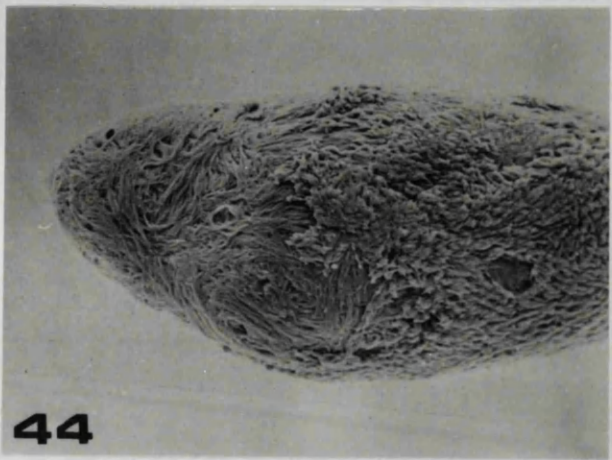
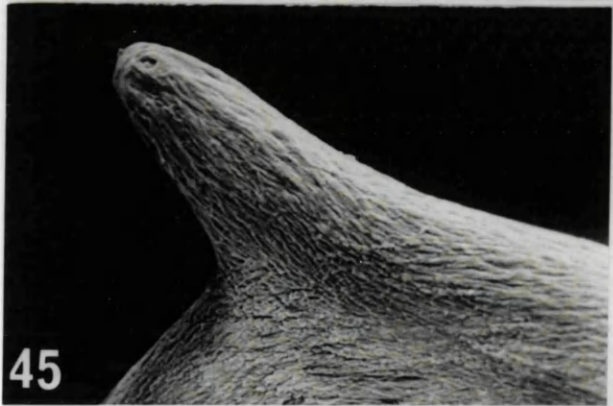
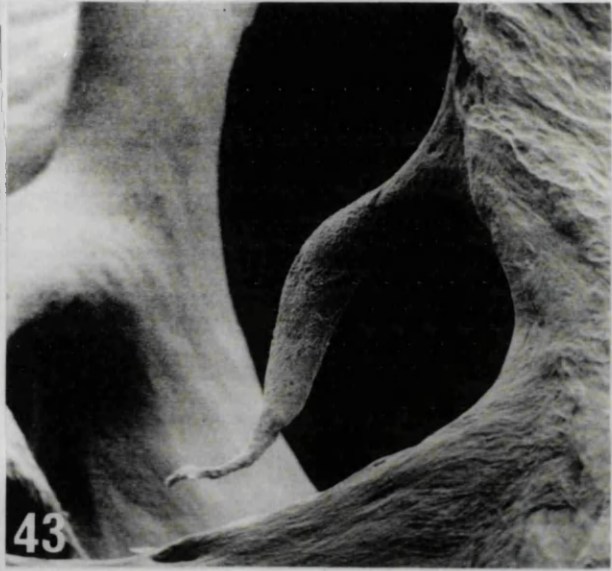
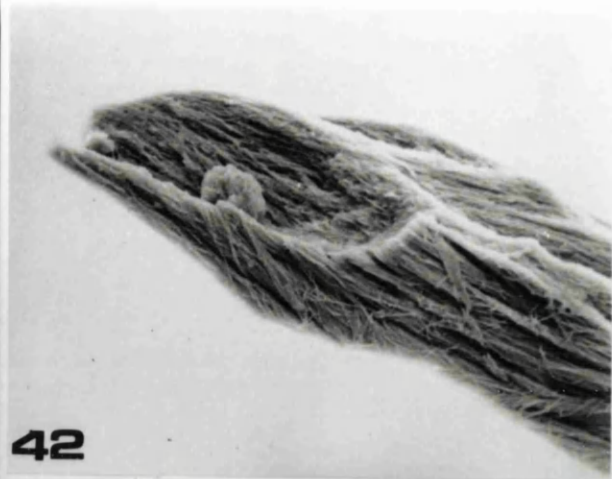
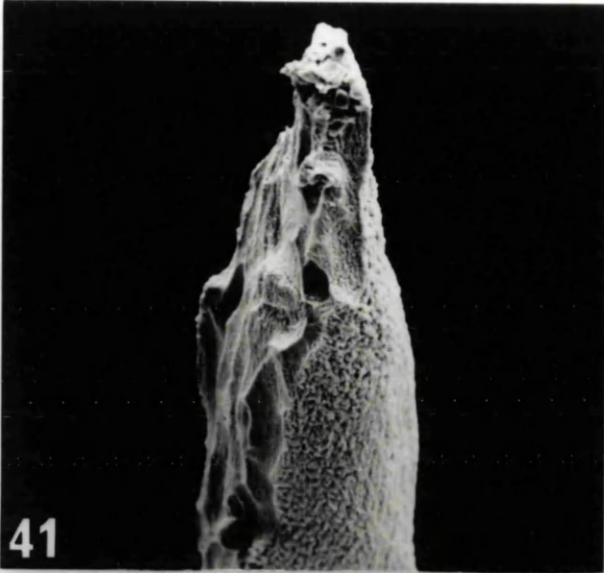
Fig. 41 88 yr female. A gradual deepening of resorption has almost disconnected this rod. However, the final fracture may have been mechanical. Fieldwidth 190 μm .

Fig. 42 71 yr osteoporotic male. Tip of a rod which has been completely "eaten away" as a result osteoclasts. Note that osteoclasts have cut right across collagen bundles at the final phase of resorption. Collagen fibrils within the bundles can easily be recognised, indicating their looser packing density. Fieldwidth 50 μm .

Fig. 43 74 yr male. A disconnected end of a trabeculum. A decline in surface activity was observed in some of such disconnected elements. Fieldwidth 540 μm .

Fig. 44 71 yr osteoporotic male. This broken tip of a trabeculum has been swathed by new collagen bundles. The collagen at the tip has been completely mineralised while rest of the surface show characteristics of a mineralising front. Fieldwidth 190 μm .

Fig. 45 88 yr female. Stereopair showing broken end of a trabeculum "wrapped" by collagen bundles. Fieldwidth 190 μm .



CHAPTER 7

SUMMARY AND CONCLUSIONS

7.1 TRABECULAR BONE

Trabecular bone has been the subject of many investigations since the early nineteenth century, with the relationship between trabecular patterns and stress trajectories being a major, and sometimes controversial, issue. Clinical interest in trabecular bone is also considerable due to the fact that two important fracture sites, the lumbar vertebrae and proximal end of the femur, are composed mainly of trabecular bone.

The methodologies usually involved in the analysis of trabecular bone are direct extensions from that used for other tissues such as compact bone or soft tissues. To derive the required quantities in bone histomorphometrical analysis, it is the usual practice to use various stereological methods or image analysis techniques to analyse thin histological sections from limited areas of bone. Three dimensional information is usually obtained by reconstruction of the third dimension from two dimensional data sets. In the 1st chapter of this thesis, it was argued that such techniques are incapable of describing accurately such unique qualities of trabecular bone as spatial distribution, connectivity or shape. Clinical techniques of bone mass measurements are also unsuitable for this purpose.

7.2 NOVEL METHODS

One of the main problems in understanding trabecular bone was that there was no suitable technique that would permit proper three dimensional observation of its architecture. In the 2nd chapter, various experiments were carried out to develop new techniques to study and analyse trabecular bone architecture three dimensionally. The limitations of different microscopic techniques were discussed. Stereopairs were unsatisfactory for an efficient analysis due to limited angles of view. In the SEM, stereopairs were further limited by the area scanned and the volume sampled. A greater volume could be sampled with a confocal laser scanning microscope (BioRad – MRC 500), but the maximum area scanned was insufficient (the image was further degraded by fixed reflections from within the optical system).

Two new techniques, the 3-D "integrgrams" and "continuous motion parallax method" were developed during the experiments. The "hologram" type of effect produced by integrgrams allowed a better comprehension of connectedness and spatial distribution of trabeculae than that would be possible from a single stereopair. If the cost of integrgram production can be kept low, they would be useful in educating both the general public and health personnel in the structure of trabecular bone and its changes in disease states such as osteoporosis (but the method is too expensive for research purposes). The continuous motion parallax method developed using a high definition light microscope with an increased depth of field (Olbrich 4000) is the best and most economical method available to date for a complete three dimensional observation of trabecular bone

architecture. Since a volume of tissue can be viewed from 360° of projections, a more accurate three dimensional understanding could be obtained. The method will be useful both in education and research.

Confocal microscopes can be used to estimate the porosity of trabecular bone and the high definition light microscope (Olbrich 4000) would be useful in analysing the spatial distribution of osteoid patches. Future research should concentrate on developing these methods.

Another observation made during the above experimental work was that trabecular bone shows extreme regional variations in a site such as a lumbar vertebral body so that whole sections should be analysed to understand the whole structure. Of the methods tested, the simple method of producing 35mm macro stereophotographs found to be most suitable for this purpose.

7.3 TRABECULAR BONE ARCHITECTURE OF THE LUMBAR VERTEBRAL BODY

Mid-sagittal sections of 4th lumbar vertebral bodies were analysed in chapter 3 using macro stereophotographs generated by tilting the specimens 10°. Three distinct zones of trabeculae were identified in young sections. It was found that the conventional terms such as "vertical" and "horizontal", do not do justice to the real structure. A model for trabecular bone architecture at the mid-sagittal plane of young vertebral bodies was proposed. The model composed of large, incomplete cylinders at the middle zone branching off to give rise to smaller, incomplete tubes or a cross braced structure at the periphery. Long rod-shaped horizontal trabeculae were identified at the middle zone while they were shorter in the peripheral zones. The real lengths of the horizontal trabeculae in the different zones could be calculated for the first time using the parallax measuring facility of the stereoscope. The proposed two dimensional model for osteoporotic architecture consists of spaced, thick, vertical trabeculae running from one end plate to other; connected by long, thin horizontal or oblique trabeculae with no definite length distributions. The zonal arrangement was not evident in this model. A highly significant age related decrease in both vertical and horizontal trabeculae was also observed. The quantitative analysis also proved the accuracy of proposed models.

The observation of the highly vascular nature of the middle zone led to an extensive literature survey on the development and vascularisation of lumbar vertebral bodies. A strong relationship was discerned between the adult vertebral trabecular structure and the developmental and vascular patterns. This is a significant observation as hitherto it was believed that trabeculae are laid down along stress trajectories of the vertebral bodies. The contribution of each of these factors in establishing the adult trabecular bone architecture of the lumbar vertebral body is not clear. In order to understand this process completely, future studies should concentrate on following development and vascularisation of lumbar vertebrae from neonates to adult. The literature survey also showed that vascular changes take place in the vertebral body on aging. Further, there is a rise in intraosseous pressure in old vertebral bodies. Research should also be carried out to determine the effects of such changes on changing trabecular bone structure with age.

The methods described here are purely post-mortem research oriented and cannot be employed clinically or in vivo situations. None of the existing techniques can analyse accurately

the *in vivo* changes in trabecular bone architecture with age. It is also not easy to develop such techniques. However, one objective of the present work was to point out the importance of changing architecture with age and its implications on age related fractures. It is now clear that why a mass based theory of bone loss would not completely predict fracture risk of elderly patients.

Similar work should also be carried out on vertebral trabecular bone from other locations and especially from other clinically important sites such as the proximal end of the femur, where trabecular patterns play important roles in age related fractures.

7.4 FREQUENCY DOMAIN ANALYSIS

Chapter 4 reported the first use of the powerful capabilities of fast Fourier transform in analysing age changes in vertebral trabecular bone. Many difficulties were encountered in developing a proper technique, and the major concern was the image input. Confocal microscopes would offer the best means of producing suitable images if they could be developed to image larger areas of bone.

It was possible to derive quantitative information more efficiently and accurately using frequency methods. Not only could changes in trabecular spacing be calculated with minimum examiner variation, but the technique also offers the advantage of being able to calculate spacing in any desired direction. This is not possible with other techniques. The power spectra of trabecular bone images can also be utilised as "fingerprints" to identify different trabecular patterns: information that is not apparent from the image can be obtained.

Another interesting finding was that if samples of uniform thickness could be radiographed under standard conditions, the image intensity could be used to compare the volume density of trabecular bone in different regions of vertebral sections and between different age groups.

The technique of studying individual groups of trabeculae using templated images also brought some interesting results. It was possible, for example, to identify which group of trabecular elements contributes more to volume density in a particular region. Further, age related bone loss could be studied separately in different trabecular groups. It was found that the loss is first apparent in the horizontal trabeculae at the anterior and posterior regions of the peripheral zones of vertebral sections. This new technique should further be explored to test its capabilities in providing further information.

The spatial domain study should be considered as preliminary. To confirm the results, it would be necessary to test the reproducibility of these experiments using a larger sample than that was used in the present study. Further, trabecular bone in the proximal end of the femur should also be subjected to frequency domain analysis to explore possibilities of acquiring more information on age related bone loss in this important site. Future research might also use clinical images to test their suitability in analysing in the frequency domain.

7.5 QUALITY OF TRABECULAR BONE

Chapter 5 presented results of an analysis of the changing quality of trabecular bone during aging. The stiffness of trabecular bone derived from mid-sagittal vertebral sections was tested and fracture patterns were studied using macro stereophotographs and the SEM. Non-mineralised matrix contributed to stiffness in all the age groups tested. Different degrees of mineralisation were observed in old specimens. Some old specimens were properly mineralised while some more younger and especially osteoporotic specimens showed poor mineralisation. It was concluded that the status of mineralisation of trabecular bone in old age is not always normal. This is a significant finding as to date it is believed that in osteoporosis, the quality of bone remains normal but the loss is only in quantity. This lead should be followed in future studies using larger numbers of samples to analyse the spatial distribution of non-mineralised matrix patches and correlating the results with stiffness of the same samples to determine the contribution of defective mineralisation to osteoporotic fractures.

The study also demonstrated that fracture patterns in trabecular bone were related not only to the architectural arrangement of trabeculae within the vertebral body, but also to the organisation of collagen (lamellae) within an individual trabeculum.

7.6 TRABECULAR BONE SURFACE

Chapter 6 described a study of trabecular bone surfaces using the SEM. Previously described surface morphologies for other sites (eg. forming, resorbing and resting) were identified on trabecular surfaces and their changes with age were studied. A proper coupling between the surface activities was evident in younger samples indicating a maintenance of both bone mass and the structural integrity, while in some old and osteoporotic samples, an uncoupling of activities were observed which may have been responsible for loss of bone and disruption of the trabecular architecture.

New information was obtained regarding mechanisms involved in trabecular bone loss. Two distinct patterns of resorption were identified which could have been resulted from different movement patterns of osteoclasts. Superficial planing of plates and thinning of rods may have been brought about by lateral movements of osteoclasts during resorptive phases, while deep resorption, involving perforations, grooving or tunnelling, may have resulted from static resorption.

The mechanisms involved in compensatory thickening of trabeculae in old and osteoporotic trabecular bone were also identified. Uncoupling between formation and resorption was such that on some occasions formation seemed to have been initiated only after several episodes of resorption. The mineralising fronts were unusually large and sometimes almost covered a trabeculum thus causing a change in trabecular size and shape.

It was also shown that trabecular disconnections were not always microfractures, but resulted from osteoclastic resorption of the complete thickness of the trabeculum.

Microcallus formation was also observed but was not adequately studied. Future work should concentrate on studying and quantifying these important lesions. Further, the appearance and progression of perforations should be investigated thoroughly to find their age of appearance

and location. Similar studies should also be carried out on trabecular bone from other clinically important sites, such as the proximal end of the femur and the iliac crest.

7.7 FINAL REMARKS

In summary, the present study investigated trabecular bone; developed new three dimensional methods for viewing and analysing its architecture; analysed the structure, age and osteoporotic changes of the 4th lumbar vertebral body in 3-D; used fast Fourier transforms to develop and analyse trabecular bone in the frequency domain; investigated changes in quality of trabecular bone, changes in trabecular micromorphology and surface activities on aging and in osteoporosis. This work confirmed some beliefs, refuted others, introduced novel methods, concepts and derived significant results. I hope that it has made some contribution to the field of bone research.

APPENDIX - I

Details of subjects from whom bone used in this study was obtained.

AGE (years)	SEX	CAUSE OF DEATH	SAMPLE SITE (Lumbar vertebrae = L) (Femoral head = FH) (Iliac crest = IC)
30	F	Acute heart failure	L1-L5
30	F	Accidental	L3-L4
31	M	Accidental	L4
33	M	Acute heart failure	FH
33	M	Accidental	FH
33	M	Not known	FH
35	M	Not known	FH
35	M	Acute heart failure	L2-L4
36	F	Cerebral infarction	IC
39	M	Acute heart failure	IC
41	M	Acute heart failure	L4
41	M	Myocardial infarction	L4
42	F	Suffocation	L2-L4
45	M	Acute heart failure	L4
50	M	Acute heart failure	L4
51	F	Broncho pneumonia	L4
55	F	Acute heart failure	L4
59	M	Acute heart failure	L4
58	M	Acute heart failure	L4
60	M	Acute heart failure	L4
62	M	Broncho pneumonia	L4
63	F	Not known	FH
64	M	Acute heart failure	L4
64	F	Septicaemia	L4-L5
64	M	Acute heart failure	L4,FH
64	M	Not known	FH
69	M	Cerebral haemorrhage	L4
69	M	Acute heart failure	L3-L4
71	F	Accidental	L4
71	M	Cerebral haemorrhage	L3-L4
73	F	Acute heart failure	FH

74	F	Broncho pneumonia	L4
74	M	Acute heart failure	L4
75	F	Acute heart failure	L4
75	M	Acute heart failure	FH
77	F	Not known	FH
77F	F	Acute heart failure	FH
77	M	Myocardial infarction	L4-L5
80	M	Broncho pneumonia	L4
85	F	Acute heart failure	FH
85	F	Acute heart failure	L1-L5,FH
86	F	Acute heart failure	FH
88	F	Broncho pneumonia	L1-L5,FH,IC
88	F	Acute heart failure	L3-L4,IC
89	M	Acute heart failure	L4
89	F	Broncho pneumonia	L1-L4,FH
89	F	Broncho pneumonia	L1-L5,FH
89	M	Broncho pneumonia	L2-L4
91	F	Acute heart failure	L4-L5
95	F	Broncho pneumonia	L5,FH

APPENDIX II

MULTIPLE REGRESSION ANALYSIS

Calculated values for L and R²

MALE		FEMALE	
L	R ² %	L	R ² %
-2	67.6	-2	66.7
-1.8	72.6	-1.8	70.6
-1.6	72.4	-1.6	71.0
-1.4	77.5	-1.4	75.1
-1.2	77.3	-1.2	75.6
-1.0	82.2	-1.0	79.6
-0.8	81.9	-0.8	80.0
-0.6	86.0	-0.6	83.6
-0.4	85.5	-0.4	83.7
-0.2	87.6	-0.2	86.2
0.0	89.1	0.0	88.0
0.2	88.0	0.2	87.2
0.4	87.9	0.4	87.8
0.6	86.7	0.6	86.6
0.8	85.2	0.8	86.0
1.0	84.1	1.0	84.6
1.2	81.4	1.2	82.9
1.4	80.7	1.4	81.6
1.6	77.0	1.6	79.0

APPENDIX III

The following aspects of this work were published as abstracts and presented at scientific meetings during the course of this study.

Boyde A, Jayasinghe JAP, Jequier B (1988) Three dimensional integram images of trabecular bone. *Bone* 10:150 (1989).

Jayasinghe JAP, Boyde A (1989) A preliminary study of normal and osteoporotic trabecular bone using frequency domain analysis. *Bone* 11:227 (1990).

Boyde A, Radcliffe R, Watson TF, Jayasinghe JAP (1989) Continuous motion parallax in the display and analysis of trabecular bone structure. *Bone* 11:228 (1990).

Jayasinghe JAP, Boyde A (1990) An analysis of changing spatial frequency of vertebral trabecular bone with age. *Bone*, in press.

Jayasinghe JAP, Boyde A (1991) Micro-Anatomy of spongy bone in human lumbar vertebrae. *Calcified Tissue International Suppl.* 48:A59 (1991).